UNIVERSITY OF NEWCASTLE

SCHOOL OF MEDICINE & PUBLIC HEALTH

Thesis

NEURAL CORRELATES OF COGNITIVE IMPAIRMENT IN A SAMPLE OF YOUNG PEOPLE AT RISK OF DEVELOPING SCHIZOPHRENIA

by

Tim Ehlkes

Submitted for the degree of

Doctor of Philosophy

2013

STATEMENT OF ORIGINALITY

This thesis contains no material which has been accepted for the award of any other degree or diploma in any university or other tertiary institution and, to the best of my knowledge and belief, contains no material previously published or written by another person, except where due reference has been made in the text.

I give consent to the final version of my thesis being made available worldwide when deposited in the University's Digital Repository, subject to the provisions of the Copyright Act 1968.

... signed

Tim Ehlkes

STATEMENT OF COLLABORATION

I hereby certify that the work embodied in this thesis has been done in collaboration with other researchers. I have included as part of the thesis a statement clearly outlining the extent of collaboration, with whom and under what auspices.

... signed

Tim Ehlkes

ACKNOWLEDGEMENTS

I wish to express my gratitude and special thanks to Prof. U. Schall.
You have been the greatest supervisor, mentor, and friend anyone could wish for.
Thanks for everything Ulli.

My sincerest thanks and appreciation go to Paul Rasser for his cheerfulness, scientific expertise, for providing countless hours of skills training, and for creating such a great lab atmosphere. You are fantastic Paul. Without you this project wouldn't have been half as much fun.

My sincere thanks also go to Prof. P. Michie for her guidance, kind help and valuable feedback during the work on my PhD project.

Last but not least I would like to thank all those who supported me throughout this study. In particular, I would like to thank the MinT consortium for their support and for making this research opportunity possible.

ABSTRACT

The reliable identification of the schizophrenia prodrome is a prerequisite for early intervention in young people considered "at-risk" of developing this severe mental illness. Clinical at-risk criteria, however, still lack predictive specificity to reliably predict outcome. Brain imaging research has added substantial evidence to the notion of emerging and progressive grey and white matter abnormalities in the early phase of illness. The purpose of this study was to investigate structural brain changes associated with the clinical profile of the At-Risk Mental State (ARMS) syndrome, along with cognitive and psychophysiological measures that have been linked schizophrenia.

Forty-two young individuals meeting ARMS criteria of the Comprehensive Assessment of At-risk Mental State (CAARMS) were included in the study. Surface-based methods were applied to quantify measures of cortical structure in high-resolution MRI scans. Participants underwent clinical and cognitive assessments. Event-related potentials (i.e. Mismatch Negativity and P3a) were recorded whilst study participants performed an auditory oddball task. A median-split of dividing the study participants into two groups with low versus high symptom expression (ARMS-LS vs. ARMS-HS) based on CAARMS symptom ratings revealed significantly reduced mean cortical grey matter thickness in the more symptomatic group. There was no significant group difference in total brain volume, grey or white matter volume, or pial or white matter surface areas. ARMS-HS presented significantly impaired in socio-occupational and social/role functioning, as well as performed lower in verbal fluency when compared to ARMS-LS.

Vertex-wise correlation analyses confirmed significant associations ($p < .05$ corrected) of CAAMRS symptom rating scores with reduced grey matter thickness in left and right superior frontal gyri, right anterior cingulate, and right medial occipito-temporal cortex (i.e. lingual gyrus). Reduced grey matter in frontal, prefrontal, and occipital cortical areas were associated with low function ratings. Verbal Fluency task performance largely overlapped with the

frontal brain areas identified for low function ratings by reduced regional grey matter thickness correlation maps.

These findings suggest that emerging psychopathology as defined by CAARMS for ARMS (i.e. low-grade psychotic symptom expression and functional impairment) is associated with reduced cortical grey matter thickness, a putative measure of brain pathology. Future research should investigate whether regional cortical grey matter reduction is associated with a higher risk of developing schizophrenia.

TABLE OF CONTENTS

STATEMENT OF ORIGINALITY I

STATEMENT OF COLLABORATION II

ACKNOWLEDGEMENTS III

ABSTRACT IV

TABLE OF CONTENTS VI

INDEX OF FIGURES IX

INDEX OF TABLES X

INDEX OF APPENDICES XI

GLOSSARY XIV

1 INTRODUCTION 16

1.1 BRIEF OVERVIEW OF SCHIZOPHRENIA 17

1.2 IDENTIFYING THE PRODROME OF PSYCHOTIC ILLNESS 19

1.3 EARLY SIGNS OF BRAIN PATHOLOGY AND THEIR ASSOCIATION WITH EMERGING CLINICAL SYMPTOMS 20

1.4 FUNCTIONAL AND ANATOMICAL CORRELATES OF IMPAIRED WORKING MEMORY AND EXECUTIVE DYSFUNCTION IN THE EARLY STAGES OF SCHIZOPHRENIA 23

1.5 ELECTROPHYSIOLOGICAL CORRELATES OF EARLY PSYCHOSIS AND THEIR ASSOCIATION WITH NEUROANATOMICAL ABNORMALITIES 27

1.6 OBJECTIVE AND HYPOTHESES 29

2 METHODOLOGY 31

2.1 PARTICIPANTS' RECRUITMENT AND COHORT CHARACTERISTICS 32

2.2 INSTRUMENTS 33

2.2.1 PSYCHOPATHOLOGY AND SYMPTOM RATINGS 34

2.2.2 FUNCTIONING MEASURES 38

2.2.3 NEUROCOGNITIVE MEASURES 39

2.2.4 SOCIAL COGNITION MEASURES 43

2.2.5 ELECTROENCEPHALOGRAPHIC DATA 44

2.3 MAGNETIC RESONANCE IMAGING DATA 46

2.3.1 MRI Data Acquisition 46
2.3.2 Brain Anatomy Relevant to Image processing 46
2.3.3 MRI Pre-Processing 48
2.3.4 FreeSurfer Image Analysis Suite 48
2.3.5 FreeSurfer's Cortical Reconstruction & Volumetric Segmentation 49
2.3.6 Modification to FreeSurfer's default workflow 52
2.4 Data Analysis using SPSS 53
2.4.1 Median-Split Group Analysis by CAARMS composite score 53
2.5 Data Analysis using FreeSurfer 53

3 RESULTS 55

3.1 ARMS Cohort Characteristics 56
3.1.1 Demographic and Clinical Data 56
3.1.2 Function Ratings 57
3.1.3 Neurocognitive Measures 57
3.1.4 Social Cognition Measures 58
3.1.5 Electroencephalographic Data 59
3.2 Median-Split Group Analysis by CCS 60
3.2.1 Demographic and Clinical Data 60
3.2.2 Brain Morphology 61
3.2.3 Function Ratings 62
3.2.4 Neurocognitive Measures 62
3.2.5 Social Cognition Measures 64
3.2.6 Electroencephalographic Data 64
3.2.7 Summary and Conclusion 65
3.3 Regional Grey Matter Thickness vs. Assessment Data 66
3.3.1 Symptom Ratings 67
3.3.2 Function Ratings 69
3.3.3 Neurocognitive Measures 74
3.3.4 Social Cognition Measures 81
3.3.5 Electroencephalographic Data 81

4 DISCUSSION **82**

4.1 BRAIN MORPHOLOGICAL CORRELATES OF PSYCHOPATHOLOGY **84**

4.2 GREY MATTER CORRELATES OF COGNITIVE PERFORMANCE **86**

4.3 STUDY STRENGTHS AND LIMITATIONS **96**

4.4 FUTURE DIRECTIONS **97**

APPENDIX **99**

SECTION I COHORT CHARACTERISTICS **100**

SECTION II GREY MATTER THICKNESS VS. ASSESSMENT DATA **103**

(I) SYMPTOM RATINGS 103

(II) FUNCTIONING MEASURES 107

(III) NEUROCOGNITIVE MEASURES 112

(IV) SOCIAL COGNITION MEASURES 146

(V) ELECTROENCEPHALOGRAPHIC DATA 150

BIBLIOGRAPHY **155**

COLLABORATION WITH OTHER RESEARCHERS **167**

INDEX OF FIGURES

FIGURE 3.1.5-1 MMN/P3A WAVEFORMS TO DURATION AND FREQUENCY DEVIANT TONES 59

FIGURE 3.2.6-1 GROUP AVERAGE MMN/P3A WAVEFORMS TO DURATION AND FREQUENCY DEVIANT TONES OF ARMS-LS VS. ARMS-HS 65

FIGURE 3.3.1-1 STATISTICAL CORRELATION MAPS OF GREY MATTER THICKNESS WITH CAARMS COMPOSITE SCORES (CCS) 67

FIGURE 3.3.1-2 STATISTICAL CORRELATION MAPS OF GREY MATTER THICKNESS WITH CAARMS NEGATIVE SYMPTOM SCORES 68

FIGURE 3.3.2-1 STATISTICAL CORRELATION MAPS OF GREY MATTER THICKNESS WITH GAF SCORES 69

FIGURE 3.3.2-2 STATISTICAL CORRELATION MAPS OF GREY MATTER THICKNESS WITH SOFAS SCORES 70

FIGURE 3.3.2-3 STATISTICAL CORRELATION MAPS OF GREY MATTER THICKNESS WITH GF:SOCIAL SCORES 71

FIGURE 3.3.2-4 STATISTICAL CORRELATION MAPS OF GREY MATTER THICKNESS WITH GF:ROLE SCORES 72

FIGURE 3.3.3-1 STATISTICAL CORRELATION MAPS OF GREY MATTER THICKNESS WITH VFT CONDITION 2 PRIMARY MEASURE SCALED SCORES 74

FIGURE 3.3.3-2 STATISTICAL CORRELATION MAPS OF GREY MATTER THICKNESS WITH VFT CONDITION 3 TOTAL CORRECT RESPONSE SCALED SCORES 75

FIGURE 3.3.3-3 STATISTICAL CORRELATION MAPS OF GREY MATTER THICKNESS WITH VFT CONDITION 3 TOTAL SWITCHING ACCURACY SCALED SCORES 76

FIGURE 3.3.3-4 STATISTICAL CORRELATION MAPS OF GREY MATTER THICKNESS WITH TOWER TASK PRIMARY MEASURE TOTAL ACHIEVEMENT SCALED SCORES 77

FIGURE 3.3.3-5 STATISTICAL CORRELATION MAPS OF GREY MATTER THICKNESS WITH CVLT-II LIST A SHORT DELAY FREE RECALL STD. SCORES 78

FIGURE 3.3.3-6 STATISTICAL CORRELATION MAPS OF GREY MATTER THICKNESS WITH CVLT-II LIST A LONG DELAY CUED RECALL STD. SCORES 79

FIGURE 3.3.3-7 STATISTICAL CORRELATION MAPS OF GREY MATTER THICKNESS WITH CVLT-II RECOGNITION CORRECT STD. SCORES “TOTAL HITS”.....80

INDEX OF TABLES

TABLE 2.2.1-1 INSTRUMENTS 33

TABLE 2.2.1-1 CAARMS-DEFINED ULTRA HIGH RISK AND PSYCHOTIC DISORDER THRESHOLD CRITERIA 35

TABLE 2.3.4-1 FREESURFER AUTORECON PROCESSING STAGES 49

TABLE 2.3.5-1 LIST OF ANATOMICAL PARCELLATIONS (APARC.A2009S) 51

TABLE 3.1.3-1 NEUROPSYCHOLOGICAL VS. FUNCTIONAL MEASURES 57

TABLE 3.2.1-1 DEMOGRAPHIC AND CLINICAL DATA: LOW-SYMPTOMATIC VS. HIGH-SYMPTOMATIC STUDY PARTICIPANTS BY CCS MEDIAN-SPLIT 61

TABLE 3.2.2-1 BRAIN MORPHOLOGICAL CHARACTERISTICS: LOW-SYMPTOMATIC VS. HIGH-SYMPTOMATIC STUDY PARTICIPANTS BY CCS MEDIAN-SPLIT 61

TABLE 3.2.4-1 NEUROCOGNITIVE ASSESSMENT BATTERY: LOW-SYMPTOMATIC VS. HIGH-SYMPTOMATIC STUDY PARTICIPANTS BY CCS MEDIAN-SPLIT 63

TABLE 3.2.6-1 ERP DATA: LOW-SYMPTOMATIC VS. HIGH-SYMPTOMATIC STUDY PARTICIPANTS BY CCS MEDIAN-SPLIT 64

TABLE 3.3.1-1 CCS VS. GREY MATTER THICKNESS 67

TABLE 3.3.1-2 CAARMS NEGATIVE SYMPTOM SCORE VS. GREY MATTER THICKNESS 68

TABLE 3.3.2-1 GAF VS. GREY MATTER THICKNESS 69

TABLE 3.3.2-2 SOFAS VS. GREY MATTER THICKNESS 70

TABLE 3.3.2-3 GF:SOCIAL VS. GREY MATTER THICKNESS 71

TABLE 3.3.2-4 GF:ROLE VS. GREY MATTER THICKNESS 72

TABLE 3.3.2-5 FUNCTIONAL MEASURES VS. SYMPTOM RATINGS 73

TABLE 3.3.3-1 VFT CONDITION 2 PRIMARY MEASURE SCALED SCORE VS. GREY MATTER THICKNESS 74

TABLE 3.3.3-2 VFT CONDITION 3 TOTAL CORRECT RESPONSE SCALED SCORE VS. GREY MATTER THICKNESS 75

TABLE 3.3.3-3 VFT CONDITION 3 TOTAL SWITCHING ACCURACY SCALED SCORE VS. GREY MATTER THICKNESS 76

TABLE 3.3.3-4 TOWER TASK PRIMARY MEASURE TOTAL ACHIEVEMENT SCALED SCORE VS. GREY MATTER THICKNESS 77

TABLE 3.3.3-5 CVLT-II LIST A SHORT DELAY FREE RECALL STD. SCORE VS. GREY MATTER THICKNESS 78

TABLE 3.3.3-6 CVLT-II LIST A LONG DELAY CUED RECALL STD. SCORE VS. GREY MATTER THICKNESS 79

TABLE 3.3.3-7 CVLT-II LIST RECOGNITION CORRECT STD. SCORE "TOTAL HITS" VS. GREY MATTER THICKNESS 80

INDEX OF APPENDICES (FIGURES)

APPENDIX - FIGURE 1 STATISTICAL CORRELATION MAPS OF GREY MATTER THICKNESS WITH CAARMS POSITIVE SYMPTOM SCORES.....106

APPENDIX - FIGURE 2 STATISTICAL CORRELATION MAPS OF GREY MATTER THICKNESS WITH TMT CONDITION 2 PRIMARY MEASURE SCALED SCORES 112

APPENDIX - FIGURE 3 STATISTICAL CORRELATION MAPS OF GREY MATTER THICKNESS WITH TMT CONDITION 4 PRIMARY MEASURE SCALED SCORES 114

APPENDIX - FIGURE 4 STATISTICAL CORRELATION MAPS OF GREY MATTER THICKNESS WITH TMT PRIMARY CONTRAST 2 CONTRAST SCALED SCORES 116

APPENDIX - FIGURE 5 STATISTICAL CORRELATION MAPS OF GREY MATTER THICKNESS WITH VFT CONDITION 1 PRIMARY MEASURE SCALED SCORES 117

APPENDIX - FIGURE 6 STATISTICAL CORRELATION MAPS OF GREY MATTER THICKNESS WITH VFT PRIMARY CONTRAST MEASURE 1 CONTRAST SCALED SCORES 121

APPENDIX - FIGURE 7 STATISTICAL CORRELATION MAPS OF GREY MATTER THICKNESS WITH VFT PRIMARY CONTRAST MEASURE 2 CONTRAST SCALED SCORES 123

APPENDIX - FIGURE 8 STATISTICAL CORRELATION MAPS OF GREY MATTER THICKNESS WITH CWIT CONDITION 1 PRIMARY MEASURE SCALED SCORES 124

APPENDIX - FIGURE 9 STATISTICAL CORRELATION MAPS OF GREY MATTER THICKNESS WITH CWIT CONDITION 2 PRIMARY MEASURE SCALED SCORES 125

APPENDIX - FIGURE 10 STATISTICAL CORRELATION MAPS OF GREY MATTER THICKNESS WITH CWIT CONDITION 3 PRIMARY MEASURE SCALED SCORES 126

APPENDIX - FIGURE 11 STATISTICAL CORRELATION MAPS OF GREY MATTER THICKNESS WITH CWIT PRIMARY COMBINED MEASURE COMPOSITE SCALED SCORES 127

APPENDIX - FIGURE 12 STATISTICAL CORRELATION MAPS OF GREY MATTER THICKNESS WITH CWIT PRIMARY CONTRAST MEASURE 1 CONTRAST SCALED SCORES 128

APPENDIX - FIGURE 13 STATISTICAL CORRELATION MAPS OF GREY MATTER THICKNESS WITH TOWER TASK MEAN FIRST MOVE TIME SCALED SCORES 131

APPENDIX - FIGURE 14 STATISTICAL CORRELATION MAPS OF GREY MATTER THICKNESS WITH CVLT-II LIST A SHORT DELAY CUED RECALL STD. SCORES 133

APPENDIX - FIGURE 15 STATISTICAL CORRELATION MAPS OF GREY MATTER THICKNESS WITH CVLT-II LIST A LONG DELAY FREE RECALL STD. SCORES 135

APPENDIX - FIGURE 16 STATISTICAL CORRELATION MAPS OF GREY MATTER THICKNESS WITH CVLT-II SEMANTIC CLUSTERING STD. SCORES 137

APPENDIX - FIGURE 17 STATISTICAL CORRELATION MAPS OF GREY MATTER THICKNESS WITH CVLT-II SERIAL CLUSTERING STD. SCORES 138

APPENDIX - FIGURE 18 STATISTICAL CORRELATION MAPS OF GREY MATTER THICKNESS WITH CVLT-II SERIAL CLUSTERING STD. SCORES 141

APPENDIX - FIGURE 19 STATISTICAL CORRELATION MAPS OF GREY MATTER THICKNESS WITH WMS-III DIGIT SPAN FORWARDS RAW SCORES 142
APPENDIX - FIGURE 20 STATISTICAL CORRELATION MAPS OF GREY MATTER THICKNESS WITH WMS-III DIGIT SPAN BACKWARDS RAW SCORES 143
APPENDIX - FIGURE 21 STATISTICAL CORRELATION MAPS OF GREY MATTER THICKNESS WITH WMS-III DIGIT SPAN SCALED SCORES 145
APPENDIX - FIGURE 22 STATISTICAL CORRELATION MAPS OF GREY MATTER THICKNESS WITH HINTING TASK SCORES 146
APPENDIX - FIGURE 23 STATISTICAL CORRELATION MAPS OF GREY MATTER THICKNESS WITH FALSE-BELIEF PICTURE SEQUENCING TASK SCORES 147
APPENDIX - FIGURE 24 STATISTICAL CORRELATION MAPS OF GREY MATTER THICKNESS WITH READING THE MIND IN THE EYES TEST SCORES 149
APPENDIX - FIGURE 25 STATISTICAL CORRELATION MAPS OF GREY MATTER THICKNESS WITH DURATION MMN (MV) 150
APPENDIX - FIGURE 26 STATISTICAL CORRELATION MAPS OF GREY MATTER THICKNESS WITH FREQUENCY MMN (MV) 151
APPENDIX - FIGURE 27 STATISTICAL CORRELATION MAPS OF GREY MATTER THICKNESS WITH DURATION P3A 152
APPENDIX - FIGURE 28 STATISTICAL CORRELATION MAPS OF GREY MATTER THICKNESS WITH FREQUENCY P3A 153

INDEX OF APPENDICES (TABLES)

APPENDIX - TABLE 1 DESCRIPTIVE STATISTICS OF THE ARMS COHORT WITH GROUP STATISTICS BY CCS MEDIAN-SPLIT 100
APPENDIX - TABLE 2 CCS VS. GREY MATTER THICKNESS 103
APPENDIX - TABLE 3 CNSS VS. GREY MATTER THICKNESS 104
APPENDIX - TABLE 4 CPSS VS. GREY MATTER THICKNESS 106
APPENDIX - TABLE 5 GAF VS. GREY MATTER THICKNESS 107
APPENDIX - TABLE 6 SOFAS VS. GREY MATTER THICKNESS 108
APPENDIX - TABLE 7 GF:SOCIAL VS. GREY MATTER THICKNESS 109
APPENDIX - TABLE 8 GF:ROLE VS. GREY MATTER THICKNESS 111
APPENDIX - TABLE 9 TMT CONDITION 2 PRIMARY MEASURE SCALED SCORE VS. GREY MATTER THICKNESS 112
APPENDIX - TABLE 10 TMT CONDITION 4 PRIMARY MEASURE SCALED SCORE VS. GREY MATTER THICKNESS 114

APPENDIX - TABLE 11 TMT PRIMARY CONTRAST 2 CONTRAST SCALED SCORE VS. GREY MATTER THICKNESS 116
APPENDIX - TABLE 12 VFT CONDITION 1 PRIMARY MEASURE SCALED SCORE VS. GREY MATTER THICKNESS 117
APPENDIX - TABLE 13 VFT CONDITION 2 PRIMARY MEASURE SCALED SCORE VS. GREY MATTER THICKNESS 118
APPENDIX - TABLE 14 VFT CONDITION 3 TOTAL CORRECT RESPONSE SCALED SCORE VS. GREY MATTER THICKNESS 119
APPENDIX - TABLE 15 VFT CONDITION 3 TOTAL SWITCHING ACCURACY SCALED SCORE VS. GREY MATTER THICKNESS 120
APPENDIX - TABLE 16 VFT PRIMARY CONTRAST MEASURE 1 CONTRAST SCALED SCORE VS. GREY MATTER THICKNESS 122
APPENDIX - TABLE 17 VFT PRIMARY CONTRAST MEASURE 2 CONTRAST SCALED SCORE VS. GREY MATTER THICKNESS 123
APPENDIX - TABLE 18 CWIT CONDITION 1 PRIMARY MEASURE SCALED SCORE VS. GREY MATTER THICKNESS 124
APPENDIX - TABLE 19 CWIT CONDITION 2 PRIMARY MEASURE SCALED SCORE VS. GREY MATTER THICKNESS 125
APPENDIX - TABLE 20 CWIT CONDITION 3 PRIMARY MEASURE SCALED SCORE VS. GREY MATTER THICKNESS 126
APPENDIX - TABLE 21 CWIT PRIMARY COMBINED MEASURE COMPOSITE SCALED SCORE VS. GREY MATTER THICKNESS 127
APPENDIX - TABLE 22 CWIT PRIMARY CONTRAST MEASURE 1 CONTRAST SCALED SCORE VS. GREY MATTER THICKNESS 129
APPENDIX - TABLE 23 TOWER TEST PRIMARY MEASURE TOTAL ACHIEVEMENT SCALED SCORE VS. GREY MATTER THICKNESS 129
APPENDIX - TABLE 24 TOWER TEST MEAN FIRST MOVE TIME SCALED SCORE VS. GREY MATTER THICKNESS 131
APPENDIX - TABLE 25 CVLT-II LIST A SHORT DELAY FREE RECALL STD. SCORE VS. GREY MATTER THICKNESS 132
APPENDIX - TABLE 26 CVLT-II LIST A SHORT DELAY CUED RECALL STD. SCORE VS. GREY MATTER THICKNESS 134
APPENDIX - TABLE 27 CVLT-II LIST A LONG DELAY FREE RECALL STD. SCORE VS. GREY MATTER THICKNESS 135
APPENDIX - TABLE 28 CVLT-II LIST A LONG DELAY CUED RECALL STD. SCORE VS. GREY MATTER THICKNESS 136
APPENDIX - TABLE 29 CVLT-II SEMANTIC CLUSTERING STD. SCORE VS. GREY MATTER THICKNESS 137

APPENDIX - TABLE 30 CVLT-II SERIAL CLUSTERING STD. SCORE VS. GREY MATTER THICKNESS 138
APPENDIX - TABLE 31 RECOGNITION CORRECT STD. SCORES "TOTAL HITS" VS. GREY MATTER THICKNESS 139
APPENDIX - TABLE 32 WMS-III LETTER-NUMBER SEQUENCING SCALED SCORE VS. GREY MATTER THICKNESS 141
APPENDIX - TABLE 33 WMS-III DIGIT SPAN FORWARDS RAW SCORE VS. GREY MATTER THICKNESS 142
APPENDIX - TABLE 34 WMS-III DIGIT SPAN BACKWARDS RAW SCORE VS. GREY MATTER THICKNESS 144
APPENDIX - TABLE 35 WMS-III DIGIT SPAN SCALED SCORE VS. GREY MATTER THICKNESS 145
APPENDIX - TABLE 36 HINTING TASK VS. GREY MATTER THICKNESS 146
APPENDIX - TABLE 37 FALSE-BELIEF PICTURE SEQUENCING TASK VS. GREY MATTER THICKNESS 147
APPENDIX - TABLE 38 READING THE MIND IN THE EYES VS. GREY MATTER THICKNESS 149
APPENDIX - TABLE 39 DURATION MMN VS. GREY MATTER VS. GREY MATTER THICKNESS 150
APPENDIX - TABLE 40 FREQUENCY MMN VS. GREY MATTER THICKNESS 151
APPENDIX - TABLE 41 DURATION P3A VS. GREY MATTER THICKNESS 152
APPENDIX - TABLE 42 FREQUENCY P3A VS. GREY MATTER THICKNESS 154

GLOSSARY

ARMS	At-Risk Mental State
ARMS-HS	High-Symptom Group by CAARMS Composite Score Median-Split
ARMS-LS	Low-Symptom Group by CAARMS Composite Score Median-Split
BLIPS	Brief Limited Intermittent Psychotic Symptoms
BOLD	Blood Oxygenation Level-Dependent
BPRS	The Brief Psychiatric Rating Scale
CAARMS	Comprehensive Assessment of At-Risk Mental State
CCS	CAARMS Composite Score
CNSS	CAARMS Negative Symptom Score
CPSS	CAARMS Positive Symptom Score
CSF	Cerebrospinal Fluid (CSF)
CVLT-II	California Verbal Learning Test: Second Edition
CWIT	Colour-Word Interference Test
D-KEFS	Delis-Kaplan Executive Function System
DLPFC	Dorsolateral Prefrontal Cortex

DTI	Diffusion Tensor Imaging
DUP	Duration of untreated Psychosis
EEG	Electroencephalography
EF	Executive Functioning
ERP	Event-Related Potential
eTIV	Estimated Total Intracranial Volume
FA	Fractional Anisotropy
FEP	First-Episode Psychosis
FES	First Episode Schizophrenia
fMRI	Functional Magnetic Resonance Imaging
GAF	Global Assessment of Functioning
GF:Role	Global Functioning: Role Scale
GF:Social	Global Functioning: Social Scale
GLM	General Linear Model
GM	Grey Matter
MC-Z	Monte-Carlo Simulation
MinT	Minds in Transition
MMN	Mismatch Negativity
MRI	Magnetic Resonance Imaging
N3	Non-Parametric Non-Uniform Intensity Normalization
NMDA	N-Methyl-D-Aspartate
PANSS	Positive and Negative Syndrome Scale
PET	Positron Emission Tomography
PPI	Prepulse Inhibition
SOFAS	Social and Occupational Functioning Scale
SWM	Spatial Working Memory
TMT	Trail Making Test
ToM	Theory of Mind
TT	Tower Task
UHR	Ultra High-Risk
VBM	Voxel-Based-Morphometry
VFT	Verbal Fluency Test
WASI	Wechsler Abbreviated Scale Of Intelligence
WM	White Matter
WMS-III	Wechsler Memory Scale: Third Edition

INTRODUCTION

1 INTRODUCTION

1.1 Brief Overview of Schizophrenia

Schizophrenia is a severe mental illness that afflicts around 1% of the world's population [McGrath & Susser, 2009]. The disorder typically emerges in late adolescent or early adulthood with a somewhat later onset in females [Levine & Rabinowitz, 2009]. Schizophrenia is characterized by a profound disruption in cognition and emotion. Illness onset usually follows a prodromal phase of behavioural dysfunction and attenuated psychotic symptoms, which are non-specific and lack predictive validity to be considered diagnostic [Schultze-Lutter et al., 2010]. The prodromal phase is generally followed by an acute stage of schizophrenia, marked by the sudden onset of severe psychotic symptoms. Thereafter there is considerable variation in the course of schizophrenia with variable symptom expression in terms of severity and their timing. The majority of patients manifest a fluctuating course, in which symptoms may be continuous but generally rise and fall in intensity; others follow a stable course with little symptom variation; and only few remit to a clinically significant degree [Rosen & Garety, 2005]. The impact of schizophrenia on social and occupational life can be devastating and many of those affected suffer a lifetime of disability. Mortality is also high due to a high suicide risk [Kao & Liu, 2011]. Yet, the basic understanding of schizophrenia as a disease process remains largely speculative.

Historically, schizophrenia symptoms are categorized as positive and negative symptoms. Positive symptoms include delusions, hallucinations, and disorganized speech, which also characterize psychosis. By contrast, negative symptoms reflect a deficiency of normal social and interpersonal behaviours and include affective flattening, alogia and avolition [American Psychiatric Association, DSM-IV-TR, 2000]. Cognitive dysfunction is recognized as one of the most pervasive features of schizophrenia. Despite considerable heterogeneity, the pattern of compromised neuropsychological ability typically involves many specific cognitive domains, including language, memory, attention, and executive functioning [Bowie & Harvey, 2005; Heinrichs &

Zakzanis, 1998]. These deficits can be detected prior to illness onset [Heinrichs & Zakzanis, 1998] and remain largely stable across changes in clinical status (i.e. psychotic symptoms) [Cantor-Graae, Warkentin, & Nilsson, 1995], suggesting that cognitive deficits are a core feature of the disorder which are independent of positive and, perhaps, negative symptoms of schizophrenia.

The aetiology of schizophrenia remains unknown but is likely to involve both biological (e.g. genetic, neurodevelopmental) and environmental factors (e.g. viral infection, fetal/perinatal insult) [Tandon, Keshavan, & Nasrallah, 2008]. The liability to schizophrenia is highly heritable and varies with degree of genetic relatedness. Concordance rates of 10% in first-degree relatives, and 44% in monozygotic twins have been reported [McGue & Gottesman, 1991]. A number of genes have been identified that are associated with the pathophysiology of schizophrenia, but none exhibits full responsibility for the disease. To this day no unitary clinical feature has been identified that is distinct to schizophrenia.

Aberrant neurotransmission, mainly involving glutamate and dopamine neurotransmission are persistently implicated in the neuropathology of the disorder. Particularly pharmacological intervention with dopamine-2 (D2) receptor antagonists have been effective in alleviating psychotic symptoms [Seeman, 2009]. However, this intervention has little effect on negative and cognitive symptoms [Davis et al., 1991]. Furthermore, glutamate hypofunction also appears to play an important role in the pathophysiology of schizophrenia [Coyle, 2004; Coyle, 2006]. Glutamate is the most abundant excitatory neurotransmitter in the human brain. One of the chief receptors for glutamate is the N- methyl-D-aspartate (NMDA) receptor subtype, which has been implicated in schizophrenia [Gaspar et al., 2009]. For instance, blocking of the NMDA receptor by non-competitive antagonists consistently induces positive, negative and cognitive symptoms in healthy volunteers akin to disorder itself [Olney & Farber, 1995]. Conversely, agents that act to enhance NMDA receptor function have shown potential in ameliorating symptoms and cognitive deficits in patients [Lavoie et al., 2008].

Empirical data from post-mortem and in vivo brain imaging studies have provided detailed evidence in support of the view that schizophrenia is a disorder with abnormal brain structure and function. Meta-analytic data derived from studies employing voxel-based-morphometry (VBM) have implicated a network of frontal, temporal, limbic and thalamic regions as those most consistently showing reduced brain volume in schizophrenia [Honea et al., 2005; Glahn et al., 2008; Ellison-Wright et al., 2008]. Similarly, when probing brain function of patients with schizophrenia using functional Magnetic Resonance Imaging (fMRI), abnormal frontal and temporal lobe activity was uncovered in association with specific cognitive tasks [Ortiz-Gil et al., 2011]. While the timing of brain structural and functional abnormalities in relation to illness onset remains unclear, it has been demonstrated that structural abnormalities progress with illness chronicity [Olabi et al., 2011]. The pattern of pathological change is similar in first-episode and chronic schizophrenia but more pronounced in the latter [Chan et al., 2011]. Furthermore, prospective studies have indicated that grey matter (GM) changes observed in schizophrenia are detectable prior to the onset of the first psychotic episode [Sun et al., 2009; Ziermans et al., 2012], suggesting that these may be critical to clinical manifestation of the disorder.

1.2 Identifying the Prodrome of Psychotic Illness

The early identification of individuals at a high risk of developing schizophrenia has become a focus of psychiatric research in recent years since it holds the promise of targeting early intervention towards a population at considerable risk of developing a severe mental illness. When exclusively focusing on the predictive criteria of at risk criteria alone, however, the false-positive rates are considerably high at 60-90% and vary depending on the settings where the clinical assessment has taken place (i.e. general versus specialised early psychosis clinics) [Klosterkotter et al., 2011]. Notwithstanding, most young people meeting At-risk Mental State (ARMS) criteria are help-seeking as a result of experiencing a recent decline in global and/or socio-occupational functioning and often present with a clinically significant

behavioural or psychological syndrome that is associated with disability and/or severe distress.

Attenuated or very brief episodes of limited psychotic symptoms and/or a 1st degree biological relative with the diagnosis of schizophrenia, together with a recent functional decline, are common ARMS criteria [Mason et al., 2004; Yung et al., 2004]. These early clinical signs are usually accompanied by mild to moderate cognitive impairment [Pflueger et al., 2007] while brain imaging research has provided evidence of emerging brain pathology [Jung et al., 2010].

Chapter 1.3 and 1.4 review the relationship of morphological and functional abnormalities in the early phase of illness, spanning from the "At-risk Mental State" to the clinical manifestation of the first psychotic episode in order to call attention to early disease function/structure signatures of the prodrome. Chapter 1.5 focuses on electrophysiological findings in early psychosis and how they relate to structural and functional deficits. This line of research may further our understanding of the underlying pathophysiology of the emerging illness and potentially holds clues regarding the neurobiology of the disorder.

1.3 Early signs of brain pathology and their association with emerging clinical symptoms

Brain imaging research has provided clear evidence of widespread grey and white matter abnormalities in first episode schizophrenia (FES) [Rasser et al., 2010; Cohen et al., 2011]. Initial support derives from Crespo-Facorro et al. (2011) who reported a reduction of whole brain cortical thickness in 142 FES patients when compared to 83 healthy control subjects. Cortical thinning was particularly pronounced in frontal, temporal and parietal cortices, changes that are also well established for more chronic patients diagnosed with schizophrenia [Shenton et al., 2001].

These early morphological deficits are also clinically relevant due to their correlation with clinical signs and symptoms of the disorder. Lui et al. (2009) reported a significant decrease of GM volume in the superior/middle temporal and cingulate gyrus in the right hemisphere in a sample of 68 antipsychotic-naïve FES patients versus 68 matched control subjects. The degree of GM

volume reduction in these brain regions correlated with clinical outcome as rated on the Global Assessment of Functioning Scale (GAF) as well as with the severity of a range of positive symptoms, including thought disturbance and paranoia, and impulsive aggression (as rated on the Positive and Negative Syndrome Scale; PANSS). Positive symptoms also correlate with reduced Fractional Anisotropy (FA) – a measure of white matter integrity – in frontotemporal tracts in treatment-naïve FES [Cheung et al., 2011] whereas negative symptoms appear to correlate with cerebellar and inferior frontal GM volume reduction [Berge et al., 2011].

Importantly, most of these neuroanatomical abnormalities appear to predate the clinical manifestation of FES and are present in individuals at "ultra high-risk" (UHR) of developing psychosis [Pantelis et al., 2007; Mechelli et al., 2011; Borgwardt, McGuire, & Fusar-Poli, 2011]. Pantelis et al. (2003) reported less GM in the right medial temporal, lateral temporal, inferior frontal, and cingulate cortex when comparing "ultra high-risk" individuals who later did develop psychosis with those who did not. In a longitudinal comparison, follow-up MRIs after at least 12 months also revealed the progressive nature of the neuroanatomical abnormalities in the course of emerging illness with further GM reductions in left parahippocampal, fusiform, orbitofrontal and cerebellar cortices, and cingulate gyri in those who went on to become psychotic. Similarly, Sun et al. (2009) reported longitudinal brain surface contractions of UHR cases who developed psychosis during a one-year follow-up when compared to those who did not. The authors employed Cortical Pattern Matching [Sowell et al., 2001] to assess brain surface contraction as an index of local brain tissue loss over time. In contrast to the average rate of < 0.2 mm/year surface contraction in non-converters, the converters showed greater brain surface contraction in bilateral dorsolateral prefrontal regions, with a maximum magnitude of 0.4 mm/year. A recent meta-analysis [Smieskova et al., 2010] based on 25 brain imaging studies confirmed small to medium volume reductions in prefrontal, cingulate, insular and cerebellar GM in high-risk individuals who went on to develop psychosis compared to those who did not. These findings, however, remain somewhat preliminary given methodological limitations in the reviewed literature which include differences in scanning parameters and analytical

processes across the studies, often small sample sizes which lack appropriate matching for gender, handedness, and co-morbidities (e.g. substance abuse) as well as potential effects due to antipsychotic pharmacotherapy which appears to be associated with cerebral GM reduction in established schizophrenia [Navari & Dazzan, 2009; Ho et al., 2011] but also early psychosis [Smieskova et al., 2009]. However, Fusar-Poli et al. (2011b) confirmed cerebral GM reductions meta-analytically across 14 voxel-based morphometric studies conducted on antipsychotic-naïve patients. The authors reported reduced GM in temporal, anterior cingulate, cerebellar and insular regions around the onset of psychosis.

There is also corresponding white matter (WM) pathology, as indexed by FA, lateral to the right putamen and in the left superior temporal lobe in ARMS individuals who develop psychosis over a follow-up period of 2 years compared to those who did not. Moreover, reduced FA in left middle temporal gyrus has been reported to correlate with the level of positive symptom expression [Bloemen et al., 2010]. Peters and colleagues (2009) reported reduced FA in superior and middle portions of frontal white matter cross-sectionally in clinical at-risk individuals when compared to healthy control subjects. When analysing the same cohorts, however, no group differences were found in uncinate and arcuate fasciculi, dorsal and anterior cingulate and subdivisions of the corpus callosum [Peters et al., 2008]. These findings are to be interpreted with caution given the methodological differences between the two reports. This discrepancy in findings may arise from the differences in Diffusion Tensor Imaging (DTI) methodology and their respective limitations. VBA [Peters et al., 2009] allows for automated whole brain analysis without a priori hypotheses but is prone to false positive findings whereas fibre tracking [Peters et al., 2008] seems not to reliably capture some of the early WM pathology in at-risk and first-episode patients [Peters et al., 2010].

Finally, emerging cognitive deficits also appear to be associated with prodromal neuroanatomical deficits. For instance, GM density measures [Meijer et al., 2011] suggest that impaired semantic fluency performance – which is considered a measure of executive function – is linked to structural abnormalities in task-related brain areas, such as the right insula, right

superior/middle temporal cortex and left anterior cingulate in ARMS individuals who go on to develop psychosis versus to those who did not. Also deficits in spatial working memory (SWM) performance have been reported in high-risk populations [Smith, Park, & Cornblatt, 2006]. SWM deficits have also been shown to be associated with grey and white matter abnormalities in FES patients [Cocchi et al., 2009]. Taken together, these reports lead to the speculation that abnormalities in neural networks involved with SWM may be present prior to the clinical manifestation of psychosis. This is of clinical relevance since SWM performance appears to predict clinical outcome in ARMS including severity of negative symptom expression in those who go on and develop psychosis [Wood et al., 2003].

Taken together, these findings support the notion of a progressive grey and white matter pathology in prodromal schizophrenia that particularly affects the frontal, temporal, parietal, and cingulate cortex and possibly the cerebellum. Furthermore, the degree of the morphological deficits is also predictive of clinical outcome (i.e. transition from "at risk mental state" to psychosis) along with the severity of clinical symptoms. There is also some evidence that the emerging neuroanatomical deficits in the prodromal phase of illness are closely linked to impaired brain function in a region-specific pattern, which will be further explored below.

1.4 Functional and anatomical correlates of impaired working memory and executive dysfunction in the early stages of Schizophrenia

Impaired cognition is a robust feature of ARMS [Kim et al., 2011; Eastvold, Heaton, & Cadenhead, 2007; Lencz et al., 2006] and FES [Flashman & Green, 2004]. Most commonly reported are working memory deficits in schizophrenia when employing the *n*-back task whilst recording brain activity in response to task-related changes of blood oxygen levels with fMRI.

A robust finding is aberrant blood oxygenation level-dependent (BOLD) activity in the dorsolateral prefrontal cortex (DLPFC) along with impaired working memory performance in schizophrenia [Manoach, 2003]. Broome and

colleagues (2009), for instance, reported reduced cortical activation in the inferior frontal, dorsolateral prefrontal and parietal cortex of individuals with first-episode schizophreniform psychosis, and intermediate degrees of activation in ARMS individuals when compared to healthy control subjects. When further differentiating ARMS individuals according to their duration of at-risk status, Smieskova and colleagues (2012) found reduced activation in the right inferior frontal gyrus and insula when comparing individuals with higher transition probability (short-term ARMS) to those with vulnerability but very low transition probability to psychosis (long-term ARMS). As a putative sign of illness progression, first-episode psychosis (FEP) patients exhibited decreased activation bilaterally in inferior frontal gyrus and insula, and in the left prefrontal cortex relative to long-term ARMS individuals whereas FEP and short-term ARMS individuals presented with reduced activation in parietal and middle frontal brain regions when compared to healthy control subjects.

Crossley et al. (2009) investigated regional activation and functional connectivity in FES, ARMS, and healthy subjects whilst performing the *n*-back task. Healthy subjects presented with deactivation of the superior temporal cortex in contrast to FES patients who showed a BOLD increase when performing the task while ARMS group exhibited a somewhat intermediate activation pattern relative to the other two groups. The authors also reported negative coupling between superior temporal gyrus and middle frontal gyrus in their healthy participants that was reversed in FES and intermediate in ARMS.

Taken together, the reports are consistent in their findings of reduced prefrontal (i.e. DLPFC), parietal, frontal and temporal brain activation when performing the *n*-back task. The cross-sectional findings also suggest a change in the fronto-temporal processing of the *n*-back task around the clinical manifestation of schizophrenia. However, the studies are limited when attempting to map out the working memory deficits and their cortical correlates across a continuum around the early stages of illness. In this respect, longitudinal studies – which ideally also incorporate structural brain measures – are better placed. When following up a ARMS cohort over one year with repeated fMRI, Fusar-Poli et al. (2011c), for instance, found reduced task

dependent activation in the left middle frontal gyrus, supramarginal gyrus and inferior parietal lobule in ARMS individuals at baseline when compared to healthy control subjects. Reduced left middle frontal gyrus volume also correlated with reduced activation in this brain region. Clinical and functional improvement after one year was associated with increased activation in anterior cingulate and right parahippocampal gyrus. This study, however, did not report functional/structural correlates, which are indicative of a progression towards schizophrenia.

The progressive nature of working memory deficits in the early phase of illness is also reflected by other working memory tasks. Fusar-Poli et al. (2010) assessed longitudinal changes in ARMS individuals and healthy control subjects with the Paired Associate Learning (PAL) task. At baseline, ARMS subjects showed reduced activation in the left precuneus/occipital gyrus, left superior parietal lobule and in the right middle temporal gyrus when compared to healthy control subjects. After a year, the general clinical status of the ARMS cohort had improved. This was accompanied by greater activation in the left lingual and in the left superior parietal lobule relative to baseline, which however did not correlate with changes in the clinical measures.

The previous studies are limited in adapting task difficulty to performance levels of study participants. This may result in ceiling or floor effects in the BOLD dynamics, thereby trivialising the relevance of any group differences. A preferred approach is therefore incorporating graded task difficulty as an independent variable when analysing BOLD differences between groups. Rasser et al. (2005) adopted a visual spatial working memory/planning task [Schall et al., 2003a] and recorded fMRI in remitted FES patients and closely matched healthy control subjects whilst performing the Tower of London task in the scanner. FES showed less task difficulty-dependent BOLD activity in DLPFC and parietal lobule as well as less deactivation in superior temporal cortex compared to the control group. Moreover, these differences in the BOLD activation pattern were also correlated with GM reduction in the respective areas of the cerebral cortex in FES, thus establishing a direct link between impaired executive function and apparent brain pathology in FES.

Other visual spatial working memory tasks have also confirmed a similar pattern of deficits in the emerging illness. Broome et al. (2010), for instance, employed an object-location paired-associate memory task which progressively activates the medial frontal and medial posterior parietal cortex with increasing task difficulty. The authors reported a reduced BOLD response in ARMS individuals in medial frontal cortex and right precuneus, which was more profound in FES when compared to healthy subjects, respectively.

The neural network subserving working memory processes overlaps with other executive functions. Hence, the regional pattern of structure/function deficits is usually very similar. For instance, ARMS subjects consistently show abnormal activation in prefrontal, frontal, temporal and cingulate cortex when performing verbal fluency tasks and thereby often show intermediate activation patterns somewhere between healthy control subjects and FES patients [Broome et al., 2009; Fusar-Poli et al., 2011b; Lord et al., 2011].

Performance on response inhibition tasks – e.g. measured as Go/No-Go procedure – is also impaired in ARMS subjects along with reduced BOLD activity in right frontal and bilateral temporal cortex when compared to healthy subjects [Jacobson et al., 2010]. The same study also revealed an aberrant activation pattern in anterior cingulate, insula and middle frontal gyrus for error-related processing in the "at-risk" group. By contrast, no differences in fronto-temporal BOLD activation were reported between ARMS and healthy subjects when investigating response inhibition with the Hayling Sentence Completion Task [Allen et al., 2010]. The authors reported increased BOLD in caudate and anterior cingulate in their "at-risk" cohort, which may reflect increased processing load due to cognitive impairment.

Collectively, the reviewed functional brain imaging studies clearly demonstrate that those brain areas emerging with GM deficits in the early phase of illness are also functionally compromised. While longitudinal studies are unfortunately sparse, the overall picture is consistent with an emerging neuroanatomical deficit that apparently drives the early cognitive deficits in a brain region-specific pattern as they are identified in the early phase of illness.

1.5 Electrophysiological correlates of early psychosis and their association with neuroanatomical abnormalities

One of the most robust findings in schizophrenia is a reduced event-related potential (ERP) termed mismatch negativity (MMN), which is recorded during a passive auditory listening oddball task [Umbricht & Krljes, 2005; Todd et al., 2012; Shelley et al., 1991; Näätänen & Kahkonen, 2009]. Psychopharmacological research has linked reduced MMN to impaired N-Methyl-D-Aspartate (NMDA) receptor function [Lavoie et al., 2008; Umbricht et al., 2002] which, in turn, has been implicated in the neuropathology of schizophrenia [Moghaddam & Javitt, 2012; Marek et al., 2010].

If at all, MMN amplitude reduction shows only very weak associations with clinical symptoms of the disorder. It rather appears to be associated with clinical outcome, such as global function levels [Light & Braff, 2005], but also with the course of illness (i.e. progressive MMN reduction with chronicity [Todd et al., 2008]) and the prediction of treatment response to clozapine in chronic schizophrenia [Schall et al., 1999]. Some research further suggests an association of reduced MMN amplitudes with some of the cognitive deficits found in FES, such as poor performance on the Trail-Making Test, the Mental Control Subtest of the Wechsler Memory Scale III, and the Rey Auditory Verbal Learning Test [Kaur et al., 2011].

Although largely generated in the primary auditory cortex with possibly a second generator in prefrontal cortex [Schall et al., 2003b; Rinne et al., 2000], reduced MMN amplitudes – particularly in response to pitch oddballs – correlate with widespread GM deficits in frontal, temporal and parietal cortices in schizophrenia [Rasser et al., 2011]. MMN amplitudes recorded in ARMS subjects usually tend to fall in the intermediate range between FES and healthy control subjects [Jahshan et al., 2012], with some recent studies suggesting that "at-risk" individuals who later develop FES have smaller MMN amplitudes than those who will not [Atkinson, Michie, & Schall, 2012; Shaikh et al., 2012; Bodatsch et al., 2011].

A few studies further suggest impaired sensory gating of the P50 auditory ERP in "at-risk" populations. For instance, Brockhaus-Dumke et al. (2008)

reported impaired P50 suppression in prodromal ARMS subjects who developed psychosis within a clinical follow-up period of 2 years. By contrast, no such deficit was observed in ARMS subjects who did not develop psychosis within the follow-up period. The authors also reported less N100 suppression in their prodromal sample similar to FES. Again, no such deficit was found in ARMS individuals who did not develop psychosis within the follow-up period. A previous study [Myles-Worsley et al., 2004] also found impaired P50 suppression in prodromal individuals but not in "at-risk" individuals who were solely defined by genetic risk such as having a first-degree biological relative diagnosed with schizophrenia.

Disrupted sensorimotor gating has also been closely linked to schizophrenia and abnormal dopamine neuro-modulation in concert with other neurotransmitters [Swerdlow et al., 2006; Minassian, Feifel, & Perry, 2007; Swerdlow & Geyer, 1998]. Usually the electromyographic eye blink response to startling noises is recorded with and without a non-startling acoustic prepulse (prepulse inhibition or PPI). "Sensorimotor gating" refers to the inhibition of the eye blink response when the startling noise is preceded by a prepulse at short lead intervals (i.e. 60-120 ms). When compared to healthy subjects, ARMS individuals show impaired sensorimotor gating, which tends to improve along with clinical improvement [Ziermans et al., 2011].

Reduced P300 amplitudes are also robustly linked to schizophrenia [Bramon et al., 2004]. Fusar-Poli et al. (2011d) reported reduced P300 amplitude and reduced brain volumes in prefrontal and parietal areas in 39 ARMS individuals at their first clinical presentation versus 41 healthy control subjects. Parietal brain volumes correlated with P300 amplitudes at baseline. However, neither parietal brain volumes nor P300 amplitudes changed longitudinally. On the other hand, parietal (as well as parahippocampal) brain volumes predicted transition to psychosis while progressive GM changes were only reported for prefrontal and some subcortical areas.

Taken together, electrophysiological findings in the early phase of illness suggest impaired auditory information processing occurring in the prodrome. These findings may assist to improve the early identification of "at-risk"

individuals, particularly when psychophysiological measures are combined with clinical ARMS criteria.

1.6 Objective and Hypotheses

From a clinical perspective, identification of early stages of a severe mental illness like schizophrenia is currently considered a better option to implement targeted intervention to alleviate or even prevent the transition to psychosis [McGorry, Yung, & Phillips, 2003]. However, the early detection of the schizophrenia prodrome in young people considered "at-risk" of developing this severe mental illness still lacks sufficient predictive specificity to unequivocally justify, for instance, the introduction of antipsychotic pharmacotherapy in the At-risk Mental State (ARMS).

The main objective of this PhD project was to evaluate clinical symptoms and measures of brain function (as assessed by performance on standardized neuropsychological tests) in relation to structural *in vivo* cortical brain abnormalities in a population identified as "ultra high-risk" (UHR) of developing schizophrenia on the basis of clinical criteria [McGorry, Yung, & Phillips, 2003]. UHR individuals present with non-specific, attenuated or brief limited intermittent psychotic symptoms and are also often affected by functional impairment and social disabilities prior to making the transition into schizophrenia [Klosterkotter et al., 2001]. Moreover, UHR individuals frequently suffer from a spectrum of cognitive impairments with deficits particularly in verbal fluency and verbal memory predictive of a subsequent transition to psychosis [Fusar-Poli et al., 2012a].

Structural magnetic resonance imaging data have added further evidence to the notion of emerging and progressive grey and white matter pathology in the early stages of illness that appears to predominantly affect frontal, temporal, parietal, and cingulate cortical areas (reviewed in chapter 1.3). Furthermore, several studies have confirmed early brain pathology in UHR populations [Sun et al., 2009; Mechelli et al., 2011; Ziermans et al., 2012]. These data have also indicated an association between the degree of morphological deficit and the

onset of psychosis, thus suggesting a neuropathological process leading to the transition to psychosis.

To the best of the author's knowledge, no study so far has comprehensively investigated in ARMS individuals the association of brain structure with performance levels in various cognitive domains which had been linked to schizophrenia. It is hypothesised that:

(i) the defining clinical criteria of ARMS (i.e. recent functional decline and emerging psychotic symptoms) are associated with emerging brain pathology (i.e. GM/WM reductions) in an UHR cohort.

(ii) that regional GM and WM deficits determine functional outcome, cognitive performance, social cognition and MMN and P3 amplitudes, respectively.

In order to test these hypotheses group comparisons of UHR individuals (groups matched for age, gender, handedness, IQ, pharmacotherapy, and substance use) with low versus high symptom expression (as assessed on the CAARMS) were performed. Total brain volume, GM and WM volume, cortical GM thickness and surface area were statistically compared between these two groups. Associations of putative regional GM and WM deficits with measures of functional outcome, cognitive performance, social cognition, and MMN and P3 amplitudes, respectively, were tested by correlation analyses.

METHODOLOGY

2 METHODOLOGY

2.1 Participants' Recruitment and Cohort Characteristics

Ethical clearance for the study was obtained through Hunter New England (HNE) Human Research Ethics Committee and the University of Newcastle Human Ethics Research Committee. Forty-two young individuals (18 males and 24 females) meeting ARMS criteria and participating in the Minds in Transition[1] (MinT) study were included. Clinical status was determined according to the Comprehensive Assessment of At-risk Mental States [Yung et al., 2005]; that is (i) recent deterioration of functioning plus a family history of a psychotic disorder in a first-degree relative or diagnosis of schizotypal personality traits or (ii) individual suffers from attenuated symptoms or (iii) brief limited intermittent psychotic symptoms (BLIPS). Participants were screened for head injury, organic brain impairment, estimated premorbid IQ of < 70, poor hearing (defined as thresholds above 20 dB SPL), and a history of nasal trauma. Participants were excluded for (i) current antipsychotic drug treatment, unless treatment of < 2 weeks and discontinued following independent psychiatric review, and (ii) current or past history of substance dependence (excluding nicotine). Treatment with antidepressants and/or occasional recreational substance use was not an exclusion criterion. Participants underwent electrophysiological recordings, MRI scanning, and further clinical, neurocognitive and socio-cognitive assessments. All participants were outpatients of the Bondi Junction Community Mental Health Centre (Sydney, Australia).

[1] MinT: www.mint.org.au

2.2 Instruments

The battery of clinical, neurocognitive, and socio-cognitive instruments (Table 2.2.1-1) was administered by trained psychologists using standard procedures.

Table 2.2.1-1 Instruments

Psychopathology and Symptom Ratings
Comprehensive Assessment of At Risk Mental States (CAARMS)
Brief Psychiatric Rating Scale (BPRS)
Alcohol Use Disorders Identification Test (AUDIT)
Cannabis Use Disorders Identification Test (CUDIT)
Opiate Treatment Index (OTI, all drug types)
Structured Clinical Interview for DSM-IV Axis I Disorders (SCID-CV; for >18 years of age)
K-SADS (K-SADS; for <18 years of age)
Schizotypal Personality Questionnaire (SPQ)
Beck Depression Inventory II (BDI-II)
Beck Anxiety Inventory (BAI)
Eysenck Personality Questionnaire – Revised (EPQ-R)
- Neuroticism Sub-scale
Prescription medication
Functioning Measures
Global Assessment of Functioning Scale (GAF)
Social and Occupational Functioning Scale (SOFAS)
Global Functioning: Social Scale (GF:Social)
Global Functioning: Role Scale (GF:Role)
Neurocognitive Measures
Wechsler Abbreviated Scale of Intelligence (WASI)
- Vocabulary
- Matrix Reasoning
California Verbal Learning Test for Children (CVLT-C; for <16 years of age)
California Verbal Learning Test: Second Edition (CVLT-II; for >16 years of age)
Wechsler Memory Scale: Third Edition (WMS-III)
- Digit Span
- Letter Number Sequencing
Delis-Kaplan Executive Function Scale (D-KEFS)
- Trail Making Test
- Verbal Fluency Test
- Colour-Word Test
- Tower Task
University of Pennsylvania Smell Identification Test (UPSIT)
Social Cognitive Measures
False-belief Picture Sequencing Task
Reading the Mind in the Eyes Test
Hinting Task

2.2.1 Psychopathology and Symptom Ratings

Comprehensive Assessment of At Risk Mental States (CAARMS) [Yung et al., 2005]: This semi-structured interview schedule was developed at the Personal Assessment and Crisis Evaluation (PACE) Clinic in Melbourne. It is designed to measure intensity, frequency, duration and recency of sub-threshold psychotic symptoms. In addition, it measures other symptoms indicative for risk of psychosis, such as negative, dissociative, and basic symptoms. The CAARMS includes the following subscales, each rated from 0 to 6 in intensity and frequency: disorders of thought content, perceptual abnormalities, conceptual disorganization, motor changes, concentration and attention, emotion and affect, subjectively impaired energy and impaired tolerance to normal stress. The CAARMS criteria define three groups as "ultra high-risk" (UHR) for psychosis: (1) Attenuated Psychosis Group, (2) Brief Limited Intermittent Psychotic Syndrome (BLIPS) Group, and (3) Vulnerability Group. A threshold for frank psychosis is also defined. This definition is not entirely concordant with the DSM-IV [American Psychiatric Association, DSM-IV-TR, 2000], but it is based on the presence of clear-cut threshold level psychotic symptoms (delusions, hallucinations and formal thought disorder) occurring several times per week for at least 1 week. The CAARMS criteria are presented in detail in Table 2.2.1-1.

Table 2.2.1-1 CAARMS-defined Ultra High Risk and Psychotic Disorder Threshold Criteria

UHR Status
Attenuated Psychosis Group (i) Sub-threshold intensity Severity scale score of 3–5 on disorders of thought content subscale, 3–4 on perceptual abnormalities subscale and/or 4–5 on disorganized speech subscale of the CAARMS. Frequency scale score of 3–6 on disorders of thought content, perceptual abnormalities and/or disorganized speech subscale of the CAARMS for at least 1 week. OR Frequency scale score of 2 on disorders of thought content, perceptual abnormalities and disorganized speech subscale of the CAARMS on more than two occasions. (ii) Sub-threshold frequency Severity scale score of 6 on disorders of thought content subscale, 5–6 on perceptual abnormalities subscale and/or 6 on disorganized speech subscale of the CAARMS. Frequency scale score of 3 on disorders of thought content, perceptual abnormalities and/or disorganized speech subscale of the CAARMS (for both categories). Symptoms present in past year and for not longer than 5 years.
BLIPS Group Severity scale score of 6 on disorders of thought content subscale, 5 or 6 on perceptual abnormalities subscale and/or 6 on disorganized speech subscale of the CAARMS. Frequency scale score of 4–6 on disorders of thought content, perceptual abnormalities and/or disorganized speech subscale. Each episode of symptoms is present for less than 1 week and symptoms spontaneously remit on every occasion. Symptoms occurred during last year and for not longer than 5 years.
Vulnerability Group Family history of psychosis in first-degree relative OR schizotypal personality disorder in identified patient. 30% drop in GAF score from premorbid level, sustained for 1 month. Change in functioning occurred within last year and maintained at least 1 month.
Psychotic disorder threshold Severity scale score of 6 on disorders of thought content subscale, 5 or 6 on perceptual abnormalities subscale and/or 6 on disorganized speech subscale of the CAARMS. Frequency scale score of greater than or equal to 4 on disorders of thought content, perceptual abnormalities and/or disorganized speech subscale. Psychotic symptoms present for longer than 1 week.

BLIPS = Brief Limited Intermittent Psychotic Symptoms | CAARMS =Comprehensive Assessment of At-risk Mental States | GAF = Global Assessment of Functioning | UHR = Ultra High Risk

- CAARMS total score: Summative measure of intensity scores for all CAARMS items.
- *CAARMS composite score* (CCS): This summative measure was derived from a selection of CAARMS subscale intensity scores: unusual thought content, non-bizarre ideas, perceptual abnormalities, disorganized speech, alogia, avolition/apathy, anhedonia, social isolation, impaired role function, disorganizing/odd/stigmatizing behaviour, aggression/dangerous behaviour, mania, depression, mood swings/liability, and anxiety.

- *CAARMS negative symptom score* (CNSS): A summative measure derived from a selection of CAARMS subscale intensity scores: alogia, avolition/apathy, and anhedonia,
- *CAARMS positive symptom score* (CPSS): CAARMS subscale intensity score for Perceptual Abnormalities

The Brief Psychiatric Rating Scale (BPRS) Expanded Version [McGorry, Goodwin, & Stuart, 1988]: A semi-structured interview schedule designed to assess the severity of psychotic symptomatology (positive symptoms; general psychopathology; affective symptoms) using a 24-item symptom scale. Symptoms are rated on a seven-point scale from 1 (not present) to 7 (extremely severe).

Alcohol Use Disorders Identification Test (AUDIT) [Saunders et al., 1993]: A 10-item screening questionnaire designed to identify individuals with hazardous and harmful patterns of alcohol consumption.

Cannabis Use Disorders Identification Test (CUDIT) [Chow, Pietranico, & Mukerji, 1975]: A 10-item screening questionnaire designed to screen for current cannabis use disorders (abuse or dependence) according to DSM-IV.

Opiate Treatment Index (OTI) [Darke et al., 1991]: A structured interview designed to evaluate treatment outcome. It covers 6 treatment domains; drug use, HIV risk-taking behaviour, social functioning, forensic issues, health status and psychological functioning. The drug use section allows the calculation of a quantity/frequency estimate.

Structured Clinical Interview for DSM-IV Axis I Disorders (SCID-CV; for >18 years of age) [First et al., 1996]: A semi-structured interview administered to determine DSM-IV diagnosis.

Kiddie-Schedule for Affective Disorders and Schizophrenia - Present and Lifetime Version (K-SADS-PL; for <18 years of age) [Kaufman et al., 1997]: A semi-structured diagnostic interview designed to assess current and lifetime history of psychopathology in children and adolescents according to DSM-IV (and DSM-III-R) criteria. The K-SADS-PL assesses a variety of diagnoses including, schizophrenia, schizoaffective disorder, major depression, bipolar disorder,

ADHD, and eating disorders. The K-SADS-PL is administered by interviewing the parent(s) and the child involved, and estimating summary scores synthesized from parent and child data.

Schizotypal Personality Questionnaire (SPQ): [Raine, 1991] A self-report scale comprised of 74 true-false ("yes" or "no") items organized into nine distinct domains, which are modelled upon the diagnostic criteria for schizotypal personality disorder (SPD) included in the Diagnostic and Statistical Manual of Mental Disorders (DSM-IV) [American Psychiatric Association, DSM-IV-TR, 2000]. All items answered "yes" are scored 1 point. Performance was measured using a total score (sum of points for all 74 items).

Beck Depression Inventory II (BDI-II) [Beck et al., 1996]: A 21-item multiple-choice self-report inventory developed to measure the intensity, severity, and depth of depression in patients with psychiatric diagnoses. The BDI-II is scored by summing the ratings for the 21 items. Each item is rated on a 4-point scale, ranging from 0 to 3 in intensity. The maximum total score is 63.

Beck Anxiety Inventory (BAI) [Beck et al., 1988]: A 21-item multiple-choice self-report inventory developed to measure symptoms specific to anxiety, and unrelated to depression. The BAI is scored by summing the ratings for the 21 items. Each item is rated on a 4-point scale, ranging from 0 to 3 in intensity. The maximum total score is 63.

Eysenck Personality Questionnaire – Revised (EPQ-R) [Eysenck, Eysenck, & Barrett, 1985]: A 102-item self-assessment questionnaire designed to assess three major dimensions of personality; extraversion vs. introversion, neuroticism, and psychoticism. In addition, a "lie scale" is part of the questionnaire that is designed to assess the degree of socially desirable responding. Only the neuroticism subscale was administered to participants of this study.

2.2.2 Functioning Measures

Global Assessment of Functioning Scale (GAF) [American Psychiatric Association, DSM-IV-TR (GAF), 2000]: A numeric scale used to rate a patient's overall social, psychological, and occupational functioning in the past month. The rating is performed on a 100-point scale, ranging from "severe impairment" (1-10), to "superior functioning" in a wide range of activities (91-100).

Social and Occupational Functioning Assessment Scale (SOFAS) [American Psychiatric Association, DSM-IV-TR (SOFAS), 2000]: A global measure assessing an individual's overall level of social and occupational functioning in the past month. The SOFAS ranges from 0 to 100 with higher scores indicating superior functioning in a wide range of activities and lower scores indicating lower functioning. The SOFAS is similar to the GAF score (see above) but differs in that it is rated independent of an individual's level of psychopathology.

Global Functioning: Social Scale (GF:Social) [Auther, Smith, & Cornblatt, 2006]: The GF:Social provides a rating of an individual's functioning in the social domain. Performance is rated on a 10-point scale and scored independently of symptom severity. A rating score of 10 indicates "superior functioning" and 1 corresponds with extreme dysfunction. Ratings are based on the past month. The GF:Social is designed to cover the age range typical of the prodromal phase, and incorporates detailed anchor points appropriate to capturing subtle prodromal social function deficits. Quantity and quality of peer relationships, level of peer conflict, age-appropriate intimate relationships, and involvement with family members are assessed. Emphasis is placed on age-appropriate social contacts and interactions outside of the family, with a particular focus on social withdrawal and isolation [Cornblatt et al., 2007].

Global Functioning: Role Scale (GF:Role) [Niendam et al., 2006]: The GF:Role allows a rating of an individual's functioning in the role domain. Performance is rated on a 10-point scale as the GF:Social (see above). Anchor points of the GF:Role refer to performance in school, occupation or as a homemaker (depending on age). Ratings are based on demands of the role, level of independence or support provided to the individual, and the individual's overall performance in the role given the level of that support [Cornblatt et al., 2007].

2.2.3 Neurocognitive Measures

Wechsler Abbreviated Scale of Intelligence (WASI) [Wechsler, 1999]: A test that produces an estimate of general intellectual ability, normed for individuals aged 6 to 89 years. The WASI was administered in the two-subtest form; Vocabulary and Matrix Reasoning. Higher scores on the WASI indicate greater intellectual ability.

- The Vocabulary subtest is a 42-item test that requires the participant to define 4 images and 37 words, which are presented both orally and visually.
- The Matrix Reasoning subtest requires the participant to complete a series of 35 incomplete grid patterns by selecting the missing portion of the pattern from five possible response choices.

California Verbal Learning Test: Second Edition (CVLT-II; for >16 years of age) [Delis et al., 2000]: A multi-trial recall and recognition word list learning test specific to episodic verbal learning and memory. In the CLVT-II participants are asked to memorize a list of 16 common words, each of which belongs to one of four categories. Participants are then asked to recall as many of these words as possible. List presentation followed by recall occurs on five occasions. The recall of the same list is repeated after learning a distracter word list. The CLVT produces a multitude of measures reflecting encoding, storage and short term and delayed retrieval of information. Raw scores for Trials 1-5 were converted to Standard scores using a normalised T-metric [M= 50; SD= 10]. The remainder of the scores were normed on a linear z-score metric [M= 0; SD= 1]. Norms were established for 7 age groups ranging from 16 through to 89 years of age.

California Verbal Learning Test for Children (CVLT-C; for <16 years of age) [Delis et al., 1994]: Children version of the CVLT-II.

Wechsler Memory Scale: Third Edition (WMS-III) [Wechsler, 1997]: A neuropsychological test designed to assess auditory and visual memory abilities. Two subtests of the WMS-III were administered; the Letter-Number Sequencing Task and the Digit Span Test, both of which are measures of short-term/working memory [Lichtenberger, Kaufman, & Lai, 2002; Mitrushina & Boone, 2005]

- Letter-Number Sequencing Task: Participants hear a sequence of alternating digits and letters and are asked to repeat the digits and letters from the sequence, starting with the digits in numerical order, followed by the letters in alphabetical order.
- Digit Span Test: The test is divided into two phases referred to as Digit Span Forward and Digit Span Backward. In both phases the participants hear a sequence of digits at a rate of one per second. After the presentation participants are instructed to repeat the sequence. In the Digit Span Forward digits are presented in the same order whereas in the Digit Span Backward in the reversed order. The sequence length is increased stepwise until the participant can no longer correctly repeat the sequence. Digit Span Forward is regarded as a measure of attention and/or short-term memory, whereas the Digit Span Backward is regarded a measure of working memory.

Delis-Kaplan Executive Function System (D-KEFS) [Delis, Kaplan, & Kramer, 2001]: A set of nine stand-alone tests assessing key components of executive function in both children and adults. The term "executive function" refers to a set of cognitive abilities, which are a prerequisite for adaptive behaviour, which occurs in a planned, organized, and contextually appropriate manner using working memory and attention. It includes the ability of problem solving and thinking ahead while monitoring and perhaps altering a course of action. Executive function is primarily mediated by the frontal lobes [Johnson-Selfridge & Zalewski, 2001]. Four subtests of the D-KEFS were administered: Trail Making, Verbal Fluency, Colour Word Interference, and Tower Task.

- Trail Making Test (TMT): The test provides a measure of attention and psychomotor speed. The task requires the participant to connect dots of 32 consecutive targets on a sheet of paper as fast as possible based on 5 different conditions. Participants were only required to complete Condition 2 & 4. In Condition 2 (Number Sequencing) all targets are numbers (i.e. 1, 2, 3, etc.) and the task is to connect consecutive numbers thereby measuring visuomotor speed. Condition 4 is a Number-Letter Switching task asking the participant to connect numbers and letters in alternating order (e.g., 1, A, 2, B, etc.) thereby assessing parallel attention plus visuomotor speed. The

"executive component" is measured by the time needed to complete Condition 4 minus Condition 2 (task switching ability). The TMT was scored using (i) the Primary Measure for each condition, a scaled score [*M*= 10; *SD*= 3], derived from the raw score for completion time in seconds, respectively, and (ii) the Primary Contrast Measure, derived by subtracting the Condition 2 scaled score from the Condition 4 scaled score and converting the difference into a contrast scaled score.

- Verbal Fluency Test (VFT): The test requires the participant to verbally generate as many words as possible within 60 seconds in three conditions: Condition 1 (Letter Fluency; e.g., words starting with the letter "F"), Condition 2 (Category Fluency; e.g., Animals), and Condition 3 Category Switching (e.g., Fruits vs. Furniture in alternating order). Performance of the VFT was scored using (i) the Primary Measure for each condition, a scaled score [*M*= 10; *SD*= 3] derived from the raw sore for total number of correct responses without repetitions, respectively, (ii) the Total Switching Accuracy, a scaled score derived from the raw score for total number of correct category switches in Condition 3, and (iii) the Primary Contrast Measure for "Condition 1 vs. Condition 2" and "Condition 3 vs. Condition 2" derived by subtracting the scaled scores of Condition 2 from Condition 1 , and Condition 2 from Condition 3, respectively, and converting the difference into a contrast scaled score.

- Colour-Word Interference Test (CWIT): The test primarily measures the participant's capacity to inhibit conflicting responses, e.g. naming the words "blue", "red", and "green" printed with incongruent ink. The test is based on the Stroop effect [Stroop, 1935]. In detail, the CWIT consists of four trials/conditions performed in order: Condition 1 (Colour Naming), Condition 2 (Word Reading), Condition 3 (Inhibition), and Condition 4 (Inhibition vs. Colour Naming). In Condition 1 the participant is presented with a page containing a series of blue, green, and/or red squares. The participant is required to name the colour of each square as quickly as possible without making mistakes. In Condition 2 the participant is presented with a page containing the words "blue", "green", and "red" printed in black

ink. The participant is asked to read out the words as quickly as possible without making mistakes. In Condition 3 the participant is presented with a page containing the words “blue”, “green”, and “red” printed in incongruently in blue, green, or red ink. The participant is asked to name the colour of the ink in which each word is printed as quickly as possible without making mistakes. For Condition 4 the participants is presented with a page containing the words “blue”, “green”, and “red” written in blue, green, or red ink while half of the words are enclosed within boxes. The participants is required to name the colour of the ink in which each word is printed - but read out the printed word if enclosed within a box - as quickly as possible without making mistakes. Performance of the CWIT is measured using (i) the Primary Measure for each condition, a scaled score [*M*= 10; *SD*= 3] derived from the raw score for completion time in seconds, respectively, and (ii) the Primary Combined Measure, derived by adding the Condition 1 and Condition 2 scaled scores and converting the sum into a composite scaled score, and (iii) the Primary Contrast Measure, derived by subtracting the Condition 1 scaled score from the Condition 3 scaled score and converting the difference into a contrast scaled score.

- Tower Task (TT): TT assesses visual attention and visuo-spatial planning skills. This problem-solving task involves moving disks varying in size from small to large across three pegs to build a designated tower in fewest numbers of moves possible from an initial starting configuration. The rules are only moving one disk at a time and never placing a larger disk on top of a smaller one. The D-KEFS TT is similar to the Tower of London Task (TOL) [Shallice, 1982]. Performance of TT was measured using (i) the Primary Measure, derived by summing the item achievement raw scores across all items administered and converting the sum into a scaled score [*M*= 10; *SD*= 3], and (ii) the Mean First Move Time, a scaled score derived by dividing the total number of items administered by the total first-move times and converting the ratio score into a scaled score.

University of Pennsylvania Smell Identification Test (UPSIT) [Doty et al., 1984]: A self-administered recognition-format measure of odour identification. The

UPSIT uses microencapsulated odorants that are released by scratching standardized odour-impregnated test booklets, and refers to the ability to identify and name the corresponding odour based on multiple choice. Impairment of olfactory identification ability has been demonstrated in individuals at ultra-high risk for psychosis who later developed schizophrenia [Brewer et al., 2003].

2.2.4 Social Cognition Measures

The term "social cognition" generally refers to higher order communication skills required to sustain complex social interactions. This includes Theory of Mind (ToM), which is the ability to represent one's own, and other individuals mental states by using contextual cues to reason about, predict, and explain behaviour in terms of psychological causation. ToM was assessed using the non-verbal False-belief Picture Sequencing Task and the Reading the Minds in the Eyes Task, and complemented by the verbal Hinting Task.

False-belief Picture Sequencing Task [Langdon & Coltheart, 1999]: Participants are presented with a set of eight picture stories each depicted as a four-card picture sequence, and presented in pseudorandom order. The participant is required to complete each story by sorting the picture cards into a logical sequence of events. The set of picture stories consisted of 4 False-belief sequences, probing the participants' ability to infer false beliefs and to correctly predict that others can act on the basis of beliefs that misrepresent reality, and 4 control sequences depicting physical cause-and-effect and testing the participants' ability to infer causal relations. Scoring was calculated as follows: 2 points if first card was correct; 2 points if last card was correct; 1 point each if second and third cards were correct (total per sequence 0-6). Mean performance across the four sets of False-belief picture sequences was used for statistical analysis. Data on control sequences was disregarded.

Reading the Mind in the Eyes Test [Baron-Cohen et al., 2001]: A 36-item test in which the participant is presented with photographs of the eye-region of different actors/actresses. The participant is asked to choose a word from a 4-choice response list, which best describes what the person in the photograph

is feeling or thinking. The test measures the capacity to discriminate the mental state of others from emotion expressions in the eye region of the face. Each item answered correctly is scored 1 point. Performance was measured using a total score (sum of points for all 36 items).

Hinting Task [Corcoran, Mercer, & Frith, 1995]: The assessment consists of 10 short stories describing a social interaction between two characters presented to the participant on a sheet of paper and on audio. Each story is read aloud to the participant who is then required to make inferences about the intent behind a hint dropped by one of the story characters. After each story the examiner will ask a question and provide extra information, if required. Correct responses/inferences are scored 2 points, if no extra information was required, and 1 point if required. Performance was measured using a total score (sum of points for all 10 stories).

2.2.5 Electroencephalographic Data

2.2.5.1 EEG Data Acquisition

Participants were presented with three runs of 697 tones (500 ms stimulus onset asynchrony (SOA)) consisting of 78% standard tones (50 ms, 1000 Hz, 80 dB sound pressure level [SPL]) and three types of deviant tones: 7.3% Duration (100 ms, 1000 Hz, 80 dB SPL), 7.3% Frequency (50 ms, 1200 Hz, 80 dB SPL), and 7.3% Intensity (50 ms, 1000 Hz, 90 dB SPL).

Each run was preceded by a sequence of 240 tones (500 ms SOA) consisting of a string of 80 of each of the deviants to be used as standards (e.g. 80 duration deviants, followed by 80 frequency deviants, followed by 80 intensity deviants), and presented in counterbalanced order for each of the 3 runs.

Tones were generated using the Presentation® software[1] and presented binaurally over headphones (HD-280 Pro; Sennheiser, Tullamore, Ireland). During stimuli presentation, participants were instructed to watch a silent video and to ignore the sounds presented via headphones.

[1] http://www.neurobs.com

Electroencephalographic data were acquired and processed with Neuroscan hardware and Software [1] (Neuroscan, El Paso, Texas). The data were continuously sampled from F3, FZ, F4, C3, CZ, C4, P3, PZ, P4, and left and right mastoid. The nose tip was used as a reference. The sampling rate was 500 Hz using a 30 Hz Low pass / 0.05 Hz High pass filter, and a 50 Hz notch filter.

2.2.5.2 EEG Data Processing

Data were analyzed offline. All files were low pass/zero-phase shift-filtered at 30 Hz (12dB), and segmented into epochs beginning 100 ms prior to stimulus onset and ending 450 ms post stimulus onset. Epochs containing artifacts exceeding +/- 150 μV were excluded from analyses. Eyeblink artifacts were corrected with procedures implemented in Neuroscan [Semlitsch et al., 1986]. Epochs were baseline corrected using the entire interval. Separate averages for each deviant and standard type were calculated, and baseline corrected using the pre-stimulus interval.

Mean amplitude measures of duration and frequency MMN and P3a were obtained from subtracting the relevant deviant as standard from the deviant ERP. The resulting waveforms were low pass/zero-phase shift-filtered at 20 Hz (12dB) and baseline corrected using the pre-stimulus interval. Mean amplitude data was derived from the Fz site and calculated as the mean across a 170-230 ms interval for duration MMN, 150-210 ms interval for frequency MMN, 274-324 ms interval for duration P3a, and 250-300 ms interval for frequency P3a, respectively. Intervals were chosen on the basis of the total grand average waveforms and are slightly shorter for P3a than MMN as this seemed more appropriate based on the grand average plots. Data analyses focused on duration and frequency deviant data while intensity deviant data were discarded with rationale being that the former two are more commonly employed in schizophrenia research.

[1] http://www.neuroscan.com

2.3 Magnetic Resonance Imaging Data

2.3.1 MRI Data Acquisition

Magnetic Resonance Imaging (MRI) brain scans were collected on a 1.5 Tesla Siemens Avanto MRI scanner (Siemens, Germany) at the Prince of Wales Hospital (Sydney, Australia) using the acquisition and data quality management protocol of the Australian Schizophrenia Research Bank[1] (ASRB).

Scanning parameters of the T1-weighted magnetization-prepared rapid acquisition gradient echo (MPRAGE) sequence were as follows:

- 176 sagittal slices of 1 mm thickness without intersection gap
- Repetition time (TR) = 1980 milliseconds (ms)
- Echo time (TE) = 4.3 ms
- Inversion time (TI) = 1100 ms
- Flip angle (FA) 15 °
- Matrix = 256 x 256
- Field of view (FOV) = 250 x 250 mm
- Resulting voxel size = 0.98 x 0.98 x 1.0 mm^3

MRI analysis was conducted at the Priority Research Centre for Translational Neuroscience and Mental Health (Newcastle, Australia).

2.3.2 Brain Anatomy Relevant to Image processing

The cerebrum is divided into right and left hemispheres. These are broadly similar in shape, arranged bilaterally around the sagittal midline, and connected by the commissural fibres of the corpus callosum.

The outer surface of the cerebrum is called the cerebral cortex, a thin layer of grey matter with an average thickness of approximately 2.5 mm [Brodmann, 1909]. The surface structure of the cerebral cortex is highly convoluted and

[1] http://www.schizophreniaresearch.org.au

folded in a manner that greatly increases its surface area. The in-folds of the surface are called gyri (singular: gyrus), separated from each other by fissures referred to as sulci (singular: sulcus).

Parsed on the basis of cell architecture, the cortex can be subdivided into numerous cortical areas, which are interconnected to other areas by a complex web of white matter (WM) fibre tracts. Most cortical areas are replicated bilaterally in each hemisphere, with some areas showing strong lateralization.

On the outside, the cerebral cortex is closely enveloped by the innermost layer of the meninges, the pia-mater, forming the outer cortical (or pial) surface. On the inside, the inner cortical (or WM) surface is formed by the GM-WM boundary of the cerebral cortex.

2.3.3 MRI Pre-Processing

MRI raw data was anonymized (Dicom Anonymizer Pro)[1], converted into the MINC file format (LONI Debabeler)[2], and checked for incidental findings and scanning artifacts using MINC Display[3]. A cutting plane in z-direction, just below the cerebellum was determined, and each subject's MRI was cropped to exclude tissue below the cerebellum.

The resulting volumes were used for (i) a preliminary non-parametric non-uniform intensity normalization (N3) [Sled, Zijdenbos, & Evans, 1998] and subsequent creation of a cerebral mask using the Hybrid Watershed Algorithm [Segonne et al., 2004], and (ii) a more stringent N3 correction by employing the mask created in (i). The latter N3-corrected volume was used in Cerebrum extraction by applying a combination of the Brain Extraction Tool [Smith, 2002] and the Hybrid Watershed Algorithm [Segonne et al., 2004]. The cerebral mask was visually inspected and edited where needed. Automated Talairach 12-parameter affine transformation was computed using an algorithm developed by Avi Snyder[4] and incorporated and distributed in FreeSurfer. Cortical reconstruction and volumetric segmentation was conducted using FreeSurfer[5].

2.3.4 FreeSurfer Image Analysis Suite

Morphological characteristics of each subject's cerebral cortex were quantified using the FreeSurfer image analysis suite (Version 5.1.0 Darwin), which provides a set of powerful tools to analyse the key features in the human brain. FreeSurfer is developed and maintained by the Athinoula A. Martinos Center for Biomedical Imaging, (Massachusetts, USA).

---

[1] Dicom Anonymizer Pro (www.neologica.it)

[2] LONI debabeler (http://www.loni.ucla.edu/Software/Debabeler)

[3] MINC Display (http://www.bic.mni.mcgill.ca)

[4] 4dfp image registration tools (http://nrg.wikispaces.com/4dfp+tools)

[5] FreeSurfer (http://surfer.nmr.mgh.harvard.edu/)

FreeSurfer was executed in clustered directive (Table 2.3.4-1); following the recommended reconstruction workflow for manual intervention[1].

Table 2.3.4-1 FreeSurfer Autorecon Processing Stages[2]

Clustered Directive	Step	Stepwise-Directive
autorecon1	1	Motion Correction and Conform
	2	N3 (Non-Uniform intensity normalization)
	3	Talairach transform computation
	4	Intensity Normalization 1
	5	Skull Strip
autorecon2	6	EM Register (linear volumetric registration)
	7	CA Intensity Normalization
	8	CA Non-linear Volumetric Registration
	9	Remove neck
	10	EM Register, with skull
	11	CA Label (Aseg: Volumetric Labelling) and Statistics
	12	Intensity Normalization 2
	13	White matter segmentation
	14	Edit WM With Aseg
	15	Fill (start here for WM edits)
	16	Tessellation (begins per-hemisphere operations)
	17	Smooth1
	18	Inflate1
	19	Q Sphere
	20	Automatic Topology Fixer
	21	White Surfs (start here for brain edits for pial surf)
	22	Smooth2
	23	Inflate2
autorecon3	24	Spherical Mapping
	25	Spherical Registration
	26	Spherical Registration, Contralateral hemisphere
	27	Map average curvature to subject
	28	Cortical Parcellation (Labelling)
	29	Cortical Parcellation Statistics
	30	Pial Surfs
	31	Cortical Ribbon Mask
	32	Cortical Parcellation mapped to Aseg
	33	Brodmann and exvio EC labels

2.3.5 FreeSurfer's Cortical Reconstruction & Volumetric Segmentation

The pre-processed MRI data was segmented based on signal intensity and geometric properties of the GM-WM boundary. Cerebral hemispheres were automatically disconnected from the brainstem and from each other. GM-WM

[1] http://surfer.nmr.mgh.harvard.edu/fswiki/RecommendedReconstruction

[2] http://surfer.nmr.mgh.harvard.edu/fswiki/recon-all

boundaries in each hemisphere were tessellated with a triangular mesh of approximately 160,000 vertices per hemisphere, and automatically corrected for topological defects.

The folded surface tessellation was then inflated outwards to locate the GM-Cerebrospinal fluid (CSF) boundary. Surfaces were deformed following the greatest shift in intensity that defines transition to other tissue types, to produce accurate and smooth representations of the WM surface (GM-WM boundary), as well as the pial surface (GM-CSF boundary). Reconstructed surfaces were visually inspected and any inaccuracies in segmentation edited manually.

Each hemisphere's cortical representation was morphed to a standard spherical atlas using a high-resolution, surface-based averaging technique that allows for accurate matching of cortical locations.

The cortex was automatically parcellated using standard anatomical nomenclature (Table 2.3.5-1) [Destrieux et al., 2010], and each vertex on the reconstructed surface was assigned to an anatomical label.

Cortical GM thickness data were obtained for each vertex on the tessellated WM surface; computed as the average distance of the WM surface to the closest vertex of the pial surface and from that vertex back to closest vertex of the WM surface [Fischl & Dale, 2000].

Mean cortical GM thickness (mm), pial surface area (mm^2), and WM surface area (mm^2) for each hemisphere and anatomical label were computed from the reconstructed surfaces and WM volumes (mm^3) computed from the automatic segmentation volume, which was derived from FreeSurfer's volume-based stream [Fischl et al., 2002; Fischl et al., 2004]. Data were extracted and used for statistical analyses. Mean global cortical GM thickness across both hemispheres was calculated as follows:

$$\bar{x} = \frac{[(lh.thick * lh.surf) + (rh.thick * rh.surf)]}{(lh.surf + rh.surf)}$$

lh.thick = left hemisphere mean cortical thickness | *rh.thick = right hemisphere mean cortical thickness*

lh.surf = left hemisphere WM surface area | *rh.surf = right hemisphere WM surface area*

The Estimated Total Intracranial Volume (mm^3) (eTIV) for each subject was obtained from the Talairach transformation of the N3-corrected input volume to MNI 305 atlas space [Buckner et al., 2004], and used to correct volumetric measures (i.e. GM volume, WM volume) using the formula:

$$eTIV\ corrected\ volume = volume * [mean\ eTIV\ across\ subjects / individual\ eTIV]$$

Table 2.3.5-1 List of anatomical parcellations (aparc.a2009s) [Destrieux et al., 2010]

Index	Anatomical Parcellation	Long name (Bold = Terminologia Anatomica Nomenclature)
1	G_and_S_frontomargin	Fronto-marginal gyrus (of Wernicke) and sulcus Inferior occipital gyrus (O3) and sulcus Paracentral lobule and sulcus
2	G_and_S_occipital_inf	Inferior occipital gyrus (O3) and sulcus
3	G_and_S_paracentral	Paracentral lobule and sulcus
4	G_and_S_subcentral	Subcentral gyrus (central operculum) and sulci Transverse frontopolar gyri and sulci
5	G_and_S_transv_frontopol	Transverse frontopolar gyri and sulci
6	G_and_S_cingul-Ant	Anterior part of the cingulate gyrus and sulcus (ACC)
7	G_and_S_cingul-Mid-Ant	Middle-anterior part of the **cingulate gyrus and sulcus** (aMCC)
8	G_and_S_cingul-Mid-Post	Middle-posterior part of the **cingulate gyrus and sulcus** (pMCC)
9	G_cingul-Post-dorsal	Posterior-dorsal part of the **cingulate gyrus** (dPCC)
10	G_cingul-Post-ventral	Posterior-ventral part of the cingulate gyrus (vPCC, **isthmus of the cingulate gyrus**)
11	G_cuneus	Cuneus (O6)
12	G_front_inf-Opercular	Opercular part of the inferior frontal gyrus
13	G_front_inf-Orbital	Orbital part of the inferior frontal gyrus
14	G_front_inf-Triangul	Triangular part of the inferior frontal gyrus
15	G_front_middle	Middle frontal gyrus (F2)
16	G_front_sup	Superior frontal gyrus (F1)
17	G_Ins_lg_and_S_cent_ins	Long insular gyrus and central sulcus of the insula
18	G_insular_short	Short insular gyri
19	G_occipital_middle	Middle occipital gyrus (O2, lateral occipital gyrus)
20	G_occipital_sup	Superior occipital gyrus (O1)
21	G_oc-temp_lat-fusifor	Lateral occipito-temporal gyrus (fusiform gyrus, O4-T4)
22	G_oc-temp_med-Lingual	Lingual gyrus, lingual part of the medial occipito-temporal gyrus, (O5)
23	G_oc-temp_med-Parahip	Parahippocampal gyrus, parahippocampal part of the medial occipito-temporal gyrus, (T5)
24	G_orbital	Orbital gyri
25	G_pariet_inf-Angular	Angular gyrus
26	G_pariet_inf-Supramar	Supramarginal gyrus
27	G_parietal_sup	Superior parietal lobule (lateral part of P1)
28	G_postcentral	Postcentral gyrus
29	G_precentral	Precentral gyrus
30	G_precuneus	**Precuneus** (medial part of P1)
31	G_rectus	Straight gyrus, Gyrus rectus
32	G_subcallosal	Subcallosal area, subcallosal gyrus
33	G_temp_sup-G_T_transv	Anterior transverse temporal gyrus (of Heschl)
34	G_temp_sup-Lateral	Lateral aspect of the superior temporal gyrus
35	G_temp_sup-Plan_polar	Planum polare of the superior temporal gyrus
36	G_temp_sup-Plan_tempo	Planum temporale or temporal plane of the superior temporal gyrus
37	G_temporal_inf	Inferior temporal gyrus (T3)
38	G_temporal_middle	Middle temporal gyrus (T2)

Index	Anatomical Parcellation	Long name (Bold = Terminologia Anatomica Nomenclature)
39	Lat_Fis-ant-Horizont	Horizontal ramus of the anterior segment of the lateral sulcus
40	Lat_Fis-ant-Vertical	Vertical ramus of the anterior segment of the lateral sulcus
41	Lat_Fis-post	Posterior ramus (or segment) of the lateral sulcus
42	Pole_occipital	Occipital pole
43	Pole_temporal	Temporal pole
44	S_calcarine	Calcarine sulcus
45	S_central	**Central sulcus** (Rolando's fissure)
46	S_cingul-Marginalis	Marginal branch (or part) of the cingulate sulcus
47	S_circular_insula_ant	Anterior segment of the circular sulcus of the insula
48	S_circular_insula_inf	Inferior segment of the circular sulcus of the insula
49	S_circular_insula_sup	Superior segment of the circular sulcus of the insula
50	S_collat_transv_ant	Anterior transverse collateral sulcus
51	S_collat_transv_post	Posterior transverse collateral sulcus
52	S_front_inf	Inferior frontal sulcus
53	S_front_middle	Middle frontal sulcus
54	S_front_sup	Superior frontal sulcus
55	S_interm_prim-Jensen	Sulcus intermedius primus (of Jensen)
56	S_intrapariet_and_P_trans	**Intraparietal sulcus** (interparietal sulcus) and transverse parietal sulci
57	S_oc_middle_and_Lunatus	Middle occipital sulcus and lunatus sulcus
58	S_oc_sup_and_transversal	Superior occipital sulcus and **transverse occipital sulcus**
59	S_occipital_ant	Anterior occipital sulcus and **preoccipital notch** (temporo-occipital incisure)
60	S_oc-temp_lat	Lateral occipito-temporal sulcus
61	S_oc-temp_med_and_Lingual	Medial occipito-temporal sulcus (**collateral sulcus**) and lingual sulcus
62	S_orbital_lateral	Lateral orbital sulcus
63	S_orbital_med-olfact	Medial orbital sulcus **(olfactory sulcus)**
64	S_orbital-H_Shaped	**Orbital sulci** (H-shaped sulci)
65	S_parieto_occipital	Parieto-occipital sulcus (or fissure)
66	S_pericallosal	Pericallosal sulcus (**S of corpus callosum**)
67	S_postcentral	Postcentral sulcus
68	S_precentral-inf-part	Inferior part of the **precentral sulcus**
69	S_precentral-sup-part	Superior part of the **precentral sulcus**
70	S_suborbital	Suborbital sulcus (sulcus rostrales, supraorbital sulcus)
71	S_subparietal	Subparietal sulcus
72	S_temporal_inf	Inferior temporal sulcus
73	S_temporal_sup	Superior temporal sulcus (parallel sulcus)
74	S_temporal_transvers	Transverse temporal sulcus

2.3.6 Modification to FreeSurfer's default workflow

Changes were made to the autorecon1 directive (see Table 2.3.4-1), where "Non-Uniform Intensity Normalization" and "Skull Strip" were omitted. Instead, a more complex N3 correction and brain extraction were included in data pre-processing (Chapter 2.3.3) that delivered superior results to FreeSurfer's default procedure. For autorecon2, expert options were used with "Intensity Normalization 2" (i.e. mri_normalize –prune 1) and "White Matter Segmentation" (i.e. mri_segment –t 8).

2.4 Data Analysis using SPSS

Statistical data analysis was conducted using SPSS 19.0 for Mac OS X (SPSS Inc., Chicago, IL, USA). *P*-values at the level < .05 (two-tailed) are reported as significant in the text. Data were tested for normal distribution using the Kolmogorov-Smirnov test (p< .05). Estimates of mean cortical grey matter thickness by anatomical parcellation (Table 2.3.5-1) and hemisphere were extracted from FreeSurfer.

Spearman's rank correlation coefficients were used to test associations between clinical and functional measures, neuropsychological variables, and grey matter thickness data, respectively, and Pearson's correlation coefficients were calculated to assess the relationship of MMN and P3a amplitudes in response to duration and frequency deviants with grey matter thickness data.

2.4.1 Median-Split Group Analysis by CAARMS composite score

The outcome on selected CAARMS subscales was used to compute a CAARMS composite score (CCS) in order to divide the study sample into a low- versus high-symptom group by median-split (ARMS-LS vs. ARMS-HS).

Group characteristics of ARMS-LS and ARMS-HS study participants were assessed using independent-samples t-test for continuous variables, and the X^2 (Chi-Square) or Yates' X^2 [Preacher, 2001] if indicated for N<5 to test for categorical variables. Statistical comparisons of non-normally distributed variables were performed using the Mann-Whitney Test.

2.5 Data Analysis using FreeSurfer

Statistical maps were created using FreeSurfer. Each subject's cortical representation was morphed to a standard spherical representation and smoothed with a full-width-half-maximum (FWHM) Gaussian kernel of 15mm across the surface. A general linear model (GLM) was fit at each surface vertex to perform inter-subject averaging and statistical inference on the cortical surface. Left and right hemispheres were tested separately. The contrast matrices used investigated (i) differences in average cortical GM thickness between ARMS-LS and ARMS-HS, which was an independent-samples *t*-test at

p< .05, and (ii) the correlation of cortical GM thickness with variable of interest (i.e. clinical and functional measures, neuropsychological variables and ERP data (as outlined in Table 2.2.1-1, respectively) across all subjects tested at p< .05. For visual display data was rendered on the FreeSurfer average brain template.

To reduce the probability of false-positive vertices (type I errors), all statistical maps were corrected for multiple comparisons using cluster size inference by means of Monte-Carlo simulation (MC-Z) [Hagler, Saygin, & Sereno, 2006]. The initial cluster forming threshold employed was p< .05 for each contrast, respectively. MC-Z simulation tests against an empirical null distribution of maximum cluster size, using synthesized Z-distributed data, and smoothed with the residual FWHM over 10,000 iterations. A threshold of p< .05 was used for simulation, which is the probability of forming a maximum cluster of that size or larger under the null hypothesis.

RESULTS

3 RESULTS

3.1 ARMS Cohort Characteristics

Detailed descriptive statistics of the ARMS cohort are reported in APPENDIX - SECTION I (page 100).

3.1.1 Demographic and Clinical Data

The cohort consisted of 42 individuals, 18 males (43%) and 24 females (57%) with a mean age of 19.36 years [*SD* 2.17].

At the time of recruitment 3 study participants were taking antipsychotic medication at a sub-therapeutic dose (e.g. quetiapine 50 mg/day) for less than 2 weeks which was discontinued following psychiatric review. Thirteen participants were treated with antidepressants (i.e. selective serotonin re-uptake inhibitors or SSRIs). Among those, one participant reported taking low dose of antipsychotics for < 2 weeks prior to study inclusion

Twenty six participants disclosed drug abuse within the last 6 months prior to study inclusion, with cannabis being used by 23 participants, stimulants (e.g. amphetamines, cocaine) by 14, and both cannabis and stimulants by 11 participants, respectively. No subject met diagnostic criteria for substance dependence/abuse for recreational drugs.

The participants' general intellectual ability was assessed with the Wechsler Abbreviated Scale of Intelligence (WASI). The participants' average WASI Full-2-Subscale IQ score was average (107.9 [*SD* 16.5]), with a mean Vocabulary T score of 53.8 [*SD* 13.3] and a mean Matrix Reasoning T score of 54.7 [*SD* 7.8].

All 42 participants met criteria for the At-risk Mental State as assessed by the CAARMS. Participants rated on average 46.7 [*SD* 21.3] on the CAARMS (total score), 33.4 [*SD* 14.7] on the CCS (summative symptom intensity rating of selected CAARMS, and 42.9 [*SD* 8.2] on the BPRS (total score). BPRS scores were significantly correlated with the total CAARMS rating scores (*rho (40)*= .74, *p*< .001), and the CCS (*rho (40)*= .68, *p*< .001), respectively.

3.1.2 Function Ratings

The study participants were moderately impaired as rated on GAF (56.1 [*SD* 12.3]), SOFAS (62 [*SD* 13.5]), GF:Role (6.5 [*SD* 1.2]), and GF:Social (6.7 [*SD* 1.2]), respectively. Level of functioning was also correlated with more severe symptom expression (i.e. CCS) with GAF (*rho (42)*= -.36, *p*= .019), SOFAS (*rho (42)*= -.36, *p*= .020), GF:Social (*rho (42)*= -.34, *p*= .028), and GF:Role (*rho (42)*= -.34, *p*= .029), respectively.

3.1.3 Neurocognitive Measures

Neuropsychological status was assessed using the Delis-Kaplan Executive Functioning System (D-KEFS), the California Verbal Learning Test (CVLT-II), and the Wechsler Memory Scale (WMS-III).

Better performance on the Verbal Fluency Test (Condition 1; Condition 3), the Tower Task (Total Achievement) and the CVLT-II (free and cued short delay and long delay List A recall), and greater impairment on the Trail Making Test (Condition 2; Condition 4) and the Colour Word Interference Test (Condition 3) were significantly correlated with higher levels of functioning as rated on the SOFAS, GF:Role and/or GF:Social, respectively (see Table 3.1.3-1 details). Finally, better working memory performance on the WMS-III digit span scaled sub-score was associated with higher SOFAS ratings.

Table 3.1.3-1 Neuropsychological vs. Functional Measures

	GAF		**SOFAS**		**GF:Social**		**GF:Role**	
	rho (42)	*p*	*rho (42)*	*p*	*rho (42)*	*p*	*rho (42)*	*p*
D-KEFS Trail Making Test								
Condition 2 (Number Sequencing) Primary Measure Scaled Score	.17	.274	.38	**.012**	.34	**.025**	.39	**.010**
Condition 4 (Number-Letter Switching) Primary Measure Scaled Score	.20	.210	.42	**.006**	.33	**.033**	.38	**.014**
Primary Contrast 2 (Condition 4 - Condition 2) Contrast Scaled Score	.15	.344	.10	.547	.04	.823	.07	.655
D-KEFS Verbal Fluency Test								
Condition 1 (Letter Fluency) Primary Measure Scaled Score	.21	.183	.47	**.002**	.33	**.031**	.31	**.048**
Condition 2 (Category Fluency) Primary Measure Scaled Score	.04	.779	.30	.055	-.03	.862	.27	.081

	GAF		SOFAS		GF:Social		GF:Role	
	rho (42)	*p*	*rho (42)*	*p*	*rho (42)*	*p*	*rho (42)*	*p*
Condition 3 (Category Switching) Total Correct Response Scaled Score	.18	.255	.36	**.018**	.26	.101	.32	**.037**
Condition 3 (Category Switching) Total Switching Accuracy Scaled Score	.26	.091	.40	**.008**	.35	**.021**	.40	**.008**
Primary Contrast Measure 1 (Condition 1 - Condition 2) Contrast Scaled Score	.10	.532	.12	.454	.29	.063	.06	.707
Primary Contrast Measure 2 (Condition 3 - Condition 2) Contrast Scaled Score	.03	.840	-.01	.943	.16	.322	.01	.932
D-KEFS Colour-Word Interference Test								
Condition 1 (Colour Naming) Primary Measure Scaled Score	.19	.221	.42	**.005**	.38	**.013**	.39	**.010**
Condition 2 (Word Reading) Primary Measure Scaled Score	.17	.275	.30	.054	.31	**.048**	.17	.274
Condition 3 (Inhibition) Primary Measure Scaled Score	.37	.015	.44	**.004**	.34	**.030**	.36	**.018**
Primary Combined Measure (Condition 1 + Condition 2) Composite Scaled Score	.21	.192	.39	**.011**	.35	**.022**	.28	.072
Primary Contrast Measure 1 (Condition 3 - Condition 1) Contrast Scaled Score	.29	.062	.11	.475	.09	.553	.01	.957
D-KEFS Tower Task								
Primary Measure Total Achievement Scaled Score	.44	.004	.56	**.000***	.27	.081	.40	**.009**
Mean First Move Time Scaled Score	.07	.645	.10	.530	.04	.785	.14	.376
California Verbal Learning Test - II								
List A Short Delay Free Recall Std. Score	.34	**.027**	.33	**.034**	.31	**.047**	.37	**.016**
List A Short Delay Cued Recall Std. Score	.39	**.011**	.38	**.012**	.32	**.038**	.44	**.004**
List A Long Delay Free Recall Std. Score	.47	**.002**	.51	**.001**	.40	**.009**	.45	**.003**
List A Long Delay Cued Recall Std. Score	.39	**.011**	.31	**.049**	.24	.123	.29	.067
Semantic Clustering Std. Score	.10	.515	.01	.925	.21	.183	.04	.797
Serial Clustering Std. Score	.02	.878	.06	.722	-.18	.262	.10	.511
Recognition Correct Std. Scores "TOTAL HITS"	.40	**.009**	.28	.072	.15	.331	.25	.115
Wechsler Memory Scale - III								
Letter-Number Sequencing Scaled Score	.21	.184	.28	.074	.26	.104	.26	.100
Digit Span Forwards Raw Score	-.01	.941	.23	.156	.10	.520	.12	.467
Digit Span Backwards Raw Score	.07	.673	.33	**.036**	.00	.986	.23	.154
Digit Span Scaled Score	.10	.533	.39	**.012**	.13	.426	.28	.078

| Bold = Sig. correlations at *p*< .05 (uncorrected) | Asterisk = Sig. correlations at *p*< .0005 (Bonferroni adjusted)

3.1.4 Social Cognition Measures

Social cognition was assessed with the False-belief Picture Sequencing Task (4.96 [*SD* 1.19]), the Reading the Mind in the Eyes Test (22.36 [*SD* 2.16]), and the Hinting Task (17.95 [*SD* 1.81]). The Hinting Task significantly correlated with higher function ratings on GAF (*rho (40)*= .35, *p*= .022), SOFAS (*rho (40)*=

.36, *p*= .020), GF:Social (*rho (40)*= .35, *p*= .023), and GF:Role (*rho (40)*= .33, *p*= .034), respectively.

3.1.5 Electroencephalographic Data

ERP data analysis was limited to 37 of the 42 study participants due to incomplete/missing data and/or noisy recordings. This sub-sample consisted of 17 males and 20 females with a mean age of 19.3 years [*SD* 2.12]. Participants did not differ from the full cohort in respect to clinical ratings (45.04 [*SD* 21.07] on the CAARMS and 32.12 [*SD* 14.34] for the CCS).

MMN and P3a amplitudes to durations and frequency deviant tones are presented in Figure 3.1.5-1. MMN mean amplitudes were -2.14 [*SD* 2.22] µV in response to duration and -1.66 [*SD* 2.24] µV in response to frequency deviants. P3a mean amplitudes were 1.77 [*SD* 2.4] µV for duration and 1.22 [*SD* 2.09] µV for frequency deviants. More severe symptom expression (i.e. larger CCS scores) was associated with reduced P3a amplitudes (*rho (37)*= -.34, *p*= .037) elicited by duration deviants.

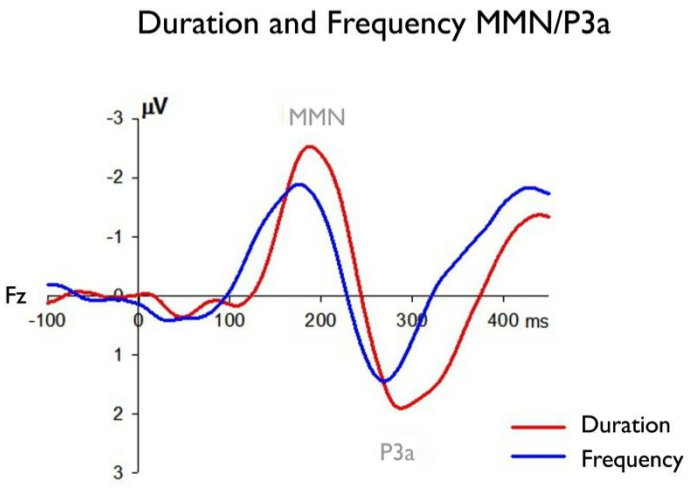

Figure 3.1.5-1 Grand average event related potentials (i.e. MMN/P3a waveforms) at the frontal central electrode site (Fz) to duration and frequency deviant tones obtained from 37 ARMS individuals during an auditory oddball task (see Chapter 2.2.5 for details).

3.2 Median-Split Group Analysis by CCS

The rationale of the median-split approach was to divide the study sample into a low- versus high-symptom group (ARMS-LS vs. ARMS-HS) and to allow for group analyses in the absence of healthy control data by introducing ARMS-LS as a "clinical control group".

It was hypothesized that severity of At-risk Mental State is related to neuropathology (i.e. decreased cortical thickness, brain volume, and/or surface area). Accordingly, neuropathology in ARMS-HS was presumed more pronounced when compared to ARMS-LS.

To test this hypothesis, the ARMS cohort was divided by a median-split of the CCS, which ranged from 0 to 62 with a median of 36 (Q1= 23; Q3= 43), yielding two equally sized groups of 21 participants.

Mean GM thickness, GM and WM volume, pial surface area, and WM surface area by hemisphere, respectively, were statistically compared between these two groups and potential confounding factors (i.e. age, gender, handedness, pharmacotherapy, and substance use) incorporated in the analyses in cases where groups differ significantly on these factors.

In addition to the assessment of brain morphological differences, the two groups were statistically compared with respect to functional status, cognitive performance, social cognition, and MMN and P3 amplitudes.

3.2.1 Demographic and Clinical Data

The two groups did not significantly differ in age, (t (40)= -.351, p= .727), gender composition (X^2 (1, n= 42)= 0, p= 1.00), or handedness (Yates' X^2 (2, n= 42)= .529, p= .768) nor regarding the use of alcohol (Yates' X^2 (1, n= 42)= 1.782, p= .182), nicotine (X^2 (1, n= 42)= .404, p= .525), cannabis (X^2 (1, n= 42)= 0.096, p= .757), or stimulants (Yates' X^2 (1, n= 42)= 0, p= 1.00). Moreover, the groups did not differ significantly in general intellectual ability (t (40)= .037, p= .971 (WASI Full-2-Subscale IQ)) nor antidepressant pharmacotherapy (Yates' X^2 (1, n= 39)= 2.168, p= .141). See Table 3.2.1-1 for details.

Table 3.2.1-1 Demographic and Clinical Data: Low-symptomatic (ARMS-LS) vs. high-symptomatic (ARMS-HS) study participants by CCS Median-Split

Variable	ARMS-LS (n=21)		ARMS-HS (n=21)		ARMS-LS vs. ARMS-HS		
	M	*SD*	*M*	*SD*	*t*	*df*	*p*
Age [years]	19.24	2.14	19.48	2.25	-0.351	40	.727
CAARMS composite score	21.57	10.32	45.17	6.60	-8.826	40	< .000
WASI full-2-Subscale IQ	107.95	15.83	107.76	17.48	0.037	40	.971
	n		*n*		X^2	*df*	*p*
Gender [female | male]	12 | 9		12 | 9		0.000	1	1.000
Cannabis [no | yes[3]]	9 | 12		10 | 11		0.096	1	.757
Stimulants [no | yes[3]]	14 | 7		14 | 7		0.000	1	1.000
Nicotine [no | yes[1]]	7 | 14		9 | 12		0.404	1	.525
	n		*n*		Yates' X^2	*df*	*p*
Handedness [right, left, ambidextrous]	16 | 2 | 3		18 | 2 | 1		0.529	2	.768
Alcohol [no | yes[2]]	4 | 17		9 | 12		1.782	1	.182
Antidepressants (SSRI) [no | yes]	16 | 4		10 | 9		2.168	1	.141
Antipsychotics [no | yes[4]]	19 | 1		18 | 2		0.000	1	1.000

| [1] within last week | [2] within last month | [3] within last 6 months | [4] At study entry < 2 weeks
| WASI = Wechsler Abbreviated Scale of Intelligence

3.2.2 Brain Morphology

Total Intracranial Volume (eTIV) did not differ significantly between the two groups. There were also no significant group differences in eTIV-corrected GM and WM volume, pial surface area, and/or WM surface area by hemisphere, respectively. By contrast, the mean cortical GM thickness (mm) was significantly reduced in ARMS-HS compared to ARMS-LS when averaged across all vertices of both cerebral hemispheres (2.63 [*SD* .10] vs. 2.70 [*SD* .08]; *t* (40)= 2.43, *p*= .020, *r*= -.36), which was also confirmed separately for the left hemisphere (2.64 [*SD* .10] vs. 2.70 [*SD* .08]; *t* (40)= 2.25, *p*= .030, *r*= -.31) and right hemisphere (2.63 [*SD* .10] vs. 2.70 [*SD* .08]; *t* (40)= 2.55, *p*= .015, *r*= -.36), respectively (see Table 3.2.2-1 for details).

Table 3.2.2-1 Brain Morphological Characteristics: Low-symptomatic (ARMS-LS) vs. high-symptomatic (ARMS-HS) study participants by CCS Median-Split

Variable	Hemisphere	ARMS-LS (n=21)		ARMS-HS (n=21)		ARMS-LS vs. ARMS-HS		
		M	*SD*	*M*	*SD*	*t*	*df*	*p*
Mean GM Thickness [mm]	L	2.70	0.08	2.64	0.10	2.250	40	**.030**
Mean GM Thickness [mm]	R	2.70	0.08	2.63	0.10	2.545	40	**.015**
Mean GM Thickness [mm]	L&R	2.70	0.08	2.63	0.10	2.433	40	**.020**
GM Volume• [mm^3]	L	268,238	9,818	266,071	9,513	0.726	40	.472
GM Volume• [mm^3]	R	269,010	9,103	265,212	9,655	1.312	40	.197
GM Volume• [mm^3]	L&R	537,248	18,813	531,284	18,971	1.023	40	.312
WM Volume• [mm^3]	L	236,737	8,576	242,155	12,364	-1.650	40	.107
WM Volume• [mm^3]	R	237,645	9,011	242,259	12,654	-1.361	40	.181

Variable	Hemisphere	ARMS-LS (n=21)		ARMS-HS (n=21)		ARMS-LS vs. ARMS-HS		
		M	*SD*	*M*	*SD*	*t*	*df*	*p*
WM Volume• [mm^3]	L&R	474,382	17,248	484,414	24,911	-1.517	40	.137
Pial Surface [mm^2]	L	105,952	11,731	109,528	10,155	-1.056	40	.297
Pial Surface [mm^2]	R	106,139	12,265	109,436	10,085	-0.951	40	.347
Pial Surface [mm^2]	L&R	212,091	23,977	218,964	20,202	-1.005	40	.321
WM Surface [mm^2]	L	89,858	10,081	93,833	7,930	-1.420	40	.163
WM Surface [mm^2]	R	90,244	10,349	93,917	8,263	-1.271	40	.211
WM Surface [mm^2]	L&R	180,101	20,398	187,750	16,134	-1.348	40	.185

| No adjustments were made for multiple comparisons | • Corrected for estimated Intracranial Volume (eTIV)
| Bold = Sig. correlations at $p < .05$ (uncorrected)

3.2.3 Function Ratings

ARMS-LS and ARMS-HS differed significantly in functional status according to the SOFAS (66.29 [*SD* 12.39] vs. 57.71 [*SD* 13.45]; *t* (40)= 2.15, *p*= .038, *r*= .32), GF:Social (7.1 [*SD* 1.11] vs. 6.33 [*SD* 1.09]; *t* (40)= 2.24, *p*= .031, *r*= .33), and the GF:Role (6.9 [*SD* 1.1] vs. 6.17 [*SD* 1.21]; *t* (42)= 2.07, *p*= .045, *r*= .30), respectively. ARMS-LS consistently presented higher levels of functioning across theses assessments. When assessed with the GAF (58.48 [*SD* 13.98] vs. 53.62 [*SD* 10.21]; *t* (40)= 1.29, *p*= .206), ARMS-LS performed better than ARMS-HS in terms of mean scores (i.e. higher level of functioning); however, no significant differences between the two groups were confirmed.

3.2.4 Neurocognitive Measures

Group statistics (ARMS-LS vs. ARMS-HS) on performance measures of the neurocognitive assessment battery revealed significant group differences on the Verbal Fluency Test Condition 3 (Category Switching) Total Correct Response Scaled Score (12.52 [*SD* 4.14] vs. 10.38 [*SD* 2.31]; *t* (40)= 2.070, *p*= .045, *r*= .30), as well as on three sub-scores of the Colour-Word Interference Test; Condition 1 (Colour Naming) Primary Measure Scaled Score (9.76 [*SD* 2.30] vs. 7.76 [*SD* 2.77]; *U* (42)= 119.50, *p*= .010, *r*= .40), Condition 3 (Inhibition) Primary Measure Scaled Score (9.90 [*SD* 3.71] vs. 8.43 [*SD* 3.04]; *U* (42)= 141.50, *p*= .045, *r*= .31), and on the Primary Combined Measure (Condition 1 + Condition 2) Composite Scaled Score (10.19 [*SD* 2.62] vs. 8.76 [*SD* 2.34]; *U* (42)= 134.00, *p*= .028, *r*= .34). See Table 3.2.4-1 for details.

Table 3.2.4-1 Neurocognitive Assessment Battery: Low-symptomatic (ARMS-LS) vs. high-symptomatic (ARMS-HS) study participants by CCS Median-Split

Variable	ARMS-LS			ARMS-HS			ARMS-LS vs. ARMS-HS		
	n	*M*	*SD*	n	*M*	*SD*	*t*	*df*	*p*
California Verbal Learning Test - II									
List A Short Delay Free Recall Std. Score	21	0.55	0.91	21	0.07	1.34	1.346	40	.186
List A Short Delay Cued Recall Std. Score	21	0.24	0.93	21	-0.21	1.32	1.284	40	.206
List A Long Delay Free Recall Std. Score	21	0.38	0.96	21	0.05	1.17	1.008	40	.319
List A Long Delay Cued Recall Std. Score	21	0.24	0.85	21	-0.33	1.50	1.519	40	.137
Semantic Clustering Std. Score	21	0.14	1.61	21	0.12	1.13	0.055	40	.956
Serial Clustering Std. Score	21	0.14	1.34	21	0.02	1.38	0.283	40	.779
Recognition Correct Std. Scores "TOTAL HITS"	21	0.00	0.77	21	-0.40	0.96	1.507	40	.140
Wechsler Memory Scale - III									
Letter-Number Sequencing Scaled Score	20	9.65	2.74	21	9.95	2.38	-0.378	39	.707
Digit Span Forwards Raw Score	20	10.25	2.71	21	10.29	1.42	-0.053	39	.958
Digit Span Backwards Raw Score	20	6.75	2.69	21	6.43	1.57	0.470	39	.641
Digit Span Scaled Score	20	9.90	3.43	21	9.43	1.50	0.575	39	.569
D-KEFS Trail Making Test									
Condition 2 (Number Sequencing) Primary Measure Scaled Score	21	10.14	2.87	21	9.00	3.15	1.230	40	.226
Condition 4 (Number-Letter Switching) Primary Measure Scaled Score	21	8.62	3.81	21	8.52	3.39	0.086	40	.932
Primary Contrast 2 (Condition 4 - Condition 2) Contrast Scaled Score	21	8.52	2.80	21	10.05	2.25	-1.944	40	.059
D-KEFS Verbal Fluency Test									
Condition 1 (Letter Fluency) Primary Measure Scaled Score	21	10.52	3.80	21	10.24	3.91	0.240	40	.812
Condition 2 (Category Fluency) Primary Measure Scaled Score	21	12.00	3.24	21	12.43	3.66	-0.402	40	.690
Condition 3 (Category Switching) Total Correct Response Scaled Score	21	12.52	4.14	21	10.38	2.31	2.070	40	**.045**
Condition 3 (Category Switching) Total Switching Accuracy Scaled Score	21	12.86	3.34	21	11.57	2.09	1.497	40	.142
Primary Contrast Measure 1 (Condition 1 - Condition 2) Contrast Scaled Score	21	8.57	3.16	21	7.81	3.11	0.788	40	.435
Primary Contrast Measure 2 (Condition 3 - Condition 2) Contrast Scaled Score	21	10.43	3.17	21	8.33	3.53	2.025	40	.050
D-KEFS Tower Task									
Primary Measure Total Achievement Scaled Score	21	10.38	1.60	21	10.33	2.83	0.067	40	.947
Mean First Move Time Scaled Score	21	10.52	1.86	21	10.48	1.78	0.085	40	.933
	n	*M*	*SD*	n	*M*	*SD*	*U*	*df*	*p*
Colour-Word Interference Test									
Condition 1 (Colour Naming) Primary Measure Scaled Score	21	9.76	2.30	21	7.76	2.77	119.50	42	**.010**
Condition 2 (Word Reading) Primary Measure Scaled Score	21	10.19	3.20	21	9.29	2.92	167.50	42	.174
Condition 3 (Inhibition) Primary Measure Scaled Score	21	9.90	3.71	21	8.43	3.04	141.50	42	**.045**
Primary Combined Measure (Condition 1 + Condition 2) Composite Scaled Score	21	10.19	2.62	21	8.76	2.34	134.00	42	**.028**

Variable	ARMS-LS			ARMS-HS			ARMS-LS vs. ARMS-HS		
	n	*M*	*SD*	n	*M*	*SD*	*t*	*df*	*p*
Primary Contrast Measure 1 (Condition 3 - Condition 1) Contrast Scaled Score	21	10.14	3.28	21	10.67	2.80	218.00	42	.949

|No adjustments were made for multiple comparisons |Bold = Sig. correlations at *p*< .05 (uncorrected)

3.2.5 Social Cognition Measures

There were no significant differences between the two groups (ARMS-LS vs. ARMS-HS) regarding the participants' performance on the False-belief Picture Sequencing Task (4.89 [*SD* 1.24] vs. 5.02 [*SD* 1.15]; *t* (40)= -0.37, *p*= .716), the Reading the Mind in the Eyes Test (22.14 [*SD* 2.5] vs. 22.57 [*SD* 1.81]; *t* (40)= -0.64, *p*= .527), nor the Hinting Task (17.91 [*SD* 1.92] vs. 18.00 [*SD* 1.73] *t* (40)= -0.17, *p*= .867).

3.2.6 Electroencephalographic Data

ERP group analysis included 37 participants (19 ARMS-LS and 18 ARMS-HS individuals). MMN amplitudes in response duration and frequency deviants had means and standard deviations of -2.31 [*SD* 2.19] µV vs. -1.96 [*SD* 2.31] µV and -1.87 [*SD* 2.31] µV vs. -1.44 [*SD* 2.19] µV. P3a amplitudes were 2.51 [*SD* 2.37] µV vs. 0.98 [*SD* 2.24] µV and 1.09 [*SD* 2.03] µV vs. 1.37 [*SD* 2.20] µV, respectively. No significant differences between the two groups were revealed for MMN or P3a amplitudes in response to duration or frequency deviants, respectively. See Table 3.2.6-1 and Figure 3.2.6-1 for details.

Table 3.2.6-1 ERP Data: Low-symptomatic (ARMS-LS) vs. high-symptomatic (ARMS-HS) study participants by CCS Median-Split

Variable	ARMS-LS			ARMS-HS			ARMS-LS vs. ARMS-HS		
	n	*M*	*SD*	n	*M*	*SD*	*t*	*df*	*p*
Duration MMN [µV]	19	-2.31	2.19	18	-1.96	2.31	-0.482	35	.633
Duration P3a [µV]	19	2.51	2.37	18	0.98	2.24	2.023	35	.051
Frequency MMN [µV]	19	-1.87	2.31	18	-1.44	2.19	-0.578	35	.567
Frequency P3a [µV]	19	1.09	2.03	18	1.37	2.20	-0.396	35	.694

|No adjustments were made for multiple comparisons

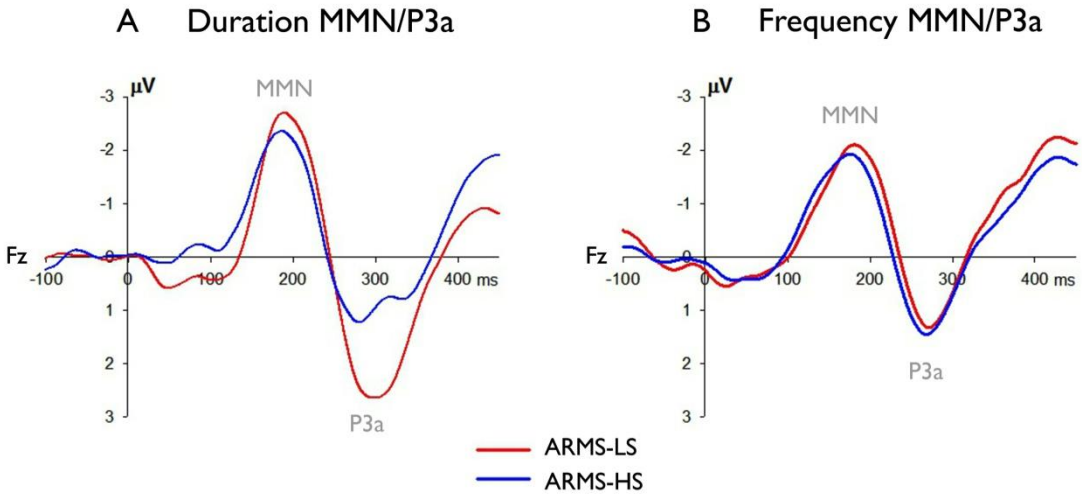

Figure 3.2.6-1 Group average event related potentials (i.e. MMN/P3a waveforms) at the frontal central electrode site (Fz) to (A) duration and (B) frequency deviant tones of study participants with low versus high symptom expression (ARMS-LS vs. ARMS-HS) by CCS Median-Split recorded during an auditory oddball task (see Chapter 2.2.5 for details).

3.2.7 Summary and Conclusion

Group analysis by severity of At-risk Mental State (ARMS-LS vs. ARMS-HS) revealed significant group differences for mean cortical GM thickness data. In both hemispheres mean GM thickness was significantly reduced in the clinically more affected At-risk sub-sample (ARMS-HS). The effect size for the difference in mean GM thickness (averaged across both hemispheres) was small to moderate. Since the groups did not differ in their mean age, gender, handedness, history of substance abuse, and exposure to psychotropic medication, these factors are unlikely to contribute to GM group differences.

Notably, the two groups did not differ in eTIV, or in any other morphological measure assessed while differences in cortical GM thickness appeared to determine the degree of psychopathology in ARMS. Correlation analysis of the full ARMS dataset confirmed a significant association of mean GM thickness with CCS for the left hemisphere (*rho (40)*= -.326, *p*= .035), right hemisphere (*rho (40)*= -.334, *p*= .031), and the entire cortex (*rho (40)*= -.307, *p*= .048).

ARMS-HS status was accompanied by significantly more pronounced impairments in the functional domain according to the SOFAS, GF:Social and GF:Role. Effect sizes were small to moderate for all of these measures. Group

differences were also revealed in the neurocognitive domain where the two groups differed on a sub-score of the Verbal Fluency Test (Condition 3 (Category Switching) Total Correct Response Scaled Score), as well as on three sub-scores of the Colour-Word Interference Test (i.e., Condition 1 (Colour Naming) Primary Measure Scaled Score; Condition 3 (Inhibition) Primary Measure Scaled Score; Primary Combined Measure (Condition 1 + Condition 2) Composite Scaled Score). Effect sizes were small to moderate for all of these measures. The two groups did not differ significantly in social cognition, nor regarding psychophysiological data.

3.3 Regional Grey Matter Thickness vs. Assessment Data

Results from the previous analyses have provided evidence that reduced total mean GM thickness is associated with severity of at-risk mental state. The current section explores this finding in more detail at a regional level via correlation analyses and investigates the potential association of regional GM reduction with functional outcome, cognitive performance, social cognition, and psychophysiological data (i.e., MMN and P3a amplitudes), respectively.

To test this hypothesis, vertex-wise correlation analyses across the surface of each hemisphere ($p < .05$ corrected) was performed for each functional domain. Correlation maps were produced from general linear models at each location (vertex) across the surface with red colour maps indicating positive correlations and blue colour maps indicating negative correlations. Statistical maps with significant correlations and corresponding data tables are presented in the following section; those confirming correlations at $p < .05$ (uncorrected) but not surviving correction for multiple comparisons using cluster size inference by means of Monte-Carlo simulation are presented in APPENDIX - SECTION II (starting from page 103).

3.3.1 Symptom Ratings

CAARMS composite ratings

High CCS symptom rating scores correlated with reduced GM thickness in the left and right superior frontal cortex, the right precentral cortex, the right anterior cingulate, and the right medial occipito-temporal cortex (i.e. lingual gyrus) while negative symptom expression (CAARMS negative symptom score) correlated with reduced GM in left and right superior occipital cortex. No significant regional correlations were confirmed for GM thickness by CAARMS positive symptom score (CPSS).

Table 3.3.1-1 CCS vs. Grey Matter Thickness

Cluster	Anatomical Parcellation *	Hemisphere	Talairach (X Y Z)			Size (mm^2)	Cluster-wise *p*
1	G_front_sup	L	-6.7	-25.0	51.8	2911.26	< 0.001
2	G_front_sup	R	7.4	-8.3	58.9	4669.03	< 0.001
3	G_oc-temp_med-Lingual	R	5.4	-85.4	0.5	1897.78	0.008
4	G_and_S_cingul-Ant	R	11.7	38.9	2.0	2089.20	0.004

| * Annotation by Vertex of max sig. in cluster

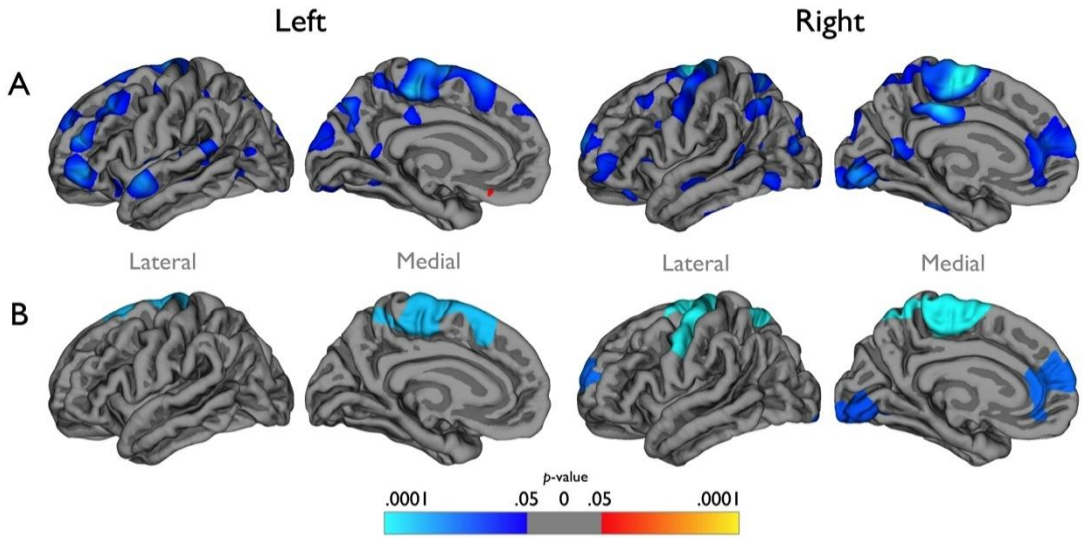

Figure 3.3.1-1 Statistical correlation maps of cerebral grey matter thickness with CAARMS composite scores (CCS) for left and right hemispheres. (A) Statistical maps with a significance threshold of *p*= .05 (uncorrected). (B) Statistical maps from (A) corrected for multiple comparisons using cluster size inference by means of Monte-Carlo simulation with 10.000 iterations and a significance threshold of *p*= .05.

Table 3.3.1-2 CAARMS negative symptom score vs. Grey Matter Thickness

Cluster	Anatomical Parcellation *	Hemisphere	Talairach (X Y Z)			Size (mm^2)	Cluster-wise *p*
1	S_oc_sup_and_transversal	L	-31.0	-69.6	29.0	2729.26	< 0.001
2	G_occipital_sup	R	13.0	-82.2	30.4	1461.12	0.041

| * Annotation by Vertex of max sig. in cluster

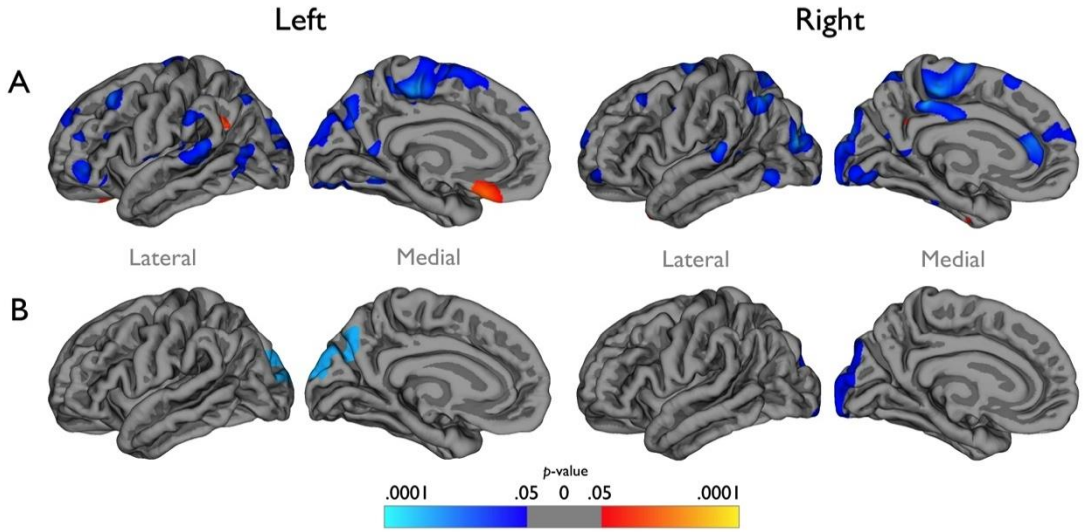

Figure 3.3.1-2 Statistical correlation maps of cerebral grey matter thickness with CAARMS negative symptom scores for left and right hemispheres. (A) Statistical maps with a significance threshold of *p*= .05 (uncorrected). (B) Statistical maps from (A) corrected for multiple comparisons using cluster size inference by means of Monte-Carlo simulation with 10.000 iterations and a significance threshold of *p*= .05.

3.3.2 Function Ratings

Low global (GAF), socio-occupational (SOFAS), and social/role function ratings (GF:Social, GF:Role) were associated with reduced regional GM thickness in frontal, prefrontal, and occipito-temporal cortex. Cortical GM correlation maps for each functional assessment rating score are reported below.

Global Assessment of Functioning (GAF)

Lower ratings scores (i.e. more impaired global function levels) were significantly correlated with reduced GM thickness in left middle frontal gyrus, left occipital pole, and right precentral gyrus.

Table 3.3.2-1 GAF vs. Grey Matter Thickness

Cluster	Anatomical Parcellation *	Hemisphere	Talairach (X Y Z)			Size (mm^2)	Cluster-wise *p*
1	G_front_middle	L	-39.0	45.8	2.4	1409.63	0.048
2	Pole_occipital	L	-11.0	-99.1	7.0	1431.88	0.044
3	G_precentral	R	35.0	-6.7	52.0	2883.62	< 0.001

| * Annotation by Vertex of max sig. in cluster

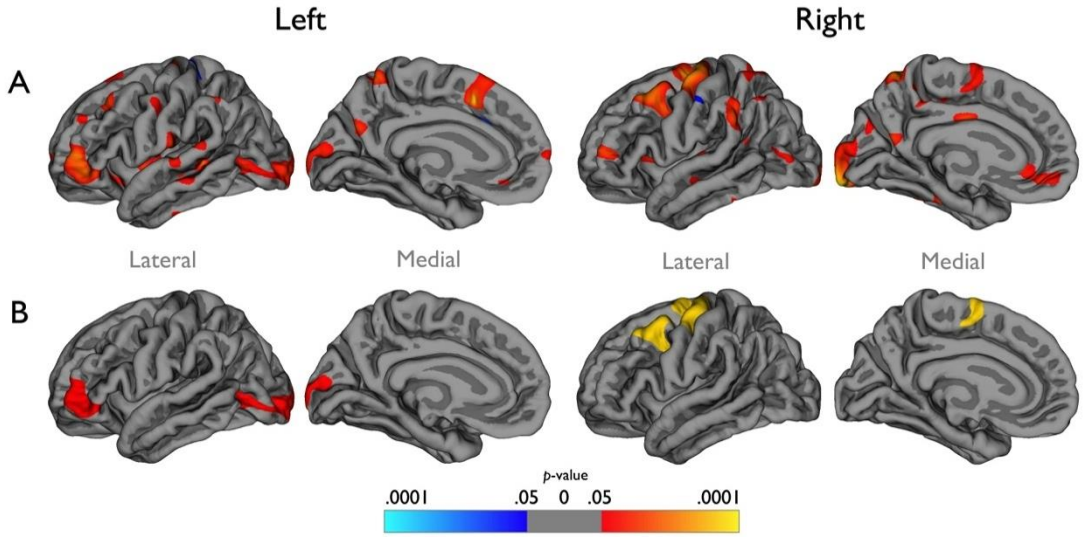

Figure 3.3.2-1 Statistical correlation maps of cerebral grey matter thickness with GAF scores for left and right hemispheres. (A) Statistical maps with a significance threshold of *p*= .05 (uncorrected). (B) Statistical maps from (A) corrected for multiple comparisons using cluster size inference by means of Monte-Carlo simulation with 10.000 iterations and a significance threshold of *p*= .05.

Social and Occupational Function Assessment Scale (SOFAS)

Lower levels of socio-occupational functioning correlated with decreased regional cortical GM thickness in middle frontal cortex, left subcentral cortex, right precentral sulcus and right medial occipito-temporal cortex.

Table 3.3.2-2 SOFAS vs. Grey Matter Thickness

Cluster	Anatomical Parcellation *	Hemisphere	Talairach (X Y Z)			Size (mm^2)	Cluster-wise *p*
1	G_front_middle	L	-36.8	50.1	-2.7	3476.39	< 0.001
2	G_and_S_subcentral	L	-56.7	-10.3	12.8	2417.96	< 0.001
3	S_front_middle	R	28.0	45.7	3.3	1946.56	0.007
4	S_precentral-inf-part	R	35.8	6.1	32.9	1717.02	0.016
5	S_oc-temp_med_and_Lingual	R	37.6	-24.9	-19.9	2356.46	0.002

| * Annotation by Vertex of max sig. in cluster

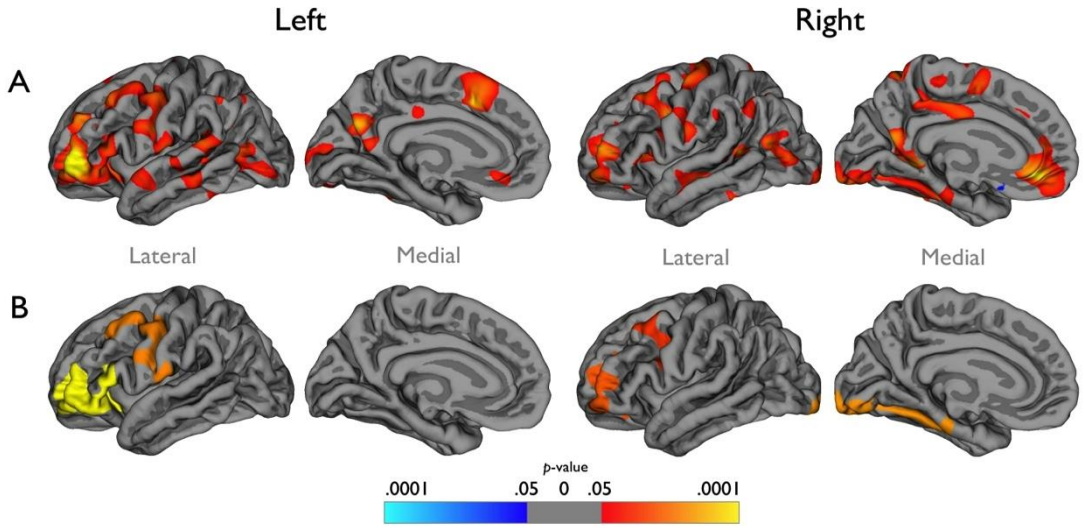

Figure 3.3.2-2 Statistical correlation maps of cerebral grey matter thickness with SOFAS scores for left and right hemispheres. (A) Statistical maps with a significance threshold of *p*= .05 (uncorrected). (B) Statistical maps from (A) corrected for multiple comparisons using cluster size inference by means of Monte-Carlo simulation with 10.000 iterations and a significance threshold of *p*= .05.

Global Functioning: Social Scale (GF:Social)

Lower levels of global function rating scores correlated with reduced GM thickness bilaterally in middle frontal and precentral cortex, left fronto-marginal cortex, and right occipital pole.

Table 3.3.2-3 GF:Social vs. Grey Matter Thickness

Cluster	Anatomical Parcellation *	Hemisphere	Talairach (X Y Z)			Size (mm^2)	Cluster-wise *p*
1	G_and_S_frontomargin	L	-30.8	48.1	0.2	4522.73	< 0.001
2	Pole_occipital	R	20.9	-95.2	-6.7	1780.13	0.012
3	G_front_middle	R	36.1	18.5	44.6	1805.93	0.011
4	S_front_sup	R	20.8	10.0	47.3	1725.87	0.015

| * Annotation by Vertex of max sig. in cluster

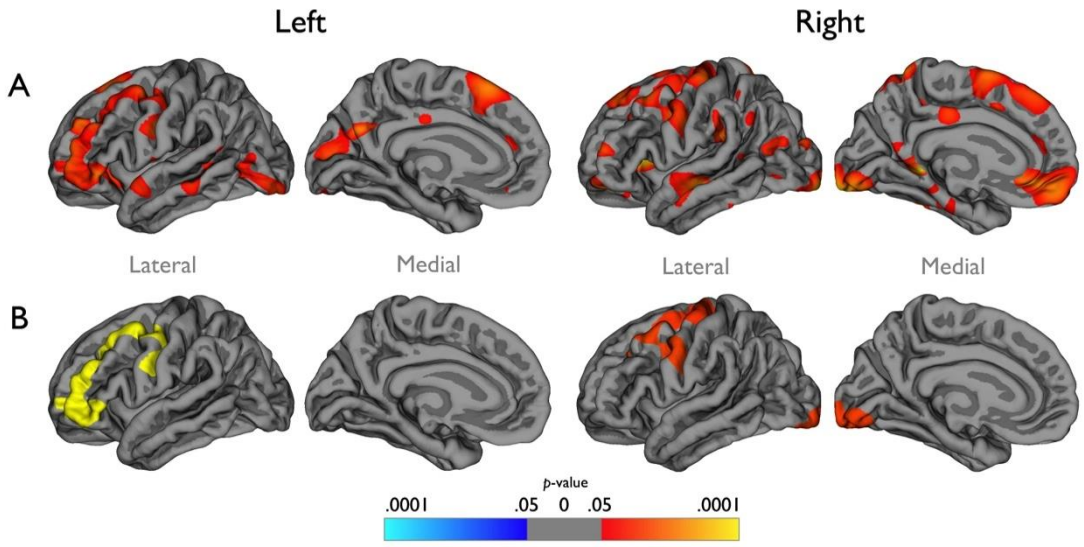

Figure 3.3.2-3 Statistical correlation maps of cerebral grey matter thickness with GF:Social scores for left and right hemispheres. (A) Statistical maps with a significance threshold of *p*= .05 (uncorrected). (B) Statistical maps from (A) corrected for multiple comparisons using cluster size inference by means of Monte-Carlo simulation with 10.000 iterations and a significance threshold of *p*= .05.

Global Functioning: Role Scale (GF:Role)

Poor role functioning correlated with reduced GM thickness bilaterally in middle frontal cortex, left precentral cortex, right middle temporal gyrus, and right occipito-temporal sulcus.

Table 3.3.2-4 GF:Role vs. Grey Matter Thickness

Cluster	Anatomical Parcellation *	Hemisphere	Talairach (X Y Z)			Size (mm^2)	Cluster-wise *p*
1	G_front_middle	L	-38.1	47.6	0.8	4225.97	< 0.001
2	G_and_S_subcentral	L	-59.7	-9.9	11.0	1939.76	0.005
3	S_oc-temp_lat	R	47.7	-43.4	-11.5	2294.17	0.002
4	S_front_middle	R	28.2	46.6	1.5	2850.37	0.001
5	G_temporal_middle	R	48.3	-3.1	-25.9	1422.16	0.049

| * Annotation by Vertex of max sig. in cluster

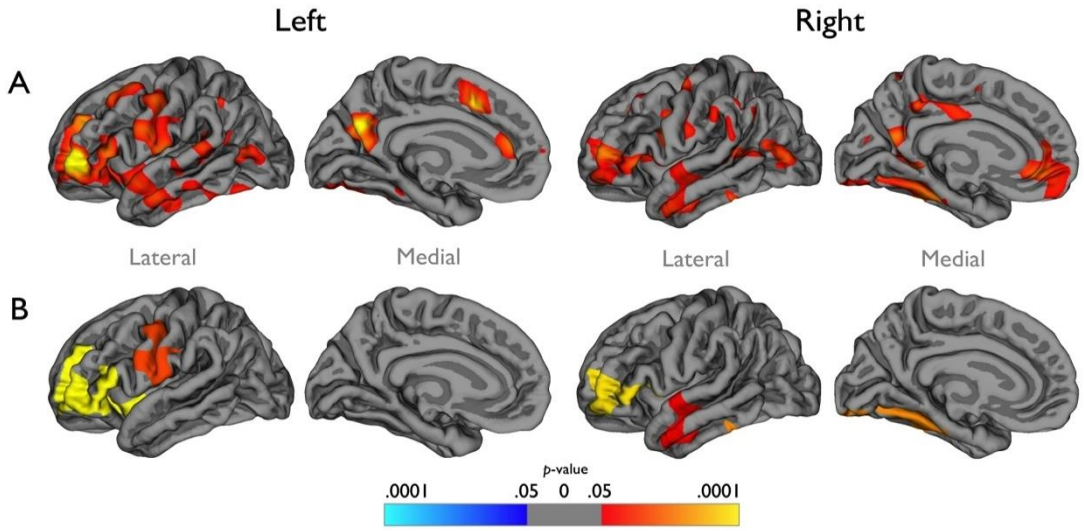

Figure 3.3.2-4 Statistical correlation maps of cerebral grey matter thickness with GF:Role scores for left and right hemispheres. (A) Statistical maps with a significance threshold of *p*= .05 (uncorrected). (B) Statistical maps from (A) corrected for multiple comparisons using cluster size inference by means of Monte-Carlo simulation with 10.000 iterations and a significance threshold of *p*= .05.

The pattern of reduced regional cortical GM by degree of functional impairment is consistent across the four instruments thereby mirroring the inter-correlation of the four rating instruments. Function rating scores also correlated with CCS but not negative symptom ratings (see Table 3.3.2-5). However, the degree of negative symptom expression was associated with reduced GM thickness in occipito-parietal cortex.

Table 3.3.2-5 Functional Measures vs. Symptom Ratings

	GAF		SOFAS		GF:Social		GF:Role	
	rho (42)	*p*	*rho (42)*	*p*	*rho(42)*	*p*	*rho(42)*	*p*
GAF			0.78	< .000	0.54	< .000	0.70	< .000
SOFAS	0.78	< .000			0.63	< .000	0.83	< .000
GF:Social	0.54	< .000	0.63	< .000			0.50	.001
GF:Role	0.70	< .000	0.83	< .000	0.50	.001		
CCS	-0.36	.019	-0.36	.020	-0.34	.028	-0.34	.029
CNSS	-0.24	.122	-0.26	.095	-0.19	.217	-0.28	.072

| GAF = Global Assessment of Functioning Scale | SOFAS = Social and Occupational Functioning Scale
| GF:Social = Global Functioning: Social Scale | GF:Role = Global Functioning: Role Scale
| CCS = CAARMS composite score | CNSS = CAARMS negative symptom score

Taken together the correlation maps identify the dorsolateral prefrontal, frontal, and occipital cortex as the neural substrate of impaired function levels across the global, social and occupational domains, thus pointing to deficits in executive function (e.g., working memory, planning, and attention as they are mediated, for instance, by the dorsolateral prefrontal cortex) and impaired communication skills including social cognition which involve left frontal and right inferior temporal cortex. The latter also partly overlaps with the frontal clusters identified for symptom expression associations with reduced regional GM. Reductions in other cortical regions, such as the prefrontal, anterior limbic, parietal, and occipital cortex, are associated with low-grade psychotic symptoms. The subsequent section will investigate more specifically the associations of regional GM deficits with deficits in the respective cognitive domains.

3.3.3 Neurocognitive Measures

Delis-Kaplan Executive Functioning System: Verbal Fluency Test (VFT)

VFT CONDITION 2 (CATEGORY FLUENCY)

Lower performance on the VFT Condition 2 (i.e. the total number of correct responses without repetitions generated for the target category) correlated with reduced GM thickness in left anterior cingulate and medial orbito-frontal cortex.

Table 3.3.3-1 VFT Condition 2 Primary Measure Scaled Score vs. Grey Matter Thickness

Cluster	Anatomical Parcellation *	Hemisphere	Talairach (X Y Z)			Size (mm^2)	Cluster-wise *p*
1	G_and_S_cingul-Ant	L	-7.3	39.7	-4.2	1653.76	.025

| * Annotation by Vertex of max sig. in cluster

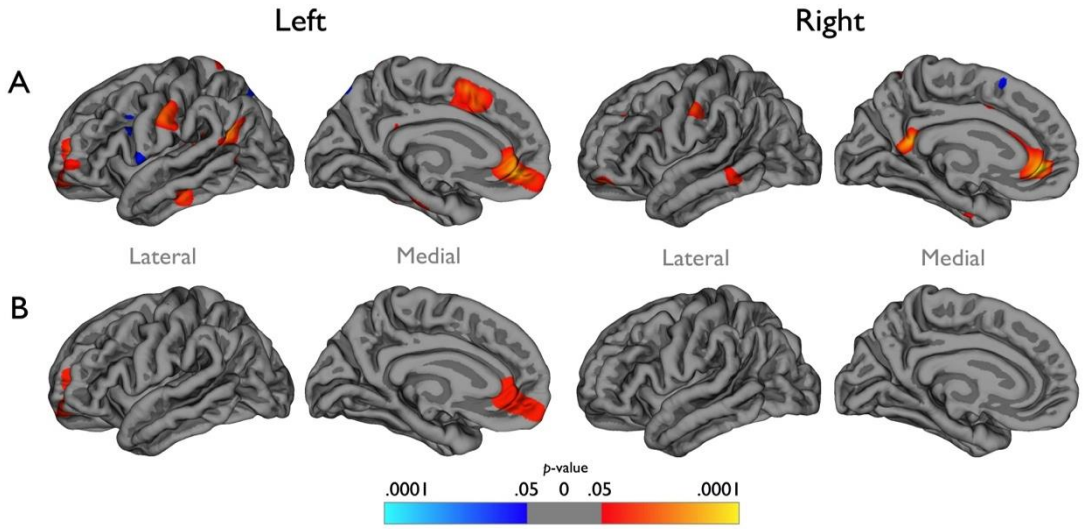

Figure 3.3.3-1 Statistical correlation maps of cerebral grey matter thickness with VFT Condition 2 Primary Measure Scaled Scores for left and right hemispheres. (A) Statistical maps with a significance threshold of *p*= .05 (uncorrected). (B) Statistical maps from (A) corrected for multiple comparisons using cluster size inference by means of Monte-Carlo simulation with 10.000 iterations and a significance threshold of *p*= .05.

VFT CONDITION 3 (CATEGORY SWITCHING): TOTAL CORRECT RESPONSES

Fewer correct responses on the VFT Condition 3 (i.e. total number of correct responses without repetitions generated for each of the two target categories summed together) were associated with reduced GM thickness in the left middle frontal cortex, as well as superior temporal areas, and inferior parietal/occipital cortex in both hemispheres.

Table 3.3.3-2 VFT Condition 3 Total Correct Response Scaled Score vs. Grey Matter Thickness

Cluster	Anatomical Parcellation *	Hemisphere	Talairach (X Y Z)			Size (mm^2)	Cluster-wise *p*
1	S_temporal_sup	L	-38.6	-53.7	24.6	2257.97	0.003
2	S_front_middle	L	-28	45.1	5.1	2318.34	0.003
3	G_and_S_occipital_inf	L	-22.2	-82.9	-4.3	2079.55	0.006
4	S_temporal_sup	R	39.4	-56.3	20.4	2331.5	0.003
5	Pole_occipital	R	14.6	-85.8	-2.2	1491.87	0.050

| * Annotation by Vertex of max sig. in cluster

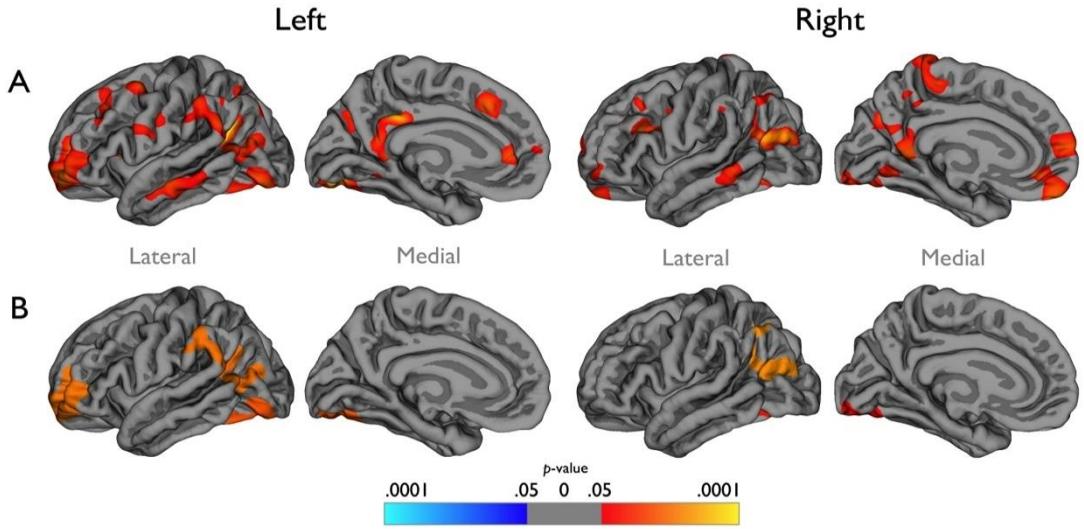

Figure 3.3.3-2 Statistical correlation maps of cerebral GM thickness with VFT Condition 3 Total Correct Response Scaled Scores for left and right hemispheres. (A) Statistical maps with a significance threshold of *p*= .05 (uncorrected). (B) Statistical maps from (A) corrected for multiple comparisons using cluster size inference by means of Monte-Carlo simulation with 10.000 iterations and a significance threshold of *p*= .05.

VFT CONDITION 3 (CATEGORY SWITCHING): TOTAL SWITCHING ACCURACY

Lower Total Switching Accuracy on the VFT Condition 3 (i.e. the total number of correct switches from one target category to the other category) was associated with reduced GM thickness in left middle frontal and precentral/inferior frontal areas, and bilaterally in fusiform and lateral occipital cortex.

Table 3.3.3-3 VFT Condition 3 Total Switching Accuracy Scaled Score vs. Grey Matter Thickness

Cluster	Anatomical Parcellation *	Hemisphere	Talairach (X Y Z)			Size (mm^2)	Cluster-wise *p*
1	S_front_middle	L	-26.8	45.9	3.1	2269.29	0.003
2	S_central	L	-38.1	-18.5	32.5	3044.8	< 0.001
3	G_and_S_occipital_inf	L	-22.6	-82.8	-4.7	2221.72	0.004
4	Pole_occipital	R	12.3	-90.1	-1.9	1875.53	0.012

| * Annotation by Vertex of max sig. in cluster

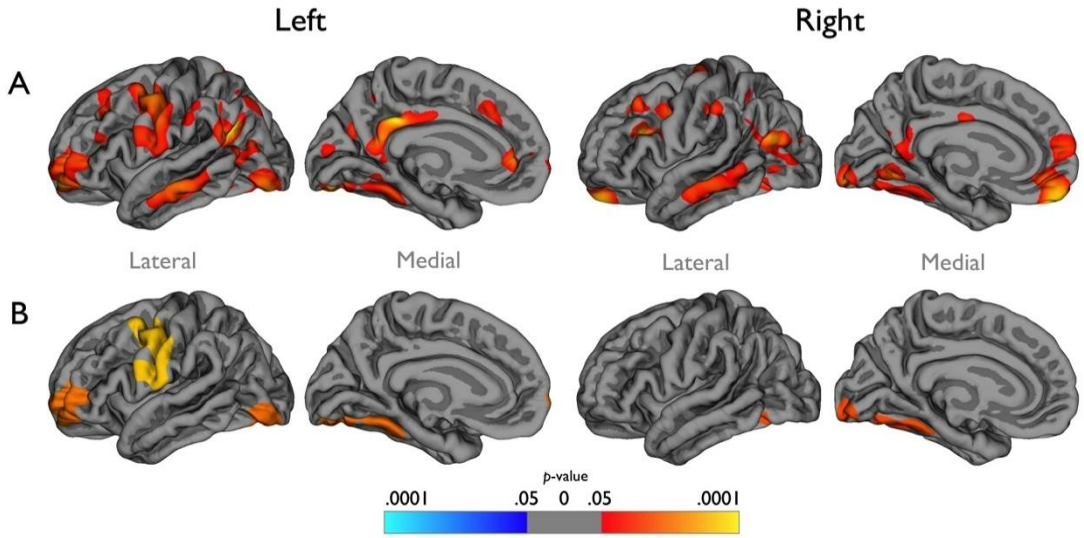

Figure 3.3.3-3 Statistical correlation maps of cerebral grey matter thickness with VFT Condition 3 Total Switching Accuracy Scaled Scores for left and right hemispheres. (A) Statistical maps with a significance threshold of *p*= .05 (uncorrected). (B) Statistical maps from (A) corrected for multiple comparisons using cluster size inference by means of Monte-Carlo simulation with 10.000 iterations and a significance threshold of *p*= .05.

Delis-Kaplan Executive Functioning System: Tower Task

TOWER TASK TOTAL ACHIEVEMENT

Better Tower Task Total Achievement scores (i.e., requiring fewer moves to correctly complete a task) correlated with reduced GM thickness in medial occipito-temporal cortex.

Table 3.3.3-4 Tower Task Primary Measure Total Achievement Scaled Score vs. Grey Matter Thickness

Cluster	Anatomical Parcellation *	Hemisphere	Talairach (X Y Z)			Size (mm^2)	Cluster-wise *p*
1	G_oc-temp_med-Lingual	L	-5.8	-71.2	-3.7	1579.83	0.033

| * Annotation by Vertex of max sig. in cluster

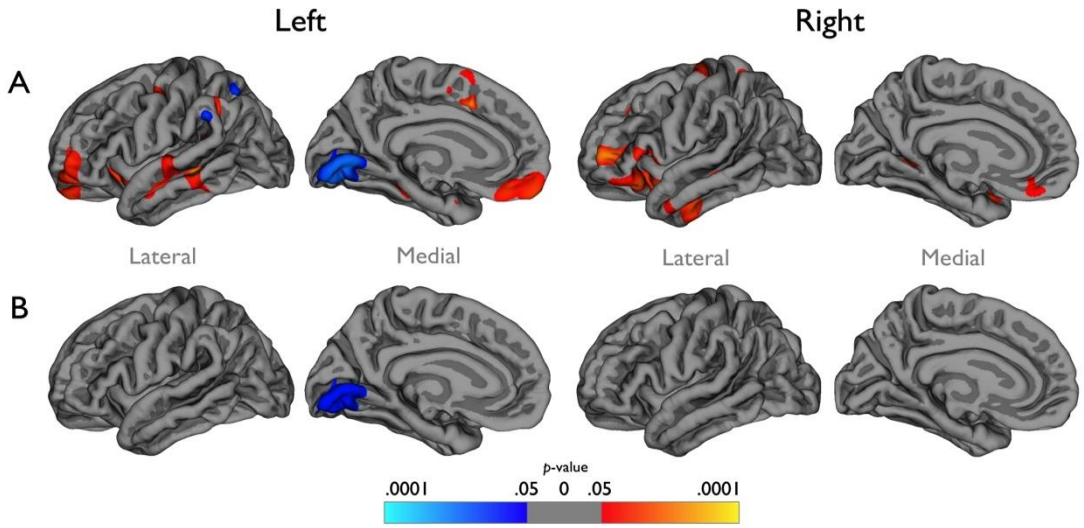

Figure 3.3.3-4 Statistical correlation maps of cerebral grey matter thickness with Tower Task Primary Measure Total Achievement Scaled Scores for left and right hemispheres. (A) Statistical maps with a significance threshold of *p*= .05 (uncorrected). (B) Statistical maps from (A) corrected for multiple comparisons using cluster size inference by means of Monte-Carlo simulation with 10.000 iterations and a significance threshold of *p*= .05.

California Verbal Learning Test (CVLT-II)

Reduced GM thickness bilaterally in superior frontal, left middle-anterior cingulate and right precentral cortex correlated with impaired performance on recall of word List A for both 'Short Delay Free Recall' and 'Long Delay Cued Recall' tasks.

CVLT-II SHORT DELAY FREE RECALL

Table 3.3.3-5 List A Short Delay Free Recall Std. Score vs. Grey Matter Thickness

Cluster	Anatomical Parcellation *	Hemisphere	Talairach (X Y Z)			Size (mm^2)	Cluster-wise *p*
1	G_and_S_cingul-Mid-Ant	L	-10.4	14.3	45.7	1870.71	0.013
2	G_precentral	R	26.5	-15.5	64.2	1819.59	0.015

| * Annotation by Vertex of max sig. in cluster

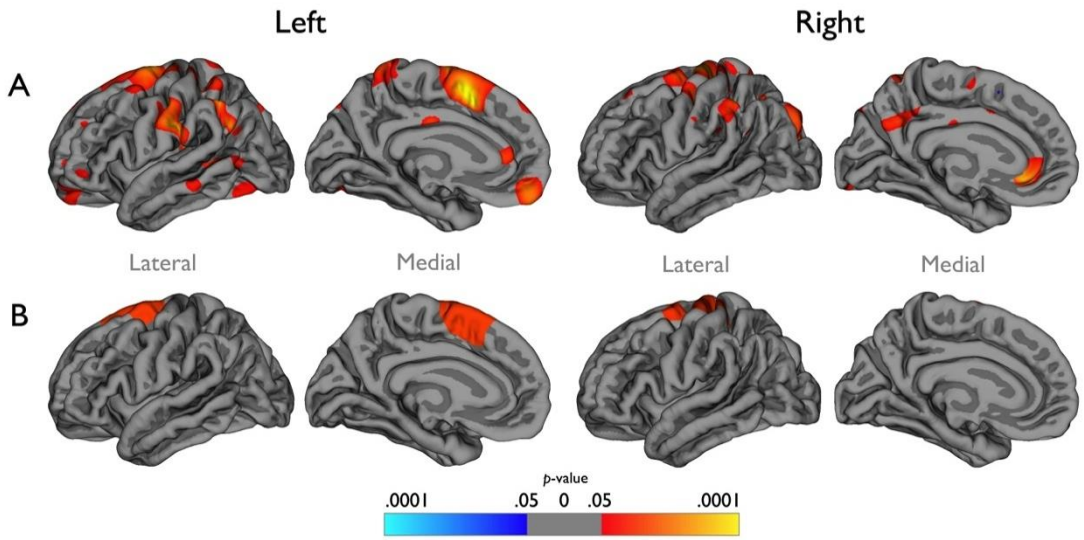

Figure 3.3.3-5. Statistical correlation maps of cerebral grey matter thickness with List A Short Delay Free Recall Std. Scores for left and right hemispheres. (A) Statistical maps with a significance threshold of *p*= .05 (uncorrected). (B) Statistical maps from (A) corrected for multiple comparisons using cluster size inference by means of Monte-Carlo simulation with 10.000 iterations and a significance threshold of *p*= .05.

CVLT-II LONG DELAY CUED RECALL

Table 3.3.3-6 List A Long Delay Cued Recall Std. Score vs. Grey Matter Thickness

Cluster	Anatomical Parcellation *	Hemisphere	Talairach (X Y Z)			Size (mm^2)	Cluster-wise *p*
1	G_and_S_cingul-Mid-Ant	L	-10.9	15.3	41.8	1468.16	0.047
2	G_precentral	R	27.5	-12.6	64	1764.8	0.020

| * Annotation by Vertex of max sig. in cluster

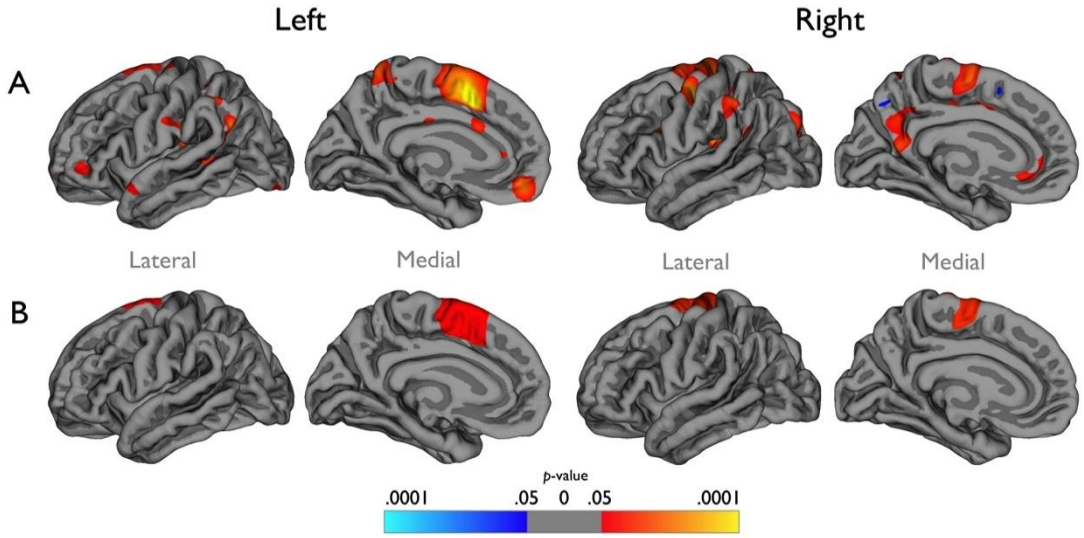

Figure 3.3.3-6 Statistical correlation maps of cerebral grey matter thickness with List A Long Delay Cued Recall Std. Scores for left and right hemispheres. (A) Statistical maps with a significance threshold of *p*= .05 (uncorrected). (B) Statistical maps from (A) corrected for multiple comparisons using cluster size inference by means of Monte-Carlo simulation with 10.000 iterations and a significance threshold of *p*= .05.

CVLT-II RECOGNITION "TOTAL HITS"

Fewer recognitions ("TOTAL HITS") of word List A items were correlated with a pattern of reduced GM thickness that encompassed segments of precentral, postcentral, and superior frontal cortical areas of the right hemisphere.

Table 3.3.3-7 Recognition Correct Std. Score "TOTAL HITS" vs. Grey Matter Thickness

Cluster	Anatomical Parcellation *	Hemisphere	Talairach (X Y Z)			Size (mm^2)	Cluster-wise *p*
1	S_central	R	38.9	-7.9	45	4623.71	< 0.001

| * Annotation by Vertex of max sig. in cluster

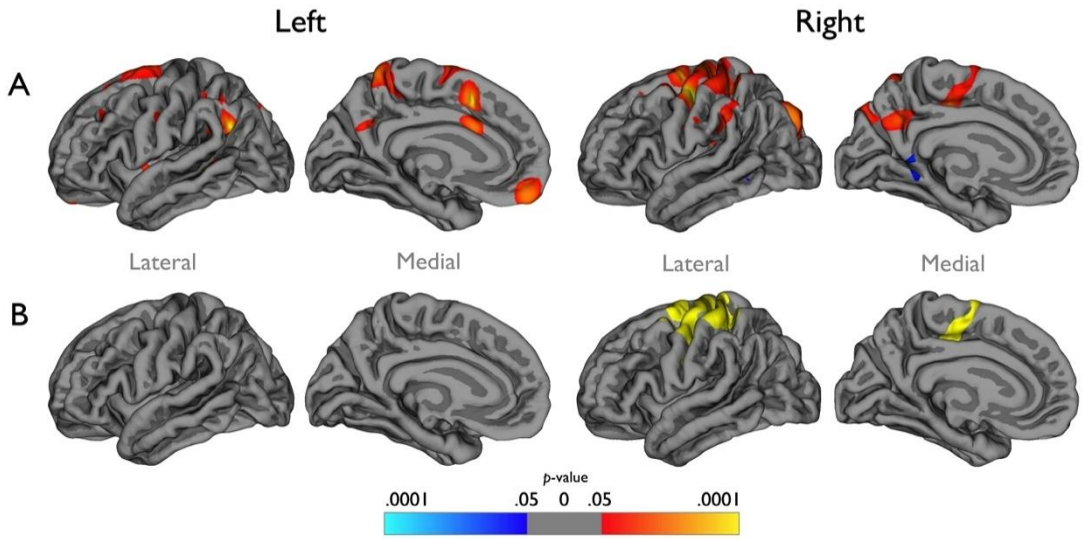

Figure 3.3.3-7 Statistical correlation maps of cerebral grey matter thickness with Recognition Correct Std. Scores "TOTAL HITS" for left and right hemispheres. (A) Statistical maps with a significance threshold of *p*= .05 (uncorrected). (B) Statistical maps from (A) corrected for multiple comparisons using cluster size inference by means of Monte-Carlo simulation with 10.000 iterations and a significance threshold of *p*= .05.

Wechsler Memory Scale (WMS-III)

Lower scores of the Letter-Number Sequencing Task correlated with reduced regional GM in superior frontal, precentral (gyrus frontalis inferior), insular, middle temporal and inferior parietal regions and bilaterally in the precuneus. Moreover, lower scores on the Digit Span Test were associated with reduced GM thickness in precentral (gyrus frontalis inferior) and inferior temporal cortex and increased GM thickness in superior frontal, middle frontal and lingual cortex. However, these correlation clusters were not confirmed by Monte Carlo simulation (Figures and Tables in APPENDIX, pages 141 *ff*).

3.3.4 Social Cognition Measures

Correlation analyses of regional GM thickness with socio-cognitive assessments revealed significant brain structure/function associations at $p < .05$. For instance, lower performance on the Hinting Task and the False-belief Picture Sequencing Task were correlated with reduced GM thickness bilaterally in the supra marginal gyrus, left superior frontal and middle temporal gyrus, and right parahippocampal gyrus, while lower performance on the Reading the Mind in the Eyes Test was associated with reduced GM thickness in the left supramarginal and anterior cingulate gyrus, and right superior frontal and inferior parietal areas (Figures and Tables in APPENDIX, pages 146 *ff*). However, these clusters were not confirmed by Monte Carlo simulation.

3.3.5 Electroencephalographic Data

Reduced regional GM thickness in superior frontal, pericalcarine, lateral occipital, and temporal pole areas was associated with smaller MMN amplitudes in response to duration deviants whereas reduced GM in superior temporal and insular areas correlated with smaller MMN amplitudes in response to frequency deviants. Increased GM thickness in inferior frontal, superior temporal and posterior cingulate areas correlated with smaller P3a amplitudes in response to duration deviants whereas reduced GM in precentral, superior frontal, and superior temporal areas were associated with smaller P3a amplitudes in response to frequency deviants. However, none of these correlation clusters were statistically confirmed by Monte Carlo simulation (Figures and Tables in APPENDIX, pages 150 *ff*).

DISCUSSION

4 DISCUSSION

Schizophrenia is marked by a profound disruption in cognition and emotion; many patients attempt suicide, and most experience a lifetime of disability. Yet, the disorder is still poorly understood, despite a 100-year history of schizophrenia research. More recently the concept of duration of untreated psychosis (DUP) has attracted much interest for its alleged effects on treatment response in schizophrenia. A longer DUP has been directly associated with poor response to antipsychotic medication, more pronounced symptom expression, reduced quality of life following transition to schizophrenia, a generally a poorer prognosis [Marshall et al., 2005; Harris et al., 2005], and reduction in whole brain GM volume [Malla et al., 2011]. These findings have motivated a more proactive early intervention in the prodromal phase of illness away from solely responding to acute psychosis. Hence, the reliable identification of the schizophrenia prodrome in young people considered "at-risk" of developing this severe mental illness is an important prerequisite to this approach which is about to enter mainstream clinical practice despite the limitations in the predictive specificity of the clinical criteria that define, for instance, the At-Risk Mental State (ARMS) syndrome. These limitations are increasingly addressed by brain imaging research, which has added substantial evidence to the notion of emerging and progressive grey and white matter abnormalities in the early phase of illness [Pantelis et al., 2003; Sun et al., 2009]. Moreover, deficits in the neurocognitive [Fusar-Poli et al., 2012a] and neurophysiological [Shin et al., 2009; Bodatsch et al., 2011] domain also appear to hold great promise as putative predictors of transition to psychosis.

The main objective of the current project was to evaluate potential associations of early brain pathology (i.e. reduced grey and/or white matter) with the clinical signs and symptoms of emerging psychosis along with cognitive performances across different domains linked to schizophrenia in order to identify regional morphological deficits and their neuropsychological correlates in ARMS.

ARMS is defined by a significant drop of global functioning over a period of 12 months and having a close biological relative with a psychotic disorder or experiencing attenuated or very brief episodes of psychotic symptoms. Young

people meeting this profile have a profound risk of developing a psychotic disorder such as schizophrenia [McGorry, Yung, & Phillips, 2003].

Forty-two help-seeking young individuals meeting ARMS criteria determined by the Comprehensive Assessment of At-Risk Mental States (CAARMS) underwent clinical & cognitive assessments, electrophysiological recordings (EEG) and structural magnetic resonance imaging (MRI) obtained from a 1.5 Tesla scanner in the current study. FreeSurfer surface-based analysis was applied to evaluate early brain pathology in the study cohort using total brain volume, GM and WM volume, cortical GM thickness and surface area in each hemisphere, respectively, as measures of interest. Potential associations of morphological deficits with functional outcome, cognitive performance, social cognition, and psychophysiological data (i.e., MMN and P3a amplitudes), respectively, were investigated at a regional level using vertex-wise correlation analyses.

4.1 Brain Morphological correlates of Psychopathology

Brain imaging research has provided evidence of widespread grey and white matter abnormalities in young patients who have recently been diagnosed with schizophrenia [Rasser et al., 2010; Cohen et al., 2011]. Most of these neuroanatomical abnormalities appear to predate the clinical manifestation of schizophrenia and are present in individuals at "ultra high-risk" of developing psychosis [Pantelis et al., 2007; Mechelli et al., 2011; Borgwardt, McGuire, & Fusar-Poli, 2011]. Furthermore, research data indicate that the degree of the morphological deficit is also predictive of clinical outcome (i.e. transition from "At-risk mental state" to psychosis) [Fusar-Poli et al., 2011a], emphasizing the critical role of brain structural changes as putative signs of a neuropathology in the emerging disorder. Hence, it was hypothesized that the defining clinical criteria of ARMS (i.e. recent functional decline and emerging psychotic symptoms) correlate with putative signs of emerging brain pathology (i.e. GM/WM reductions). A median-split group analysis of UHR individuals with low versus high symptom expression (ARMS-LS vs. ARMS-HS) by CAARMS composite score (CCS) was performed, thus evaluating brain morphological differences within the symptom continuum of ARMS. Statistical

analyses revealed significantly reduced mean cortical GM thickness in the clinically more affected At-risk sub-sample versus the clinically less affected UHR group. Reduced GM thickness in ARMS-HS was accompanied by significantly more pronounced impairment across socio-occupational (SOFAS) and social/role functioning (GF:Social, GF:Role) when compared to ARMS-LS. The effect size between groups was small to moderate on all of these measures. Potential confounding factors, such as mean age, gender and handedness, history of substance abuse, and exposure to psychotropic medication are unlikely to have biased the observed GM group differences.

These findings suggest a potential role of GM thickness in predicting the level of ARMS psychopathology versus other morphometric measures, such as grey and white matter volumes or brain surface data. These data are also consistent with a previous report of reduced hemispheric mean cortical thickness of UHR individuals as intermediate between schizophrenia patients and healthy control subjects [Jung et al., 2011].

Psychopathology and impaired brain function associations of cortical GM thickness at a regional level was further evaluated by generating correlation maps with summative scores of CAARMS symptom ratings and function levels as rated on the Global Assessment of Functioning (GAF), socio-occupational Function Assessment (SOFA), and social/role functioning (GF:Role, GF:Social) using FreeSurfer. High total symptom rating scores (CCS) correlated ($p< .05$ corrected) with reduced GM thickness in left and right superior frontal gyri, right anterior cingulate, and right medial occipito-temporal cortex (i.e. lingual gyrus) while negative symptom expression correlated with reduced GM in left and right superior occipital gyri. The study cohort was moderately impaired across function levels of global, social and occupational domains. The frontal, prefrontal, and occipito-temporal cortex in both hemispheres were identified as the neural substrate of this impairment, thus pointing to deficits in executive function (e.g., working memory, planning, and attention), as they are mediated, for instance, by the dorsolateral prefrontal cortex [Minzenberg et al., 2009], and to deficits in communication skills, including impaired social cognition, which involve left frontal and right inferior temporal cortex [Beer & Ochsner, 2006].

Taken together, these findings suggest that regional GM thinning correlates with the degree of psychopathology in ARMS. Correlation maps identified the frontal, prefrontal, and occipito-temporal cortex as the neural substrate of functional impairment. Reduced regional GM in the prefrontal, anterior limbic, parietal, and occipital cortex was associated with low-grade psychotic symptoms. Moreover, cortical thickness and volume reduction of the affected brain areas have also been reported in FES and chronic schizophrenia [Kuperberg et al., 2003; Schultz et al., 2010; Nakamura et al., 2013], suggesting that the degree of GM reduction in ARMS may also determine the probability of developing a psychotic illness at a later stage. This, however, will require longitudinal data linking baseline GM data to clinical outcome. A longitudinal approach would also provide information about the potential trajectory of morphological brain changes in relation to changing psychopathology.

The subsequent section will discuss the findings of impaired cognition in ARMS and its relationship to GM thickness.

4.2 Grey Matter correlates of cognitive performance

Executive Functioning (EF): Impaired EF is considered a core cognitive deficit in schizophrenia [Wobrock et al., 2009]. EF refers to a set of cognitive abilities, which are a prerequisite for adaptive behaviour that occurs in a planned, organized, and contextually appropriate manner using working memory and attention. It includes the ability of problem solving and thinking ahead while monitoring and perhaps altering a course of action, which is primarily mediated by the frontal lobes [Johnson-Selfridge & Zalewski, 2001]. Different domains of executive functioning were tested in the UHR cohort by employing four subtests of the Delis-Kaplan Executive Function Scale (D-KEFS): the Trail Making Test, Verbal Fluency Test, Colour-Word Interference Test, and Tower Task.

The Trail Making Test (TMT) provides a measure of visual attention, psychomotor speed, and mental flexibility. The task requires the participant to connect a scattering of consecutive targets on a sheet of paper as fast as possible. It consists of two parts: In the first part (Condition 2) all targets are

numbers (i.e. 1, 2, 3, etc.) and the task is to connect consecutive numbers thereby measuring visuomotor speed. In the second part (Condition 4) targets are numbers and letters and the task is to connect items in alternating order (e.g., 1, A, 2, B, etc.). The “executive component” of Task Switching is measured by computing a contrast score of the time needed to complete Condition 4 minus Condition 2.

Zakzanis and colleagues [Zakzanis, Mraz, & Graham, 2005] investigated the functional anatomy of the TMT using fMRI, while participants performed the task using a custom-built fMRI-compatible writing device. The authors reported distinct left-sided dorsolateral and medial frontal activity for the "executive component" of the task, along with further task-induced activation in the insula, the middle and superior temporal cortices as well as in supplementary motor areas. In schizophrenia, many of these brain regions are also structurally compromised [Shenton et al., 2001], and lower performance on the TMT has been linked to GM volume reductions, particularly in the dorsolateral prefrontal cortex using VBM [Bonilha et al., 2008]. The current ARMS cohort found a correlation ($p< .05$ uncorrected) of reduced TMT performance (Primary Contrast 2; task switching ability) with clusters of increased GM thickness bilaterally in medial orbitofrontal and precentral regions, left insular and superior temporal, and right middle temporal cortex. These findings of a reversed relationship of task performance with regional GM thickness, however, were not statistically confirmed by Monte Carlo simulation although these areas largely overlap with TMT task-induced fMRI activation patterns as they were reported by Zakzanis et al. (2005). Hence, the normal structure/function relationship in these brain areas may be affected by a subtle disease process that is below the statistical detection threshold in the current study. A larger sample size would be required to further investigate this observation.

Verbal Fluency Test (VFT) is a widely used test of language production. It requires the participants to verbally list as many words as possible under constrained search conditions based on phonemic or semantic criteria (i.e. Letter Fluency and Category Fluency, respectively). Both measures are intended to make comparable demands on EF, as both imply efficient organisation of

verbal retrieval and recall, self-monitoring (i.e., the participant must keep track of responses already given), effortful self-initiation and inhibition of inappropriate responses [Ruff et al., 1997]. The Category Switching condition of the task probes the participants' ability to generate words fluently while simultaneously shifting between semantic concepts (e.g., fruits and furniture). Processing demands created by the dual nature of this condition are believed to increase sensitivity to frontal-system dysfunction [Delis, Kaplan, & Kramer, 2001].

Two indices from Category Switching condition were used for the GM correlation analyses: (1) the number of correct responses for each of the two target categories summed together (Total Correct Responses) and (2) the number of accurate switches between semantic concepts/categories (Total Switching Accuracy).

Meta-analytic data derived from Bokat & Goldberg (2003) have indicated that schizophrenia patients are disproportionately deficient in Category Fluency relative to Letter Fluency. Similarly, Magaud et al. (2010) have found altered Category Fluency but no Letter Fluency in UHR individuals when compared to help-seeking control subjects that did not meet UHR criteria, and Becker et al. (2010) reported that Category Fluency predicted development of psychosis in their sample. Moreover, GM density measures [Meijer et al., 2011] suggest that impaired Category Fluency is linked to structural abnormalities in the right insula, right superior/middle temporal cortex and left anterior cingulate in ARMS individuals who go on to develop psychosis versus to those who do not. In the current ARMS sample lower Category Fluency, which significantly correlated with reduced GM thickness in left anterior cingulate and medial orbito-frontal cortex. By contrast, no such significant correlations were found for Letter Fluency. In addition, Category Switching performance (i.e. Total Switching Accuracy and Total Correct Responses scaled scores) was significantly associated with reduced GM thickness. Specifically Total Switching Accuracy correlated with regional GM in left middle frontal and precentral areas, and bilaterally in fusiform and lateral occipital cortex whereas Total Correct Responses correlated with GM in left middle frontal cortex, superior

temporal, and inferior parietal/occipital cortex bilaterally. Interestingly, performance on Category Switching Total Correct Responses was also significantly impaired in the clinically more affected ARMS sub-sample. These findings suggest that impaired Category Fluency, and particularly Category Switching in UHR, are linked to reduced regional GM in brain areas involved with task processing.

The Colour-Word Interference Test (CWIT) is a measure of verbal inhibition. The test is based on the Stroop effect [Stroop, 1935]. Stroop tests the participants' ability to control cognitive interference such as identifying the colour of a printed colour word in an incongruent condition (e.g., the word "green" printed in red ink). Three sub-tests of the CWIT were administered; Colour Naming, Word Reading, and Inhibition (or Interference condition).

Using VBM, Takeuchi et al. (2012) found reduced regional GM volume in the anterior cingulate cortex, right inferior frontal gyrus, and cerebellum in healthy subjects to be associated with impaired Stroop interference inhibition. The spatial distribution of these correlation clusters as they were identified by meta-analysis largely overlaps with those of fMRI activation when performing the Stroop task [Laird et al., 2005]. When comparing fMRI data to healthy control subjects, schizophrenia patients presented with reduced BOLD in dorsolateral prefrontal, anterior cingulate and parietal regions and increased BOLD activation in temporal regions and posterior cingulate [Weiss et al., 2007].

The current study, however, did not reveal any significant GM thickness correlation with performance measures of the CWIT, albeit statistically uncorrected correlation maps indicate an association of reduced verbal response inhibition (Inhibition Primary Measure Scaled Score; Inhibition vs. Colour Naming Primary Contrast Measure 1) with increased GM thickness in right anterior cingulate and left superior frontal cortex and reduced GM thickness in left lingual gyrus (statistical maps presented in APPENDIX, pages 126 & 128). Lower verbal response inhibition (Inhibition Primary Measure Scaled Score) was also associated with higher levels of functioning as rated on the SOFAS, GF:Role and GF:Social, respectively.

Visual attention and visuo-spatial planning skills were assessed with the Tower Task (TT). This paper-based problem-solving task is similar to the Tower of London Task (TOL) [Shallice, 1982] and involves mentally planning the minimum number of moves required to moving disks of varying sizes staggered on pegs from an initial starting configuration to a predefined goal configuration. The rules are only moving one disk at a time and never placing a larger disk on top of a smaller one.

It is well documented that frontal brain lesions result in poor TOL performance [e.g., Pantelis et al., 1997]. In healthy subjects, Schall et al. (2003a) have shown TOL task-difficulty-dependent increase of BOLD contrast and regional cerebral blood flow (rCBF) for the cerebellum and the left dorsolateral prefrontal cortex. Rasser et al. (2005) reported that reduced left-hemispheric prefrontal/frontal and bilateral parietal BOLD activation when performing the Tower of London Task also correlates with reduced regional GM thickness in first-episode schizophrenia patients in these brain areas.

The current data suggests that better TT performance (i.e. fewer moves to correctly complete the task; Tower Task Total Achievement Score) correlates with reduced GM thickness in medial occipito-temporal cortex (i.e., lingual gyrus). For uncorrected data, positive correlations were revealed for GM clusters bilaterally in prefrontal, left superior/middle temporal and right inferior temporal cortices. Lower TT performance as a function of reduced GM thickness, particularly in the prefrontal cortex is consistent with the reviewed literature. The reverse function/structure relationship found for the medial occipito-temporal cortex, however, requires further investigations. This brain area is closely associated with more basic visual processing, including encoding of visual information. Rasser et al. (2005) reported TOL task-difficulty dependent increase of BOLD contrast in the left inferior occipital lobe in healthy subjects, whereas in schizophrenia this relationship was diminished towards an increase of BOLD response in the left middle and inferior frontal gyrus, notably at the same level of TOL performance with no group difference in GM thickness of the inferior occipital lobe. These findings rather indicate a rather secondary TOL task-specific functional involvement of this cortical region in schizophrenia.

Learning and Memory: Impaired visual learning and memory as well as impaired verbal learning and memory are fundamental dimensions of cognitive deficits found in schizophrenia [Nuechterlein et al., 2004] with the latter being the most consistent cognitive deficit across studies [Bowie & Harvey, 2005]. Learning and memory deficits are also among the strongest predictors of social and occupational outcome [Green et al., 2000], and further appear to be critical in determining clinical outcome in ARMS [Simon et al., 2012].

The ability to store and retrieve information adequately is crucial for social interaction and occupational success. Impairments in this domain severely compromise the patient's ability to perform everyday activities. The assessment of learning and memory abilities is complex, given the inter-relationship between multiple cognitive processes and subsystems that are required to encode and retrieve multi-modal information (e.g., verbal vs. visual/spatial). The current study used the California Verbal Learning Test (CLVT-II) with the two commonly used subtests of the Wechsler Memory Scale III (WMS-III): the Letter-Number Sequencing Task and the Digit Span Test to assess working memory.

The CLVT-II is a multi-trial recall and recognition word-list learning test specific to episodic verbal learning and memory [Elwood, 1995]. For the task a list of 16 common words (List A) drawn from four categories in mixed order are read to the participant over five sequential trials, with recall being tested after each list presentation. Following an interference trial for which the participant is required to learn and recall a different list of 16 items (List B), the participant is again asked to recall the words from List A; this is the Short Delay Free Recall trial. The participant is then cued with each of the four categories of words in List A; this is the Short Delay Cued Recall trial. After a twenty-minute delay - during which the participant does other tasks - Long Delay Free Recall and Long Delay Cued Recall trials are administered. Finally, the subject is read a list of 48 words and is asked to indicate whether or not each item was part of List A; this is the “Total Hits” recognition trial.

Key variables of the CVLT-II include recall and recognition scores, learning strategies (e.g., semantic clustering; primary-recency effects), and error types

(e.g., intrusions). When factor analysis was conducted in the standardization sample using 19 CVLT-II variables, six factors emerged; the first being "general verbal learning" which consisted of multiple measures of immediate and delayed recall and recognition [Delis et al., 2000]. The current study identified significant GM correlations with three of these measures as part of the general verbal learning factor: impaired performance for both Short Delay Free Recall and Long Delay Cued Recall which correlated with reduced GM thickness bilaterally in superior frontal, left middle-anterior cingulate and right precentral cortex, and fewer “TOTAL HITS” in the recognition trial with a pattern of reduced GM thickness that encompassed segments of the superior frontal, precentral, and postcentral cortical areas of the right hemisphere.

Uncorrected correlation data further indicates a more extensive pattern of function/structure associations bilaterally in the anterior cingulate, which has been implicated to be affected in schizophrenia where learning and memory strategies are also found to be impaired. For instance, a VBM study by Rannikko et al. (2012) reported significant associations between higher serial cluster scores and smaller GM volume of the anterior cingulate gyrus and larger GM volume of the intracalcarine cortex in a sample of schizophrenia patients when adjusting for total GM volume, gender, and antipsychotic medication. More pronounced learning and memory deficits have also been associated with an earlier onset of schizophrenia [Tuulio-Henriksson et al., 2004]. The current data also show that impaired verbal learning performance (i.e. free and cued short delay and long delay recall scores) predict lower levels of functioning in UHR as rated on the SOFAS, GF:Role and/or GF:Social, respectively. Hence, verbal learning and memory deficits are associated with putative frontal GM pathology, which also appears to determine functional level in UHR.

Two subtests of the WMS-III were administered; the Letter-Number Sequencing Task and the Digit Span Test, both of which are measures of short-term/working memory [Lichtenberger, Kaufman, & Lai, 2002; Mitrushina & Boone, 2005].

The current findings suggest that lower scores of the Letter-Number Sequencing Task correlate with reduced regional GM primarily in left superior frontal,

precentral/inferior frontal, insular, middle temporal and inferior parietal regions and bilaterally with GM thickness in precuneus, whereas lower scores on the Digit Span Test were found to be associated with reduced GM thickness in precentral/inferior frontal and inferior temporal areas, and increased GM thickness in superior frontal, middle frontal and lingual cortex. These correlation clusters were not confirmed by Monte Carlo simulation for either of the WMS-III subtests despite the overlap of these clusters with functional PET data [Haut et al., 2000]. The authors reported task-related neural activation in the orbital frontal lobe, dorsolateral prefrontal cortex, and posterior parietal cortex.

Social Cognition: There is growing evidence of more specific "socio-cognitive" deficits in schizophrenia, which, for instance, translate into poor social skills. "Socio-cognitive" refers to higher order communication skills that have evolved to sustain complex social interactions. This includes Theory of Mind (ToM), which is the ability to represent one's own and other individuals mental states by using contextual cues to reason about, predict, and explain behaviour in terms of psychological causation.

Impaired ToM competence has been described in a variety of neuropsychiatric conditions [Brune, 2005], including schizophrenia [Bora, Yucel, & Pantelis, 2009] where it also better predicts real-world functioning than cognitive skills, such as attention processing [Brune et al., 2007]. A recent study that compared ToM competence in individuals at UHR to IQ and age-matched healthy control subjects found baseline deficits in social cognition in the UHR sample. Moreover, impaired ToM task performance in the UHR group was found to correlate with measures of executive function (set-shifting task), suggesting that deficits in social cognition may be attributed to prefrontal dysfunction [Chung et al., 2008]. Based on a recent meta-analysis of ToM in schizophrenia [Bora, Yucel, & Pantelis, 2009] the current study assessed UHR participants with the (non-verbal) False-belief Picture Sequencing Task [Langdon & Coltheart, 1999] and Reading the Minds in the Eyes Task [Baron-Cohen et al., 2001] as well as with the language-based Hinting Task [Corcoran, Mercer, & Frith, 1995].

Several studies have contributed to the delineation of the functional anatomy of ToM by employing Positron Emission Tomography (PET) and fMRI, but findings to date remained somewhat inconsistent. A recent review identified the medial prefrontal and orbitofrontal region to be activated when performing various ToM tasks. The anterior temporal lobe and superior temporal regions were also associated with ToM in ≤50% of the reviewed studies [Carrington & Bailey, 2009].

The current study only revealed some trends in statistically uncorrected data. ToM performance scores showed a tendency towards ceiling effects, which may have caused loss of power in correlation analyses. Lower performance levels on the Hinting Task and the False-belief Picture Sequencing Task were correlated with reduced GM thickness bilaterally in the supramarginal gyrus, left superior frontal and middle temporal gyrus, and right parahippocampal gyrus, while lower performance on the Reading the Mind in the Eyes Test was associated with reduced GM thickness in the left supramarginal and anterior cingulate gyrus, and right superior frontal and inferior parietal areas. These brain areas have been reported to be structurally and functionally compromised in schizophrenia [Shenton et al., 2001; Antonova et al., 2004; Thompson et al., 2001].

Psychophysiological Data: In the current study two ERPs were recorded by employing an auditory oddball paradigm; mismatch negativity (MMN) and the subsequent positive component, the P3a. MMN is a negative-going ERP component that represents an auditory deviants detection process that is dependant on short-term or sensory memory [Näätänen, 1990]. This process does not depend on active attention. The positive-going P3a has been conceptualised to reflect fronto-central attention orienting processes [Friedman, Cycowicz, & Gaeta, 2001]. P3a is elicited following the conscious detection of the deviant stimuli [Light, Swerdlow, & Braff, 2007].

Many studies have demonstrated that MMN and P3a are reduced in schizophrenia [Umbricht & Krljes, 2005; Todd et al., 2012; Näätänen & Kahkonen, 2009; Grillon et al., 1990; Turetsky et al., 2000]. Emerging evidence also suggests that MMN amplitudes, as well as P3a, are reduced in individuals

suffering from very early stages of a psychotic illness, including those identified as UHR [Atkinson, Michie, & Schall, 2012; Jahshan et al., 2012]. Moreover, some recent data indicates that "at-risk" individuals who later develop FES have smaller MMN amplitudes than those who do not [Shaikh et al., 2012; Bodatsch et al., 2011].

While previous studies have linked MMN amplitude reduction to widespread GM deficits in frontal, temporal and parietal cortices in schizophrenia [Rasser et al., 2011; Salisbury et al., 2007], the current study revealed no such association at a statistically significant level. However, uncorrected correlation data indicates a relationship between smaller MMN amplitudes in response to duration deviants and reduced GM thickness in superior frontal, pericalcarine, lateral occipital, and temporal pole areas in ARMS, and smaller MMN amplitudes in response to frequency deviants with reduced GM in superior temporal and insular cortices, respectively.

P3a has been linked to neural generators within the prefrontal, superior temporal, and anterior cingulate cortex [Linden, 2005]. The current study revealed a trend of P3a amplitude reduction in the clinically more affected At-risk sub-sample (ARMS-HS) when compared to those with lower symptom profiles (ARMS-LS). However, these findings were just below threshold of statistical significance. Similarly, only trend significant correlations with statistically uncorrected data were revealed. These indicated a positive association between P3a amplitude to duration deviants with GM thickness in inferior frontal, superior temporal and posterior cingulate areas, and a negative association between P3a amplitudes to frequency deviants with GM thickness in precentral, superior frontal, and superior temporal areas.

The current section discussed the association of regional GM thickness and impaired cognition in ARMS. Taken together, data of the current study suggest an emerging neuroanatomical deficit in ARMS that appears to drive an early cognitive deficit in a brain region in a brain function-specific pattern. This seems to be best reflected in the verbal fluency, and learning and memory data discussed above. Verbal Fluency task performance in particular largely overlapped with the frontal brain areas identified for low function ratings by

reduced regional GM thickness correlation maps, suggesting putative associations with frontal GM pathology which also appears to determine functional level in UHR, which, in turn, may contribute to the identification of ARMS.

4.3 Study Strengths and Limitations

To the best of the author's knowledge the current study is the first to have shown GM associations with clinical, functional and cognitive features as they emerge in the At-Risk Mental State. All participants included in the study were help-seeking young individuals who were free of antipsychotic medication, thus controlling for potential effects of antipsychotic treatment on brain structural changes [Navari & Dazzan, 2009].

A major strength of the study lies in its methodology with respect to MR image analysis. All subjects were investigated in the same MR scanner using identical pulse sequences, while scanner software version was maintained throughout the project. MR image processing was conducted using a freely available, standardized and validated software tool (FreeSurfer) that has been used in a wide variety of settings. FreeSurfer allows to spatially align anatomical regions across subjects with a high level of accuracy by explicitly modelling and controlling for variations in cortical folding patterns, resulting into much better matching of homologous cortical regions than volumetric techniques which utilise only a small number of landmarks on the cortical surface in reference to the Anterior Commissure – Posterior Commissure line. However, a critical element of accurate and reliable FreeSurfer processing involves manual intervention to the automated processing stream in cases where the produced output is not correct (e.g., incorrect segmentation and quantification of grey and white matter). Manual correction of these defects is time consuming, requires great attention to detail, and precise knowledge of brain anatomy. In the current study, a single rater processed all MR imaging data, thus maintaining consistency in editing procedures, and precluding putative bias arising from inter-rater inconsistencies. Moreover, at time of image processing the rater was also blind to symptom group and any other of the reported variables. FreeSurfer

Version, Workstation Type and Operating System Version were maintained throughout the project, thus excluding potential effects thereof.

Notwithstanding, the current project also suffers from several limitations. For instance, the relatively small sample size, particularly in relation to the large number of variables investigated, has not provided sufficient power to investigate all aspects of potential brain structure/function associations, leaving some findings "at trend level".

In particular, median-split group analysis suffered from lack in statistical power. For instance, post-hoc power analysis based on group comparison (i.e. t-test) of P3a amplitudes to duration deviants with an effect size of $r = .32$ suggests an estimated sample size of 74 participants required to obtain significant results at the conventional level of 80% power. Moreover, the study was limited by its cross-sectional design. Thus, inferences on trajectory of psychopathology, brain structure and measures of brain function cannot be made from the current data.

The study also lacks a healthy control group which would provide a crucial anchor point for data interpretation; that is whether GM differences between low and high symptom groups follow on from a continuum of ranging from "healthy" and "moderately affected" to more "severely affected" ARMS. On the other hand, however, splitting the UHR group based on clinical criteria has created a "clinical control group" which is comparable in most aspect to the clinically more severely affected UHR group.

4.4 Future Directions

Future research should address some of the limitations of this project, such as the need for a larger sample size, introduction of a control group, and implementation of longitudinal study design. Collection of longitudinal data would allow to monitor transition rates to schizophrenia, evaluate how a change in clinical status relates to altered brain structure, and, in turn, how these alterations translate into changes in symptoms, cognition, and other measures of brain function..

Future research should also include the rapidly increasing knowledge about the molecular genetics of schizophrenia in order to comprehensively investigate

the biological pathways from gene and gene products to brain pathology. Brain imaging research has already shown how and where early signs of illness emerge in the brains of young people developing schizophrenia whereas psychophysiological and cognitive research has informed us about the impaired processes and functions in the affected brain areas. It is only a matter time before these lines of research eventually merge to open up novel approaches to early detection, intervention and perhaps illness prevention.

APPENDIX

SECTION I Cohort Characteristics

Appendix - Table 1 Descriptive statistics of the ARMS cohort with Group statistics by CCS Median-Split

Variable	ARMS					ARMS-LS			ARMS-HS			ARMS-LS vs. ARMS-HS		
	n	min	max	*M*	*SD*	n	*M*	*SD*	n	*M*	*SD*	*t*	*df*	*p*
Age (years)	42	14	24	19.36	2.17	21	19.24	2.14	21	19.48	2.25	-0.351	40	.727
CAARMS	42	0	85	46.68	21.29	21	29.38	14.98	21	63.98	8.72	-9.145	40	< .000
CAARMS Composite Score	42	0	62	33.37	14.69	21	21.57	10.32	21	45.17	6.60	-8.826	40	< .000
CAARMS Negative Symptoms Score	42	0	15	5.82	4.23	21	3.19	3.11	21	8.45	3.53	-5.128	40	< .000
CAARMS Positive Symptoms Score	42	0	5	2.643	2.022	21	1.905	1.947	21	3.381	1.857	-2.514	40	.016
BPRS	40	26	58	42.90	8.21	20	38.75	7.85	20	47.05	6.36	-3.673	38	.001
SPQ Total Score	41	0	68	32.41	18.11	20	28.40	20.42	21	36.24	15.11	-1.402	39	.169
Beck Depression Inventory II (BDI-II)	42	0	53	24.54	14.30	21	19.57	2.91	21	29.50	3.00	-2.374	40	.022
Beck Anxiety Inventory (BAI)	42	0	41	18.62	12.34	21	14.52	2.53	21	22.71	2.61	-2.256	40	.030
Global Assessment Of Functioning	42	20	80	56.05	12.34	21	58.48	13.98	21	53.62	10.21	1.285	40	.206
Social And Occupational Function Assessment Scale	42	30	90	62.00	13.49	21	66.29	12.39	21	57.71	13.45	2.149	40	.038
Global Functioning: Social Scale	42	3.5	9	6.71	1.15	21	7.10	1.11	21	6.33	1.09	2.243	40	.031
Global Functioning: Role Scale	42	4	9	6.54	1.20	21	6.91	1.10	21	6.17	1.21	2.069	40	.045
WASI Vocabulary T Score	42	28	76	53.76	13.25	21	54.14	11.98	21	53.38	14.71	0.184	40	.855
WASI Matrix Reasoning T Score	42	37	67	54.67	7.77	21	54.67	7.32	21	54.67	8.38	0.000	40	1.000
WASI full-2-Subscale IQ	42	75	138	107.86	16.47	21	107.95	15.83	21	107.76	17.48	0.037	40	.971
CVLT-II List A Short Delay Free Recall Std. Score	42	-4	2	0.31	1.16	21	0.55	0.91	21	0.07	1.34	1.346	40	.186
CVLT-II List A Short Delay Cued Recall Std. Score	42	-4	1.5	0.01	1.15	21	0.24	0.93	21	-0.21	1.32	1.284	40	.206
CVLT-II List A Long Delay Free Recall Std. Score	42	-4	1.5	0.21	1.07	21	0.38	0.96	21	0.05	1.17	1.008	40	.319
CVLT-II List A Long Delay Cued Recall Std. Score	42	-5	1.5	-0.05	1.24	21	0.24	0.85	21	-0.33	1.50	1.519	40	.137
CVLT-II Semantic Clustering Std. Score	42	-2	4.5	0.13	1.38	21	0.14	1.61	21	0.12	1.13	0.055	40	.956
CVLT-II Serial Clustering Std. Score	42	-2	5	0.08	1.35	21	0.14	1.34	21	0.02	1.38	0.283	40	.779

Variable	ARMS					ARMS-LS			ARMS-HS			ARMS-LS vs. ARMS-HS		
	n	min	max	*M*	*SD*	n	*M*	*SD*	n	*M*	*SD*	*t*	*df*	*p*
CVLT-II Recognition Correct Std. Scores "TOTAL HITS"	42	-4	2.5	-0.20	0.88	21	0.00	0.77	21	-0.40	0.96	1.507	40	.140
WMS-III Letter-Number Sequencing Scaled Score	41	5	15	9.80	2.53	20	9.65	2.74	21	9.95	2.38	-0.378	39	.707
WMS-III Digit Span Forwards Raw Score	41	5	15	10.27	2.12	20	10.25	2.71	21	10.29	1.42	-0.053	39	.958
WMS-III Digit Span Backwards Raw Score	41	2	11	6.59	2.17	20	6.75	2.69	21	6.43	1.57	0.470	39	.641
WMS-III Digit Span Scaled Score	41	4	15	9.66	2.60	20	9.90	3.43	21	9.43	1.50	0.575	39	.569
TMT Condition 2 (Number Sequencing) Primary Measure Scaled Score	42	2	15	9.57	3.03	21	10.14	2.87	21	9.00	3.15	1.230	40	.226
TMT Condition 4 (Number-Letter Switching) Primary Measure Scaled Score	42	1	13	8.57	3.56	21	8.62	3.81	21	8.52	3.39	0.086	40	.932
TMT Primary Contrast 2 (Condition 4 - Condition 2) Contrast Scaled Score	42	2	15	9.29	2.63	21	8.52	2.80	21	10.05	2.25	-1.944	40	.059
VFT Condition 1 (Letter Fluency) Primary Measure Scaled Score	42	2	18	10.38	3.81	21	10.52	3.80	21	10.24	3.91	0.240	40	.812
VFT Condition 2 (Category Fluency) Primary Measure Scaled Score	42	3	19	12.21	3.42	21	12.00	3.24	21	12.43	3.66	-0.402	40	.690
VFT Condition 3 (Category Switching) Total Correct Response Scaled Score	42	5	19	11.45	3.49	21	12.52	4.14	21	10.38	2.31	2.070	40	.045
VFT Condition 3 (Category Switching) Total Switching Accuracy Scaled Score	42	6	18	12.21	2.82	21	12.86	3.34	21	11.57	2.09	1.497	40	.142
VFT Primary Contrast Measure 1 (Condition 1 - Condition 2) Contrast Scaled Score	42	1	13	8.19	3.12	21	8.57	3.16	21	7.81	3.11	0.788	40	.435
VFT Primary Contrast Measure 2 (Condition 3 - Condition 2) Contrast Scaled Score	42	1	19	9.38	3.48	21	10.43	3.17	21	8.33	3.53	2.025	40	.050
TT Primary Measure Total Achievement Scaled Score	42	6	15	10.36	2.27	21	10.38	1.60	21	10.33	2.83	0.067	40	.947
TT Mean First Move Time Scaled Score	42	6	13	10.50	1.80	21	10.52	1.86	21	10.48	1.78	0.085	40	.933
UPSIT	42	27	39	33.88	2.93	21	34.29	2.87	21	33.48	3.01	0.893	40	.377

Variable	ARMS					ARMS-LS			ARMS-HS			ARMS-LS vs. ARMS-HS		
	n	min	max	*M*	*SD*	n	*M*	*SD*	n	*M*	*SD*	*t*	*df*	*p*
False Belief Picture Sequencing Task	42	1.5	6	4.96	1.19	21	4.89	1.24	21	5.02	1.15	-0.367	40	.716
Reading the Mind in the Eyes Task	42	17	26	22.36	2.16	21	22.14	2.50	21	22.57	1.81	-0.638	40	.527
Hinting Task	42	12	20	17.95	1.81	21	17.90	1.92	21	18.00	1.73	-0.169	40	.867
MMN (duration deviants) [µV]	37	-6.42	2.66	-2.14	2.22	19	-2.31	2.19	18	-1.96	2.31	-0.482	35	.633
P3a (duration deviants) [µV]	37	-1.47	8.42	1.77	2.40	19	2.51	2.37	18	0.98	2.24	2.023	35	.051
MMN (frequency deviants) [µV]	37	-6.43	3.51	-1.66	2.23	19	-1.87	2.31	18	-1.44	2.19	-0.578	35	.567
P3a (frequency deviants) [µV]	37	-2.60	6.31	1.22	2.09	19	1.09	2.03	18	1.37	2.20	-0.396	35	.694
	n			*M*	*SD*	n	*M*	*SD*	n	*M*	*SD*	*U*	*df*	*p*
Eysenck Personality Questionnaire N-Score	42	0	12	7.76	3.35	21	6.43	0.78	21	9.10	0.56	115.00	42	.007
CWIT Condition 1 (Colour Naming) Primary Measure Scaled Score	42	3	14	8.76	2.71	21	9.76	2.30	21	7.76	2.77	119.50	42	.010
CWIT Condition 2 (Word Reading) Primary Measure Scaled Score	42	2	15	9.74	3.06	21	10.19	3.20	21	9.29	2.92	167.50	42	.174
CWIT Condition 3 (Inhibition) Primary Measure Scaled Score	42	1	14	9.17	3.44	21	9.90	3.71	21	8.43	3.04	141.50	42	.045
CWIT Primary Combined Measure (Condition 1 + Condition 2) Composite Scaled Score	42	4	15	9.48	2.56	21	10.19	2.62	21	8.76	2.34	134.00	42	.028
CWIT Primary Contrast Measure 1 (Condition 3 - Condition 1) Contrast Scaled Score	42	2	17	10.40	3.02	21	10.14	3.28	21	10.67	2.80	218.00	42	.949

| No adjustments were made for multiple comparisons
| CAARMS = Comprehensive Assessment of At-risk Mental States | BPRS = Brief Psychiatric Rating Scale | SPQ = Schizotypal Personality Questionnaire
| WASI = Wechsler Abbreviated Scale of Intelligence | CVLT-II = California Verbal Learning Test: Second Edition | WMS-III = Wechsler Memory Scale: Third Edition
| TMT = Trail Making Test | VFT = Verbal Fluency Test| TT = Tower Task | CWIT = Colour-Word Interference Test | UPSIT = University of Pennsylvania Smell Identification Test

SECTION II Grey Matter Thickness vs. Assessment Data

(i) Symptom Ratings

CAARMS composite score (CCS)

Appendix - Table 2 CCS vs. Grey Matter Thickness

Cluster	Anatomical Parcellation	Hem.	Talairach (X Y Z)			Size (mm^2)	VtxMax	Max	Sig.
1	G_front_sup	L	-6.7	-25	51.8	2911.26	30575	-3.55	.00028
2	S_parieto_occipital	L	-12	-62.8	33.8	860.3	54220	-3.377	.00042
3	S_intrapariet_and_P_trans	L	-30.8	-68.8	30.8	670.75	96898	-3.037	.00092
4	S_orbital_lateral	L	-38.9	41.7	-6.6	662	129876	-3.013	.00097
5	G_and_S_subcentral	L	-48.7	-7.6	9.9	307.46	16023	-2.968	.00108
6	G_front_middle	L	-36.9	43.4	14.3	1375.87	146191	-2.943	.00114
7	G_temp_sup-Lateral	L	-55.7	0.6	-9.5	422.92	57704	-2.863	.00137
8	S_precentral-sup-part	L	-30.5	-8.6	45.8	396.86	15932	-2.367	.00430
9	G_front_sup	L	-15.1	50.3	22.8	607.27	70944	-2.349	.00448
10	G_temp_sup-Lateral	L	-62.3	-40.6	14.8	332.22	85894	-2.106	.00783
11	S_temporal_inf	L	-47.3	-61.8	-1.4	209.92	34204	-1.926	.01186
12	S_oc-temp_med_and_Lingual	L	-31.1	-56.2	-5.8	155.12	10145	-1.83	.01479
13	G_occipital_sup	L	-7.3	-88.5	18.3	619.83	69059	-1.804	.01570
14	S_temporal_sup	L	-57.4	-26.5	-9.4	156.9	99706	-1.767	.01710
15	S_circular_insula_sup	L	-32.8	0.3	10.8	47.41	73652	-1.711	.01945
16	G_cingul-Post-dorsal	L	-4.8	-27.7	33.3	95.39	88101	-1.688	.02051
17	S_central	L	-41.4	-19.1	45.6	77.38	58040	-1.656	.02208
18	S_orbital-H_Shaped	L	-21.5	34.8	-12.3	61.64	134241	-1.646	.02259
19	G_occipital_middle	L	-45	-69.4	12.7	100.64	51760	-1.612	.02443
20	G_cingul-Post-ventral	L	-6.4	-51.4	13.8	47.86	136463	-1.554	.02793
21	S_circular_insula_ant	L	-29.6	22	-12.7	126.26	13104	-1.522	.03006
22	S_oc_middle_and_Lunatus	L	-32.7	-78.6	7	94.89	52130	-1.499	.03170
23	S_circular_insula_inf	L	-41.8	-22.9	-2.9	25.59	85225	1.49	.03236
24	Pole_occipital	L	-24.5	-90.2	-8.2	283.17	148887	-1.475	.03350
25	G_pariet_inf-Angular	L	-38.3	-62.7	45.4	46.58	35402	-1.457	.03491
26	S_postcentral	L	-31	-36.3	49.6	87.01	108824	-1.439	.03639
27	S_front_sup	L	-20.3	5.2	48.5	34.72	92967	-1.406	.03926
28	G_temp_sup-G_T_transv	L	-47.6	-22.8	7.2	7.64	33423	-1.357	.04395
29	G_rectus	L	-6.1	25.3	-16.4	13.42	20385	1.345	.04519
30	S_pericallosal	L	-7.2	-22.5	27.5	3	143001	-1.308	.04920
1	G_front_sup	R	7.4	-8.3	58.9	4669.03	54910	-5.589	.00000
2	G_cingul-Post-dorsal	R	5	-25.1	37	675.37	111343	-3.795	.00016
3	S_circular_insula_sup	R	33.9	11.3	11.4	719.17	83119	-3.396	.00040
4	G_occipital_sup	R	15.4	-83.2	30.7	514.67	74313	-2.919	.00121
5	G_oc-temp_med-Lingual	R	5.4	-85.4	0.5	1897.78	25448	-2.861	.00138
6	G_and_S_cingul-Ant	R	11.7	38.9	2	2089.2	51186	-2.772	.00169
7	S_temporal_sup	R	49.2	-42.6	5.7	326.25	90962	-2.757	.00175
8	G_cingul-Post-ventral	R	12.6	-51.5	14.6	552.11	33662	-2.631	.00234
9	G_pariet_inf-Angular	R	42.8	-56.6	44.9	677.13	147423	-2.628	.00236
10	G_occipital_middle	R	37.5	-79.1	18.1	348.74	12953	-2.414	.00385
11	G_and_S_subcentral	R	43.4	-16.2	19.7	234.63	147801	-2.39	.00407

Cluster	Anatomical Parcellation	Hem.	Talairach (X Y Z)			Size (mm^2)	VtxMax	Max	Sig.
12	G_temporal_inf	R	49.4	-30.6	-19.4	349.16	163080	-2.25	.00562
13	S_orbital-H_Shaped	R	20.9	31	-15	141.56	153761	-1.97	.01072
14	G_orbital	R	37.6	49.7	-5.9	469.95	77217	-1.917	.01211
15	G_and_S_occipital_inf	R	44.9	-65.4	-3.4	484.79	128204	-1.896	.01271
16	S_temporal_sup	R	40	-55.2	17.3	66.87	31430	-1.874	.01337
17	S_temporal_sup	R	49.5	-13.3	-9.1	213.38	163497	-1.764	.01722
18	G_front_middle	R	38.4	22.8	40	207.79	94040	-1.757	.01750
19	S_front_inf	R	32	11.1	26.7	98.63	96015	-1.757	.01750
20	S_orbital_med-olfact	R	16	19.3	-14.1	54.76	89127	-1.527	.02972
21	S_front_sup	R	25.4	22.4	36.6	69.96	56644	-1.501	.03155

| Anatomical Parcellation (aparc.a2009s): Annotation that VtxMax falls into
| VtxMax = Vertex of max sig. in cluster | Max = −log10 (p-value) of VtxMax | Sig. = *p*-value of VtxMax

CAARMS negative symptom score (CNSS)

Appendix - Table 3 CNSS vs. Grey Matter Thickness

Cluster	Anatomical Parcellation	Hem.	Talairach (X Y Z)			Size (mm^2)	VtxMax	Max	Sig.
1	S_oc_sup_and_transversal	L	-31	-69.6	29	2729.26	157716	-3.48	.00033
2	G_front_sup	L	-7.1	-24.1	50.9	1415.12	12306	-2.977	.00105
3	S_circular_insula_sup	L	-33.4	-0.2	9.3	173.35	16872	-2.44	.00363
4	S_oc-temp_med_and_Lingual	L	-31	-56.4	-4.8	246.08	91435	-2.42	.00380
5	G_front_middle	L	-36.8	23.9	39.9	324.42	47059	-2.397	.00401
6	S_interm_prim-Jensen	L	-48.7	-50.4	28.4	159.26	29969	2.366	.00431
7	G_rectus	L	-5	21.5	-18.1	330.19	41272	2.302	.00499
8	G_and_S_subcentral	L	-50.2	-6.4	8.7	248.97	56345	-2.227	.00593
9	G_temporal_inf	L	-47.8	-61.5	-1.5	630.39	143677	-2.152	.00705
10	G_pariet_inf-Angular	L	-38.5	-63.1	45.6	236.09	78323	-2.146	.00714
11	S_temporal_sup	L	-55.2	-35.9	6	488.03	135405	-2.124	.00752
12	S_orbital_lateral	L	-39.2	41.2	-7	243.06	129877	-2.018	.00959
13	G_precuneus	L	-6.9	-53.7	11.3	90.25	127203	-1.977	.01054
14	G_and_S_occipital_inf	L	-26.2	-81.7	-7.8	554.66	107754	-1.967	.01079
15	G_pariet_inf-Supramar	L	-60.2	-27.8	30.5	190.26	129985	-1.883	.01309
16	G_temp_sup-G_T_transv	L	-42.1	-23.5	9.1	100.17	47566	-1.842	.01439
17	G_parietal_sup	L	-21.9	-51.9	60.7	108.57	66920	-1.767	.01710
18	G_front_middle	L	-36.7	43.9	14.4	88.8	18145	-1.738	.01828
19	G_front_sup	L	-15	50.3	24.1	286.35	138232	-1.693	.02028
20	S_front_inf	L	-39.6	25.6	16.4	81.42	154648	-1.643	.02275
21	S_circular_insula_inf	L	-45.9	-19.7	-2.4	28.92	43367	1.526	.02979
22	S_orbital-H_Shaped	L	-21.3	32.3	-10.7	30.3	134233	-1.503	.03141
23	S_cingul-Marginalis	L	-7.9	-26	38.3	29.73	88071	-1.483	.03289
24	S_temporal_sup	L	-55.8	-22.9	-10.8	35.61	139241	-1.48	.03311
25	G_oc-temp_med-Parahip	L	-30.5	-24.9	-18.7	63.24	115190	-1.442	.03614
26	G_postcentral	L	-43.4	-18.4	48.7	19.25	144645	-1.385	.04121
27	S_oc_middle_and_Lunatus	L	-29.8	-86	0.5	59	39258	-1.372	.04246
28	S_postcentral	L	-35.3	-41.8	45.9	14.57	67045	-1.351	.04457
29	G_front_inf-Orbital	L	-43.9	28.7	-11.2	26.48	117419	-1.346	.04508
1	G_pariet_inf-Angular	R	41.3	-55.5	43.5	1053.53	147411	-3.73	.00019
2	G_occipital_middle	R	36.6	-80.7	18.7	857.02	305	-3.267	.00054
3	S_cingul-Marginalis	R	7.2	-34	40.4	452.39	96599	-3.259	.00055

Cluster	Anatomical Parcellation	Hem.	Talairach (X Y Z)			Size (mm^2)	VtxMax	Max	Sig.
4	G_occipital_sup	R	13	-82.2	30.4	1461.12	104498	-2.976	.00106
5	G_and_S_paracentral	R	5.9	-26.6	50.6	1052.48	119315	-2.826	.00149
6	S_circular_insula_sup	R	37.3	16.9	9.6	535.34	47351	-2.802	.00158
7	G_and_S_subcentral	R	43.5	-17.3	18.8	153.89	35602	-2.459	.00348
8	G_and_S_cingul-Ant	R	7.1	33.5	10.6	384.91	116317	-2.451	.00354
9	G_temp_sup-Lateral	R	64.7	-29.7	10.6	134.01	160049	-2.277	.00528
10	G_parietal_sup	R	18.9	-56.5	58.2	417.41	774	-2.23	.00589
11	G_cingul-Post-ventral	R	11.9	-51.4	13.1	132.09	1232	-2.03	.00933
12	G_and_S_occipital_inf	R	44.9	-65.4	-3.4	385.53	128204	-1.865	.01365
13	G_precentral	R	28	-11.1	58.6	169.74	115239	-1.802	.01578
14	G_oc-temp_med-Lingual	R	14.6	-75.1	-3.1	561.9	22540	-1.752	.01770
15	G_front_middle	R	37.7	23.7	39.6	115.66	56892	-1.71	.01950
16	G_front_sup	R	12.4	60.3	11.9	429.31	84492	-1.684	.02070
17	G_front_sup	R	6.8	23.3	51.4	83.83	103067	-1.668	.02148
18	S_temporal_sup	R	48.7	-43.5	7.3	33.17	10081	-1.586	.02594
19	G_and_S_frontomargin	R	35.7	53.1	-9.8	125.05	27142	-1.582	.02618
20	S_subparietal	R	11.6	-49.3	29	21.93	65901	1.54	.02884
21	G_temp_sup-G_T_transv	R	43	-22.9	9.5	31.73	69393	-1.522	.03006
22	S_parieto_occipital	R	23.3	-60.9	23	62.94	86380	-1.492	.03221
23	G_precentral	R	51.8	1.8	32	56.86	55132	-1.481	.03304
24	Pole_temporal	R	39.6	-7	-30.3	43.63	127479	1.436	.03664
25	G_temporal_inf	R	49.4	-30.6	-19.4	26.44	163080	-1.369	.04276
26	Pole_temporal	R	37.6	12.6	-31.9	17.22	104946	1.337	.04603

| Anatomical Parcellation (aparc.a2009s): Annotation that VtxMax falls into
| VtxMax = Vertex of max sig. in cluster | Max = −log10 (p-value) of VtxMax | Sig. = *p*-value of VtxMax

CAARMS positive symptom score (CPSS)

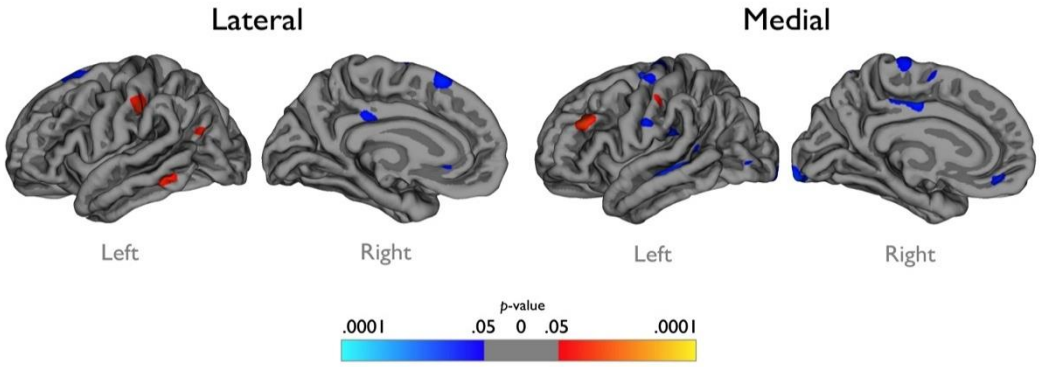

Appendix - Figure 1 Statistical correlation maps of cerebral grey matter thickness with CPSS for left and right hemispheres. Statistical maps with a significance threshold of *p*= .05 (uncorrected).

Appendix - Table 4 CPSS vs. Grey Matter Thickness

Cluster	Anatomical Parcellation	Hem.	Talairach (X Y Z)			Size (mm^2)	VtxMax	Max	Sig.
1	Lat_Fis-post	L	-41.5	-26.3	22.1	156.38	77936	2.288	.00515
2	S_postcentral	L	-49.1	-21.8	37.2	366.94	150306	2.019	.00957
3	S_temporal_inf	L	-54.4	-44	-8.8	138.51	137091	1.732	.01854
4	G_front_sup	L	-6.6	24	51	335.99	37242	-1.676	.02109
5	G_pariet_inf-Angular	L	-44.3	-66.3	23.2	77.02	130069	1.66	.02188
6	G_cingul-Post-dorsal	L	-4.5	-29.1	31.6	62.94	158977	-1.553	.02799
7	S_precentral-sup-part	L	-17.4	-14.5	60	28.86	131184	-1.447	.03573
8	S_pericallosal	L	-3	24.7	-3.3	27.15	133919	-1.437	.03656
9	S_postcentral	L	-20.4	-33.6	58.7	1.59	98278	1.309	.04909
1	S_cingul-Marginalis	R	10.5	-22.4	35.9	384.16	98565	-2.979	.00105
2	S_precentral-sup-part	R	17.1	-9.3	56.4	411.79	102306	-2.507	.00311
3	S_temporal_sup	R	49.3	-36.7	-2.6	471.44	132588	-2.357	.00440
4	Pole_occipital	R	18.7	-95.5	-6.3	417.72	2484	-2.131	.00740
5	G_front_middle	R	46.1	33.1	22.8	184.47	41804	2.073	.00845
6	G_pariet_inf-Supramar	R	47.9	-22.9	20.3	355.92	8455	-1.962	.01091
7	S_suborbital	R	9.8	40.3	-13.5	102.16	125162	-1.745	.01799
8	S_central	R	11	-29.4	58.5	88.72	105801	-1.624	.02377
9	G_postcentral	R	62.1	-8.5	25.1	43.27	2594	-1.567	.02710
10	S_temporal_sup	R	47.9	-44.1	8.7	45.88	158017	-1.506	.03119
11	G_precentral	R	39.9	-8.4	55	42.59	116143	-1.478	.03327
12	G_and_S_paracentral	R	5.3	-19.4	66.1	90.18	25607	-1.476	.03342
13	G_postcentral	R	53.1	-15.5	40.6	38.78	59965	1.438	.03648
14	G_front_sup	R	7.9	-0.2	56.9	45.57	72203	-1.398	.03999
15	S_oc-temp_med_and_Lingual	R	37.5	-25.6	-19.8	19.99	2478	-1.38	.04169
16	S_circular_insula_inf	R	35.7	-17.6	-0.5	20.04	114841	1.364	.04325
17	S_temporal_sup	R	52.6	-54.6	10	13.55	39045	1.36	.04365
18	S_calcarine	R	22.7	-62.6	4.3	10.92	54743	-1.337	.04603
19	G_occipital_middle	R	44.1	-78	3.1	19.82	59190	-1.337	.04603
20	G_parietal_sup	R	10.8	-56.2	59.9	2.73	42607	-1.314	.04853

| Anatomical Parcellation (aparc.a2009s): Annotation that VtxMax falls into
| VtxMax = Vertex of max sig. in cluster | Max = −log10 (p-value) of VtxMax | Sig. = *p*-value of VtxMax

(ii) Functioning Measures

Global Assessment Of Functioning (GAF)

Appendix - Table 5 GAF vs. Grey Matter Thickness

Cluster	Anatomical Parcellation	Hem.	Talairach (X Y Z)			Size (mm^2)	VtxMax	Max	Sig.
1	G_and_S_cingul-Mid-Ant	L	-10.8	14.9	42.3	457.85	55201	3.257	.00055
2	G_front_middle	L	-39	45.8	2.4	1409.63	106438	2.519	.00303
3	S_temporal_sup	L	-48.4	-37.8	3.6	307.09	86588	2.392	.00406
4	G_precuneus	L	-8.5	-49.4	59.1	282.5	82304	2.356	.00441
5	G_precentral	L	-24.4	-13.3	60.9	226.47	138011	2.344	.00453
6	G_and_S_subcentral	L	-56.4	-15.7	14.4	431.24	121967	2.321	.00478
7	S_parieto_occipital	L	-9	-62.9	30.1	342.55	130388	2.144	.00718
8	G_front_middle	L	-35.6	25.7	37.7	208.42	139595	2.064	.00863
9	G_Ins_lg_and_S_cent_ins	L	-35.6	-3.7	-3.5	393.09	85341	1.948	.01127
10	G_pariet_inf-Supramar	L	-49.5	-44.7	43.6	141.24	40986	1.863	.01371
11	G_temp_sup-Plan_tempo	L	-60	-35.8	13.1	141.75	156343	1.815	.01531
12	G_and_S_cingul-Mid-Ant	L	-13.4	22.5	26.4	70.65	117206	-1.809	.01552
13	Pole_occipital	L	-11	-99.1	7	1431.88	5269	1.799	.01589
14	S_intrapariet_and_P_trans	L	-29.6	-64.2	38.2	250.93	87019	1.723	.01892
15	S_circular_insula_ant	L	-31.5	25.9	-9.3	147.37	83664	1.672	.02128
16	G_temp_sup-Lateral	L	-62.4	-20.1	2.6	94.96	100781	1.651	.02234
17	G_front_sup	L	-8.4	62.1	3	73.53	58422	1.528	.02965
18	G_postcentral	L	-21.7	-30.5	64.3	56.9	34608	-1.515	.03055
19	G_front_middle	L	-30	11.3	48.7	110.64	145339	1.512	.03076
20	G_temporal_middle	L	-61.8	-28.4	-9.1	133.3	122732	1.493	.03214
21	G_precentral	L	-52.3	-4.5	38.4	133.52	75966	1.488	.03251
22	S_suborbital	L	-10.2	32.7	-10.9	55.04	67898	1.483	.03289
23	G_front_middle	L	-24.3	43.5	26.7	53.03	82456	1.463	.03443
24	G_temporal_inf	L	-52.7	-21.4	-26.6	22.33	130749	1.395	.04027
25	S_central	L	-35.4	-17.7	33.8	22.86	25631	1.382	.04150
26	S_temporal_sup	L	-47.6	-24.2	-5.3	14.81	98159	1.343	.04539
27	S_parieto_occipital	L	-14.3	-71.3	19.5	14.95	74386	1.32	.04786
1	G_precentral	R	35	-6.7	52	2883.62	116179	3.972	.00011
2	Pole_occipital	R	18.9	-94.7	-6.4	1451.88	40284	3.892	.00013
3	G_parietal_sup	R	12.4	-53.2	58.2	738.09	19539	2.829	.00148
4	S_cingul-Marginalis	R	11.9	-33.9	38.6	228.02	141655	2.572	.00268
5	S_parieto_occipital	R	10.1	-56.7	24.6	232.68	16997	2.371	.00426
6	G_front_inf-Opercular	R	42.5	7.5	7.9	266.18	117158	2.292	.00511
7	G_pariet_inf-Supramar	R	59.1	-37.8	31.9	358.12	126825	2.188	.00649
8	G_temporal_inf	R	48.9	-41.5	-13.8	200.01	53529	2.124	.00752
9	G_oc-temp_lat-fusifor	R	36.5	-29	-19.9	207.9	90274	2.116	.00766
10	G_front_middle	R	39.2	48.1	5.3	380.19	77252	2.046	.00899
11	G_and_S_cingul-Mid-Post	R	4.2	-8.4	31.1	98.96	146640	2.005	.00989
12	G_and_S_cingul-Ant	R	8.3	40.1	-11.3	344.53	154890	1.739	.01824
13	S_circular_insula_sup	R	31.8	15.4	2.7	104.43	124914	1.726	.01879
14	S_temporal_sup	R	54.5	-16.2	-14.9	291.73	70456	1.716	.01923
15	G_pariet_inf-Angular	R	40.9	-56.2	43.7	261.15	147418	1.69	.02042
16	S_temporal_transverse	R	51.6	-17.7	4.5	44.04	113117	1.551	.02812
17	S_temporal_sup	R	43.3	-48	17.2	27.09	68949	1.523	.02999

Cluster	Anatomical Parcellation	Hem.	Talairach (X Y Z)			Size (mm^2)	VtxMax	Max	Sig.
18	S_cingul-Marginalis	R	9.3	-44.6	51.4	53.5	123807	1.51	.03090
19	S_pericallosal	R	7.2	-36.1	24.8	17.08	15138	-1.505	.03126
20	G_occipital_middle	R	46.7	-76.4	7.6	94.96	148795	1.504	.03133
21	S_postcentral	R	38.3	-27	42.9	44.84	109264	-1.489	.03243
22	G_cuneus	R	7.2	-74.8	30	112.55	94284	1.448	.03565
23	G_postcentral	R	54.5	-13.5	42.8	44.36	43027	-1.441	.03622
24	G_and_S_transv_frontopol	R	19.4	57.5	10.3	46.22	8247	1.399	.03990
25	S_cingul-Marginalis	R	11.8	-23.1	45.5	28.47	23725	1.364	.04325

| Anatomical Parcellation (aparc.a2009s): Annotation that VtxMax falls into
| VtxMax = Vertex of max sig. in cluster | Max = −log10 (p-value) of VtxMax | Sig. = *p*-value of VtxMax

Social and Occupational Function Assessment Scale (SOFAS)

Appendix - Table 6 SOFAS vs. Grey Matter Thickness

Cluster	Anatomical Parcellation	Hem.	Talairach (X Y Z)			Size (mm^2)	VtxMax	Max	Sig.
1	G_front_middle	L	-36.8	50.1	-2.7	3476.39	106209	5.309	.00000
2	G_precuneus	L	-8.1	-63.4	29.1	751.91	17222	3.706	.00020
3	G_and_S_cingul-Mid-Ant	L	-10.8	16.6	39.7	699.72	100514	3.489	.00032
4	G_front_middle	L	-24	44.4	26.8	399.24	152192	2.79	.00162
5	S_intrapariet_and_P_trans	L	-30.6	-64.5	35.9	486.67	52046	2.605	.00248
6	G_and_S_subcentral	L	-56.7	-10.3	12.8	2417.96	7300	2.581	.00262
7	G_temp_sup-Plan_tempo	L	-60.5	-36.1	13.3	732.71	156344	2.545	.00285
8	G_precentral	L	-22.6	-13.8	60.3	312.84	92564	2.404	.00394
9	S_temporal_sup	L	-44.4	-67.7	11.8	964.77	156674	2.106	.00783
10	S_oc-temp_lat	L	-47.5	-43.2	-12.4	248.01	70074	2	.01000
11	G_pariet_inf-Supramar	L	-49.4	-46.9	43.3	131.96	53848	1.976	.01057
12	G_precuneus	L	-4.8	-55.4	16.2	85.54	159400	1.827	.01489
13	G_temporal_middle	L	-62.1	-33.5	-8.5	288.6	49545	1.823	.01503
14	G_temp_sup-Lateral	L	-55.4	2.6	-9.1	233.54	42274	1.74	.01820
15	G_cuneus	L	-4.3	-87.8	12.4	305.17	112517	1.7	.01995
16	S_suborbital	L	-10.5	33.1	-11.3	176.87	30918	1.698	.02004
17	S_oc-temp_med_and_Lingual	L	-24.5	-45	-3	189.71	130911	1.659	.02193
18	G_temp_sup-Lateral	L	-63.6	-19.9	2.1	160.29	31025	1.589	.02576
19	S_orbital-H_Shaped	L	-25.8	35.3	-8.8	62.2	67759	1.562	.02742
20	S_front_sup	L	-23.6	17.8	35.2	129.03	72756	1.561	.02748
21	G_cingul-Post-dorsal	L	-4.7	-22.7	33.4	44.86	95282	1.523	.02999
22	G_pariet_inf-Angular	L	-40.2	-63.4	43.4	29.94	35406	1.451	.03540
23	S_precentral-inf-part	L	-35.1	2.6	28.2	10.35	41319	1.381	.04159
24	Pole_occipital	L	-27.1	-87.2	-7.4	86.53	79705	1.352	.04446
25	S_temporal_sup	L	-37.4	-58.3	26.4	5.77	96746	1.32	.04786
26	G_front_middle	L	-40.8	33.7	21.6	5.63	131534	1.313	.04864
1	S_oc-temp_lat	R	47.5	-43.2	-11.5	481.6	91453	4.986	.00001
2	G_and_S_cingul-Ant	R	10.3	36.6	-10.4	1270.21	110715	4.088	.00008
3	S_parieto_occipital	R	10.5	-56.2	24.4	1292.59	142005	3.559	.00028
4	S_precentral-sup-part	R	34.7	-5.9	48.2	1378.57	65466	3.397	.00040
5	S_front_middle	R	28	45.7	3.3	1946.56	44932	3.371	.00043
6	G_front_inf-Opercular	R	41.3	9.5	8.1	646.01	1105	3.341	.00046
7	S_temporal_sup	R	49.3	-43.9	7.2	268.54	162396	2.989	.00103
8	G_parietal_sup	R	11.4	-51.1	57.1	321.67	81666	2.899	.00126

Cluster	Anatomical Parcellation	Hem.	Talairach (X Y Z)			Size (mm^2)	VtxMax	Max	Sig.
9	S_cingul-Marginalis	R	11.3	-34.1	38.9	749.26	141656	2.882	.00131
10	S_precentral-inf-part	R	35.8	6.1	32.9	1717.02	152607	2.861	.00138
11	G_pariet_inf-Angular	R	38.8	-56.1	42.3	689.17	106992	2.834	.00147
12	S_oc-temp_med_and_Lingual	R	37.6	-24.9	-19.9	2356.46	127758	2.823	.00150
13	S_temporal_sup	R	39.4	-64.3	15.3	616.94	2363	2.468	.00340
14	G_and_S_cingul-Mid-Post	R	9.2	1	51.8	271.33	139818	2.293	.00509
15	S_circular_insula_sup	R	30.9	18.9	2.9	131.4	110406	2.167	.00681
16	S_temporal_sup	R	47	-16.3	-9.3	869.52	40836	2.144	.00718
17	S_front_sup	R	20.6	11.1	48.1	226.78	17680	2.14	.00724
18	G_and_S_subcentral	R	63.1	-7.3	21.6	397.71	153617	2.061	.00869
19	G_and_S_paracentral	R	7.1	-27	55.9	99.69	5870	1.618	.02410
20	S_temporal_sup	R	56.5	-31.6	5.1	76.09	52721	1.611	.02449
21	G_subcallosal	R	7.2	13.5	-13.5	10.32	125484	-1.482	.03296
22	G_pariet_inf-Supramar	R	59.4	-25.6	33.1	45.88	97097	1.445	.03589
23	G_parietal_sup	R	25.1	-48	60.3	40.7	81396	1.38	.04169
24	G_front_sup	R	8.1	33.2	30.4	25.27	122995	1.333	.04645
25	G_subcallosal	R	7	15.9	-12.5	0.45	5006	-1.322	.04764

| Anatomical Parcellation (aparc.a2009s): Annotation that VtxMax falls into
| VtxMax = Vertex of max sig. in cluster | Max = −log10 (p-value) of VtxMax | Sig. = *p*-value of VtxMax

Global Functioning: Social Scale (GF:Social)

Appendix - Table 7 GF:Social vs. Grey Matter Thickness

Cluster	Anatomical Parcellation	Hem.	Talairach (X Y Z)			Size (mm^2)	VtxMax	Max	Sig.
1	G_and_S_frontomargin	L	-30.8	48.1	0.2	4522.73	106224	3.195	.00064
2	G_precuneus	L	-6.8	-63.8	28.5	1136.03	7845	2.682	.00208
3	G_front_sup	L	-6.9	25.3	48.9	893.36	50660	2.64	.00229
4	G_front_middle	L	-23.9	45	26.4	276.18	13484	2.358	.00439
5	S_circular_insula_ant	L	-30.2	27.3	-7	363.49	110817	2.092	.00809
6	G_and_S_occipital_inf	L	-31.8	-88.3	-7.6	984.47	6369	1.994	.01014
7	G_temp_sup-Plan_tempo	L	-57.7	-34.1	11.1	87.17	68486	1.85	.01413
8	S_temporal_sup	L	-53.4	-47.6	16.1	151.83	29339	1.846	.01426
9	G_temp_sup-Lateral	L	-54.5	3.5	-10.2	210.79	161223	1.814	.01535
10	G_temporal_middle	L	-61.7	-31.5	-8.9	439.47	107608	1.808	.01556
11	G_and_S_cingul-Ant	L	-13.3	40.5	16.1	112.92	153279	1.553	.02799
12	G_and_S_cingul-Mid-Post	L	-3.7	-16.9	32.1	32.57	8461	1.55	.02818
13	G_and_S_subcentral	L	-55.4	-5.9	8.7	55.97	128920	1.532	.02938
14	S_precentral-inf-part	L	-34.3	6.1	30.1	18.02	108114	1.447	.03573
15	S_intrapariet_and_P_trans	L	-30.9	-65.6	37.8	41.06	5189	1.397	.04009
16	S_suborbital	L	-8.2	35.4	-15	9.44	154241	1.33	.04677
17	G_front_inf-Triangul	L	-46.2	24.5	12.2	8.41	27273	1.324	.04742
18	S_oc_sup_and_transversal	L	-28.8	-69.1	20.5	0.42	157753	1.301	.05000
19	Lat_Fis-ant-Vertical	L	-41.1	22.1	7.1	0.45	27300	1.301	.05000
1	Pole_occipital	R	20.9	-95.2	-6.7	1780.13	114146	4.023	.00009
2	G_cingul-Post-ventral	R	13.2	-40.8	2.4	540.8	115389	3.922	.00012
3	S_circular_insula_sup	R	30.1	20.6	3.2	645.97	84168	3.747	.00018
4	G_parietal_sup	R	10.2	-47.3	64	309.95	67063	2.908	.00124
5	S_oc-temp_lat	R	47.7	-42.6	-12.1	298.59	114778	2.86	.00138
6	S_temporal_sup	R	48.4	-15.1	-8.4	1038.08	44124	2.852	.00141
7	G_and_S_cingul-Ant	R	10	36	-10.9	1024.16	84685	2.789	.00163

Cluster	Anatomical Parcellation	Hem.	Talairach (X Y Z)			Size (mm^2)	VtxMax	Max	Sig.
8	G_front_middle	R	36.1	18.5	44.6	1805.93	152429	2.711	.00195
9	S_front_sup	R	20.8	10	47.3	1725.87	48397	2.69	.00204
10	Lat_Fis-post	R	43.4	-29.5	25.2	487.95	120544	2.634	.00232
11	G_front_sup	R	6.6	7.6	59.1	1330.24	119331	2.423	.00378
12	G_front_middle	R	35.1	48.1	8.8	537.33	46737	2.397	.00401
13	G_orbital	R	33.6	48.2	-11.1	385.35	20280	2.325	.00473
14	S_intrapariet_and_P_trans	R	38.8	-55.6	42	152.7	6287	2.131	.00740
15	G_occipital_middle	R	26.6	-85.8	19.6	155.67	38992	2.05	.00891
16	G_and_S_cingul-Mid-Post	R	4.4	-19.8	35.1	125.27	125633	1.972	.01067
17	S_temporal_sup	R	39.4	-63.6	14.6	303.88	21549	1.895	.01274
18	G_and_S_cingul-Mid-Ant	R	10.5	13.4	40.1	79.2	133115	1.839	.01449
19	S_oc-temp_med_and_Lingual	R	33.9	-21.3	-20	248.47	53121	1.802	.01578
20	S_cingul-Marginalis	R	15.8	-35.6	38.5	110.89	150147	1.664	.02168
21	S_temporal_sup	R	50	-45.5	8.1	58.15	128074	1.609	.02460
22	S_calcarine	R	24.4	-66.2	6.7	69.95	157101	1.54	.02884
23	G_and_S_cingul-Ant	R	12.6	44.3	11.6	141.03	134473	1.509	.03097
24	S_orbital-H_Shaped	R	22.1	32.9	-15.7	31.42	50953	1.483	.03289
25	G_pariet_inf-Angular	R	52.5	-49.9	34.3	99	13893	1.468	.03404
26	G_oc-temp_med-Parahip	R	20.4	-31.5	-9.4	39.38	97470	1.46	.03467
27	S_intrapariet_and_P_trans	R	33.5	-40.6	49.1	32.79	133145	1.451	.03540
28	G_and_S_occipital_inf	R	42.7	-68.3	-2.1	44.91	91223	1.391	.04064
29	G_cuneus	R	8.7	-76.3	32.2	6.62	130089	1.319	.04797

| Anatomical Parcellation (aparc.a2009s): Annotation that VtxMax falls into
| VtxMax = Vertex of max sig. in cluster | Max = −log10 (p-value) of VtxMax | Sig. = *p*-value of VtxMax

Global Functioning: Role Scale (GF:Role)

Appendix - Table 8 GF:Role vs. Grey Matter Thickness

Cluster	Anatomical Parcellation	Hem.	Talairach (X Y Z)			Size (mm^2)	VtxMax	Max	Sig.
1	G_front_middle	L	-38.1	47.6	0.8	4225.97	146300	5.621	.00000
2	G_precuneus	L	-6.5	-63.6	27.5	1234.74	74714	4.58	.00003
3	G_and_S_cingul-Mid-Ant	L	-10.8	16.9	39.2	523.04	100513	3.76	.00017
4	G_and_S_cingul-Ant	L	-7.7	37.4	9.5	352.81	140728	2.807	.00156
5	G_and_S_subcentral	L	-59.7	-9.9	11	1939.76	138537	2.563	.00274
6	G_front_middle	L	-35.6	24.5	41.8	804.34	119259	2.264	.00545
7	S_precentral-sup-part	L	-24.4	-12.6	58.3	218.43	92579	2.163	.00687
8	S_oc-temp_lat	L	-47.4	-44.3	-11.2	529.65	137146	2.077	.00838
9	G_temp_sup-Plan_tempo	L	-61.9	-35.5	12.6	562.26	111453	2.075	.00841
10	G_temporal_middle	L	-58.2	-7.8	-20.5	1004.18	136814	2.021	.00953
11	S_oc-temp_med_and_Lingual	L	-26.9	-43.6	-3.3	251.37	25555	1.974	.01062
12	S_occipital_ant	L	-41	-63.1	8.5	553.16	43497	1.963	.01089
13	S_intrapariet_and_P_trans	L	-29.8	-63.1	33	290.47	157696	1.96	.01096
14	G_pariet_inf-Angular	L	-49.5	-48.1	43.3	131.85	98077	1.866	.01361
15	G_oc-temp_lat-fusifor	L	-39.6	-67.1	-11.3	510.12	149003	1.81	.01549
16	S_temporal_sup	L	-54.8	-22.1	-1.7	167.87	38045	1.697	.02009
17	S_intrapariet_and_P_trans	L	-35.4	-45.6	32.7	104.18	36765	1.688	.02051
18	G_oc-temp_med-Parahip	L	-30.7	-14.7	-24.9	66.44	89680	1.571	.02685
19	S_temporal_sup	L	-37.8	-53.6	17.1	91.24	68624	1.462	.03451
20	S_precentral-inf-part	L	-37	1.9	25.9	40.63	116691	1.458	.03483
21	S_circular_insula_sup	L	-33.2	-0.5	10.4	29.07	141540	1.437	.03656
22	G_oc-temp_lat-fusifor	L	-29.7	-39.1	-15.2	24.69	114811	1.39	.04074
23	S_temporal_sup	L	-55.2	-19	-12.9	22.47	89862	1.352	.04446
24	G_front_sup	L	-8.5	59.8	4.2	8.77	11752	1.327	.04710
1	S_oc-temp_lat	R	47.7	-43.4	-11.5	2294.17	10148	5.58	.00000
2	S_front_middle	R	28.2	46.6	1.5	2850.37	131588	3.935	.00012
3	S_precentral-inf-part	R	45.3	5.7	16.6	449.16	129692	3.646	.00023
4	S_precentral-sup-part	R	34.9	-5.2	46.5	378.29	29785	3.073	.00085
5	G_pariet_inf-Angular	R	36.6	-57.6	43.1	496.65	131989	2.827	.00149
6	G_precuneus	R	7.5	-57.7	23.3	429.07	130102	2.816	.00153
7	S_front_sup	R	26.1	25.9	33.7	531.8	93901	2.765	.00172
8	S_cingul-Marginalis	R	13.5	-36.1	39	721.94	85546	2.608	.00247
9	G_and_S_cingul-Ant	R	11.6	37	-8.7	1050.47	37965	2.592	.00256
10	S_calcarine	R	17.8	-45.4	2.1	537.03	63750	2.273	.00533
11	G_occipital_middle	R	47.1	-74.4	8	522.47	59181	2.202	.00628
12	S_temporal_sup	R	47.8	-42.8	7	395.3	90952	2.145	.00716
13	S_precentral-sup-part	R	22.9	-9.7	55.1	162.61	92162	2.14	.00724
14	G_temporal_middle	R	48.3	-3.1	-25.9	1422.16	92008	2.129	.00743
15	S_precentral-inf-part	R	35.8	6.1	32.9	169.18	152607	1.956	.01107
16	G_parietal_sup	R	11.8	-50.5	57.2	128.76	36758	1.895	.01274
17	G_oc-temp_med-Parahip	R	35.3	4.2	-14	77.25	113520	1.778	.01667
18	S_circular_insula_sup	R	31	17.7	3.5	94.87	51095	1.76	.01738
19	G_and_S_subcentral	R	62.9	-7.1	22	340.31	153619	1.752	.01770
20	G_pariet_inf-Angular	R	48.7	-50	32.9	127.85	54222	1.742	.01811
21	G_pariet_inf-Supramar	R	52.2	-39.4	41.4	134.18	52438	1.666	.02158
22	G_pariet_inf-Supramar	R	59.4	-24	33.2	113.64	27974	1.632	.02333
23	G_pariet_inf-Supramar	R	62	-37	19.9	80.36	159278	1.517	.03041
24	S_front_sup	R	21.3	11.8	45	54.78	25587	1.515	.03055
25	G_and_S_cingul-Mid-Post	R	9.9	0	50.4	18.66	92854	1.37	.04266

Cluster	Anatomical Parcellation	Hem.	Talairach (X Y Z)			Size (mm^2)	VtxMax	Max	Sig.
26	G_cuneus	R	6.7	-77	20.1	18.28	68568	1.337	.04603

| Anatomical Parcellation (aparc.a2009s): Annotation that VtxMax falls into
| VtxMax = Vertex of max sig. in cluster | Max = −log10 (p-value) of VtxMax | Sig. = *p*-value of VtxMax

(iii) Neurocognitive Measures

Delis-Kaplan Executive Function System (D-KEFS)

<u>D-KEFS Trail Making Test (TMT) Condition 2 (Number Sequencing)</u>

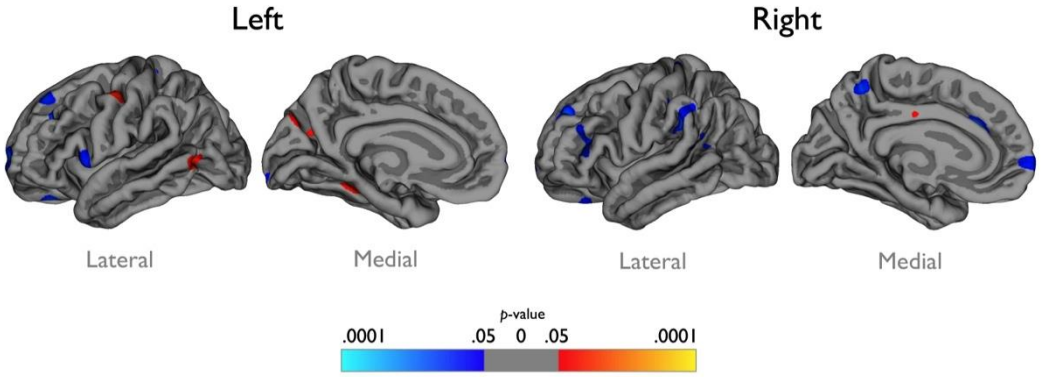

Appendix - Figure 2 Statistical correlation maps of cerebral grey matter thickness with TMT Condition 2 Primary Measure Scaled Scores for left and right hemispheres. Statistical maps with a significance threshold of *p*= .05 (uncorrected).

Appendix - Table 9 TMT Condition 2 Primary Measure Scaled Score vs. Grey Matter Thickness

Cluster	Anatomical Parcellation	Hem.	Talairach (X Y Z)			Size (mm^2)	VtxMax	Max	Sig.
1	S_orbital_med-olfact	L	-14.4	32	-19.5	204.18	20337	-2.445	.00359
2	S_postcentral	L	-46.9	-34.3	38.8	149.57	95619	-2.239	.00577
3	G_and_S_transv_frontopol	L	-14.4	59.9	0.4	200.62	35000	-2.012	.00973
4	G_temporal_middle	L	-51.2	-57.9	4.6	347.19	27621	1.960	.01096
5	S_front_sup	L	-26.9	33.9	29	258.54	132879	-1.886	.01300
6	G_precentral	L	-49.1	-6	44.8	88.63	843	1.756	.01754
7	G_front_sup	L	-17	39	39.6	103.28	60170	-1.751	.01774
8	S_parieto_occipital	L	-17.8	-60.3	28.1	263.58	3779	1.748	.01786
9	S_intrapariet_and_P_trans	L	-18.1	-63.8	39.5	68.85	71436	-1.742	.01811
10	S_circular_insula_inf	L	-47	-11.3	-8.8	148.46	35762	-1.688	.02051
11	G_oc-temp_lat-fusifor	L	-29.1	-42.5	-12.7	133.62	44084	1.598	.02523
12	G_front_inf-Opercular	L	-49.9	10.4	2.5	188	20449	-1.535	.02917
13	G_temporal_middle	L	-58.2	-31.9	-12.4	71.45	79552	1.511	.03083
14	S_temporal_sup	L	-56.2	-45.1	1.3	28.96	51880	1.510	.03090
15	Pole_occipital	L	-17	-96	-2.8	36.74	132472	-1.389	.04083
16	S_oc-temp_lat	L	-47.1	-42.9	-12.1	7.22	3307	1.335	.04624
17	G_parietal_sup	L	-14.9	-53.5	56.9	5.13	152140	-1.325	.04732
18	S_postcentral	L	-18.7	-33.4	62.2	4.95	98347	-1.319	.04797

Cluster	Anatomical Parcellation	Hem.	Talairach (X Y Z)			Size (mm^2)	VtxMax	Max	Sig.
19	S_postcentral	L	-30.9	-33.7	39.5	3.41	72466	-1.312	.04875
1	G_temp_sup-Plan_tempo	R	52.2	-35	29.6	422.86	107301	-2.206	.00622
2	G_and_S_cingul-Ant	R	14.6	31	22.3	216.54	154397	-2.172	.00673
3	G_front_sup	R	18.7	46.7	28.7	223.76	95575	-2.109	.00778
4	G_precuneus	R	8.4	-48.6	51.9	139.7	8853	-1.924	.01191
5	S_precentral-inf-part	R	41.6	5.4	20.3	64.01	115592	1.825	.01496
6	S_temporal_sup	R	50.6	-39.6	15	148.39	112981	-1.822	.01507
7	S_circular_insula_inf	R	47.7	-7.4	-10.7	129.24	54708	-1.766	.01714
8	S_front_inf	R	44.8	31.4	6	368.29	116198	-1.755	.01758
9	S_orbital-H_Shaped	R	29.4	43.6	-11.2	78.03	42050	1.638	.02301
10	G_pariet_inf-Angular	R	34.6	-62.1	43.7	73.32	66027	1.602	.02500
11	G_postcentral	R	25.8	-26.5	64.9	78.75	1824	-1.546	.02844
12	G_orbital	R	14.3	31.7	-22.8	70.86	6635	-1.535	.02917
13	S_temporal_sup	R	49.2	-50.5	12.8	31.66	27835	-1.524	.02992
14	S_postcentral	R	44.7	-21.6	40.3	37.72	50382	-1.521	.03013
15	G_and_S_transv_frontopol	R	8.6	59.5	-3.2	152.03	51228	-1.481	.03304
16	S_temporal_sup	R	53.7	-28.9	-8.1	17.01	79955	1.408	.03908
17	G_and_S_cingul-Mid-Post	R	3.9	-14.3	32.9	9.3	68412	1.381	.04159
18	S_central	R	31.8	-15.5	39.2	6.54	151720	-1.341	.04560

| Anatomical Parcellation (aparc.a2009s): Annotation that VtxMax falls into
| VtxMax = Vertex of max sig. in cluster | Max = −log10 (p-value) of VtxMax | Sig. = *p*-value of VtxMax

D-KEFS Trail Making Test (TMT) Condition 4 (Number-Letter Switching)

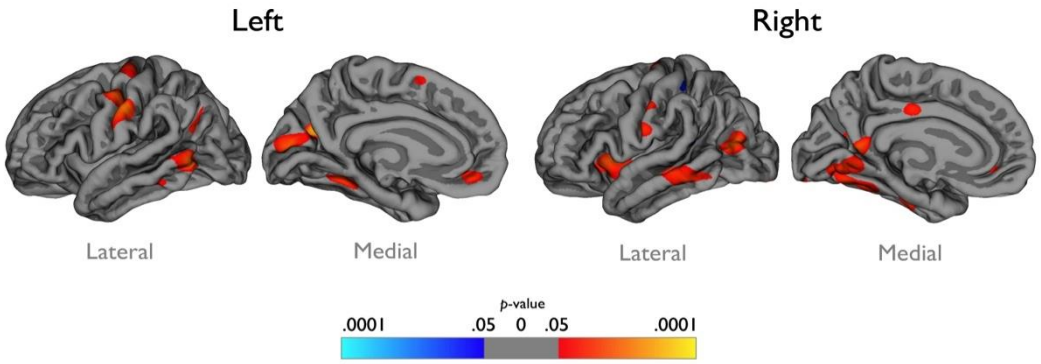

Appendix - Figure 3 Statistical correlation maps of cerebral grey matter thickness with TMT Condition 4 Primary Measure Scaled Scores for left and right hemispheres. Statistical maps with a significance threshold of *p*= .05 (uncorrected).

Appendix - Table 10 TMT Condition 4 Primary Measure Scaled Score vs. Grey Matter Thickness

Cluster	Anatomical Parcellation	Hem.	Talairach (X Y Z)			Size (mm^2)	VtxMax	Max	Sig.
1	S_parieto_occipital	L	-20.2	-62.6	25.4	901.95	74348	3.333	.00046
2	G_temporal_middle	L	-54.5	-58.1	2.7	508.71	86279	2.650	.00224
3	G_postcentral	L	-58	-13.1	35.9	787.63	66832	2.528	.00296
4	G_precentral	L	-49.6	-6.6	43.2	200.33	144394	2.228	.00592
5	G_oc-temp_lat-fusifor	L	-26.9	-47.1	-10.9	168.68	128309	1.910	.01230
6	S_suborbital	L	-8.2	40.2	-13.4	190.78	12549	1.798	.01592
7	G_precentral	L	-34.3	-12.1	61.1	145.33	97985	1.779	.01663
8	S_central	L	-41.5	-23.2	52.1	108.57	99116	1.777	.01671
9	G_and_S_subcentral	L	-53	-10.2	13.9	108.08	138568	1.771	.01694
10	S_temporal_sup	L	-39.6	-61.7	26.3	144.42	86290	1.760	.01738
11	S_intrapariet_and_P_trans	L	-17.6	-65.2	40	67.59	138827	-1.716	.01923
12	S_orbital-H_Shaped	L	-24	41.3	-10.3	53.8	33271	1.545	.02851
13	G_front_sup	L	-7.7	10.2	53.9	45.65	50695	1.465	.03428
14	S_central	L	-20.9	-28.2	52.1	23.03	116165	1.460	.03467
15	G_temporal_middle	L	-56.6	-38.9	-10.7	46.26	161980	1.395	.04027
16	G_and_S_cingul-Mid-Post	L	-7.8	-1.2	36.3	15.15	138937	1.394	.04036
17	S_front_inf	L	-37.3	15.5	20.2	13.95	129809	-1.389	.04083
18	S_oc-temp_med_and_Lingual	L	-33.6	-33.8	-10.8	18.83	70549	1.375	.04217
19	S_postcentral	L	-45.2	-33.7	37.1	27.54	66733	-1.375	.04217
20	S_orbital-H_Shaped	L	-24.4	27.6	-11.8	5.74	124738	1.327	.04710
1	S_temporal_sup	R	52.9	-28	-8.5	833.87	79958	3.375	.00042
2	G_occipital_middle	R	45.6	-68.2	14	521.35	126565	2.280	.00525
3	G_cingul-Post-ventral	R	6.2	-52.9	13.2	215.69	94311	2.232	.00586
4	G_insular_short	R	35.1	14.8	-1.6	457.83	110375	2.231	.00587
5	S_oc-temp_lat	R	44.4	-53.8	-6.5	193.64	17552	2.100	.00794
6	G_oc-temp_lat-fusifor	R	32.7	-50.9	-11.1	317.43	90857	1.990	.01023
7	G_postcentral	R	55.2	-10	34.2	309.18	59928	1.951	.01119
8	S_collat_transv_ant	R	46.6	-19.4	-23.2	168.96	163834	1.936	.01159
9	G_oc-temp_med-Lingual	R	12.4	-60.4	1.6	632.74	79533	1.927	.01183

Cluster	Anatomical Parcellation	Hem.	Talairach (X Y Z)			Size (mm^2)	VtxMax	Max	Sig.
10	S_orbital-H_Shaped	R	28.9	37.5	-11.4	141.94	16714	1.718	.01914
11	G_and_S_cingul-Mid-Post	R	4.1	-14.7	34.2	53.88	135041	1.700	.01995
12	S_temporal_sup	R	52	-39.7	15.2	41.1	88459	-1.672	.02128
13	G_precentral	R	25.2	-11.7	63.2	108.39	63420	1.663	.02173
14	G_postcentral	R	36.7	-30.9	51.8	73.66	140338	-1.626	.02366
15	G_pariet_inf-Angular	R	35.2	-64.5	43	104.91	122288	1.611	.02449
16	S_temporal_sup	R	52.6	-30.2	3.2	23.38	89	1.580	.02630
17	S_precentral-inf-part	R	39.6	6	20.8	77.07	10333	1.565	.02723
18	S_front_sup	R	21.1	11	45.8	40.02	25585	1.554	.02793
19	Pole_occipital	R	25.5	-92.4	-7	66.42	88	1.535	.02917
20	G_and_S_cingul-Ant	R	11.9	36.4	-7.9	48.83	110708	1.533	.02931
21	G_front_inf-Opercular	R	43.1	9.2	6.5	51.52	140726	1.446	.03581
22	S_parieto_occipital	R	23.3	-63.2	20	32.15	135318	1.380	.04169

| Anatomical Parcellation (aparc.a2009s): Annotation that VtxMax falls into
| VtxMax = Vertex of max sig. in cluster | Max = −log10 (p-value) of VtxMax | Sig. = *p*-value of VtxMax

D-KEFS Trail Making Test (TMT) Primary Contrast 2 (Condition 4 - Condition 2)

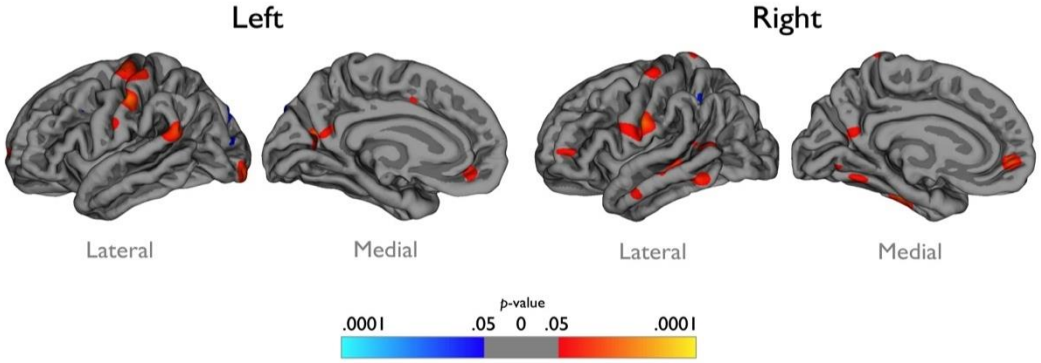

Appendix - Figure 4 Statistical correlation maps of cerebral grey matter thickness with TMT Primary Contrast 2 Contrast Scaled Scores for left and right hemispheres. Statistical maps with a significance threshold of *p*= .05 (uncorrected).

Appendix - Table 11 TMT Primary Contrast 2 Contrast Scaled Score vs. Grey Matter Thickness

Cluster	Anatomical Parcellation	Hem.	Talairach (X Y Z)			Size (mm^2)	VtxMax	Max	Sig.
1	G_postcentral	L	-56	-16.6	39.7	496.93	123406	2.398	.00400
2	S_parieto_occipital	L	-19.7	-65.7	17.7	269.68	39050	2.285	.00519
3	G_pariet_inf-Supramar	L	-58.6	-48.6	21.3	226.39	4206	2.155	.00700
4	Pole_occipital	L	-24.1	-93.8	-3.9	219.23	139261	2.095	.00804
5	G_precentral	L	-35.6	-11.5	60.1	345.47	13474	2.003	.00993
6	S_circular_insula_inf	L	-39.3	-18.4	-7	195.83	61063	1.784	.01644
7	G_occipital_sup	L	-14.9	-81.9	32.6	181.95	74414	-1.737	.01832
8	S_suborbital	L	-10.7	40.3	-11.5	164.28	141088	1.658	.02198
9	G_precuneus	L	-6.9	-54.5	21.3	70.41	159369	1.577	.02649
10	G_postcentral	L	-60.2	-7.8	22.9	115.84	81134	1.565	.02723
11	Lat_Fis-post	L	-46.3	-31.8	6	109	141855	1.557	.02773
12	G_and_S_transv_frontopol	L	-12.6	60.8	0	69.96	77338	1.533	.02931
13	G_occipital_middle	L	-31.3	-85.9	15.7	87.24	87153	-1.513	.03069
14	G_and_S_cingul-Mid-Post	L	-11.4	4.1	38.4	48.82	153598	1.464	.03436
15	S_front_inf	L	-38.4	15.9	32.1	4.57	30326	-1.324	.04742
1	S_collat_transv_ant	R	48.4	-26.4	-19.9	292.44	91537	2.424	.00377
2	G_postcentral	R	62.6	-7	23.6	420.55	9103	2.372	.00425
3	G_and_S_cingul-Ant	R	11.1	50.1	-4.3	221.95	134575	2.203	.00627
4	S_temporal_sup	R	55.1	-22.1	-10.7	390.26	17603	1.963	.01089
5	G_temporal_inf	R	56.6	-46.6	-9.7	210.23	128252	1.708	.01959
6	G_temporal_middle	R	55.9	-50.8	9.5	116.12	15707	1.693	.02028
7	S_intrapariet_and_P_trans	R	31.6	-43.1	43.2	56.65	152170	-1.683	.02075
8	S_front_sup	R	28.3	22.5	39.1	80.67	44325	1.615	.02427
9	S_parieto_occipital	R	21.6	-62.5	14.1	79.32	117672	1.587	.02588
10	G_and_S_paracentral	R	13.2	-36.9	71.1	51.46	45379	1.559	.02761
11	G_temporal_middle	R	58.5	-4.6	-21.9	43.75	70496	1.555	.02786
12	G_front_middle	R	40.2	42.4	1.3	111.74	106273	1.550	.02818
13	G_oc-temp_lat-fusifor	R	28.1	-55.4	-9.4	57.7	90827	1.541	.02877
14	G_precentral	R	39.2	-10.8	57.9	69.16	105890	1.484	.03281

Cluster	Anatomical Parcellation	Hem.	Talairach (X Y Z)			Size (mm^2)	VtxMax	Max	Sig.
15	G_precuneus	R	4.5	-56.2	21.6	49.8	64516	1.458	.03483
16	S_temporal_sup	R	44.6	-40.7	12	22.48	88506	1.457	.03491
17	G_oc-temp_med-Lingual	R	11.2	-68.8	-0.5	29.06	118318	1.355	.04416

| Anatomical Parcellation (aparc.a2009s): Annotation that VtxMax falls into
| VtxMax = Vertex of max sig. in cluster | Max = −log10 (p-value) of VtxMax | Sig. = *p*-value of VtxMax

D-KEFS Verbal Fluency Test (VFT) Condition 1 (Letter Fluency)

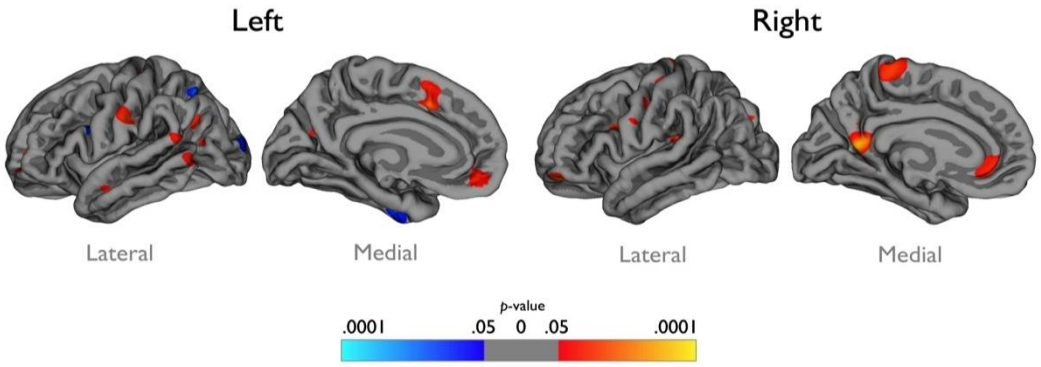

Appendix - Figure 5 Statistical correlation maps of cerebral grey matter thickness with VFT Condition 1 Primary Measure Scaled Scores for left and right hemispheres. Statistical maps with a significance threshold of *p*= .05 (uncorrected).

Appendix - Table 12 VFT Condition 1 Primary Measure Scaled Score vs. Grey Matter Thickness

Cluster	Anatomical Parcellation	Hem.	Talairach (X Y Z)			Size (mm^2)	VtxMax	Max	Sig.
1	G_and_S_cingul-Mid-Ant	L	-11.3	15.6	37.9	336.07	134120	2.450	.00355
2	S_intrapariet_and_P_trans	L	-22.2	-59	48.5	258.11	96833	-2.438	.00365
3	S_front_middle	L	-24.8	46.7	2.8	247.61	34969	2.172	.00673
4	G_postcentral	L	-57.6	-14.4	27.4	162.78	95699	2.127	.00746
5	S_front_inf	L	-40.6	13.9	20.5	126.52	57088	-2.112	.00773
6	S_collat_transv_ant	L	-39.7	-9.8	-28.5	439.58	62725	-2.031	.00931
7	S_temporal_sup	L	-39.8	-62.8	29.1	120.27	77986	1.921	.01199
8	S_postcentral	L	-36.9	-32.2	34.5	151.79	55000	-1.909	.01233
9	G_temporal_middle	L	-55	-57.7	3.5	170.16	111671	1.758	.01746
10	G_pariet_inf-Angular	L	-58	-49.2	18.4	94.07	78177	1.733	.01849
11	Pole_occipital	L	-23.8	-93.1	16.5	129.64	69098	-1.704	.01977
12	S_suborbital	L	-8.3	45.7	-13	252.8	141074	1.620	.02399
13	S_temporal_sup	L	-41.6	-68	15	59.39	141909	1.566	.02716
14	S_central	L	-16.5	-26	52.9	72.72	65409	1.564	.02729
15	S_parieto_occipital	L	-20.3	-63.6	24.9	90.28	74349	1.551	.02812
16	S_temporal_sup	L	-48.9	-4.4	-17.2	47.74	34124	1.524	.02992
17	G_oc-temp_med-Parahip	L	-28.5	-25.5	-19.8	52.45	163811	1.390	.04074
18	G_and_S_frontomargin	L	-30.1	51.5	-8.7	50.73	153910	1.357	.04395
19	G_temp_sup-G_T_transv	L	-41.7	-22.7	4.5	11.87	3092	-1.346	.04508
1	G_precuneus	R	5.4	-53.1	15.3	326.2	29354	3.173	.00067
2	G_orbital	R	33.6	46.5	-11	268.37	37654	2.398	.00400

Cluster	Anatomical Parcellation	Hem.	Talairach (X Y Z)			Size (mm^2)	VtxMax	Max	Sig.
3	S_precentral-inf-part	R	34.8	9.7	21.9	255.44	152409	2.354	.00443
4	Lat_Fis-post	R	33.4	-28	20.1	164	159775	2.181	.00659
5	G_and_S_paracentral	R	3.5	-30.2	61.1	272.8	41033	1.951	.01119
6	G_and_S_cingul-Ant	R	7.5	31.6	-8	288.18	129964	1.750	.01778
7	S_front_middle	R	26.8	45.8	3.7	67.88	99309	1.580	.02630
8	S_circular_insula_inf	R	44.3	-11.5	-10.7	82.3	23608	-1.530	.02951
9	S_front_sup	R	21.5	11.7	44.4	22.22	121140	1.486	.03266
10	G_precentral	R	46.7	-5.3	38.4	47.73	64129	1.414	.03855
11	G_precentral	R	35.8	-17.6	54.3	81.37	145221	1.413	.03864
12	G_occipital_sup	R	23.5	-77.7	33	26.99	104466	1.359	.04375
13	Pole_occipital	R	28.2	-91.2	-7.6	15.29	54777	1.355	.04416
14	G_precentral	R	57.3	1.4	26.4	21.54	26961	1.351	.04457
15	S_calcarine	R	21	-46.7	2.1	8.59	102945	1.350	.04467
16	G_precuneus	R	5.7	-54.7	28.1	1.72	78154	1.303	.04977

| Anatomical Parcellation (aparc.a2009s): Annotation that VtxMax falls into
| VtxMax = Vertex of max sig. in cluster | Max = −log10 (p-value) of VtxMax | Sig. = *p*-value of VtxMax

D-KEFS Verbal Fluency Test (VFT) Condition 2 (Category Fluency)

Appendix - Table 13 VFT Condition 2 Primary Measure Scaled Score vs. Grey Matter Thickness

Cluster	Anatomical Parcellation	Hem.	Talairach (X Y Z)			Size (mm^2)	VtxMax	Max	Sig.
1	G_and_S_cingul-Ant	L	-7.3	39.7	-4.2	1653.76	33162	3.175	.00067
2	S_temporal_sup	L	-37.4	-57.5	22.6	684.05	86315	2.698	.00200
3	G_front_sup	L	-7.8	11.8	49.7	852.27	82973	2.554	.00279
4	Lat_Fis-ant-Vertical	L	-36.6	22	8.5	90.8	110712	-2.457	.00349
5	G_postcentral	L	-60.7	-10.5	29.5	596.06	66856	2.302	.00499
6	S_temporal_inf	L	-52.3	-26.2	-18.6	257.08	130707	2.141	.00723
7	S_oc-temp_lat	L	-46.2	-41.2	-13.5	130.38	118343	1.872	.01343
8	S_temporal_inf	L	-48.4	-58	4.8	177.62	51791	1.810	.01549
9	G_oc-temp_med-Parahip	L	-28	-17.6	-24.9	251.31	39976	1.796	.01600
10	G_parietal_sup	L	-14.7	-45.9	66.2	48.34	37027	1.631	.02339
11	G_front_inf-Opercular	L	-46.5	13.6	20.3	59.14	73349	-1.618	.02410
12	G_parietal_sup	L	-10.1	-68.2	49.2	126.29	118941	-1.594	.02547
13	Lat_Fis-post	L	-43.5	-38.5	15	187.68	55448	1.562	.02742
14	G_front_inf-Opercular	L	-55.6	4	3.6	62.01	154388	-1.521	.03013
15	S_front_inf	L	-36.4	13.9	30.9	31.3	59428	-1.516	.03048
16	S_cingul-Marginalis	L	-15.9	-41.3	45.9	39.91	6029	-1.510	.03090
17	G_orbital	L	-37.2	48.4	-4.3	105.1	146314	1.500	.03162
18	G_temporal_middle	L	-54.3	-7.4	-20.3	38.18	69803	1.441	.03622
19	S_postcentral	L	-27.1	-31.5	54.9	13.46	19475	1.353	.04436
20	S_pericallosal	L	-8	-38.6	26.4	26.93	25350	1.350	.04467
1	G_and_S_cingul-Ant	R	12.8	38.1	-6.5	708.05	20540	3.872	.00013
2	G_cingul-Post-dorsal	R	5.9	-47	18.1	202.57	111444	3.125	.00075
3	G_orbital	R	32	43.7	-11.9	483.37	83903	2.635	.00232
4	G_and_S_cingul-Mid-Ant	R	9.9	5.9	35.2	125.28	138509	2.327	.00471
5	G_postcentral	R	57.8	-11.4	35.5	256.98	19614	2.087	.00818
6	S_front_middle	R	27.7	46.3	1.9	145.6	99314	1.945	.01135
7	S_oc-temp_lat	R	42.2	-55.7	-5.4	86.58	1783	1.858	.01387
8	G_temporal_middle	R	60.1	-39.9	-7.6	195.89	128165	1.814	.01535
9	S_front_sup	R	22.6	36.7	27.5	70.7	149840	1.741	.01816

Cluster	Anatomical Parcellation	Hem.	Talairach (X Y Z)			Size (mm^2)	VtxMax	Max	Sig.
10	S_precentral-inf-part	R	42.3	8.6	18	59.08	64184	1.699	.02000
11	G_parietal_sup	R	17.1	-53.7	60.8	53.59	151199	1.497	.03184
12	G_front_sup	R	8.7	17.9	51.2	40.43	119366	-1.442	.03614
13	G_oc-temp_med-Parahip	R	32.7	-8.7	-29.4	54.53	39933	1.418	.03819
14	G_and_S_subcentral	R	56	-8.8	11.5	17.42	124603	-1.389	.04083

| Anatomical Parcellation (aparc.a2009s): Annotation that VtxMax falls into
| VtxMax = Vertex of max sig. in cluster | Max = −log10 (p-value) of VtxMax | Sig. = *p*-value of VtxMax

D-KEFS Verbal Fluency Test (VFT) Condition 3 (Category Switching | Total Correct Response)

Appendix - Table 14 VFT Condition 3 Total Correct Response Scaled Score vs. Grey Matter Thickness

Cluster	Anatomical Parcellation	Hem.	Talairach (X Y Z)			Size (mm^2)	VtxMax	Max	Sig.
1	S_temporal_sup	L	-38.6	-53.7	24.6	2257.97	101067	4.529	.00003
2	S_front_middle	L	-28	45.1	5.1	2318.34	2807	3.703	.00020
3	G_and_S_occipital_inf	L	-22.2	-82.9	-4.3	2079.55	105280	3.672	.00021
4	G_cingul-Post-dorsal	L	-5.1	-38.1	31.2	437.99	88320	3.424	.00038
5	G_pariet_inf-Angular	L	-29.9	-61.9	40.6	1124.71	27759	3.073	.00085
6	G_front_sup	L	-7.4	24.8	37.4	321.66	73087	2.354	.00443
7	G_temporal_middle	L	-57.5	-18.4	-13	751.34	22276	2.272	.00535
8	G_and_S_cingul-Ant	L	-6.1	37.7	2.7	176.2	67545	2.141	.00723
9	S_circular_insula_sup	L	-28.3	18.5	7.3	84.52	1187	2.045	.00902
10	G_front_middle	L	-38.3	6.6	48.7	403.27	144549	1.943	.01140
11	G_front_middle	L	-34.9	26.2	36.1	388.04	123195	1.865	.01365
12	S_parieto_occipital	L	-15.3	-66.1	35.6	339.95	78403	1.823	.01503
13	S_central	L	-13.7	-31.3	58.1	101.15	76723	1.762	.01730
14	G_postcentral	L	-59.3	-7.7	28.7	200	45329	1.738	.01828
15	S_front_sup	L	-20.4	26.4	42	146.19	117063	1.698	.02004
16	G_oc-temp_med-Lingual	L	-19.1	-51.9	-3.8	67.46	116026	1.691	.02037
17	G_precentral	L	-57.4	1.3	20.8	144.5	14623	1.661	.02183
18	S_intrapariet_and_P_trans	L	-32.7	-42.6	34.5	71.2	50263	1.597	.02529
19	S_central	L	-37.8	-18.7	32.8	31.71	76306	1.441	.03622
20	S_temporal_transverse	L	-44.5	-30.1	4	19.06	47679	1.425	.03758
21	G_front_sup	L	-9.9	56.4	5.3	42.29	4073	1.385	.04121
22	G_pariet_inf-Angular	L	-49.8	-49.3	41.7	32.92	63627	1.370	.04266
23	S_oc_sup_and_transversal	L	-21.3	-83.2	16.8	14.05	64678	1.356	.04406
1	S_temporal_sup	R	39.4	-56.3	20.4	2331.5	117834	3.636	.00023
2	S_parieto_occipital	R	16.4	-62	34.7	570.14	106724	2.883	.00131
3	Pole_occipital	R	14.6	-85.8	-2.2	1491.87	101903	2.659	.00219
4	S_front_inf	R	41.2	25.1	22.2	552.58	23476	2.356	.00441
5	G_cingul-Post-ventral	R	9.2	-50.2	10.2	305.26	93229	2.323	.00475
6	G_rectus	R	6.4	47.8	-19.8	644.07	154962	2.315	.00484
7	S_front_sup	R	22.6	12.4	42.3	214.9	121150	2.236	.00581
8	G_front_sup	R	9.7	58.8	7.7	474.17	125076	2.170	.00676
9	G_and_S_paracentral	R	7.5	-27	53.8	636.85	41938	1.977	.01054
10	G_temporal_middle	R	63.9	-39.9	-3.9	252.82	162592	1.828	.01486
11	G_front_middle	R	37.3	24.5	36.6	99.16	103562	1.716	.01923
12	G_oc-temp_med-Lingual	R	15.7	-62.8	-1.3	320.08	143705	1.707	.01963
13	G_orbital	R	37	51.8	-7.6	139.65	77196	1.692	.02032
14	S_precentral-inf-part	R	39.1	2.7	33.1	113.35	133804	1.634	.02323
15	S_subparietal	R	8.8	-48.5	48.5	55.89	667	1.614	.02432

Cluster	Anatomical Parcellation	Hem.	Talairach (X Y Z)			Size (mm^2)	VtxMax	Max	Sig.
16	G_precuneus	R	6.7	-40.4	41.4	69.56	6757	1.524	.02992
17	S_front_middle	R	27.4	44.1	11.9	65.63	71053	1.458	.03483
18	S_central	R	44.1	-13.9	30.4	35.07	59942	1.430	.03715
19	G_front_inf-Opercular	R	39.2	17.6	8.3	67.85	140691	1.424	.03767
20	S_postcentral	R	24.1	-39.6	56.6	21.41	14637	1.386	.04111
21	G_pariet_inf-Supramar	R	58.2	-30.2	36.6	21.51	15388	1.358	.04385
22	Pole_temporal	R	40.9	14.6	-26.7	18.39	7899	-1.352	.04446
23	S_front_middle	R	26.9	35.1	24	20.61	123219	1.335	.04624
24	G_cuneus	R	4.4	-72.6	25.6	5.11	141961	1.317	.04819

| Anatomical Parcellation (aparc.a2009s): Annotation that VtxMax falls into
| VtxMax = Vertex of max sig. in cluster | Max = −log10 (p-value) of VtxMax | Sig. = *p*-value of VtxMax

D-KEFS Verbal Fluency Test (VFT) Condition 3 (Category Switching | Total Switching Accuracy)

Appendix - Table 15 VFT Condition 3 Total Switching Accuracy Scaled Score vs. Grey Matter Thickness

Cluster	Anatomical Parcellation	Hem.	Talairach (X Y Z)			Size (mm^2)	VtxMax	Max	Sig.
1	S_front_middle	L	-26.8	45.9	3.1	2269.29	44898	4.266	.00005
2	S_temporal_sup	L	-37.4	-58.1	25.9	1281.82	12788	4.018	.00010
3	G_cingul-Post-dorsal	L	-4.7	-38	30.9	645.5	88322	4.004	.00010
4	S_central	L	-38.1	-18.5	32.5	3044.8	144778	3.410	.00039
5	G_and_S_occipital_inf	L	-22.6	-82.8	-4.7	2221.72	105279	3.306	.00049
6	G_and_S_cingul-Ant	L	-7.6	39.5	1.7	248.01	7574	2.687	.00206
7	G_temporal_middle	L	-59.6	-19.2	-12.2	1152.79	161094	2.499	.00317
8	G_pariet_inf-Angular	L	-30.7	-62.5	41.2	875.1	96879	2.482	.00330
9	G_oc-temp_med-Lingual	L	-19.8	-51.5	-3.6	146.14	54351	2.144	.00718
10	G_front_middle	L	-33.8	27.4	34.7	338.5	26470	2.039	.00914
11	G_temporal_middle	L	-50.5	-61.7	10.3	624.95	38673	2.008	.00982
12	G_front_sup	L	-8.5	26.1	34.1	231.11	119732	1.878	.01324
13	S_parieto_occipital	L	-19.2	-67.6	26.9	254.71	130254	1.806	.01563
14	S_front_inf	L	-40.9	32.1	16.6	132.27	146131	1.779	.01663
15	S_circular_insula_sup	L	-28.5	17.2	8	44.84	73715	1.752	.01770
16	G_front_sup	L	-20.7	28.5	43.4	137.02	55094	1.610	.02455
17	G_pariet_inf-Supramar	L	-59.1	-27.4	30.1	160.37	98555	1.589	.02576
18	G_parietal_sup	L	-12.2	-48.8	62.3	56.87	26841	1.546	.02844
19	G_precuneus	L	-9.5	-50.5	47.4	39.95	147683	1.543	.02864
20	G_cuneus	L	-3.3	-84.9	14.5	93.71	9645	1.509	.03097
21	S_postcentral	L	-25.1	-35.8	49.4	21.15	26666	1.389	.04083
22	S_oc_sup_and_transversal	L	-20.7	-83.5	17.2	17.91	130309	1.384	.04130
23	S_oc-temp_lat	L	-39.9	-53.6	-8.2	44.16	53279	1.369	.04276
24	Lat_Fis-ant-Horizont	L	-42.7	31.1	-3.8	12.16	20568	1.363	.04335
25	G_parietal_sup	L	-23.4	-58.6	50.7	28.66	68752	1.359	.04375
26	G_front_sup	L	-10.4	53.7	5.9	10.32	76986	1.324	.04742
27	G_front_middle	L	-22.2	47	22.6	0.81	128796	1.303	.04977
1	G_orbital	R	8.6	49.7	-20.2	1339.44	154956	3.626	.00024
2	Pole_occipital	R	12.3	-90.1	-1.9	1875.53	127835	3.246	.00057
3	S_front_inf	R	40.6	25.1	21.2	615.44	882	3.055	.00088
4	S_temporal_sup	R	39.2	-66	20.7	903.39	135857	3.016	.00096
5	G_oc-temp_med-Lingual	R	18.6	-59.6	-2.8	593.61	143713	2.434	.00368

Cluster	Anatomical Parcellation	Hem.	Talairach (X Y Z)			Size (mm^2)	VtxMax	Max	Sig.
6	S_precentral-sup-part	R	32.4	-10.5	55.8	667.29	169	2.392	.00406
7	S_precentral-inf-part	R	37.7	4.8	34.8	365.13	12394	2.215	.00610
8	S_intrapariet_and_P_trans	R	36	-54.5	40.5	1000.76	71419	2.168	.00679
9	G_temporal_middle	R	61	-22.5	-10.4	1008.64	144241	2.136	.00731
10	S_postcentral	R	47.5	-21.3	35	349.91	57491	2.134	.00735
11	G_front_middle	R	36.9	26.8	38.7	545.72	33087	2.119	.00760
12	G_and_S_cingul-Mid-Post	R	4.7	-8.3	30.9	122.62	146641	1.945	.01135
13	S_front_sup	R	21.6	11.2	44.3	159.26	94706	1.942	.01143
14	S_front_middle	R	28.2	45	11.5	112.85	138391	1.794	.01607
15	S_parieto_occipital	R	12.6	-59.3	26.8	278.09	74012	1.685	.02065
16	S_circular_insula_sup	R	37.6	6.4	11.8	56.33	83141	1.679	.02094
17	G_precuneus	R	5.3	-53.2	16.1	196.42	13835	1.610	.02455
18	G_and_S_occipital_inf	R	40.5	-67.6	0.7	101.57	70237	1.585	.02600
19	S_central	R	52.6	-10.3	28.4	153.61	133407	1.555	.02786
20	G_cuneus	R	9.2	-85.6	17.4	41.84	156651	1.465	.03428
21	S_orbital_med-olfact	R	17.5	11.7	-13.1	14.51	39755	-1.461	.03459
22	S_subparietal	R	8.3	-34.3	33.4	8.67	55431	1.337	.04603
23	G_pariet_inf-Angular	R	55.3	-47.5	30.9	12.51	42216	1.330	.04677
24	G_postcentral	R	24.1	-27.8	66.3	26.36	123642	1.329	.04688
25	Pole_temporal	R	41	14.2	-25.7	5.3	75054	-1.316	.04831
26	G_orbital	R	25.3	19.2	-18.3	4.04	74949	-1.312	.04875
27	S_postcentral	R	25.3	-39.8	57.3	1.95	6480	1.306	.04943

| Anatomical Parcellation (aparc.a2009s): Annotation that VtxMax falls into
| VtxMax = Vertex of max sig. in cluster | Max = −log10 (p-value) of VtxMax | Sig. = *p*-value of VtxMax

D-KEFS Verbal Fluency Test (VFT) Primary Contrast Measure 1 (Condition 1 - Condition 2)

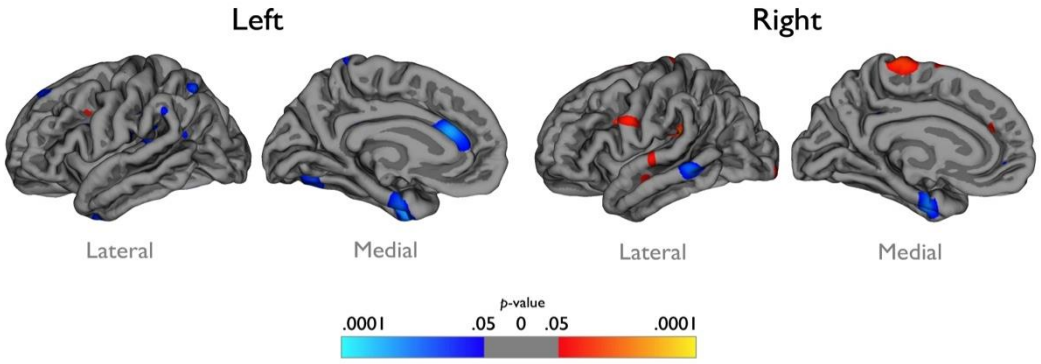

Appendix - Figure 6 Statistical correlation maps of cerebral grey matter thickness with VFT Primary Contrast Measure 1 Contrast Scaled Scores for left and right hemispheres. Statistical maps with a significance threshold of *p*= .05 (uncorrected).

Appendix - Table 16 VFT Primary Contrast Measure 1 Contrast Scaled Score vs. Grey Matter Thickness

Cluster	Anatomical Parcellation	Hem.	Talairach (X Y Z)			Size (mm^2)	VtxMax	Max	Sig.
1	G_and_S_cingul-Mid-Ant	L	-5.6	26.5	16.5	421.48	37466	-3.070	.00085
2	Pole_temporal	L	-32.7	-4.1	-30.7	590.37	75346	-2.871	.00135
3	S_postcentral	L	-49.6	-27.8	32.5	313.78	12171	-2.209	.00618
4	G_parietal_sup	L	-23.2	-59	50.9	231.5	135471	-2.184	.00655
5	Lat_Fis-post	L	-37.7	-32.5	9.6	305.94	130054	-2.175	.00668
6	G_oc-temp_lat-fusifor	L	-31.8	-65.5	-9.5	310.78	6103	-2.044	.00904
7	G_oc-temp_lat-fusifor	L	-41.2	-37.8	-16.5	304.37	114422	-1.967	.01079
8	G_front_sup	L	-13.6	39.7	40.2	108.64	82615	-1.775	.01679
9	G_and_S_subcentral	L	-54.9	-16.4	17.4	73.39	106625	-1.628	.02355
10	G_and_S_paracentral	L	-15.1	-37.6	66.4	60.85	92942	-1.537	.02904
11	S_front_inf	L	-35.4	12.9	21.3	24.66	149465	-1.532	.02938
12	Lat_Fis-post	L	-45.7	-33.2	25.1	50.55	20917	-1.528	.02965
13	S_temporal_sup	L	-37.2	-55.2	19	35.29	61410	-1.495	.03199
14	G_pariet_inf-Supramar	L	-57.2	-40.3	34.9	33.14	111254	-1.459	.03475
15	S_front_inf	L	-36.6	11.6	31.8	27.21	59421	1.457	.03491
16	S_pericallosal	L	-8.9	-35.5	26.5	32.05	17288	-1.376	.04207
1	S_precentral-inf-part	R	35.5	4.6	26.6	212.87	82831	2.928	.00118
2	G_oc-temp_med-Parahip	R	25.6	-8.8	-28	336.61	57752	-2.742	.00181
3	Lat_Fis-post	R	40.3	-32.9	22.4	362.72	159802	2.522	.00301
4	G_temporal_middle	R	60.9	-42	-4.4	297.85	91114	-2.454	.00352
5	S_central	R	33.2	-22.9	43.4	164.95	145177	2.006	.00986
6	G_and_S_paracentral	R	4.6	-22.6	67.3	285.07	94723	1.968	.01076
7	S_circular_insula_inf	R	41.8	-9.8	-12.5	222.45	122543	-1.903	.01250
8	G_precentral	R	57.4	1.8	24.7	85.28	109686	1.654	.02218
9	S_subparietal	R	9.6	-38.3	31.7	30.14	6765	-1.598	.02523
10	S_circular_insula_sup	R	35	-7.6	15.9	76.22	50768	1.553	.02799
11	G_temp_sup-Lateral	R	64	-13.7	0.8	56.53	116020	1.552	.02805
12	Lat_Fis-ant-Horizont	R	38.5	29.8	1.2	24.64	11341	1.533	.02931
13	G_and_S_cingul-Ant	R	11.3	38.8	20.8	41.36	45688	1.520	.03020
14	Pole_occipital	R	23.6	-96.6	-2.5	62.32	3503	1.515	.03055
15	G_front_sup	R	9.5	3.5	61.6	56.2	3543	1.479	.03319
16	G_and_S_subcentral	R	51.9	-11.7	16.3	29.38	153445	1.413	.03864
17	S_temporal_sup	R	51.6	-8.5	-10.4	54.82	22951	1.402	.03963
18	G_and_S_cingul-Ant	R	11.1	45.9	-5.2	9.09	84631	-1.329	.04688
19	S_parieto_occipital	R	16.9	-52.4	19.1	9.07	47733	1.313	.04864

| Anatomical Parcellation (aparc.a2009s): Annotation that VtxMax falls into
| VtxMax = Vertex of max sig. in cluster | Max = −log10 (p-value) of VtxMax | Sig. = *p*-value of VtxMax

D-KEFS Verbal Fluency Test (VFT) Primary Contrast Measure 2 (Condition 3 - Condition 2)

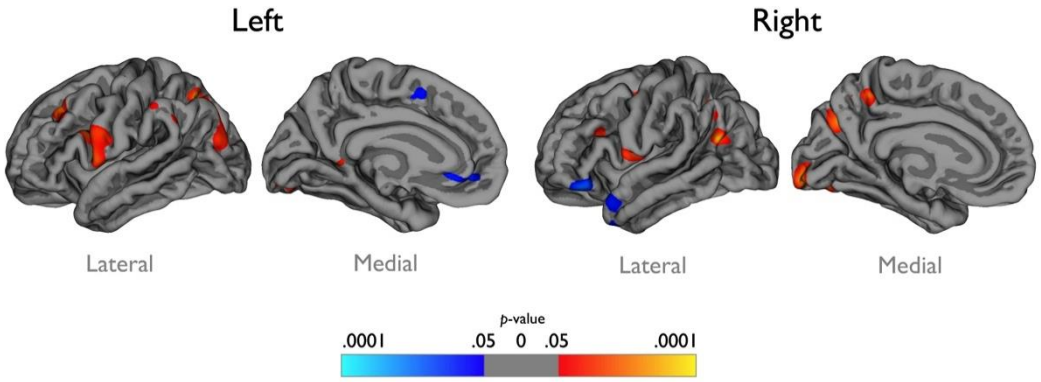

Appendix - Figure 7 Statistical correlation maps of cerebral grey matter thickness with VFT Primary Contrast Measure 2 Contrast Scaled Scores for left and right hemispheres. Statistical maps with a significance threshold of p= .05 (uncorrected).

Appendix - Table 17 VFT Primary Contrast Measure 2 Contrast Scaled Score vs. Grey Matter Thickness

Cluster	Anatomical Parcellation	Hem.	Talairach (X Y Z)			Size (mm^2)	VtxMax	Max	Sig.
1	S_intrapariet_and_P_trans	L	-17.4	-60.1	47.4	1429.01	111946	3.291	.00051
2	S_front_inf	L	-44	13.9	20.8	214.92	16769	2.796	.00160
3	G_front_middle	L	-32.5	29	35.3	510.34	149852	2.363	.00434
4	G_and_S_subcentral	L	-56.1	4.8	8.3	472.18	110468	2.224	.00597
5	Pole_occipital	L	-18.7	-86.1	-1.7	449.63	41724	2.085	.00822
6	S_circular_insula_sup	L	-33.2	18.7	10.7	54.79	64413	1.918	.01208
7	G_cingul-Post-ventral	L	-9	-46.8	7	36.77	139332	1.692	.02032
8	S_temporal_sup	L	-55.2	-24.6	-10.2	84.62	32670	1.633	.02328
9	S_oc_sup_and_transversal	L	-24	-85.7	16.3	65.86	57477	1.522	.03006
10	G_and_S_cingul-Ant	L	-6	27.9	-5.9	192.4	14827	-1.506	.03119
11	Lat_Fis-post	L	-33.2	-31.5	17.7	11.16	54124	-1.457	.03491
12	G_front_sup	L	-8.2	10.5	49	95.99	109690	-1.440	.03631
13	G_pariet_inf-Supramar	L	-56.4	-46.2	32.4	23.3	38338	1.432	.03698
14	G_pariet_inf-Supramar	L	-56.9	-33	39.7	28.16	3114	1.411	.03882
15	S_circular_insula_sup	L	-27	26.2	1.1	0.98	100902	1.302	.04989
1	S_temporal_sup	R	44.8	-56.7	21.6	396.21	93283	3.854	.00014
2	Pole_occipital	R	11.5	-91.8	-1.4	1107.59	90436	3.265	.00054
3	S_parieto_occipital	R	18.9	-64.6	33.5	381.73	146860	2.611	.00245
4	G_precuneus	R	6.7	-45.4	49.1	145.8	19596	2.398	.00400
5	G_orbital	R	47.2	32.8	-12	252.6	83952	-2.211	.00615
6	G_and_S_subcentral	R	55.2	0.8	10.1	204.34	153488	1.983	.01040
7	S_front_inf	R	40.2	24.9	20.2	153.84	14167	1.759	.01742
8	S_circular_insula_sup	R	30.9	13.1	7.9	52.73	45675	1.622	.02388
9	S_oc_sup_and_transversal	R	32.6	-65.3	25.3	43.98	52074	1.570	.02692
10	S_postcentral	R	32.5	-38.1	36.1	66.16	7338	1.562	.02742
11	G_temp_sup-Lateral	R	48.3	10.2	-20.6	90.65	148261	-1.497	.03184
12	S_precentral-sup-part	R	22	-4.7	46.6	81.63	56177	1.480	.03311
13	Pole_temporal	R	39.4	6.1	-31.5	108.92	104959	-1.462	.03451
14	S_intrapariet_and_P_trans	R	30.8	-55.1	44.1	78.87	157433	1.450	.03548
15	G_pariet_inf-Angular	R	46.2	-54.6	36.4	39.5	126466	1.422	.03784

Cluster	Anatomical Parcellation	Hem.	Talairach (X Y Z)			Size (mm^2)	VtxMax	Max	Sig.
16	G_precuneus	R	6.3	-56	49.8	1.34	16093	1.306	.04943

| Anatomical Parcellation (aparc.a2009s): Annotation that VtxMax falls into
| VtxMax = Vertex of max sig. in cluster | Max = −log10 (p-value) of VtxMax | Sig. = *p*-value of VtxMax

D-KEFS Colour Word Interference Test (CWIT) Condition 1 (Colour Naming)

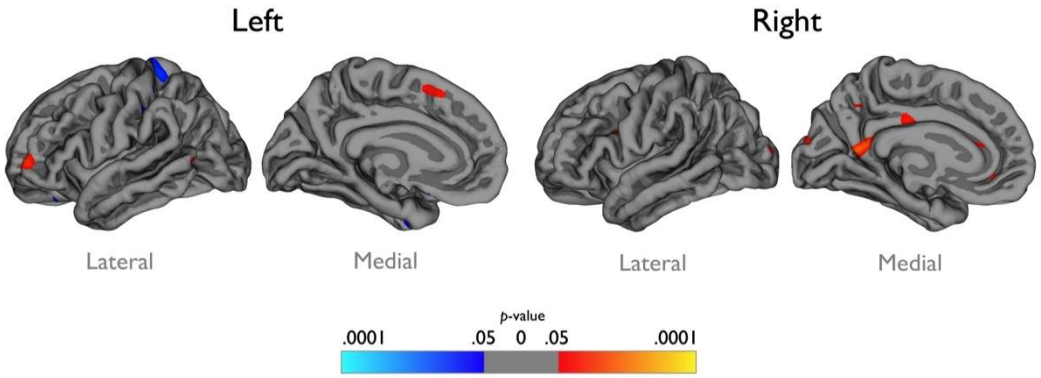

Appendix - Figure 8 Statistical correlation maps of cerebral grey matter thickness with CWIT Condition 1 Primary Measure Scaled Scores for left and right hemispheres. Statistical maps with a significance threshold of *p*= .05 (uncorrected).

Appendix - Table 18 CWIT Condition 1 Primary Measure Scaled Score vs. Grey Matter Thickness

Cluster	Anatomical Parcellation	Hem.	Talairach (X Y Z)			Size (mm^2)	VtxMax	Max	Sig.
1	G_front_middle	L	-34	50.6	0.5	379.86	94924	2.070	.00851
2	S_postcentral	L	-44.4	-31.1	34.2	195.97	19223	-1.989	.01026
3	G_and_S_paracentral	L	-18.5	-35.1	62.3	140.12	64074	-1.796	.01600
4	G_temporal_middle	L	-51	-58.3	6.2	123.43	96741	1.781	.01656
5	S_precentral-inf-part	L	-45.1	3.1	19.6	87.8	8629	1.646	.02259
6	S_oc_sup_and_transversal	L	-23.6	-78.8	16.2	55.69	786	1.591	.02564
7	G_front_sup	L	-8.9	15.7	49.6	107.41	109645	1.565	.02723
8	G_rectus	L	-7.8	12.6	-14.4	10.21	66194	-1.470	.03388
9	G_temporal_middle	L	-57.9	-31.2	-12.4	34.4	79553	1.458	.03483
10	S_precentral-sup-part	L	-38.2	-0.1	40	133.38	94705	1.438	.03648
11	Lat_Fis-post	L	-45.3	-39.3	18.9	17	45854	1.411	.03882
12	Pole_temporal	L	-32	-2.8	-31.9	28.03	75342	-1.395	.04027
13	G_postcentral	L	-41.3	-30.7	51.9	15.97	7491	-1.360	.04365
14	G_orbital	L	-17.1	31.2	-19.7	10.63	60592	-1.347	.04498
1	G_precuneus	R	5.8	-54.4	14.7	270.87	3752	2.358	.00439
2	S_intrapariet_and_P_trans	R	33.6	-61.8	40.2	233.44	38835	1.998	.01005
3	S_collat_transv_ant	R	42.1	-28.1	-15.6	107.18	162370	-1.807	.01560
4	S_precentral-inf-part	R	38.2	10.6	19.9	79.92	115578	1.676	.02109
5	G_and_S_cingul-Mid-Post	R	4.6	-18.2	30.4	64.11	38401	1.608	.02466
6	G_occipital_sup	R	12.9	-86.2	20	81.94	55484	1.499	.03170
7	S_intrapariet_and_P_trans	R	37.3	-44.3	35.7	66.71	32550	1.498	.03177
8	G_orbital	R	36	43.5	-10.7	55.11	51004	1.476	.03342
9	G_precuneus	R	8.3	-52.4	42.9	26.52	28907	1.472	.03373
10	S_precentral-inf-part	R	41.4	2.1	30.2	56.5	67450	1.451	.03540

Cluster	Anatomical Parcellation	Hem.	Talairach (X Y Z)			Size (mm^2)	VtxMax	Max	Sig.
11	G_postcentral	R	26.2	-26.5	61.6	40.2	144864	-1.440	.03631
12	G_and_S_cingul-Ant	R	11.6	35.7	-8.5	21.37	154862	1.414	.03855
13	G_front_inf-Opercular	R	40.3	7.1	9.8	13.74	133954	1.389	.04083
14	S_pericallosal	R	8.3	28.6	12.1	37.18	99345	1.379	.04178
15	Pole_occipital	R	24.7	-92.4	14.1	23.48	61941	1.343	.04539
16	S_temporal_sup	R	47.6	-39.8	14.4	2.03	159436	-1.331	.04667
17	G_precuneus	R	8.5	-52.7	54	1.53	151367	-1.312	.04875
18	S_temporal_sup	R	46.2	-41.3	4.5	0.32	63806	1.301	.05000

| Anatomical Parcellation (aparc.a2009s): Annotation that VtxMax falls into
| VtxMax = Vertex of max sig. in cluster | Max = −log10 (p-value) of VtxMax | Sig. = *p*-value of VtxMax

D-KEFS Colour Word Interference Test (CWIT) Condition 2 (Word Reading)

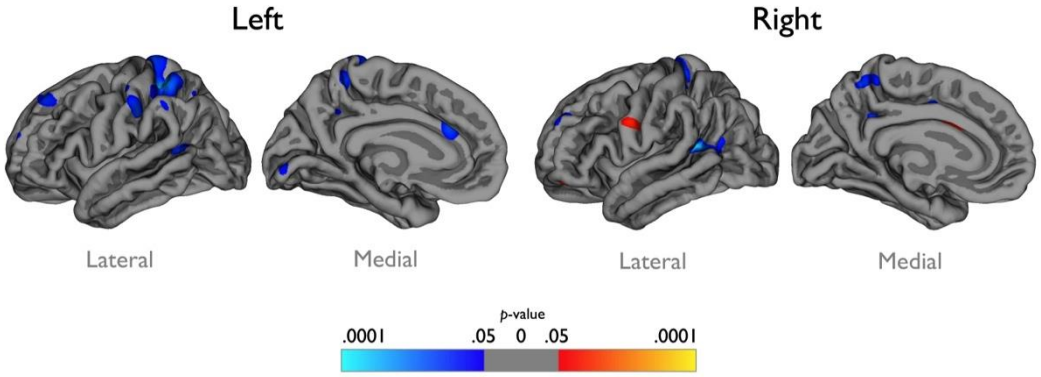

Appendix - Figure 9 Statistical correlation maps of cerebral grey matter thickness with CWIT Condition 2 Primary Measure Scaled Scores for left and right hemispheres. Statistical maps with a significance threshold of *p*= .05 (uncorrected).

Appendix - Table 19 CWIT Condition 2 Primary Measure Scaled Score vs. Grey Matter Thickness

Cluster	Anatomical Parcellation	Hem.	Talairach (X Y Z)			Size (mm^2)	VtxMax	Max	Sig.
1	S_postcentral	L	-24.1	-38.3	51.6	1291.45	151017	-3.344	.00045
2	S_intrapariet_and_P_trans	L	-19.6	-58.2	41	428.78	157426	-2.167	.00681
3	G_and_S_cingul-Mid-Ant	L	-7.4	25.9	21.8	197.73	124563	-2.149	.00710
4	S_postcentral	L	-49.6	-20.7	33.6	469.14	150395	-2.122	.00755
5	S_temporal_sup	L	-46.2	-52.2	8.9	194.29	101089	-1.993	.01016
6	S_cingul-Marginalis	L	-12.9	-44	56.3	165.98	8916	-1.935	.01161
7	G_front_sup	L	-17	38.9	38.9	142.95	60169	-1.775	.01679
8	S_precentral-sup-part	L	-24.1	-11.1	53	82.95	6181	-1.699	.02000
9	G_front_middle	L	-19.6	55.7	13.7	87.87	46713	-1.556	.02780
10	G_oc-temp_med-Lingual	L	-6.5	-84.6	2.7	72.68	11601	-1.531	.02944
11	G_pariet_inf-Supramar	L	-55.3	-39.8	38.7	30.42	96588	-1.470	.03388
12	S_subparietal	L	-12.9	-48.3	37.3	36.04	88204	-1.428	.03733
13	G_postcentral	L	-50.4	-14.8	49	27.64	80847	-1.384	.04130
14	S_temporal_transverse	L	-54.5	-24.9	3.1	16.11	24069	-1.358	.04385
15	G_temporal_middle	L	-49.6	-5.7	-25.7	4.32	113962	-1.310	.04898
1	S_temporal_sup	R	44.2	-43.1	13.8	517.98	28068	-3.405	.00039
2	S_circular_insula_inf	R	43.6	-7.9	-13.6	223.32	11989	-2.473	.00337

Cluster	Anatomical Parcellation	Hem.	Talairach (X Y Z)			Size (mm^2)	VtxMax	Max	Sig.
3	G_precuneus	R	8.9	-48.8	54.8	196.15	123792	-1.918	.01208
4	S_subparietal	R	14.6	-41.7	33.6	66.07	27489	-1.862	.01374
5	S_postcentral	R	18.5	-31.7	62.1	170.18	59801	-1.791	.01618
6	G_and_S_cingul-Mid-Post	R	10.5	-1.5	39.5	43.74	36521	-1.719	.01910
7	G_precentral	R	57.5	1.9	25.9	82.48	82968	1.666	.02158
8	G_pariet_inf-Supramar	R	47.3	-33.7	42.4	68.17	21700	-1.632	.02333
9	S_pericallosal	R	3.3	7.7	24.5	110.32	44981	1.589	.02576
10	G_front_middle	R	21	48	27.2	143.58	123171	-1.580	.02630
11	S_oc-temp_med_and_Lingual	R	26.5	-46.8	-2.8	54.18	148742	-1.561	.02748
12	G_orbital	R	33	44.2	-11.4	72.11	83899	1.556	.02780
13	S_postcentral	R	26.8	-32.2	52.2	49.38	56879	-1.502	.03148
14	S_temporal_inf	R	55.3	-46.8	-2.9	7.26	137319	-1.334	.04634
15	G_postcentral	R	33.4	-26.6	60.2	17.69	5899	-1.333	.04645
16	S_oc_middle_and_Lunatus	R	34	-75	11.2	2.58	112595	-1.304	.04966

| Anatomical Parcellation (aparc.a2009s): Annotation that VtxMax falls into
| VtxMax = Vertex of max sig. in cluster | Max = −log10 (p-value) of VtxMax | Sig. = *p*-value of VtxMax

D-KEFS Colour Word Interference Test (CWIT) Condition 3 (Inhibition)

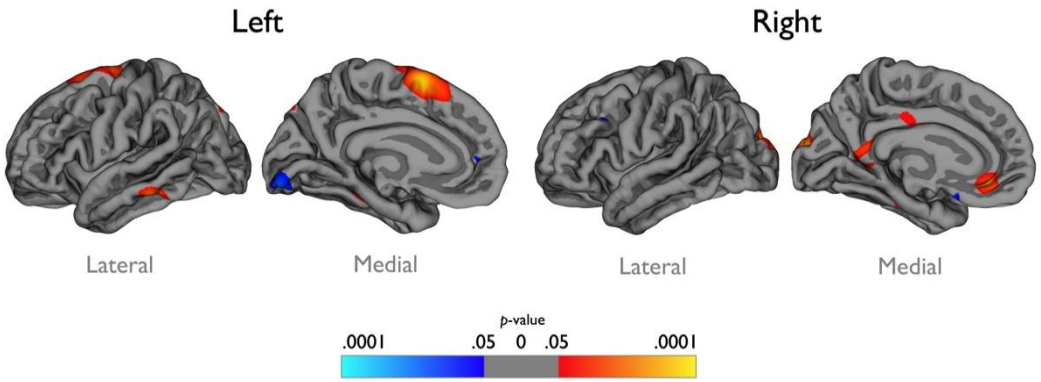

Appendix - Figure 10 Statistical correlation maps of cerebral grey matter thickness with CWIT Condition 3 Primary Measure Scaled Scores for left and right hemispheres. Statistical maps with a significance threshold of *p*= .05 (uncorrected).

Appendix - Table 20 CWIT Condition 3 Primary Measure Scaled Score vs. Grey Matter Thickness

Cluster	Anatomical Parcellation	Hem.	Talairach (X Y Z)			Size (mm^2)	VtxMax	Max	Sig.
1	G_front_sup	L	-7.2	10.3	55.3	1140.19	50692	3.466	.00034
2	G_temporal_middle	L	-59.8	-33.3	-12.3	252.85	107631	2.667	.00215
3	G_oc-temp_med-Lingual	L	-8.6	-89.2	-4.4	488.11	53432	-2.535	.00292
4	S_precentral-inf-part	L	-39.2	0	28.4	128.03	71976	1.937	.01156
5	G_and_S_frontomargin	L	-26	47.6	-3.4	185.68	48777	1.854	.01400
6	S_oc-temp_med_and_Lingual	L	-35.4	-36.3	-14.2	178.32	22823	1.698	.02004
7	G_and_S_cingul-Ant	L	-11.1	46	3.8	27.76	37401	-1.478	.03327
8	G_occipital_sup	L	-19.1	-77.3	40.9	42.71	35479	1.463	.03443
9	S_circular_insula_inf	L	-43.9	-22.3	1.7	29.65	117452	-1.442	.03614
1	G_occipital_sup	R	14.8	-88.6	20.9	541.8	135691	2.995	.00101
2	G_and_S_cingul-Ant	R	10.6	32.4	-10.1	314.22	64414	2.856	.00139

Cluster	Anatomical Parcellation	Hem.	Talairach (X Y Z)			Size (mm^2)	VtxMax	Max	Sig.
3	S_temporal_sup	R	50.9	-38.5	13.8	91.69	159409	-2.576	.00265
4	G_temp_sup-Plan_tempo	R	52.9	-25.4	7.9	388.62	159911	-2.282	.00522
5	S_circular_insula_sup	R	32.2	13	10.7	120.81	10702	2.258	.00552
6	S_oc-temp_med_and_Lingual	R	37.7	-25.4	-20.1	279.56	127759	2.034	.00925
7	G_cingul-Post-ventral	R	6.3	-47.7	17.3	297.83	85900	1.892	.01282
8	G_front_middle	R	32.5	16.1	45.2	157.51	17912	1.769	.01702
9	S_pericallosal	R	4.7	-14.4	27.3	37.69	141766	1.712	.01941
10	G_and_S_subcentral	R	57.8	-12	18.2	44.43	147865	-1.563	.02735
11	G_subcallosal	R	7.8	12	-14.3	20.88	61110	-1.557	.02773
12	S_circular_insula_inf	R	44	-20.8	-1.5	69.13	137521	-1.497	.03184
13	G_and_S_cingul-Mid-Post	R	3.9	-17.8	32.1	43.74	68419	1.447	.03573
14	S_cingul-Marginalis	R	14	-36.2	39	16.71	155902	1.392	.04055
15	S_temporal_sup	R	48.5	-42.1	4.8	6.27	98191	1.360	.04365
16	S_front_inf	R	39.1	21.5	30	20.16	133709	-1.347	.04498
17	G_orbital	R	13.7	34.2	-22.5	3.05	45615	-1.330	.04677
18	G_front_middle	R	41.9	27.2	27.5	11.27	152307	-1.328	.04699

| Anatomical Parcellation (aparc.a2009s): Annotation that VtxMax falls into
| VtxMax = Vertex of max sig. in cluster | Max = −log10 (p-value) of VtxMax | Sig. = *p*-value of VtxMax

D-KEFS Colour Word Interference Test (CWIT) Primary Combined Measure (Condition 1 + Condition 2)

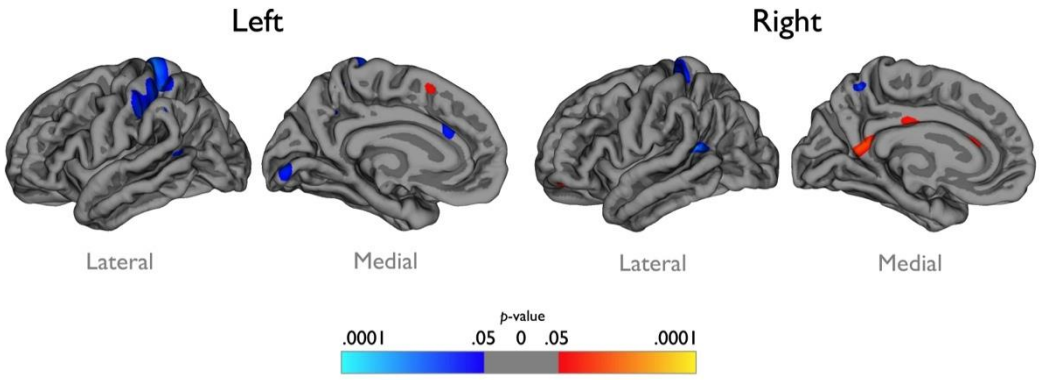

Appendix - Figure 11 Statistical correlation maps of cerebral grey matter thickness with CWIT Primary Combined Measure Composite Scaled Scores for left and right hemispheres. Statistical maps with a significance threshold of *p*= .05 (uncorrected).

Appendix - Table 21 CWIT Primary Combined Measure Composite Scaled Score vs. Grey Matter Thickness

Cluster	Anatomical Parcellation	Hem.	Talairach (X Y Z)			Size (mm^2)	VtxMax	Max	Sig.
1	G_postcentral	L	-16.2	-31.9	67.5	840.13	98340	-2.489	.00324
2	S_postcentral	L	-44.9	-30	33.5	917.58	150101	-2.482	.00330
3	G_oc-temp_med-Lingual	L	-5.4	-84.5	2.2	128.39	94612	-1.699	.02000
4	G_and_S_cingul-Mid-Ant	L	-6.4	25.2	22	94.91	60449	-1.625	.02371
5	S_temporal_sup	L	-46.1	-50.5	8.7	72.06	101086	-1.620	.02399
6	S_intrapariet_and_P_trans	L	-19.5	-58.2	41.9	66.32	9527	-1.560	.02754
7	G_front_sup	L	-8.6	15.8	50.2	45.74	109643	1.528	.02965

Cluster	Anatomical Parcellation	Hem.	Talairach (X Y Z)			Size (mm^2)	VtxMax	Max	Sig.
8	G_and_S_frontomargin	L	-24.8	47	-0.7	116.04	94928	1.527	.02972
9	S_temporal_transverse	L	-54.3	-24.3	2.5	36.33	55473	-1.491	.03228
10	S_precentral-sup-part	L	-23.1	-11.1	53	12.12	29783	-1.366	.04305
11	G_temp_sup-Plan_polar	L	-50.1	-11.1	-1.4	22.4	20667	-1.341	.04560
12	S_subparietal	L	-10.5	-49.8	38.2	11.8	62038	-1.339	.04581
13	G_pariet_inf-Supramar	L	-55.4	-40.2	37.5	4.72	43420	-1.321	.04775
14	S_cingul-Marginalis	L	-12.4	-44.2	55.9	6.3	82256	-1.313	.04864
1	S_temporal_sup	R	45.2	-40.9	14.3	228.79	52537	-2.760	.00174
2	S_circular_insula_inf	R	44.2	-8.6	-13	156.08	132253	-2.152	.00705
3	G_cingul-Post-dorsal	R	6.7	-48.7	17.9	180.18	85899	2.120	.00759
4	G_precuneus	R	9	-51.2	53.9	81.55	81770	-1.934	.01164
5	G_orbital	R	34.3	43.9	-10.7	134.3	51007	1.837	.01455
6	G_postcentral	R	27.3	-26.3	62.1	531.71	105728	-1.778	.01667
7	G_and_S_cingul-Mid-Post	R	4.9	-16.6	30.4	78.22	38400	1.589	.02576
8	S_collat_transv_ant	R	43.3	-30.1	-15.6	53.16	90929	-1.574	.02667
9	S_pericallosal	R	3.1	23.5	13.9	67.41	121885	1.469	.03396
10	S_oc-temp_med_and_Lingual	R	25.3	-47.9	-2.7	21.43	35918	-1.407	.03917
11	S_intrapariet_and_P_trans	R	33.3	-61.3	40.3	25.65	86846	1.399	.03990
12	G_front_sup	R	19.9	48.4	25.7	21.91	108162	-1.378	.04188
13	S_precentral-inf-part	R	39.6	2.3	30.4	18.58	133819	1.360	.04365

| Anatomical Parcellation (aparc.a2009s): Annotation that VtxMax falls into
| VtxMax = Vertex of max sig. in cluster | Max = −log10 (p-value) of VtxMax | Sig. = *p*-value of VtxMax

D-KEFS Colour Word Interference Test (CWIT) Primary Contrast Measure 1 (Condition 3 - Condition 1)

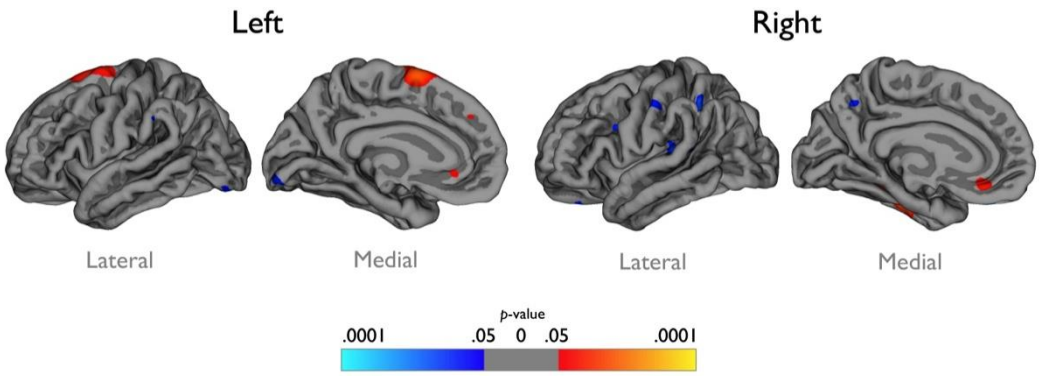

Appendix - Figure 12 Statistical correlation maps of cerebral grey matter thickness with CWIT Primary Contrast Measure 1 Contrast Scaled Scores for left and right hemispheres. Statistical maps with a significance threshold of *p*= .05 (uncorrected).

Appendix - Table 22 CWIT Primary Contrast Measure 1 Contrast Scaled Score vs. Grey Matter Thickness

Cluster	Anatomical Parcellation	Hem.	Talairach (X Y Z)			Size (mm^2)	VtxMax	Max	Sig.
1	G_front_sup	L	-6.6	8.1	58.3	676.13	152782	2.231	.00587
2	G_oc-temp_med-Lingual	L	-8.9	-90.1	-3.9	265.23	137342	-2.146	.00714
3	Lat_Fis-post	L	-38.7	-34.1	9.4	44.35	104239	-1.599	.02518
4	G_and_S_occipital_inf	L	-37.3	-84	-8.5	34.14	23651	-1.422	.03784
5	S_pericallosal	L	-5.6	28.6	-4.4	36.92	30747	1.391	.04064
6	G_pariet_inf-Supramar	L	-59	-31.7	32.6	13.22	73771	-1.356	.04406
7	S_precentral-inf-part	L	-42.5	-0.8	32.2	12.34	80264	1.349	.04477
8	S_orbital-H_Shaped	L	-21.2	34.3	-12	6.7	134242	1.346	.04508
9	G_front_sup	L	-8.1	42.8	30.7	11.31	94089	1.332	.04656
10	G_temp_sup-Plan_polar	L	-37.4	3.2	-24	1.22	79370	-1.305	.04955
1	S_collat_transv_ant	R	47	-24.8	-19.8	442.39	163106	2.926	.00119
2	Lat_Fis-post	R	39.3	-16.1	21.3	690.3	159720	-2.294	.00508
3	S_intrapariet_and_P_trans	R	32.6	-43.1	44.7	185.01	82437	-2.233	.00585
4	S_circular_insula_sup	R	32.2	13	10.7	51.44	10702	1.773	.01687
5	G_precuneus	R	8.8	-55.3	44.8	52.12	56418	-1.724	.01888
6	S_central	R	50.7	-13.2	37.5	218.02	151567	-1.681	.02084
7	S_front_inf	R	32.6	11.8	23.7	63.4	152401	-1.680	.02089
8	S_oc-temp_med_and_Lingual	R	37.6	-35.3	-11.9	77.03	161469	1.664	.02168
9	G_and_S_cingul-Ant	R	8.9	30.3	-12.6	112.26	57211	1.658	.02198
10	S_temporal_sup	R	55.1	-37.7	13.5	50.78	118085	-1.565	.02723
11	G_orbital	R	13.4	34.2	-22.4	55.03	45748	-1.553	.02799
12	S_cingul-Marginalis	R	14	-30.4	36	21.25	120046	1.519	.03027
13	S_front_inf	R	42.5	31.9	7.1	2.6	116202	-1.313	.04864

| Anatomical Parcellation (aparc.a2009s): Annotation that VtxMax falls into
| VtxMax = Vertex of max sig. in cluster | Max = −log10 (p-value) of VtxMax | Sig. = *p*-value of VtxMax

D-KEFS Tower Test (TT) Primary Measure Total Achievement

Appendix - Table 23 TT Primary Measure Total Achievement Scaled Score vs. Grey Matter Thickness

Cluster	Anatomical Parcellation	Hem.	Talairach (X Y Z)			Size (mm^2)	VtxMax	Max	Sig.
1	S_temporal_sup	L	-50.9	-34.9	-5.8	565.78	71715	4.097	.00008
2	G_and_S_cingul-Mid-Ant	L	-10.9	13.6	39.3	156.47	67693	2.699	.00200
3	G_oc-temp_med-Lingual	L	-5.8	-71.2	3.7	1579.83	46442	-2.489	.00324
4	S_temporal_sup	L	-51.4	-8.9	-19.3	755.39	46303	2.407	.00392
5	S_front_middle	L	-24.7	45.9	5.7	1015.08	18070	2.259	.00551
6	G_rectus	L	-6.8	52.1	-20.6	635.78	30885	2.029	.00935
7	G_parietal_sup	L	-23.7	-58.4	50.3	163.07	101156	-1.989	.01026
8	G_temp_sup-Plan_tempo	L	-56.6	-39.8	33.3	103.79	27483	-1.982	.01042
9	S_circular_insula_ant	L	-27.3	15.2	-9	194.23	89163	1.966	.01081
10	G_precentral	L	-44	-5.5	45.3	200.7	105532	1.840	.01445
11	S_oc-temp_med_and_Lingual	L	-26	-42.9	-3.8	122.8	25554	1.760	.01738
12	Lat_Fis-ant-Horizont	L	-40.2	30.1	-1.9	80.77	110757	1.744	.01803
13	G_pariet_inf-Supramar	L	-49.9	-45.8	39.1	100.7	128947	1.730	.01862
14	S_oc-temp_med_and_Lingual	L	-33.6	-37.1	-15.2	88.39	163076	1.642	.02280
15	S_circular_insula_inf	L	-32.1	-24.6	6.2	31.91	125359	-1.519	.03027
16	S_parieto_occipital	L	-20.2	-58.1	22	61.92	55752	1.480	.03311

Cluster	Anatomical Parcellation	Hem.	Talairach (X Y Z)			Size (mm^2)	VtxMax	Max	Sig.
17	G_temp_sup-Plan_tempo	L	-50.5	-41.7	19.4	23.72	156263	1.454	.03516
18	G_front_sup	L	-6.9	-0.5	48.9	18.18	83012	1.376	.04207
19	S_circular_insula_sup	L	-34.5	14.8	10.7	39.56	64402	1.375	.04217
20	G_front_sup	L	-6.5	13.3	56.8	44.71	82935	1.369	.04276
21	G_pariet_inf-Angular	L	-55.9	-48.6	16.8	9.83	13824	1.357	.04395
22	G_oc-temp_med-Parahip	L	-24.9	-1.2	-25.7	2.5	127415	1.345	.04519
23	G_precentral	L	-23.6	-13.9	61.9	3.36	145179	1.322	.04764
24	G_temp_sup-G_T_transv	L	-51.3	-11.6	0.5	4.12	85033	1.308	.04920
25	S_circular_insula_sup	L	-44.1	-11.9	18.3	0.93	116300	1.303	.04977
1	G_front_middle	R	39.9	46.4	1.9	760	77261	2.679	.00209
2	S_orbital-H_Shaped	R	31.7	32.4	-8.1	1311.66	93044	2.399	.00399
3	S_temporal_sup	R	48.5	-27.9	-7.7	121.43	18970	2.293	.00509
4	G_temporal_inf	R	50.9	-15.8	-24.6	407.8	128603	2.202	.00628
5	S_calcarine	R	23.1	-48.4	1.4	143.44	71737	2.161	.00690
6	G_precentral	R	28.4	-14.8	64.1	277.3	28823	2.085	.00822
7	G_front_inf-Triangul	R	51.8	25.3	4.1	381.09	76977	1.764	.01722
8	G_parietal_sup	R	19.2	-42.3	58.7	208.38	151132	1.732	.01854
9	S_front_sup	R	21	30.1	31.8	102.5	32788	1.609	.02460
10	S_orbital_med-olfact	R	13.9	22.1	-13.6	55.59	155820	1.584	.02606
11	S_temporal_sup	R	49.3	-41.2	0.6	27.77	24749	1.430	.03715
12	G_rectus	R	6.4	34	-18.1	125.69	84734	1.406	.03926
13	S_collat_transv_post	R	28.2	-72.5	-2.8	4.37	127966	1.319	.04797

| Anatomical Parcellation (aparc.a2009s): Annotation that VtxMax falls into
| VtxMax = Vertex of max sig. in cluster | Max = −log10 (p-value) of VtxMax | Sig. = *p*-value of VtxMax

D-KEFS Tower Test (TT) Mean First Move Time

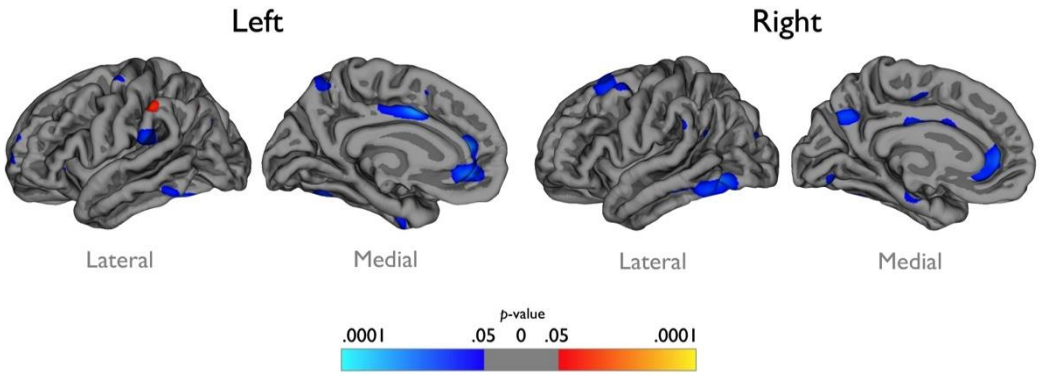

Appendix - Figure 13 Statistical correlation maps of cerebral grey matter thickness with TT Mean First Move Time Scaled Scores for left and right hemispheres. Statistical maps with a significance threshold of *p*= .05 (uncorrected).

Appendix - Table 24 TT Mean First Move Time Scaled Score vs. Grey Matter Thickness

Cluster	Anatomical Parcellation	Hem.	Talairach (X Y Z)			Size (mm^2)	VtxMax	Max	Sig.
1	G_and_S_cingul-Mid-Post	L	-4.4	3.9	33.8	400.44	147881	-2.947	.00113
2	S_front_sup	L	-26.3	5.2	44.5	319.03	1844	-2.860	.00138
3	G_and_S_cingul-Ant	L	-10.2	38.5	-5.5	802.31	47479	-2.684	.00207
4	S_central	L	-39.3	-20.2	43.6	200.63	65250	-2.240	.00575
5	S_oc-temp_lat	L	-39.5	-48.9	-12.8	385.16	90781	-2.212	.00614
6	G_pariet_inf-Supramar	L	-59.3	-28.3	21	489.76	85710	-1.940	.01148
7	G_pariet_inf-Supramar	L	-57.4	-31.8	38.7	80.41	85546	1.822	.01507
8	S_oc-temp_med_and_Lingual	L	-27.5	-52.4	-2	65.19	162914	-1.659	.02193
9	G_precuneus	L	-11.1	-56.4	54.2	177.47	16138	-1.645	.02265
10	Pole_temporal	L	-33.8	-7	-31.3	121.21	31861	-1.565	.02723
11	G_front_middle	L	-17.7	55.1	13.1	147.53	46673	-1.565	.02723
12	G_temporal_inf	L	-57.2	-45.7	-12.7	76.15	10037	-1.542	.02871
13	G_precentral	L	-37.4	-6.7	54.9	69.65	3365	-1.444	.03597
14	G_and_S_paracentral	L	-10.3	-37	62.6	29.5	133560	-1.415	.03846
15	S_postcentral	L	-31.5	-33.6	43.9	18.41	103373	-1.411	.03882
16	S_central	L	-41.4	-10.1	28.2	27.2	139781	-1.401	.03972
17	G_and_S_transv_frontopol	L	-20	59.3	1.1	42.96	11787	-1.371	.04256
18	G_pariet_inf-Angular	L	-42	-61.2	40.7	8.92	147243	1.360	.04365
19	G_front_sup	L	-9.3	13.5	47.7	10.69	9003	-1.343	.04539
20	S_circular_insula_ant	L	-26.9	26.5	-4	7.63	84852	-1.340	.04571
21	G_pariet_inf-Angular	L	-40.6	-71	32.6	2.85	94337	-1.309	.04909
1	S_oc-temp_lat	R	46	-55	-6.2	1033.88	144025	-2.994	.00101
2	G_and_S_cingul-Ant	R	7.7	39.2	1.4	402.3	37872	-2.294	.00508
3	S_pericallosal	R	7.9	-15.7	29.3	288.65	27518	-2.058	.00875
4	G_oc-temp_med-Lingual	R	19.1	-72.9	-3.9	289.68	127937	-2.010	.00977
5	G_precuneus	R	5.8	-60.4	35.9	230.73	146922	-2.009	.00979
6	S_central	R	31.9	-14.5	42.1	111.56	376	-1.927	.01183
7	G_front_sup	R	16.2	19.7	52	483.49	123072	-1.829	.01483
8	G_temp_sup-Plan_tempo	R	60.1	-35.2	28.2	53.11	21755	-1.702	.01986
9	S_temporal_sup	R	47.6	-47.1	24.6	62.78	142860	-1.675	.02113
10	G_and_S_cingul-Mid-Post	R	7.8	-10.7	47.5	77.91	133035	-1.653	.02223
11	G_front_middle	R	36.7	11.1	50.9	171.94	34789	-1.604	.02489

Cluster	Anatomical Parcellation	Hem.	Talairach (X Y Z)			Size (mm^2)	VtxMax	Max	Sig.
12	S_temporal_inf	R	54	-30.8	-12.7	69.5	94676	-1.572	.02679
13	S_oc_sup_and_transversal	R	18.6	-82	22.7	64.25	157887	-1.559	.02761
14	G_oc-temp_med-Parahip	R	22.7	-20	-19.1	18.02	143534	-1.440	.03631
15	S_precentral-sup-part	R	26.7	-2.5	41.4	8.52	145431	-1.339	.04581
16	S_precentral-inf-part	R	33.9	6.5	30.1	6.05	8990	1.335	.04624

| Anatomical Parcellation (aparc.a2009s): Annotation that VtxMax falls into
| VtxMax = Vertex of max sig. in cluster | Max = −log10 (p-value) of VtxMax | Sig. = *p*-value of VtxMax

California Verbal Learning Task II (CVLT-II)

CVLT-II List A Short Delay Free Recall

Appendix - Table 25 CVLT-II List A Short Delay Free Recall Std. Score vs. Grey Matter Thickness

Cluster	Anatomical Parcellation	Hem.	Talairach (X Y Z)			Size (mm^2)	VtxMax	Max	Sig.
1	G_and_S_cingul-Mid-Ant	L	-10.4	14.3	45.7	1870.71	33242	4.388	.00004
2	G_pariet_inf-Supramar	L	-47.8	-45	42.4	703.83	2587	3.803	.00016
3	G_pariet_inf-Supramar	L	-55.5	-18.9	26.5	1391.91	150480	3.344	.00045
4	G_rectus	L	-5.6	49.8	-17.5	557.77	103857	2.575	.00266
5	G_precentral	L	-31.4	-9.8	57.1	455.35	3394	2.569	.00270
6	S_circular_insula_inf	L	-41.5	-9.9	-13.5	230	122606	2.508	.00310
7	Lat_Fis-post	L	-30.5	-27.2	16	112.5	20679	2.469	.00340
8	G_front_middle	L	-29.4	8.8	49.3	489.78	105968	2.468	.00340
9	S_temporal_sup	L	-53.4	-46.2	3.4	227	135386	2.321	.00478
10	S_postcentral	L	-30.5	-41.9	53.9	637.35	151117	2.220	.00603
11	G_precuneus	L	-10.6	-46.4	65.9	439.75	152038	2.099	.00796
12	G_and_S_cingul-Mid-Post	L	-4.1	-14	30.7	62.56	122473	1.940	.01148
13	S_pericallosal	L	-5.1	32.8	4.3	115.84	1106	1.921	.01199
14	S_occipital_ant	L	-43.3	-59.7	3.9	329	111644	1.732	.01854
15	S_temporal_sup	L	-39.6	-61.9	26.8	68.38	21083	1.653	.02223
16	G_front_sup	L	-6.8	48.4	35.5	59.52	77139	1.635	.02317
17	G_parietal_sup	L	-19.6	-75.5	42.2	65.6	122265	1.629	.02350
18	G_temporal_middle	L	-62.6	-33	-9	90.42	1985	1.597	.02529
19	G_oc-temp_lat-fusifor	L	-42.1	-66.4	-10.6	397.79	90533	1.497	.03184
20	S_circular_insula_sup	L	-44	-12.5	18.6	59.05	116299	1.452	.03532
21	S_orbital_lateral	L	-38.9	41.7	-6.6	68.39	129876	1.439	.03639
22	S_front_middle	L	-23.4	40.1	24.4	34.38	109372	1.394	.04036
23	S_front_middle	L	-22.3	51.4	-0.3	55.96	77288	1.388	.04093
24	G_temporal_middle	L	-54.9	-6.4	-20.8	15.05	118210	1.354	.04426
25	S_intrapariet_and_P_trans	L	-29.2	-56.3	39.5	19.9	86941	1.344	.04529
1	G_precentral	R	26.5	-15.5	64.2	1819.59	70722	3.162	.00069
2	G_and_S_cingul-Ant	R	5.6	29	-8.2	382.64	64399	3.113	.00077
3	G_occipital_middle	R	33.8	-68.1	35.5	436.43	78580	2.532	.00294
4	G_parietal_sup	R	12.1	-49.1	57.7	262.08	81660	2.355	.00442
5	G_pariet_inf-Supramar	R	52.3	-37.4	42.4	311.05	159113	2.132	.00738
6	S_central	R	37.3	-9.2	48	391	145128	2.072	.00847
7	G_occipital_sup	R	23.4	-78.4	36	634.19	120290	2.062	.00867
8	G_precuneus	R	6.1	-55.4	32.4	375.33	131829	1.858	.01387
9	G_and_S_cingul-Mid-Ant	R	9.1	6.1	35.1	88.83	18270	1.800	.01585
10	S_collat_transv_ant	R	39.7	-9.9	-24.1	78.16	89682	-1.780	.01660

Cluster	Anatomical Parcellation	Hem.	Talairach (X Y Z)			Size (mm^2)	VtxMax	Max	Sig.
11	S_central	R	46.2	-8.4	24.9	109.37	55144	1.689	.02046
12	Pole_occipital	R	22.3	-91.7	-4.2	167.63	53199	1.660	.02188
13	S_circular_insula_sup	R	41.5	4	11.4	65.64	45560	1.580	.02630
14	S_precentral-inf-part	R	41.2	7.4	18.8	48.65	98413	1.549	.02825
15	G_pariet_inf-Supramar	R	50.7	-26	27	53.83	66155	1.523	.02999
16	G_front_sup	R	7.9	-4	53.7	56.04	80915	1.486	.03266
17	G_and_S_cingul-Mid-Post	R	4.7	-17.4	30.4	31.74	85764	1.477	.03334
18	G_and_S_paracentral	R	16	-35.7	65.3	61.63	50220	1.466	.03420
19	S_temporal_sup	R	51.7	-47	26.9	35.95	74715	1.453	.03524
20	G_pariet_inf-Angular	R	46.1	-50.3	43.2	27.36	14350	1.402	.03963
21	G_front_sup	R	17.8	33.3	44.2	29.41	108104	1.339	.04581
22	G_postcentral	R	58.9	-11.5	30.6	11.11	126657	1.339	.04581
23	G_and_S_cingul-Mid-Ant	R	10.2	14.5	48.8	5.2	47139	-1.325	.04732

| Anatomical Parcellation (aparc.a2009s): Annotation that VtxMax falls into
| VtxMax = Vertex of max sig. in cluster | Max = −log10 (p-value) of VtxMax | Sig. = *p*-value of VtxMax

CVLT-II List A Short Delay Cued Recall

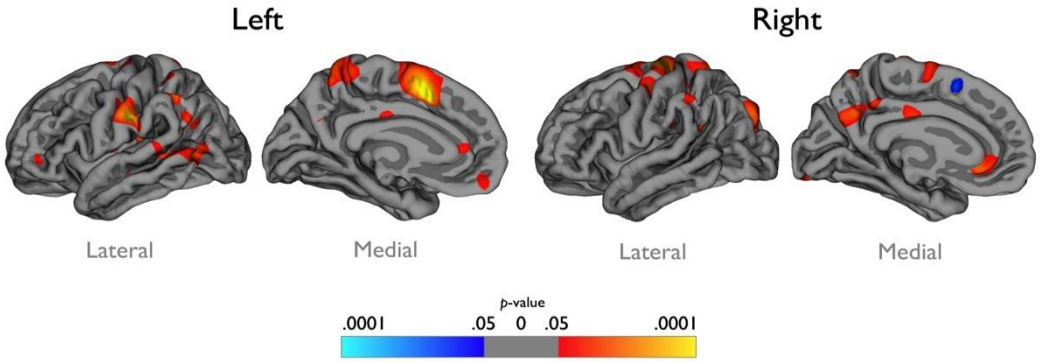

Appendix - Figure 14 Statistical correlation maps of cerebral grey matter thickness with CVLT-II List A Short Delay Cued Recall Std. Scores for left and right hemispheres. Statistical maps with a significance threshold of *p*= .05 (uncorrected).

Appendix - Table 26 CVLT-II List A Short Delay Cued Recall Std. Score vs. Grey Matter Thickness

Cluster	Anatomical Parcellation	Hem.	Talairach (X Y Z)			Size (mm^2)	VtxMax	Max	Sig.
1	G_and_S_cingul-Mid-Ant	L	-10.5	14	42.7	1018.02	117221	4.732	.00002
2	G_postcentral	L	-55.9	-16.4	27.3	1249.11	4525	3.827	.00015
3	G_pariet_inf-Supramar	L	-48.1	-44.8	42.6	273.72	92209	3.311	.00049
4	Lat_Fis-post	L	-30.7	-27.2	16.6	479.29	51398	3.001	.00100
5	S_temporal_sup	L	-53.6	-46	3.1	967.5	61477	2.507	.00311
6	G_precentral	L	-30.7	-9.8	55.2	355.55	15942	2.300	.00501
7	S_circular_insula_inf	L	-37.5	-9.9	-10.9	180.82	66253	2.165	.00684
8	G_precuneus	L	-10.2	-46.8	65.5	656.77	152065	2.015	.00966
9	S_temporal_sup	L	-40.3	-62.7	27	86.41	38613	1.893	.01279
10	G_pariet_inf-Angular	L	-50.5	-55.3	30.2	100.97	49062	1.788	.01629
11	S_postcentral	L	-30	-41.5	53.2	218.14	151116	1.768	.01706
12	G_front_middle	L	-30.2	8.7	49.8	182.17	105602	1.725	.01884
13	G_and_S_cingul-Mid-Post	L	-4	-14.8	30.7	38.91	122474	1.715	.01928
14	G_pariet_inf-Angular	L	-52.1	-51.2	21.2	60.63	106788	1.581	.02624
15	S_pericallosal	L	-5.1	32.8	4.3	60.14	1106	1.549	.02825
16	G_rectus	L	-6.6	48	-16.3	66.12	16740	1.500	.03162
17	G_and_S_frontomargin	L	-23.6	48.1	-0.6	66.9	42498	1.462	.03451
18	S_orbital_lateral	L	-37.3	43.3	-4.4	47.85	98492	1.355	.04416
19	S_temporal_sup	L	-48.7	-18.3	-8.6	6.83	52962	1.335	.04624
20	G_precuneus	L	-5.4	-59.6	29.5	3.37	120485	1.313	.04864
1	G_precentral	R	26.2	-14.4	64.5	1204.42	102337	3.409	.00039
2	G_parietal_sup	R	13.2	-48.5	57.6	511.29	95820	2.773	.00169
3	G_and_S_cingul-Ant	R	5.3	27.9	-7.3	240.03	129955	2.269	.00538
4	G_precuneus	R	6.1	-56.5	33.1	443.64	58667	2.207	.00621
5	G_occipital_sup	R	23.4	-78.9	34.7	494.15	47793	2.182	.00658
6	S_central	R	35.6	-10.4	47.4	474.22	76599	2.064	.00863
7	S_intrapariet_and_P_trans	R	33.4	-66.9	35.4	217.16	49233	1.982	.01042
8	G_front_sup	R	16.6	4	58.7	506.26	131074	1.975	.01059
9	S_collat_transv_ant	R	40	-9	-25.4	104.9	113713	-1.958	.01102
10	G_front_sup	R	10.1	15.3	49.1	103.94	47138	-1.941	.01146
11	S_circular_insula_sup	R	42.9	2	12.8	205.8	133982	1.916	.01213
12	G_and_S_cingul-Mid-Post	R	3.9	-16.1	31.2	76.83	45846	1.821	.01510
13	G_pariet_inf-Supramar	R	52.6	-37.1	42.6	126.98	39385	1.814	.01535
14	Pole_occipital	R	23	-92.3	-5.5	157.76	10017	1.799	.01589
15	G_postcentral	R	28.5	-31	57.6	189.52	5879	1.782	.01652
16	S_central	R	45.4	-8	25.3	82.45	92990	1.607	.02472
17	S_temporal_sup	R	51.5	-44.5	23.7	66.45	88404	1.602	.02500
18	S_precentral-inf-part	R	39.7	7	20	44.17	54035	1.482	.03296
19	G_pariet_inf-Supramar	R	51.3	-24.4	26.1	42.6	99594	1.472	.03373
20	G_and_S_cingul-Mid-Ant	R	10.4	5.5	35.4	18.63	138506	1.395	.04027
21	Lat_Fis-post	R	33.9	-27.8	14.6	7.36	142952	1.362	.04345
22	G_precuneus	R	7.3	-63	43.3	2.09	65934	-1.314	.04853

| Anatomical Parcellation (aparc.a2009s): Annotation that VtxMax falls into
| VtxMax = Vertex of max sig. in cluster | Max = −log10 (p-value) of VtxMax | Sig. = *p*-value of VtxMax

CVLT-II List A Long Delay Free Recall

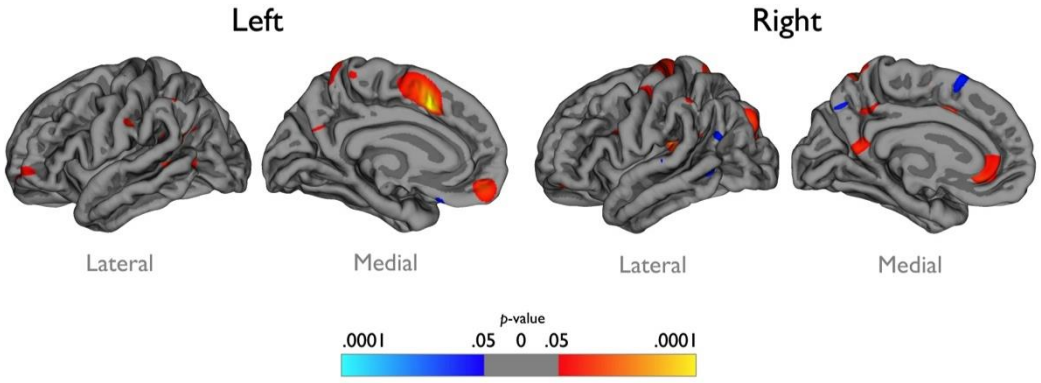

Appendix - Figure 15 Statistical correlation maps of cerebral grey matter thickness with CVLT-II List A Long Delay Free Recall Std. Scores for left and right hemispheres. Statistical maps with a significance threshold of *p*= .05 (uncorrected).

Appendix - Table 27 CVLT-II List A Long Delay Free Recall Std. Score vs. Grey Matter Thickness

Cluster	Anatomical Parcellation	Hem.	Talairach (X Y Z)			Size (mm^2)	VtxMax	Max	Sig.
1	G_and_S_cingul-Mid-Ant	L	-11	15.8	40.2	793.27	14882	4.643	.00002
2	S_temporal_sup	L	-53.2	-45.5	2.7	109.67	5132	2.135	.00733
3	G_rectus	L	-7.1	49.1	-15.5	202.14	47458	2.079	.00834
4	S_temporal_sup	L	-50.9	-50.3	20.8	189.69	35327	2.052	.00887
5	G_pariet_inf-Supramar	L	-48.5	-44.2	42.7	90.58	151442	1.922	.01197
6	G_postcentral	L	-56.3	-16	27.3	69.63	95696	1.664	.02168
7	G_parietal_sup	L	-11.3	-46.6	66.2	95.33	152063	1.624	.02377
8	G_and_S_frontomargin	L	-27.3	51.4	-8.3	214.3	83883	1.480	.03311
9	Lat_Fis-post	L	-30.9	-28.3	16.7	15.07	110948	1.476	.03342
10	S_occipital_ant	L	-43.3	-59.7	3.9	116.06	111644	1.456	.03499
11	Lat_Fis-post	L	-47.6	-41.6	21.8	18.46	156255	1.451	.03540
12	S_central	L	-42	-8.7	29.5	102.49	129337	1.439	.03639
13	S_precentral-sup-part	L	-29.8	-9.9	48.9	29.74	102410	1.426	.03750
14	G_rectus	L	-5.4	21	-19	16.12	54699	-1.414	.03855
15	S_temporal_sup	L	-39.6	-62.1	27.2	18.94	111677	1.407	.03917
16	G_and_S_paracentral	L	-3.7	-35.1	61.4	15.92	95920	1.390	.04074
17	G_precuneus	L	-5.2	-59.6	28.6	19.68	104716	1.377	.04198
18	S_collat_transv_ant	L	-44.2	-25.2	-18.2	27	46418	-1.375	.04217
19	S_postcentral	L	-26.9	-35.5	49	3.89	59803	1.315	.04842
1	G_parietal_sup	R	12.2	-48.2	58.9	341.96	151231	2.657	.00220
2	Lat_Fis-post	R	33	-27.9	15.9	279.89	104789	2.650	.00224
3	G_and_S_cingul-Mid-Ant	R	11.7	6.9	35.3	142.45	102604	2.418	.00382
4	G_occipital_sup	R	23.6	-77	33.8	239.9	104465	1.884	.01306
5	G_and_S_cingul-Ant	R	5.5	27.3	-6.8	328.74	64396	1.848	.01419
6	G_precentral	R	17.7	-17.9	64.9	481.16	70748	1.809	.01552
7	G_precuneus	R	5.8	-52.4	17.1	109.66	44555	1.792	.01614
8	S_precentral-inf-part	R	37.1	9.7	20.5	81.89	145820	1.736	.01837
9	G_precuneus	R	7.4	-63.4	42.2	41.16	23555	-1.635	.02317
10	S_subparietal	R	13.3	-47.8	39.8	147.64	38305	1.626	.02366

Cluster	Anatomical Parcellation	Hem.	Talairach (X Y Z)			Size (mm^2)	VtxMax	Max	Sig.
11	G_front_sup	R	8.6	17.6	52.3	93.55	56733	-1.622	.02388
12	G_pariet_inf-Supramar	R	52.3	-36.8	42.6	63.11	159114	1.608	.02466
13	S_oc_sup_and_transversal	R	20.1	-84.7	21	88.54	61708	1.544	.02858
14	G_pariet_inf-Angular	R	49.5	-56.9	23.2	54.33	7796	-1.543	.02864
15	G_orbital	R	34.3	44.7	-10.8	69.22	110244	1.533	.02931
16	S_temporal_inf	R	53.3	-52.2	-0.1	101.43	56035	-1.504	.03133
17	S_front_middle	R	25.1	48	4.9	49.59	94982	1.480	.03311
18	S_central	R	38.5	-8.3	48.8	71.03	76593	1.426	.03750
19	S_collat_transv_ant	R	39.3	-9.6	-24.4	33.72	89681	-1.422	.03784
20	S_temporal_sup	R	51.5	-44.1	23.2	26.25	159336	1.416	.03837
21	G_oc-temp_lat-fusifor	R	36.9	-64.7	-9.8	8.62	98958	-1.327	.04710
22	G_temp_sup-Lateral	R	65.2	-20.3	4.3	2.27	88929	-1.313	.04864
23	G_front_sup	R	7.9	-4	53.7	1.76	80915	1.307	.04932

| Anatomical Parcellation (aparc.a2009s): Annotation that VtxMax falls into
| VtxMax = Vertex of max sig. in cluster | Max = −log10 (p-value) of VtxMax | Sig. = *p*-value of VtxMax

CVLT-II List A Long Delay Cued Recall

Appendix - Table 28 CVLT-II List A Long Delay Cued Recall Std. Score vs. Grey Matter Thickness

Cluster	Anatomical Parcellation	Hem.	Talairach (X Y Z)			Size (mm^2)	VtxMax	Max	Sig.
1	G_and_S_cingul-Mid-Ant	L	-10.9	15.3	41.8	1468.16	117218	5.422	.00000
2	G_pariet_inf-Supramar	L	-47.8	-44.4	42.3	221.3	151440	2.630	.00234
3	S_precentral-sup-part	L	-31	-9.9	52	451.67	138127	2.616	.00242
4	G_rectus	L	-7.5	46.4	-15.1	245.68	103864	2.523	.00300
5	S_temporal_sup	L	-50.9	-50.3	20.8	404.27	35327	2.464	.00344
6	Lat_Fis-post	L	-30.7	-26.7	16.5	116.25	51399	2.386	.00411
7	G_precuneus	L	-8.9	-47.4	64.2	338.13	95949	2.228	.00592
8	S_temporal_sup	L	-51.4	-45.1	3.3	184.47	68687	2.030	.00933
9	S_circular_insula_inf	L	-40	-10.5	-12.6	269.26	122603	1.953	.01114
10	S_postcentral	L	-27.6	-38.1	49.6	160.86	151100	1.859	.01384
11	S_pericallosal	L	-5.5	17.4	22.8	94.15	9078	1.841	.01442
12	G_postcentral	L	-56.3	-17.1	26.5	126.23	123449	1.742	.01811
13	S_pericallosal	L	-5.4	-15.5	30.3	41.7	107270	1.621	.02393
14	G_front_middle	L	-30.6	7	49.1	127.68	48426	1.570	.02692
15	G_front_middle	L	-31.3	46	13.5	78.83	32383	1.532	.02938
16	G_and_S_frontomargin	L	-22.4	49.2	-2.1	180.23	11781	1.519	.03027
17	G_and_S_subcentral	L	-45.4	-10.4	16.9	112.52	35129	1.518	.03034
18	S_orbital_lateral	L	-38.7	40.8	-5.8	120.88	44482	1.482	.03296
19	G_and_S_occipital_inf	L	-31.3	-88.3	-8.2	59.42	132494	1.476	.03342
20	S_pericallosal	L	-1.8	31.5	4.5	22.73	124434	1.371	.04256
21	S_central	L	-45	-8.3	35	17.97	144840	1.332	.04656
22	G_and_S_paracentral	L	-4.6	-35.4	59	3.58	12333	1.319	.04797
23	G_temporal_middle	L	-50.9	-58.1	5.8	7.49	61396	1.315	.04842
1	S_central	R	37.5	-9	46.6	551.67	58169	3.233	.00058
2	Lat_Fis-post	R	32.6	-27.5	15.6	450.79	104787	2.872	.00134
3	G_precentral	R	27.5	-12.6	64	1764.8	13458	2.666	.00216
4	G_and_S_cingul-Mid-Ant	R	10.4	5.5	35.4	165.18	138506	2.310	.00490
5	G_pariet_inf-Supramar	R	52.6	-37.1	42.6	270.73	39385	2.235	.00582
6	G_precuneus	R	5.5	-53.1	17.5	436.71	44553	2.033	.00927

Cluster	Anatomical Parcellation	Hem.	Talairach (X Y Z)			Size (mm^2)	VtxMax	Max	Sig.
7	G_parietal_sup	R	14.5	-49.1	56.7	301.71	4592	1.980	.01047
8	S_precentral-inf-part	R	37.3	8.6	20.7	122.11	92322	1.932	.01169
9	G_occipital_sup	R	23.8	-77.7	31.8	282.96	7777	1.788	.01629
10	S_temporal_sup	R	51.6	-46.2	26	100.49	142843	1.658	.02198
11	G_and_S_cingul-Ant	R	6.9	29.9	-8.5	252.67	129967	1.635	.02317
12	S_central	R	43.4	-7.4	27.3	69.43	72919	1.561	.02748
13	G_precuneus	R	7.3	-63	43.3	27.82	65934	-1.500	.03162
14	S_collat_transv_ant	R	39	-10.6	-23.4	38.3	160869	-1.473	.03365
15	G_and_S_cingul-Mid-Post	R	14.6	-16.9	41.7	44.94	108508	1.463	.03443
16	S_intrapariet_and_P_trans	R	27	-56.7	43.6	31.68	117733	1.443	.03606
17	S_postcentral	R	25.9	-35.4	49.7	56.41	7475	1.430	.03715
18	G_and_S_cingul-Mid-Ant	R	10.6	14.8	47.7	22.86	103284	-1.398	.03999
19	S_front_sup	R	27.1	24.1	36.8	4.68	63856	1.317	.04819

| Anatomical Parcellation (aparc.a2009s): Annotation that VtxMax falls into
| VtxMax = Vertex of max sig. in cluster | Max = −log10 (p-value) of VtxMax | Sig. = *p*-value of VtxMax

CVLT-II Semantic Clustering

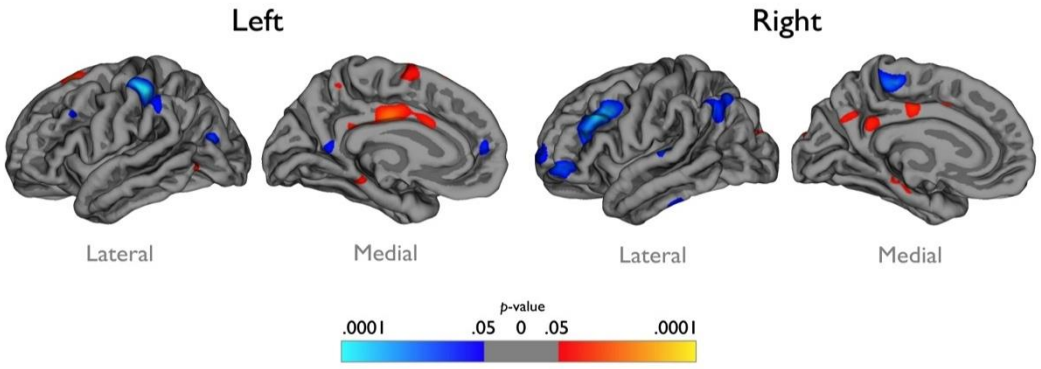

Appendix - Figure 16 Statistical correlation maps of cerebral grey matter thickness with CVLT-II Semantic Clustering Std. Scores for left and right hemispheres. Statistical maps with a significance threshold of *p*= .05 (uncorrected).

Appendix - Table 29 CVLT-II Semantic Clustering Std. Score vs. Grey Matter Thickness

Cluster	Anatomical Parcellation	Hem.	Talairach (X Y Z)			Size (mm^2)	VtxMax	Max	Sig.
1	G_postcentral	L	-46.5	-24.9	49.4	382.61	41020	-4.059	.00009
2	G_and_S_cingul-Mid-Post	L	-3.6	-12.4	31.4	593.8	11970	2.465	.00343
3	G_occipital_middle	L	-42.1	-73	18.2	130.1	3175	-2.006	.00986
4	G_front_sup	L	-11	22.7	52.3	454.86	67449	1.897	.01268
5	G_temporal_inf	L	-47.8	-63.2	-0.8	150.15	7950	1.861	.01377
6	S_postcentral	L	-49.2	-33.4	37.4	247.23	150121	-1.711	.01945
7	G_front_sup	L	-10.1	50.5	6.4	103.38	124485	-1.668	.02148
8	S_intrapariet_and_P_trans	L	-36.8	-43.6	33.7	127.3	50273	-1.570	.02692
9	G_oc-temp_med-Parahip	L	-18.7	-32.6	-9.2	33.81	48340	1.491	.03228
10	G_cingul-Post-ventral	L	-5.7	-53.3	13.6	38.5	101627	-1.489	.03243
11	S_circular_insula_inf	L	-40.1	-13.4	-10.8	47.49	12002	1.476	.03342
12	G_front_middle	L	-43.6	22.2	30.5	36.6	30334	-1.433	.03690
13	G_precuneus	L	-7.3	-46.9	53.1	20.65	147577	1.379	.04178

Cluster	Anatomical Parcellation	Hem.	Talairach (X Y Z)			Size (mm^2)	VtxMax	Max	Sig.
14	G_pariet_inf-Supramar	L	-55.9	-27.4	33.9	16.12	49967	-1.355	.04416
15	S_temporal_sup	L	-39.5	-51.9	22.4	11.53	117650	-1.347	.04498
1	G_front_middle	R	45.6	25.8	28.3	1122.96	82559	-3.617	.00024
2	G_and_S_paracentral	R	7	-28.1	55	242.24	29053	-2.608	.00247
3	G_temp_sup-Plan_tempo	R	58.2	-22.7	7.1	162.25	62270	-2.510	.00309
4	G_orbital	R	40.3	45.4	-6.7	293.66	45638	-2.133	.00736
5	S_oc_sup_and_transversal	R	19.7	-86.4	21.2	195.74	43609	2.028	.00938
6	G_pariet_inf-Angular	R	46.6	-53.9	37.6	434.43	78403	-1.922	.01197
7	G_and_S_transv_frontopol	R	18.1	59.3	0.8	245.9	37908	-1.749	.01782
8	G_and_S_cingul-Mid-Post	R	4.2	-15.9	35.7	112.1	51608	1.736	.01837
9	G_cingul-Post-dorsal	R	4.6	-44.2	27.2	59.63	85864	1.622	.02388
10	G_temporal_inf	R	55.8	-28.3	-22.5	64.26	102236	-1.561	.02748
11	G_precuneus	R	6.1	-58.2	33	70.14	122073	1.561	.02748
12	S_oc-temp_med_and_Lingual	R	22.5	-69.6	-0.7	115.92	137126	1.553	.02799
13	G_and_S_cingul-Mid-Ant	R	13.4	7.5	38.2	30.64	50092	1.479	.03319
14	G_oc-temp_med-Parahip	R	20.5	-31.5	-9	13.59	62606	1.430	.03715
15	G_oc-temp_med-Parahip	R	23.2	-22.2	-16.9	10.26	55930	1.406	.03926
16	S_temporal_sup	R	51.3	-37.3	12.4	7.8	31685	-1.381	.04159
17	S_front_middle	R	26.8	37.6	17.1	23.58	80568	-1.376	.04207
18	G_oc-temp_med-Parahip	R	22.6	-26.9	-13	0.44	90100	1.304	.04966

| Anatomical Parcellation (aparc.a2009s): Annotation that VtxMax falls into
| VtxMax = Vertex of max sig. in cluster | Max = −log10 (p-value) of VtxMax | Sig. = *p*-value of VtxMax

CVLT-II Serial Clustering

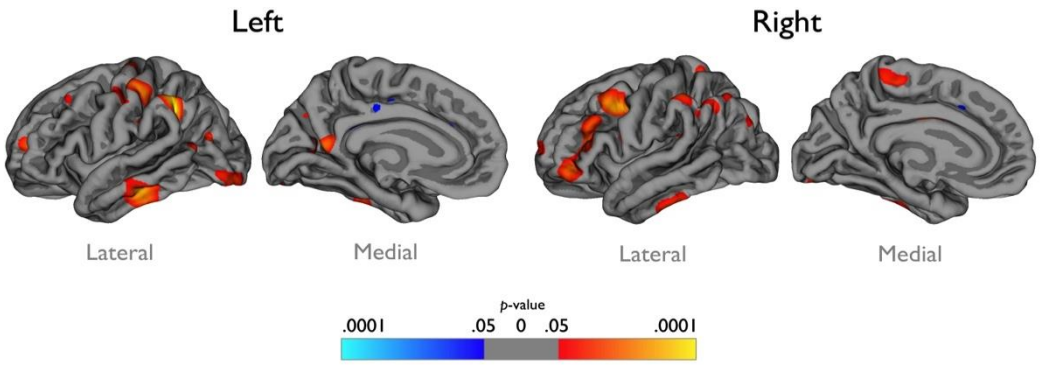

Appendix - Figure 17 Statistical correlation maps of cerebral grey matter thickness with CVLT-II Serial Clustering Std. Scores for left and right hemispheres. Statistical maps with a significance threshold of *p*= .05 (uncorrected).

Appendix - Table 30 CVLT-II Serial Clustering Std. Score vs. Grey Matter Thickness

Cluster	Anatomical Parcellation	Hem.	Talairach (X Y Z)			Size (mm^2)	VtxMax	Max	Sig.
1	G_pariet_inf-Supramar	L	-50.1	-45.2	37.9	551.41	128950	4.429	.00004
2	S_temporal_inf	L	-53	-25.5	-16.2	1117.1	98895	3.210	.00062
3	G_postcentral	L	-47.1	-23.8	48.4	298.87	2622	2.708	.00196
4	G_precuneus	L	-4.9	-56.6	15.4	148.53	88458	2.434	.00368
5	S_front_middle	L	-23.4	48.8	8.3	190.59	138279	2.286	.00518
6	G_precentral	L	-26.2	-14.5	64.6	195.27	32251	2.085	.00822

Cluster	Anatomical Parcellation	Hem.	Talairach (X Y Z)			Size (mm^2)	VtxMax	Max	Sig.
7	G_and_S_occipital_inf	L	-32.8	-87.7	-7.7	359.27	99744	1.939	.01151
8	G_occipital_middle	L	-42.5	-71.4	18.9	66.38	74335	1.902	.01253
9	S_central	L	-38.2	-10.9	39.8	218.62	131077	1.680	.02089
10	G_and_S_cingul-Ant	L	-12.2	28	20.4	68.05	109949	-1.676	.02109
11	G_temporal_middle	L	-51.7	-61.2	12	93.65	21131	1.670	.02138
12	S_pericallosal	L	-5.2	-36.6	23.7	60.87	74890	-1.649	.02244
13	G_temp_sup-Plan_tempo	L	-56.1	-25.9	4.5	125.22	101006	1.576	.02655
14	G_cuneus	L	-13.3	-64.8	14.8	110.42	87407	1.550	.02818
15	G_and_S_subcentral	L	-47.6	-9	14.2	41.39	32390	1.483	.03289
16	S_parieto_occipital	L	-16.2	-68	35.3	22.73	147316	1.461	.03459
17	S_postcentral	L	-55.9	-24.1	27.2	19.17	80822	1.426	.03750
18	G_and_S_cingul-Ant	L	-11.2	41.2	-3.1	22.55	94075	1.390	.04074
19	G_and_S_cingul-Mid-Post	L	-12.3	-11.2	43.5	13.4	27950	-1.387	.04102
20	G_cingul-Post-dorsal	L	-4.7	-21.2	36	16.52	30110	-1.384	.04130
21	G_front_middle	L	-36.9	23.8	39.2	34.67	47058	1.381	.04159
22	S_intrapariet_and_P_trans	L	-36.2	-41.8	34.3	15.65	151343	1.367	.04295
23	G_postcentral	L	-55.3	-14.6	39.8	21.74	108460	1.359	.04375
24	G_parietal_sup	L	-11.9	-50	58.9	1.29	2122	1.307	.04932
1	S_precentral-inf-part	R	37	8.5	37.1	721.49	124254	3.111	.00077
2	G_pariet_inf-Supramar	R	49.4	-31.5	43.3	342.69	112795	2.601	.00251
3	S_orbital_lateral	R	41.3	41.3	-7.7	1117.43	55242	2.377	.00420
4	Lat_Fis-post	R	36.7	-25.4	21.7	195.26	88749	2.335	.00462
5	G_parietal_sup	R	23.2	-43.7	57.9	307.15	100093	2.282	.00522
6	G_and_S_occipital_inf	R	28.8	-84.3	-6.3	230.94	132540	1.970	.01072
7	G_temporal_inf	R	55.2	-24.2	-24.6	280.52	128621	1.921	.01199
8	S_pericallosal	R	4	-3.3	27.7	90.7	146770	1.906	.01242
9	G_and_S_paracentral	R	7.2	-25.5	56.6	185.68	150250	1.803	.01574
10	G_pariet_inf-Angular	R	47.8	-52.1	39.6	165.62	78397	1.756	.01754
11	G_pariet_inf-Angular	R	40.3	-60	45.6	73.81	26068	1.725	.01884
12	S_precentral-inf-part	R	47.2	6.5	12.9	66.57	119716	1.672	.02128
13	G_and_S_transv_frontopol	R	17.4	58.3	5.2	188.81	117367	1.546	.02844
14	S_circular_insula_inf	R	45	-12.2	-9.7	26.72	32613	-1.472	.03373
15	G_occipital_middle	R	38.3	-75.8	30.3	47.17	57454	1.418	.03819
16	S_interm_prim-Jensen	R	51.7	-43.1	33.3	43.85	7838	1.413	.03864
17	G_and_S_cingul-Mid-Ant	R	11	18.8	36.6	22.6	123521	-1.402	.03963
18	G_and_S_cingul-Mid-Post	R	9.2	-8.9	37.2	12.08	48970	-1.355	.04416

| Anatomical Parcellation (aparc.a2009s): Annotation that VtxMax falls into
| VtxMax = Vertex of max sig. in cluster | Max = −log10 (p-value) of VtxMax | Sig. = *p*-value of VtxMax

Recognition Correct "TOTAL HITS"

Appendix - Table 31 Recognition Correct Std. Scores "TOTAL HITS" vs. Grey Matter Thickness

Cluster	Anatomical Parcellation	Hem.	Talairach (X Y Z)			Size (mm^2)	VtxMax	Max	Sig.
1	G_pariet_inf-Angular	L	-50.2	-55.5	28.2	477.62	106759	4.010	.00010
2	G_and_S_cingul-Mid-Ant	L	-10.7	14.4	42.2	358.27	23906	3.681	.00021
3	G_rectus	L	-4.8	49.1	-18.9	310.11	141056	2.651	.00223
4	S_pericallosal	L	-5.1	15.1	24.3	187.11	153408	2.628	.00236
5	G_precuneus	L	-7.7	-48.4	61.8	620.6	19752	2.492	.00322
6	S_circular_insula_inf	L	-34.1	-7.4	-6.4	374.38	54720	2.195	.00638

Cluster	Anatomical Parcellation	Hem.	Talairach (X Y Z)			Size (mm^2)	VtxMax	Max	Sig.
7	G_front_sup	L	-13.3	7.6	59.7	899.39	16601	2.105	.00785
8	G_pariet_inf-Supramar	L	-46.4	-44.4	41	211.35	151433	2.043	.00906
9	S_central	L	-43.2	-8	27.3	206.19	3546	2.020	.00955
10	G_precuneus	L	-6.9	-57.9	30.1	93.35	120482	1.808	.01556
11	S_circular_insula_sup	L	-32.6	21.9	9.8	49.54	154901	1.751	.01774
12	G_front_middle	L	-28.5	7.4	48.3	173.47	145350	1.729	.01866
13	G_precentral	L	-21.5	-14.4	61.8	74.11	116143	1.680	.02089
14	G_front_middle	L	-36.4	29.4	28.1	121.8	149879	1.665	.02163
15	G_temp_sup-Plan_tempo	L	-49.4	-42.9	24.9	35.24	85826	1.646	.02259
16	S_temporal_sup	L	-53.3	-46.9	3.8	56.51	31284	1.599	.02518
17	S_precentral-sup-part	L	-26.8	-9.1	45	50.45	121491	1.504	.03133
18	G_and_S_subcentral	L	-53.2	-6.1	9	46.75	128867	1.458	.03483
19	Lat_Fis-post	L	-32.6	-30.2	16.2	22.32	41070	1.445	.03589
20	G_and_S_cingul-Mid-Post	L	-8.5	-7.4	37.5	15.87	16170	-1.442	.03614
21	S_postcentral	L	-32.4	-39.3	44.3	98.14	54989	1.428	.03733
22	S_central	L	-16.1	-27.8	53.3	28.61	76727	1.411	.03882
23	S_circular_insula_sup	L	-43.3	-11	18	32.95	44946	1.402	.03963
24	S_front_middle	L	-22.9	38.4	22.9	28.53	19194	1.393	.04046
25	S_intrapariet_and_P_trans	L	-27.9	-48.3	47.2	68.18	19458	1.389	.04083
26	S_circular_insula_inf	L	-45.6	-18.1	-4.8	37.28	155558	1.384	.04130
27	G_parietal_sup	L	-20	-74.5	41.7	14.16	122262	1.361	.04355
28	S_orbital_lateral	L	-42.5	35.7	-4.5	5.58	267	1.313	.04864
29	S_postcentral	L	-31.4	-42.2	54.1	7.51	81564	1.312	.04875
30	G_front_middle	L	-31.3	46	13.5	0.74	32383	1.301	.05000
1	S_central	R	38.9	-7.9	45	4623.71	121367	4.750	.00002
2	G_occipital_sup	R	24.1	-75.9	36	938.49	17074	2.643	.00228
3	G_parietal_sup	R	13.5	-49.8	56.9	291.37	59857	2.408	.00391
4	S_intrapariet_and_P_trans	R	32.5	-63	35	312.26	157507	2.201	.00630
5	G_precuneus	R	6.5	-54.3	32.1	421.16	65879	2.128	.00745
6	G_pariet_inf-Supramar	R	49.5	-28.3	28.3	403.11	122479	1.906	.01242
7	G_cingul-Post-ventral	R	9.4	-45.1	9.6	35.11	86032	-1.769	.01702
8	G_oc-temp_med-Lingual	R	15	-46.5	-2.5	40.66	66349	-1.541	.02877
9	S_circular_insula_sup	R	44.3	3.8	9.6	46.69	117171	1.449	.03556
10	Lat_Fis-post	R	31.6	-24.5	17.7	49.98	74797	1.447	.03573
11	G_postcentral	R	57.9	-12.5	29.7	23.04	5288	1.405	.03936
12	S_precentral-inf-part	R	43.5	4.8	19.6	21.83	129706	1.394	.04036
13	S_temporal_inf	R	53	-49.5	-5.5	9.93	91295	-1.332	.04656
14	S_front_sup	R	20.1	24.5	45.8	3.99	149594	1.309	.04909
15	S_temporal_sup	R	49.7	-36.1	8.9	1.06	22016	1.308	.04920

| Anatomical Parcellation (aparc.a2009s): Annotation that VtxMax falls into
| VtxMax = Vertex of max sig. in cluster | Max = −log10 (p-value) of VtxMax | Sig. = *p*-value of VtxMax

Wechsler Memory Scale (WMS-III)

WMS-III Letter-Number Sequencing

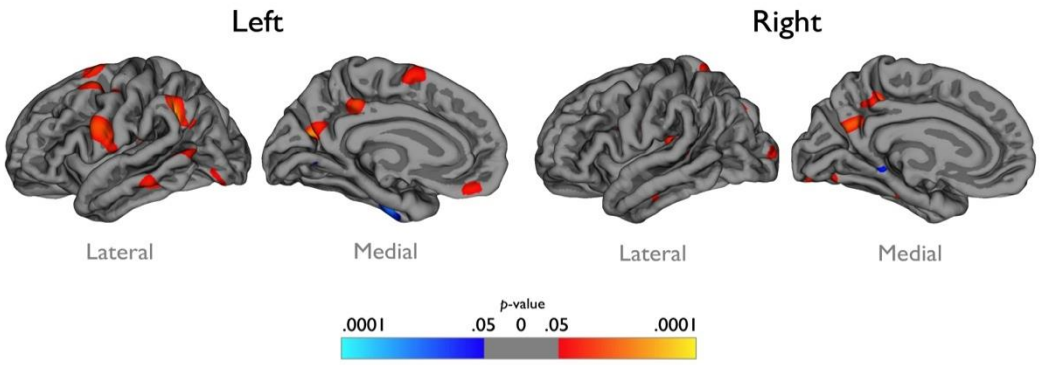

Appendix - Figure 18 Statistical correlation maps of cerebral grey matter thickness with CVLT-II Serial Clustering Std. Scores for left and right hemispheres. Statistical maps with a significance threshold of p= .05 (uncorrected).

Appendix - Table 32 WMS-III Letter-Number Sequencing Scaled Score vs. Grey Matter Thickness

Cluster	Anatomical Parcellation	Hem.	Talairach (X Y Z)			Size (mm^2)	VtxMax	Max	Sig.
1	S_interm_prim-Jensen	L	-50.3	-45.4	34.6	478.07	118900	3.289	.00051
2	S_parieto_occipital	L	-20.9	-65.3	23	656.07	33761	3.063	.00086
3	G_temporal_inf	L	-41.9	-13.3	-27.9	348.56	90260	-2.505	.00313
4	G_front_sup	L	-16.3	8.6	58.7	473.02	103608	2.272	.00535
5	S_circular_insula_sup	L	-31.3	16.1	11.4	90.06	120021	2.144	.00718
6	G_precentral	L	-58	2.7	22	482.54	23672	2.108	.00780
7	S_circular_insula_sup	L	-39.1	-18	19.6	191.79	131609	1.990	.01023
8	G_precuneus	L	-5.8	-34.6	39	297.12	21741	1.977	.01054
9	G_front_middle	L	-36.4	8.9	50.7	252.91	63836	1.965	.01084
10	S_front_middle	L	-29.2	45.4	5.9	136.99	92604	1.911	.01227
11	G_temporal_middle	L	-58.8	-31.9	-12.4	259.61	35903	1.881	.01315
12	G_temporal_middle	L	-52.4	-59.5	7.5	200.39	157011	1.738	.01828
13	S_temporal_sup	L	-38	-58.3	28.6	108.22	18320	1.673	.02123
14	G_rectus	L	-4.9	39.9	-18.8	75.71	84141	1.556	.02780
15	G_precentral	L	-45.5	-5.4	44.4	77.16	144467	1.525	.02985
16	S_temporal_sup	L	-50.9	-8	-19.8	35.99	118202	1.484	.03281
17	G_and_S_occipital_inf	L	-43.2	-76.6	-4.8	92	53174	1.369	.04276
18	G_oc-temp_med-Lingual	L	-8.9	-65.1	2.7	10.07	162588	-1.326	.04721
1	S_cingul-Marginalis	R	16.8	-39.2	42.6	337.26	19213	2.528	.00296
2	G_pariet_inf-Angular	R	33.3	-60.2	44	252.13	54650	2.462	.00345
3	G_precuneus	R	4.8	-59.3	26.8	391.14	106787	2.262	.00547
4	S_circular_insula_sup	R	41.3	1.8	13.8	134.91	100445	1.946	.01132
5	S_precentral-inf-part	R	48.1	4.6	16.5	149.47	140841	1.910	.01230
6	Pole_occipital	R	26.6	-84.4	-4.8	491.07	161841	1.876	.01330
7	G_parietal_sup	R	15	-46.1	59.7	155.75	59842	1.809	.01552
8	S_oc-temp_med_and_Lingual	R	37.3	-25.5	-18.7	145.64	114061	1.741	.01816
9	Lat_Fis-post	R	31.9	-26.1	13.8	129.73	15442	1.693	.02028
10	S_central	R	47.9	-7.2	23.3	86.4	30737	1.644	.02270

Cluster	Anatomical Parcellation	Hem.	Talairach (X Y Z)			Size (mm^2)	VtxMax	Max	Sig.
11	G_oc-temp_med-Parahip	R	16.5	-37	-2.8	36.39	161001	-1.579	.02636
12	Pole_occipital	R	23.5	-93.1	8.7	130.52	158732	1.569	.02698
13	S_temporal_inf	R	51.7	-17.3	-21.6	44.47	115142	1.544	.02858
14	G_occipital_sup	R	25	-69.4	37	106.2	15263	1.519	.03027
15	S_interm_prim-Jensen	R	40.8	-44.5	35.9	44.11	941	1.504	.03133
16	S_parieto_occipital	R	15.1	-52.1	17.8	47.18	142097	1.434	.03681
17	S_orbital_med-olfact	R	17.5	11.7	-13.1	2.33	39755	-1.377	.04198
18	S_temporal_sup	R	46.2	-36.4	8.3	17.27	113364	1.356	.04406
19	S_front_sup	R	22.2	9.4	43.5	2.35	11653	1.309	.04909

| Anatomical Parcellation (aparc.a2009s): Annotation that VtxMax falls into
| VtxMax = Vertex of max sig. in cluster | Max = −log10 (p-value) of VtxMax | Sig. = *p*-value of VtxMax

WMS-III Digit Span Forwards

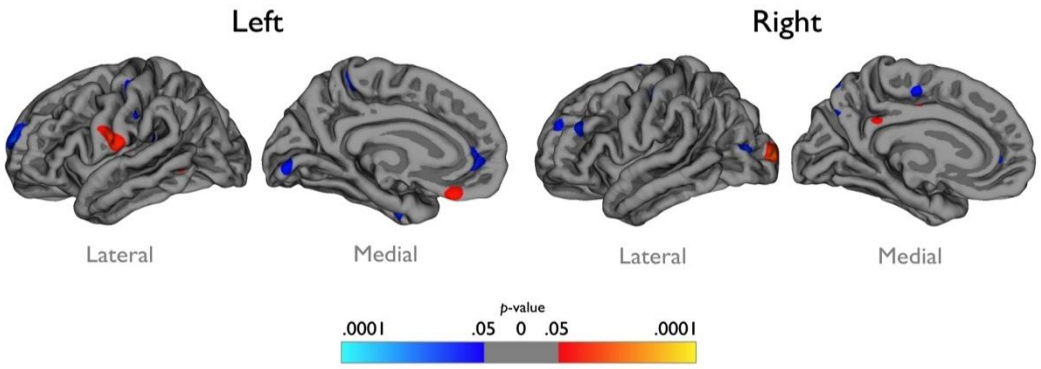

Appendix - Figure 19 Statistical correlation maps of cerebral grey matter thickness with WMS-III Digit Span Forwards Raw Scores for left and right hemispheres. Statistical maps with a significance threshold of *p*= .05 (uncorrected).

Appendix - Table 33 WMS-III Digit Span Forwards Raw Score vs. Grey Matter Thickness

Cluster	Anatomical Parcellation	Hem.	Talairach (X Y Z)			Size (mm^2)	VtxMax	Max	Sig.
1	G_front_middle	L	-17.1	55	13.3	354.14	102445	-2.723	.00189
2	S_central	L	-33.3	-18.1	45.3	368.58	70648	-1.988	.01028
3	S_central	L	-55	-4.6	16.3	271.75	133123	1.945	.01135
4	G_and_S_cingul-Ant	L	-12.7	41.3	-3.9	275.32	42066	-1.791	.01618
5	S_circular_insula_sup	L	-35.1	12.6	10.9	65.08	115681	1.736	.01837
6	S_cingul-Marginalis	L	-13.3	-35.6	55.3	144.51	82220	-1.692	.02032
7	S_postcentral	L	-51.5	-21	30.4	65.06	150413	-1.684	.02070
8	G_rectus	L	-4.1	30	-20.1	70.78	84178	1.585	.02600
9	Pole_temporal	L	-35	-9.2	-31.1	97.06	69925	-1.576	.02655
10	Lat_Fis-post	L	-36.7	-31.9	20.3	121.26	104198	-1.549	.02825
11	G_oc-temp_med-Lingual	L	-4.4	-84	1.7	83.25	3923	-1.536	.02911
12	G_front_sup	L	-15.1	11.1	55.3	33.07	117091	1.388	.04093
13	G_pariet_inf-Supramar	L	-52	-44.3	37.3	17.46	38304	1.364	.04325
14	Pole_occipital	L	-18.6	-96.6	-5.1	14.78	116616	-1.348	.04487
15	S_temporal_inf	L	-52.8	-52.6	-2.1	14.05	90558	1.330	.04677
1	S_central	R	31.5	-15.7	41.3	549.99	30588	-2.702	.00199
2	Pole_occipital	R	23.4	-93.3	9.9	273.27	158734	2.403	.00395

Cluster	Anatomical Parcellation	Hem.	Talairach (X Y Z)			Size (mm^2)	VtxMax	Max	Sig.
3	S_oc_middle_and_Lunatus	R	39.1	-73.2	10.9	252.35	61885	-2.387	.00410
4	G_and_S_cingul-Ant	R	14.8	40.2	0.2	76.77	4902	-1.817	.01524
5	G_precuneus	R	8.8	-65.7	38.3	70.8	99410	-1.757	.01750
6	G_front_middle	R	42.7	36.1	19.7	111.25	63488	-1.727	.01875
7	G_and_S_cingul-Mid-Post	R	7.5	-11.6	36.9	61.12	35191	1.723	.01892
8	S_orbital_med-olfact	R	16.3	12.5	-12.6	49.41	63740	-1.608	.02466
9	G_parietal_sup	R	10.6	-64	53.7	40.84	78241	-1.589	.02576
10	G_front_middle	R	22.6	49.7	21.4	60.65	65634	-1.458	.03483
11	G_front_sup	R	5.5	-11.9	48.9	55.74	59617	-1.448	.03565
12	G_cingul-Post-dorsal	R	4.4	-38.9	29.7	20.1	85834	1.392	.04055
13	G_front_sup	R	13.5	-1.4	63.2	12.44	11679	-1.333	.04645

| Anatomical Parcellation (aparc.a2009s): Annotation that VtxMax falls into
| VtxMax = Vertex of max sig. in cluster | Max = −log10 (p-value) of VtxMax | Sig. = *p*-value of VtxMax

WMS-III Digit Span Backwards

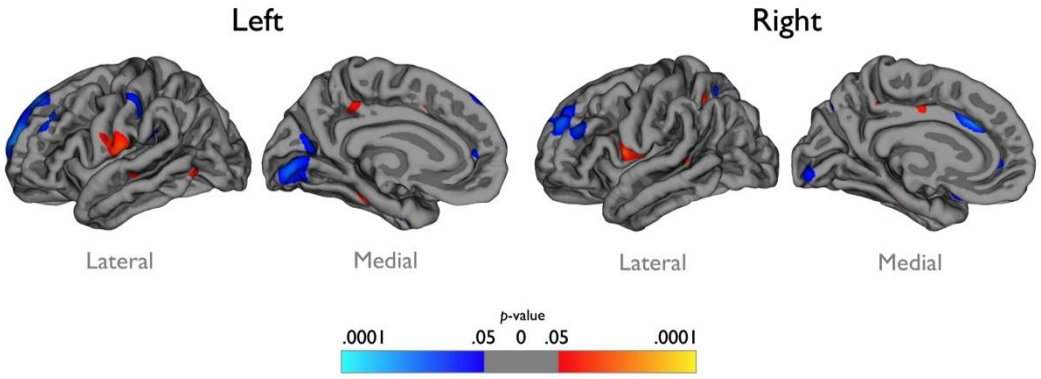

Appendix - Figure 20 Statistical correlation maps of cerebral grey matter thickness with WMS-III Digit Span Backwards Raw Scores for left and right hemispheres. Statistical maps with a significance threshold of *p*= .05 (uncorrected).

Appendix - Table 34 WMS-III Digit Span Backwards Raw Score vs. Grey Matter Thickness

Cluster	Anatomical Parcellation	Hem.	Talairach (X Y Z)			Size (mm^2)	VtxMax	Max	Sig.
1	G_front_sup	L	-14.4	55.3	14.7	830.19	48720	-2.946	.00113
2	S_front_middle	L	-33.6	35.6	23.9	589.29	149917	-2.719	.00191
3	S_circular_insula_sup	L	-31.1	11.2	11.3	168.94	141586	2.623	.00238
4	G_oc-temp_med-Lingual	L	-3.8	-81.7	1.9	614.29	48244	-2.339	.00458
5	G_and_S_subcentral	L	-62.6	-11.1	13.3	292.96	24601	1.997	.01007
6	S_oc-temp_med_and_Lingual	L	-35.3	-33.3	-16.1	135.77	114822	1.843	.01435
7	S_calcarine	L	-19.7	-56	1.5	62.31	45202	1.717	.01919
8	S_front_middle	L	-27.7	44.9	5.6	62.14	145912	1.687	.02056
9	G_cuneus	L	-4.4	-69.3	18.7	251.71	46030	-1.669	.02143
10	S_postcentral	L	-48	-21.8	34.7	184.07	41339	-1.634	.02323
11	G_temporal_inf	L	-50.5	-61.2	-0.6	126.61	75388	1.600	.02512
12	G_and_S_cingul-Ant	L	-12	44.3	5.9	47.79	153197	-1.568	.02704
13	Lat_Fis-post	L	-46.2	-32.6	24.9	69.38	85790	-1.559	.02761
14	S_temporal_sup	L	-51.6	-20.7	-3.3	59.45	160938	1.549	.02825
15	S_subparietal	L	-7.1	-37.1	39.5	78.98	159154	1.526	.02979
16	G_and_S_cingul-Mid-Ant	L	-10.7	11.3	37.8	9.3	12483	1.398	.03999
17	S_postcentral	L	-39.5	-38.1	37.1	25.93	6509	-1.386	.04111
18	S_precentral-sup-part	L	-26.8	-6.3	41.5	12.42	145426	-1.373	.04236
19	S_oc-temp_lat	L	-47.1	-42.9	-12.1	19.95	3307	1.355	.04416
20	Pole_temporal	L	-33.4	-6	-29.9	4.84	24352	-1.316	.04831
1	G_and_S_cingul-Mid-Ant	R	8.7	23.7	24.7	332.94	63546	-3.429	.00037
2	G_precentral	R	52.8	4.7	13.5	463.3	73067	2.751	.00177
3	G_front_middle	R	24	48.1	26.2	558.71	19141	-2.375	.00422
4	G_front_middle	R	43.5	36.6	20.8	222.12	13483	-2.089	.00815
5	S_orbital_med-olfact	R	16.3	12.5	-12.6	116.95	63740	-2.016	.00964
6	G_and_S_cingul-Ant	R	14.4	39.8	-0.6	92.6	125043	-1.794	.01607
7	G_precuneus	R	12.8	-66.1	40.4	111.65	99404	-1.758	.01746
8	S_intrapariet_and_P_trans	R	22	-52.9	51.8	60.76	104411	-1.697	.02009
9	G_and_S_cingul-Mid-Post	R	4.8	-9.3	36.3	35.28	146619	1.621	.02393
10	S_intrapariet_and_P_trans	R	29.2	-45.8	45.5	69.36	126096	1.609	.02460
11	S_cingul-Marginalis	R	11.9	-38.2	40.8	63.51	117526	1.606	.02477
12	S_temporal_sup	R	47.2	-34.2	6.1	53.66	160140	1.583	.02612
13	Pole_occipital	R	7.7	-88.6	0.7	117.06	75396	-1.568	.02704
14	S_parieto_occipital	R	12.5	-57.8	25.8	48.37	142003	1.509	.03097
15	S_circular_insula_inf	R	40.1	-9.8	-11.9	69.19	79098	-1.507	.03112
16	S_calcarine	R	22.1	-55.8	2.4	41.82	49531	1.477	.03334
17	S_precentral-sup-part	R	21.6	-5.5	48.7	13.24	118577	-1.374	.04227
18	S_central	R	32.1	-14.8	43.4	19.86	76615	-1.372	.04246
19	G_parietal_sup	R	15.3	-46.6	58	34.32	59845	1.367	.04295
20	G_oc-temp_lat-fusifor	R	36.8	-28.9	-20	8.18	90275	1.354	.04426
21	S_front_inf	R	35.4	17.1	20.5	10.38	4092	1.345	.04519
22	S_temporal_inf	R	53.5	-14.8	-20.3	5.55	163727	1.318	.04808
23	S_pericallosal	R	8.9	-27	28.2	0.83	135072	-1.305	.04955

| Anatomical Parcellation (aparc.a2009s): Annotation that VtxMax falls into
| VtxMax = Vertex of max sig. in cluster | Max = −log10 (p-value) of VtxMax | Sig. = *p*-value of VtxMax

WMS-III Digit Span

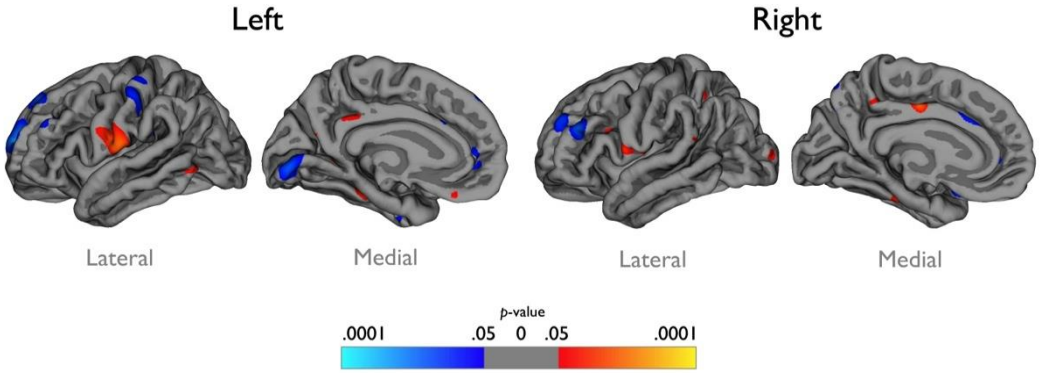

Appendix - Figure 21 Statistical correlation maps of cerebral grey matter thickness with WMS-III Digit Span Scaled Scores for left and right hemispheres. Statistical maps with a significance threshold of *p*= .05 (uncorrected).

Appendix - Table 35 WMS-III Digit Span Scaled Score vs. Grey Matter Thickness

Cluster	Anatomical Parcellation	Hem.	Talairach (X Y Z)			Size (mm^2)	VtxMax	Max	Sig.
1	G_front_sup	L	-15.9	55.6	12.3	438.89	138177	-3.064	.00086
2	G_and_S_subcentral	L	-62.8	-10	13.9	420.16	81175	2.344	.00453
3	G_front_sup	L	-12.1	43.2	37.5	182.94	37129	-2.197	.00635
4	G_oc-temp_med-Lingual	L	-4.1	-82.9	2.2	367.17	57847	-2.139	.00726
5	S_circular_insula_sup	L	-32.5	11.7	11.8	138.86	129955	2.061	.00869
6	S_oc-temp_med_and_Lingual	L	-35.3	-35.2	-15	159.96	40708	1.829	.01483
7	S_front_middle	L	-29.6	45.8	5.1	106.33	116234	1.823	.01503
8	G_front_middle	L	-36.9	38.4	23.6	205.34	138341	-1.816	.01528
9	S_calcarine	L	-20.8	-56.3	1.8	63.2	99792	1.704	.01977
10	G_postcentral	L	-53.6	-20.5	44.4	207.62	26545	-1.644	.02270
11	G_and_S_cingul-Ant	L	-11.7	44.3	5.2	65.64	83272	-1.580	.02630
12	G_temporal_inf	L	-51.8	-60.6	-0.2	111.86	17448	1.526	.02979
13	G_cingul-Post-dorsal	L	-5.1	-36.8	31.4	50.96	126845	1.487	.03258
14	G_postcentral	L	-46.6	-21.7	55.5	49.94	4028	-1.466	.03420
15	Lat_Fis-post	L	-36.7	-31.9	20.3	27.94	104198	-1.414	.03855
16	Pole_temporal	L	-34.5	-8.2	-31.8	41.39	69922	-1.407	.03917
17	G_and_S_cingul-Mid-Ant	L	-7.1	22.3	24.3	19.77	12472	-1.396	.04018
18	G_precuneus	L	-9	-60.8	23.3	33.06	69305	1.385	.04121
19	S_suborbital	L	-13.4	45.9	-4.6	50.25	64275	-1.383	.04140
20	G_rectus	L	-4.1	30	-20.1	11.61	84178	1.353	.04436
21	G_pariet_inf-Supramar	L	-45.6	-31.7	22.7	11.4	51629	-1.347	.04498
22	S_oc-temp_med_and_Lingual	L	-22.4	-43.6	-3.9	5.02	130898	1.320	.04786
1	G_and_S_cingul-Mid-Post	R	5.9	-10.8	37.2	127.15	146614	2.447	.00357
2	G_front_middle	R	42.9	36.5	20	257.88	63489	-2.329	.00469
3	S_orbital_med-olfact	R	16.6	12.3	-12.7	102.63	63742	-2.203	.00627
4	S_central	R	31.5	-15.7	41.3	135.14	30588	-1.944	.01138
5	G_precentral	R	54.1	5	13.2	135.08	73069	1.926	.01186
6	G_and_S_cingul-Mid-Ant	R	9.4	23.7	24.5	173.91	128883	-1.813	.01538
7	G_front_middle	R	23.9	48.1	24	165.65	149797	-1.811	.01545
8	G_and_S_subcentral	R	50	-9	13.2	65.82	50860	1.716	.01923
9	G_oc-temp_lat-fusifor	R	35.9	-29.7	-19.6	98.77	161579	1.695	.02018
10	G_precuneus	R	11.3	-66	40.2	74.13	44985	-1.657	.02203

Cluster	Anatomical Parcellation	Hem.	Talairach (X Y Z)			Size (mm^2)	VtxMax	Max	Sig.
11	G_and_S_cingul-Ant	R	14.8	40.3	-0.3	42.4	96377	-1.597	.02529
12	Pole_occipital	R	23.9	-92.9	9.1	77.39	87900	1.576	.02655
13	G_parietal_sup	R	10.4	-64.7	53	32.24	106849	-1.508	.03105
14	S_cingul-Marginalis	R	10.4	-39.8	42.1	69.26	15099	1.506	.03119
15	S_front_inf	R	35.9	17.9	19.8	31.17	25797	1.443	.03606
16	S_intrapariet_and_P_trans	R	29.7	-46	47.2	27.01	5154	1.417	.03828
17	S_parieto_occipital	R	12.7	-58.4	26.1	18.69	120175	1.392	.04055
18	G_pariet_inf-Supramar	R	59.2	-39.9	17.9	21.27	39444	1.384	.04130
19	G_temporal_middle	R	53.5	-13.7	-20.6	23.08	10227	1.359	.04375
20	S_oc_middle_and_Lunatus	R	36.4	-73.7	11	2.61	12951	-1.309	.04909
21	G_occipital_sup	R	24.1	-68.9	38.8	0.64	142273	1.304	.04966

| Anatomical Parcellation (aparc.a2009s): Annotation that VtxMax falls into
| VtxMax = Vertex of max sig. in cluster | Max = −log10 (p-value) of VtxMax | Sig. = *p*-value of VtxMax

(iv) Social Cognition Measures

Hinting Task

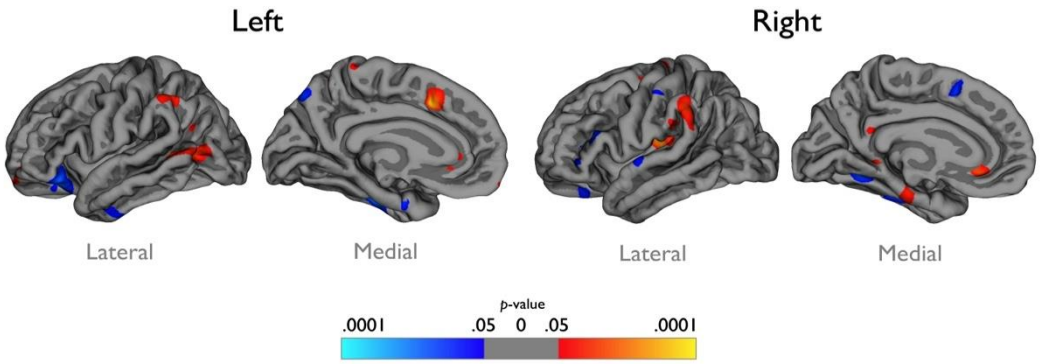

Appendix - Figure 22 Statistical correlation maps of cerebral grey matter thickness with Hinting Task scores for left and right hemispheres. Statistical maps with a significance threshold of *p*= .05 (uncorrected).

Appendix - Table 36 Hinting Task vs. Grey Matter Thickness

Cluster	Anatomical Parcellation	Hem.	Talairach (X Y Z)			Size (mm^2)	VtxMax	Max	Sig.
1	G_and_S_cingul-Mid-Ant	L	-10.8	17	38.3	288.62	30818	3.356	.00044
2	S_collat_transv_ant	L	-46.2	-24.6	-20.8	410.85	24392	-2.988	.00103
3	S_temporal_sup	L	-54.7	-48.7	4.3	766.63	135373	2.606	.00248
4	S_temporal_sup	L	-45.7	-48.7	19.7	267.25	141981	2.325	.00473
5	G_front_inf-Orbital	L	-45	30.4	-12.9	487.25	93111	-2.285	.00519
6	S_temporal_transverse	L	-44.1	-27.4	4	92.32	57283	2.109	.00778
7	G_and_S_frontomargin	L	-21.8	53.1	-10.1	339.4	67805	2.071	.00849
8	G_precuneus	L	-8.2	-68.7	47	105.79	71370	-1.811	.01545
9	G_pariet_inf-Supramar	L	-49.8	-46.2	43.4	237.01	92205	1.753	.01766
10	G_oc-temp_med-Parahip	L	-23.2	-6.4	-26.6	19.53	28280	-1.745	.01799
11	S_circular_insula_sup	L	-40.8	9.6	7.8	36.22	25921	-1.545	.02851
12	S_intrapariet_and_P_trans	L	-28.5	-56.3	40.8	34.68	11443	1.46	.03467

Cluster	Anatomical Parcellation	Hem.	Talairach (X Y Z)			Size (mm^2)	VtxMax	Max	Sig.
13	G_orbital	L	-19	32.2	-16.8	23.57	96254	-1.45	.03548
14	S_temporal_sup	L	-39.3	-61	25.6	43.84	156806	1.442	.03614
15	G_and_S_paracentral	L	-4	-34.9	64.9	29.11	109186	1.437	.03656
16	S_pericallosal	L	-2.5	31.8	1.3	18.22	83152	1.377	.04198
17	G_precuneus	L	-9.7	-51.2	56	6.47	78660	1.358	.04385
18	S_pericallosal	L	-5.8	27.1	-5.5	12.19	100417	1.325	.04732
1	Lat_Fis-post	R	35.2	-17	11.9	351.98	118001	2.728	.00187
2	S_collat_transv_ant	R	47.5	-26.7	-19.2	248.84	163102	-2.209	.00618
3	S_oc-temp_med_and_Lingual	R	29.6	-52.9	-8.2	139.33	1770	-2.013	.00971
4	S_pericallosal	R	5.5	26.3	-7.2	99.8	129953	2.004	.00991
5	G_front_inf-Triangul	R	49	25.7	14.4	172.19	58318	-1.921	.01199
6	G_pariet_inf-Supramar	R	58.1	-34	36.2	229.38	52459	1.885	.01303
7	G_and_S_cingul-Mid-Ant	R	10.7	14.8	47.1	119.65	16421	-1.84	.01445
8	G_cingul-Post-ventral	R	13.2	-40.8	2.4	22.37	115389	1.777	.01671
9	G_orbital	R	18.3	31.7	-18.4	74.62	14902	-1.679	.02094
10	G_oc-temp_med-Parahip	R	22.6	-20.6	-19.2	135.55	152	1.624	.02377
11	G_pariet_inf-Supramar	R	52.3	-25	26.8	123.03	14371	1.624	.02377
12	G_temp_sup-Lateral	R	61	-5.7	-0.6	40.93	17589	-1.509	.03097
13	G_front_inf-Triangul	R	46.6	36	-2.6	52.85	77323	-1.447	.03573
14	G_cingul-Post-dorsal	R	4.7	-44.5	23.3	25.68	111425	1.429	.03724
15	S_precentral-sup-part	R	19.9	-2.5	54.8	23.39	3362	1.419	.03811
16	G_postcentral	R	53	-15.1	46.7	24.62	67177	-1.418	.03819
17	G_precentral	R	17.1	-18.1	64.9	28.95	137990	1.372	.04246
18	S_front_inf	R	35.6	35.4	7.2	4.93	71026	-1.322	.04764

| Anatomical Parcellation (aparc.a2009s): Annotation that VtxMax falls into
| VtxMax = Vertex of max sig. in cluster | Max = −log10 (p-value) of VtxMax | Sig. = *p*-value of VtxMax

<u>False-belief Picture Sequencing Task</u>

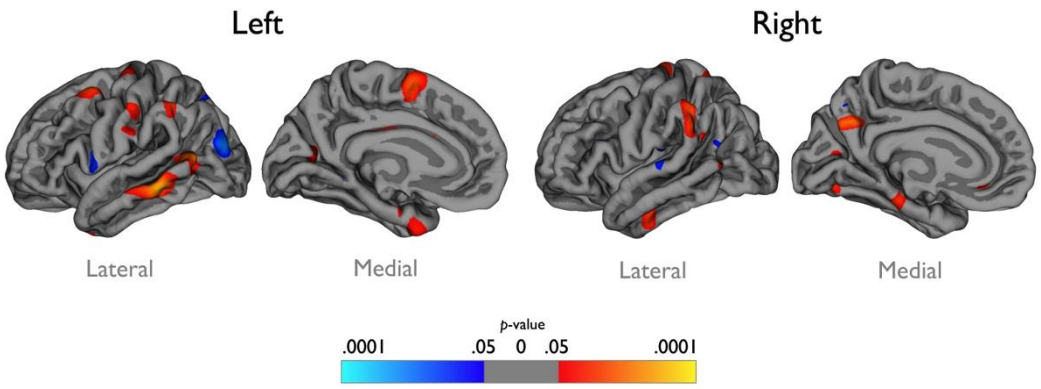

Appendix - Figure 23 Statistical correlation maps of cerebral grey matter thickness with False-belief Picture Sequencing Task scores for left and right hemispheres. Statistical maps with a significance threshold of *p*= .05 (uncorrected).

Appendix - Table 37 False-belief Picture Sequencing Task vs. Grey Matter Thickness

Cluster	Anatomical Parcellation	Hem.	Talairach (X Y Z)			Size (mm^2)	VtxMax	Max	Sig.
1	G_temporal_middle	L	-61.2	-38.2	-7.8	867.65	59129	3.182	.00066
2	G_occipital_middle	L	-39.6	-79.4	20.9	265.9	157881	-2.592	.00256
3	G_front_middle	L	-34	8.7	50.8	383.35	144587	2.585	.00260
4	G_temporal_middle	L	-53.3	-60.5	10.7	667.37	51854	2.578	.00264
5	S_precentral-inf-part	L	-51.5	4.4	8.3	172.35	154400	-2.222	.00600
6	G_front_sup	L	-6.9	3.9	55.8	301.15	60287	2.19	.00646
7	G_pariet_inf-Supramar	L	-52.2	-43.2	41.6	175.39	111201	1.907	.01239
8	S_temporal_transverse	L	-48.6	-27.6	2.9	90.91	141874	1.845	.01429
9	G_precentral	L	-31.7	-11.9	61.8	174.98	41793	1.81	.01549
10	S_parieto_occipital	L	-15.2	-65	16.7	274.64	52169	1.735	.01841
11	G_parietal_sup	L	-12	-66.6	48.2	89.32	32513	-1.656	.02208
12	G_postcentral	L	-55	-18.3	41	144.91	8739	1.627	.02360
13	Pole_temporal	L	-25.9	2.7	-33.2	114.61	13971	1.534	.02924
14	S_pericallosal	L	-3	-15.2	26.6	70	127068	1.529	.02958
15	G_postcentral	L	-57.7	-16.5	25.9	100.01	50055	1.483	.03289
16	S_circular_insula_sup	L	-33.9	-17.7	18.5	38.54	77626	1.464	.03436
17	S_oc-temp_med_and_Lingual	L	-24	-71.5	-0.3	61	46458	1.458	.03483
18	S_calcarine	L	-19.9	-48.3	-1.2	14.47	59293	-1.395	.04027
19	G_oc-temp_med-Parahip	L	-20.3	-11	-23.6	8.57	9904	1.388	.04093
20	S_temporal_sup	L	-53	-46.6	15.1	14.15	130113	1.33	.04677
21	S_pericallosal	L	-5.5	16.3	21	6.85	153390	1.316	.04831
1	G_precuneus	R	6.3	-59.4	34.2	233.68	146926	2.434	.00368
2	G_pariet_inf-Supramar	R	53.2	-16.5	17.8	181.39	45080	-2.143	.00719
3	G_pariet_inf-Supramar	R	55.6	-36.5	36.6	392.72	43725	2.109	.00778
4	S_oc-temp_med_and_Lingual	R	33.6	-32.7	-11.2	229.5	53088	2.056	.00879
5	G_precentral	R	15.8	-16.3	66.7	184.21	138005	2.026	.00942
6	G_temporal_inf	R	50	-14.3	-25.9	183.78	115154	1.905	.01245
7	G_temporal_middle	R	52.8	-58.4	6.9	106.48	75569	1.851	.01409
8	G_temp_sup-Lateral	R	62.2	-20	5.7	92.41	21955	-1.756	.01754
9	S_collat_transv_post	R	27.7	-73.2	-2.5	138.17	114329	1.74	.01820
10	S_temporal_sup	R	52.3	-45.4	25.6	72.23	74698	1.587	.02588
11	G_parietal_sup	R	14.7	-45.9	61.8	126.31	4588	1.576	.02655
12	S_temporal_sup	R	49.5	-56.5	21.3	40.93	117815	-1.528	.02965
13	G_and_S_cingul-Ant	R	8.9	30.4	-9.1	44.16	64410	1.505	.03126
14	G_cuneus	R	7	-71.3	16.3	94.79	156982	1.416	.03837
15	S_front_inf	R	41.2	21.5	17	32.36	58346	-1.413	.03864
16	G_front_middle	R	40	26.5	28.1	28.04	8952	-1.389	.04083
17	S_circular_insula_sup	R	30	24.8	5.7	10.37	96318	1.358	.04385
18	G_precuneus	R	8.3	-60.6	45.7	8.95	65927	-1.352	.04446
19	S_circular_insula_sup	R	47.2	2.7	8.3	1.55	9070	1.302	.04989

| Anatomical Parcellation (aparc.a2009s): Annotation that VtxMax falls into
| VtxMax = Vertex of max sig. in cluster | Max = −log10 (p-value) of VtxMax | Sig. = *p*-value of VtxMax

Reading the Mind in the Eyes Test

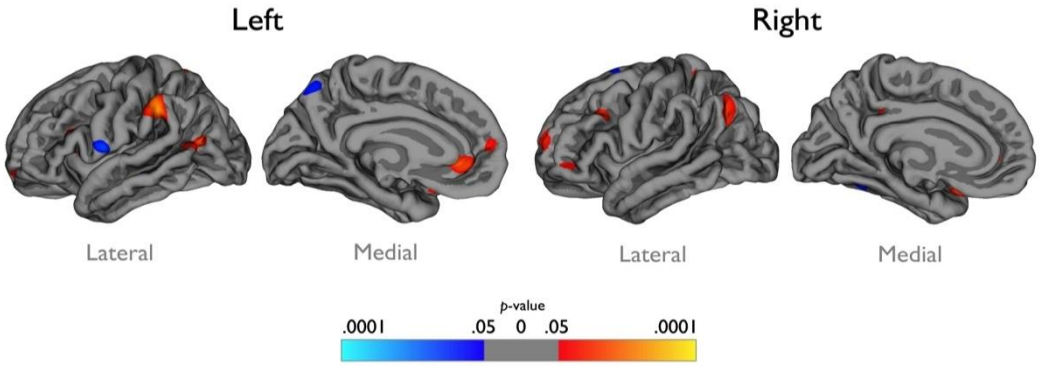

Appendix - Figure 24 Statistical correlation maps of cerebral grey matter thickness with Reading the Mind in the Eyes Test scores for left and right hemispheres. Statistical maps with a significance threshold of *p*= .05 (uncorrected).

Appendix - Table 38 Reading the Mind in the Eyes vs. Grey Matter Thickness

Cluster	Anatomical Parcellation	Hem.	Talairach (X Y Z)			Size (mm^2)	VtxMax	Max	Sig.
1	G_pariet_inf-Supramar	L	-56.6	-35.9	36.1	447.29	111236	2.831	.00148
2	S_circular_insula_sup	L	-28.4	20.7	8.1	138.67	73724	2.524	.00299
3	S_pericallosal	L	-5.4	31.2	-2.5	170.35	37346	2.184	.00655
4	S_temporal_sup	L	-40.3	-66	15.4	402.69	73978	2.12	.00759
5	G_and_S_subcentral	L	-56.6	0.5	10.2	97.62	149252	-1.937	.01156
6	S_central	L	-39.2	-16	30.7	120.66	119323	-1.799	.01589
7	S_front_inf	L	-39.4	21.2	17.8	81.42	5948	1.689	.02046
8	G_precuneus	L	-7.3	-62.1	51.4	82.11	71488	-1.558	.02767
9	G_front_sup	L	-8.9	53.9	7.2	79.28	106097	1.512	.03076
10	S_temporal_sup	L	-50.4	-28	-8.1	43.83	102954	-1.495	.03199
11	S_orbital_med-olfact	L	-16.1	15.4	-14.8	35.93	52820	1.477	.03334
12	G_parietal_sup	L	-25.9	-51.4	61.6	27.52	6477	1.436	.03664
13	G_and_S_frontomargin	L	-12.3	54.7	-10.8	83.8	51018	1.434	.03681
14	S_precentral-sup-part	L	-45.5	-3.6	41.9	46.88	144496	-1.358	.04385
15	S_front_sup	L	-29.5	20.8	36.6	7.75	56674	-1.338	.04592
16	G_and_S_subcentral	L	-48.6	-21.8	21.5	0.83	18289	1.308	.04920
1	G_front_middle	R	40.8	21.9	29.2	174.79	12372	1.989	.01026
2	S_orbital_med-olfact	R	17.3	14.7	-15.6	88.12	39761	1.922	.01197
3	G_and_S_transv_frontopol	R	20.2	58.7	8.9	264.09	77436	1.864	.01368
4	G_pariet_inf-Angular	R	41.9	-61.4	33.6	294.55	15325	1.848	.01419
5	S_postcentral	R	19.3	-40.3	58.2	79.97	108844	1.804	.01570
6	G_oc-temp_lat-fusifor	R	34.5	-52.2	-10.8	60.52	62906	-1.481	.03304
7	G_front_sup	R	10.9	13.9	57.1	51.11	144845	-1.456	.03499
8	S_subparietal	R	9.5	-35.8	35.5	20.95	31138	1.429	.03724
9	G_and_S_cingul-Ant	R	14.4	39.8	-1.7	24.76	60792	1.41	.03890
10	S_orbital_lateral	R	39.9	41.4	-6	78.2	145906	1.408	.03908
11	S_parieto_occipital	R	12	-62.7	36.9	11.68	122040	1.373	.04236

| Anatomical Parcellation (aparc.a2009s): Annotation that VtxMax falls into
| VtxMax = Vertex of max sig. in cluster | Max = –log10 (p-value) of VtxMax | Sig. = *p*-value of VtxMax

(v) Electroencephalographic Data

MMN-Duration-Deviants

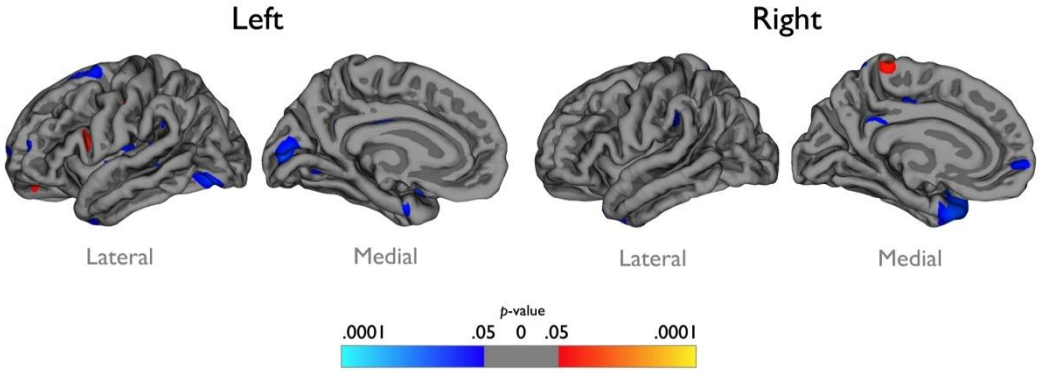

Appendix - Figure 25 Statistical correlation maps of cerebral grey matter thickness with Duration MMN (µV) for left and right hemispheres. Statistical maps with a significance threshold of *p*= .05 (uncorrected).

Appendix - Table 39 Duration MMN vs. Grey Matter vs. Grey Matter Thickness

Cluster	Anatomical Parcellation	Hem.	Talairach (X Y Z)			Size (mm^2)	VtxMax	Max	Sig.
1	S_calcarine	L	-9.9	-85.6	11.2	585.48	87492	-2.33	.00468
2	S_circular_insula_sup	L	-36.4	6.9	12	274.61	64376	-2.227	.00593
3	S_circular_insula_inf	L	-43.6	1.8	-19.8	199.69	107502	-2.025	.00944
4	G_and_S_occipital_inf	L	-41.3	-74.3	-5.6	363.55	161828	-1.992	.01019
5	G_front_sup	L	-14.7	14.4	52.8	300.04	100356	-1.817	.01524
6	G_front_inf-Opercular	L	-48.4	12.8	12.8	110.89	154486	1.752	.01770
7	Lat_Fis-post	L	-37.1	-32.7	10.3	44.51	130053	-1.721	.01901
8	S_pericallosal	L	-3.1	-16.8	26.4	64.56	62237	-1.644	.02270
9	Lat_Fis-post	L	-49.7	-40.4	28.8	39.93	156228	-1.581	.02624
10	G_oc-temp_med-Parahip	L	-23.2	-6.4	-26.6	24.36	28280	-1.581	.02624
11	G_front_middle	L	-35.8	48.5	7	84.86	29885	-1.546	.02844
12	S_oc-temp_med_and_Lingual	L	-17.5	-63.1	-1.1	96.73	10132	-1.541	.02877
13	S_circular_insula_inf	L	-34.1	-8.9	-3.8	84.24	27432	-1.534	.02924
14	G_and_S_transv_frontopol	L	-14	60.5	3.5	57.38	29853	-1.509	.03097
15	S_subparietal	L	-10	-46.8	29.1	43.68	136152	-1.478	.03327
16	S_temporal_sup	L	-47.3	-37.9	0.2	15.7	27691	-1.442	.03614
17	G_postcentral	L	-54.3	-14	38.3	43.94	150345	1.428	.03733
18	Pole_temporal	L	-32.3	1.9	-32.7	50.1	75315	-1.417	.03828
19	G_orbital	L	-15.4	44.5	-15.5	29.64	60636	1.412	.03873
20	S_precentral-sup-part	L	-26.6	-0.8	41.6	14.76	99166	-1.407	.03917
21	S_postcentral	L	-36.9	-38.5	37	1.47	123775	-1.307	.04932
1	S_circular_insula_inf	R	37.5	-12.8	-7.8	910.27	71619	-3.047	.00090
2	S_calcarine	R	19.1	-55.9	2.6	142.33	79481	1.976	.01057
3	G_and_S_cingul-Ant	R	12.5	35.3	12.1	99.46	84392	-1.701	.01991
4	G_pariet_inf-Supramar	R	53.7	-27.6	30.1	125.34	158920	-1.668	.02148
5	S_front_sup	R	24.1	33.7	28.2	38.77	108203	1.638	.02301
6	G_and_S_cingul-Mid-Post	R	13.6	-17.8	43.4	68.65	150440	-1.612	.02443

Cluster	Anatomical Parcellation	Hem.	Talairach (X Y Z)			Size (mm^2)	VtxMax	Max	Sig.
7	G_parietal_sup	R	11.5	-47	63.9	54.76	133329	-1.605	.02483
8	G_and_S_paracentral	R	2.7	-31.8	64.6	69.98	23165	1.593	.02553
9	G_front_sup	R	8.9	55.6	-4.4	99.61	68035	-1.498	.03177
10	S_precentral-sup-part	R	16	-5.4	57.3	11.2	137903	-1.394	.04036
11	G_cingul-Post-dorsal	R	4.3	-37	29.3	30.47	111402	-1.361	.04355
12	S_intrapariet_and_P_trans	R	29.8	-58.8	38.8	19.49	27739	-1.327	.04710
13	G_temp_sup-Plan_tempo	R	59.9	-31.2	12.9	0.99	74883	-1.307	.04932

| Anatomical Parcellation (aparc.a2009s): Annotation that VtxMax falls into
| VtxMax = Vertex of max sig. in cluster | Max = −log10 (p-value) of VtxMax | Sig. = *p*-value of VtxMax

MMN-Frequency-Deviants

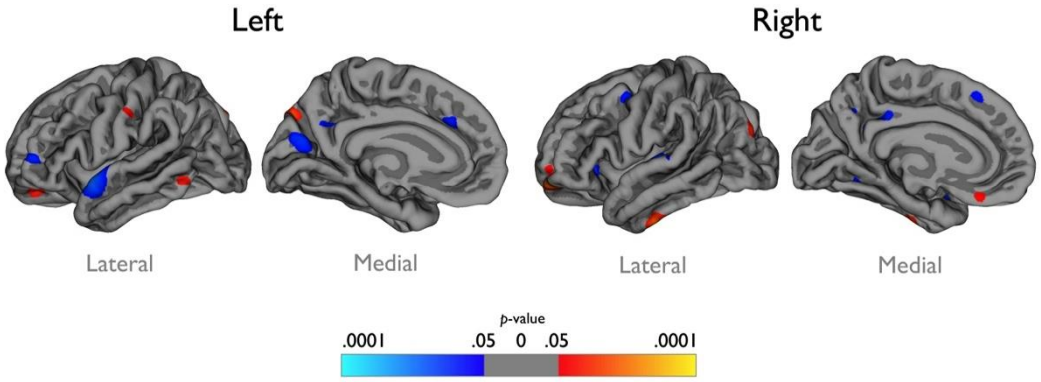

Appendix - Figure 26 Statistical correlation maps of cerebral grey matter thickness with Frequency MMN (µV) for left and right hemispheres. Statistical maps with a significance threshold of *p*= .05 (uncorrected).

Appendix - Table 40 Frequency MMN vs. Grey Matter Thickness

Cluster	Anatomical Parcellation	Hem.	Talairach (X Y Z)			Size (mm^2)	VtxMax	Max	Sig.
1	G_temp_sup-Lateral	L	-53	3	-8.4	466.17	161192	-2.561	.00275
2	G_occipital_sup	L	-17.5	-78	36.5	153.98	78448	2.063	.00865
3	S_orbital-H_Shaped	L	-17.8	43.8	-14	157.58	51034	1.786	.01637
4	G_cuneus	L	-4	-74.3	21.1	205.39	55641	-1.782	.01652
5	S_circular_insula_sup	L	-36.8	17.3	9	59.05	154850	-1.776	.01675
6	G_front_middle	L	-38.9	46.6	2.6	116.98	18172	-1.672	.02128
7	G_temporal_inf	L	-53.8	-54.1	-4.8	83.27	90583	1.622	.02388
8	S_oc-temp_lat	L	-46.9	-41.5	-13.8	41.81	56003	1.556	.02780
9	G_and_S_cingul-Ant	L	-8.8	29.7	28.6	94.83	73051	-1.552	.02805
10	S_subparietal	L	-9.2	-55.4	30	62.89	104711	-1.472	.03373
11	G_postcentral	L	-55.7	-16	35.5	47.59	150418	1.42	.03802
12	G_precentral	L	-21.4	-14.2	60.6	12.54	23444	1.394	.04036
1	S_circular_insula_sup	R	34.3	11.2	11.5	193.81	83118	-2.633	.00233
2	G_temporal_inf	R	51.6	-17.1	-29.6	192.17	23026	2.517	.00304
3	G_and_S_frontomargin	R	27	55.2	-11.7	368.66	92333	2.486	.00327
4	G_occipital_middle	R	36.8	-77.4	28.6	206.03	64665	2.096	.00802
5	S_circular_insula_inf	R	43.2	-0.8	-18.7	101.11	34041	-1.737	.01832
6	G_temp_sup-G_T_transv	R	51.1	-16.7	5.3	100.47	113106	-1.72	.01905

Cluster	Anatomical Parcellation	Hem.	Talairach (X Y Z)			Size (mm^2)	VtxMax	Max	Sig.
7	S_subparietal	R	6.9	-33.1	33.2	144.08	10797	-1.662	.02178
8	S_circular_insula_ant	R	29	25.8	-2.6	66.58	134350	-1.593	.02553
9	G_precentral	R	39.8	6.2	44.2	95.37	37181	-1.56	.02754
10	G_oc-temp_med-Lingual	R	19.6	-55.5	-3.5	45.01	35905	-1.45	.03548
11	G_temporal_middle	R	51.7	-58.5	5.7	42.63	17513	1.449	.03556
12	G_rectus	R	6.3	27.5	-17.9	35.93	55406	1.446	.03581
13	S_subparietal	R	8.6	-56	38.9	23.04	7308	-1.437	.03656
14	G_front_sup	R	8.1	28.4	44.5	47.19	139434	-1.434	.03681
15	S_precentral-inf-part	R	46.5	2.4	29.8	25.08	14807	1.417	.03828
16	G_temp_sup-Lateral	R	64.2	-24.8	6.2	18.82	31658	-1.389	.04083
17	S_circular_insula_inf	R	35.4	-11.5	-5.6	12.76	139047	-1.376	.04207
18	G_and_S_cingul-Ant	R	11.7	47.3	9.4	0.55	3071	-1.303	.04977

| Anatomical Parcellation (aparc.a2009s): Annotation that VtxMax falls into
| VtxMax = Vertex of max sig. in cluster | Max = −log10 (p-value) of VtxMax | Sig. = *p*-value of VtxMax

P3a-Duration-Deviants

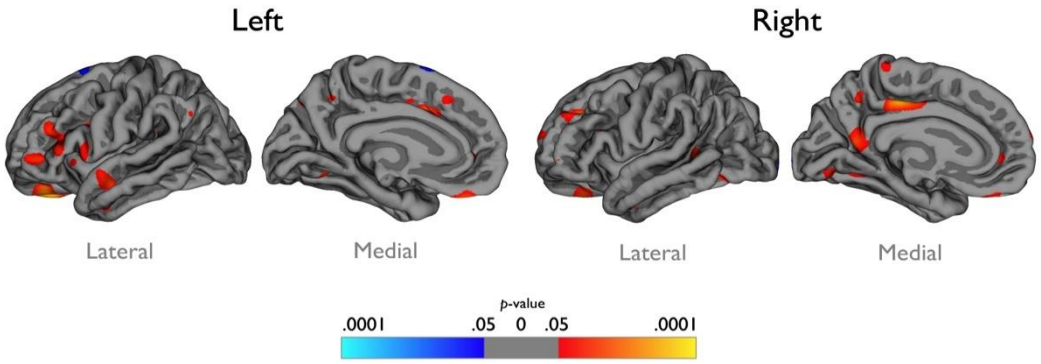

Appendix - Figure 27 Statistical correlation maps of cerebral grey matter thickness with Duration P3a (µV) for left and right hemispheres. Statistical maps with a significance threshold of *p*= .05 (uncorrected).

Appendix - Table 41 Duration P3a vs. Grey Matter Thickness

Cluster	Anatomical Parcellation	Hem.	Talairach (X Y Z)			Size (mm^2)	VtxMax	Max	Sig.
1	S_orbital_med-olfact	L	-9.3	35.1	-19.4	446.29	154148	3.468	.00034
2	G_and_S_cingul-Mid-Ant	L	-10.7	13	33.1	180.07	83568	2.044	.00904
3	S_front_inf	L	-34.9	8.3	22	121.7	80175	2.017	.00962
4	S_temporal_sup	L	-50.6	-5.4	-13.6	178.06	143431	1.93	.01175
5	Lat_Fis-ant-Horizont	L	-36.5	31.8	-2	144.86	51296	1.865	.01365
6	G_oc-temp_med-Lingual	L	-22.6	-59.3	-5.4	141.8	102076	1.808	.01556
7	G_front_middle	L	-41	35.1	18.3	440.89	94969	1.762	.01730
8	S_orbital_lateral	L	-37.1	43.7	-1.5	169.1	13757	1.753	.01766
9	S_orbital-H_Shaped	L	-31.2	31.2	-9.8	74.42	153754	1.697	.02009
10	G_front_sup	L	-8.5	14.6	58.5	74.12	152747	-1.602	.02500
11	G_precuneus	L	-9.8	-50.4	45.4	50.74	8420	1.581	.02624
12	G_parietal_sup	L	-13	-70.3	42	62.08	65986	1.564	.02729
13	S_central	L	-39.7	-18.7	41.9	30.85	25615	1.536	.02911
14	G_front_inf-Opercular	L	-50.8	12.2	6.4	90.64	60766	1.506	.03119
15	S_central	L	-18.9	-29.4	56.1	16.76	121441	1.459	.03475

Cluster	Anatomical Parcellation	Hem.	Talairach (X Y Z)			Size (mm^2)	VtxMax	Max	Sig.
16	G_and_S_cingul-Mid-Post	L	-10.9	2.4	40.8	41.13	50917	1.426	.03750
17	G_front_sup	L	-6.7	27.5	39.7	41.24	29192	1.418	.03819
18	G_insular_short	L	-32	18	-2.6	20.6	20805	1.401	.03972
19	G_and_S_cingul-Ant	L	-10.6	42.4	0.2	33.62	140685	1.385	.04121
20	Pole_temporal	L	-44.8	-4.2	-28.8	53.07	69873	1.38	.04169
21	S_central	L	-52.6	-12	30	35.02	2946	1.358	.04385
22	Lat_Fis-post	L	-41.7	-37.6	20.7	10.93	68429	1.349	.04477
23	G_pariet_inf-Angular	L	-49.7	-56.8	34.3	9.66	146890	1.348	.04487
1	S_cingul-Marginalis	R	6.4	-23.4	38.1	408.99	85724	3.557	.00028
2	S_front_sup	R	21.3	40	27.1	385.17	66662	2.598	.00252
3	S_orbital_med-olfact	R	11.9	34.8	-17.6	380.36	110803	2.453	.00352
4	S_oc-temp_lat	R	45.1	-52.8	-7.2	398.12	34330	2.375	.00422
5	S_oc-temp_med_and_Lingual	R	24	-65.1	0.2	660.91	70048	2.268	.00540
6	S_temporal_sup	R	49.9	-42.5	5	168.79	162407	2.212	.00614
7	G_precuneus	R	5	-54.8	16.2	245.15	5996	1.947	.01130
8	S_subparietal	R	8.2	-51.7	46.3	71.39	63620	1.667	.02153
9	S_precentral-inf-part	R	45.7	6.9	14.8	51.58	24974	1.57	.02692
10	G_and_S_cingul-Ant	R	14.5	43.2	-2.1	61.22	84644	1.484	.03281
11	Pole_occipital	R	17.9	-97.7	2.2	67.22	40248	-1.445	.03589
12	G_and_S_subcentral	R	46.9	-15.8	18.7	46.84	122412	1.444	.03597
13	G_front_sup	R	11.8	60.7	12.3	75.57	84493	1.429	.03724
14	S_front_inf	R	42.2	25	17.7	44.82	11764	1.413	.03864
15	G_and_S_paracentral	R	2.8	-31.9	65.2	31.52	129423	1.398	.03999
16	S_central	R	27.7	-25.9	48.7	10.57	76744	1.384	.04130
17	Pole_temporal	R	43.7	-4.1	-28.4	5.93	75140	1.328	.04699
18	S_oc_sup_and_transversal	R	23	-77.7	20.3	7.32	157901	1.319	.04797
19	G_front_middle	R	39.3	48.8	-3.1	2.92	25812	1.304	.04966

| Anatomical Parcellation (aparc.a2009s): Annotation that VtxMax falls into
| VtxMax = Vertex of max sig. in cluster | Max = −log10 (p-value) of VtxMax | Sig. = *p*-value of VtxMax

P3a-Frequency-Deviants

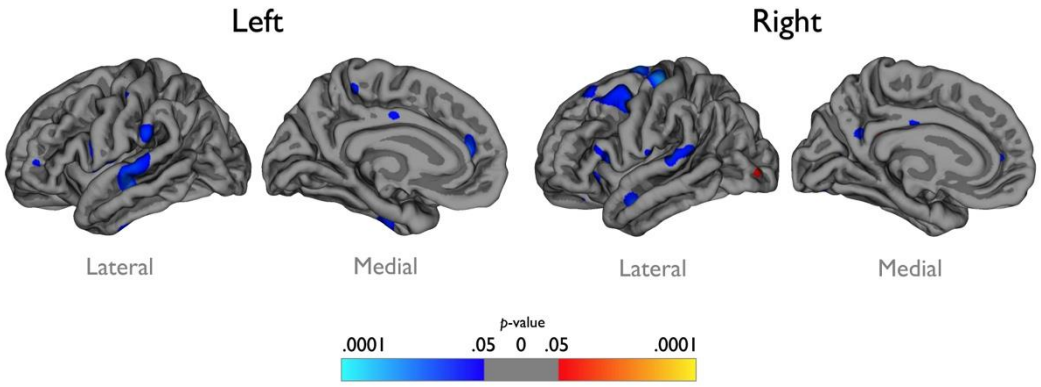

Appendix - Figure 28 Statistical correlation maps of cerebral grey matter thickness with Frequency P3a (µV) for left and right hemispheres. Statistical maps with a significance threshold of *p*= .05 (uncorrected).

Appendix - Table 42 Frequency P3a vs. Grey Matter Thickness

Cluster	Anatomical Parcellation	Hem.	Talairach (X Y Z)			Size (mm^2)	VtxMax	Max	Sig.
1	S_temporal_sup	L	-50.7	-17.7	-6.3	535.28	160968	-2.329	.00469
2	G_and_S_cingul-Ant	L	-14.5	40.7	9.9	205.62	83303	-2.239	.00577
3	S_front_sup	L	-30.9	20.1	39.6	307.88	24786	-2.204	.00625
4	S_circular_insula_sup	L	-35.6	26.4	5.2	67.03	110723	-2.12	.00759
5	G_and_S_paracentral	L	-9	-34.4	53.8	83.6	151903	-1.864	.01368
6	G_pariet_inf-Supramar	L	-62.1	-28.5	25.1	136.6	38374	-1.856	.01393
7	G_and_S_subcentral	L	-42.6	-6.6	13.9	273.34	106516	-1.855	.01396
8	G_temporal_inf	L	-45.7	-16.6	-29.1	173.73	114018	-1.772	.01690
9	G_postcentral	L	-48.7	-15.7	46.1	51.96	66786	-1.602	.02500
10	S_central	L	-26.5	-21	49.5	106.44	56211	-1.523	.02999
11	S_precentral-inf-part	L	-45.9	8.4	12.9	66.64	154460	-1.501	.03155
12	G_and_S_cingul-Mid-Post	L	-3.7	-10.1	33.9	21.62	95267	-1.451	.03540
13	G_front_middle	L	-38.7	44.2	1.8	34.7	77558	-1.44	.03631
14	G_front_inf-Orbital	L	-37.8	26.5	-8.8	8.58	43345	-1.326	.04721
15	S_intrapariet_and_P_trans	L	-43.6	-43.8	38	13.41	151410	-1.318	.04808
1	G_precentral	R	36.3	-16.3	57.8	343.61	58190	-3.041	.00091
2	G_front_inf-Opercular	R	39.3	7.7	10.4	793.49	30756	-2.612	.00244
3	G_front_sup	R	15.8	-0.1	62	195.79	131063	-2.476	.00334
4	G_pariet_inf-Supramar	R	48.1	-33.6	43.1	139.53	88142	-2.192	.00643
5	G_temp_sup-Plan_tempo	R	60.7	-27.7	7.8	343.49	118057	-2.143	.00719
6	S_temporal_sup	R	49.5	-1.3	-18.2	166.65	40873	-1.913	.01222
7	G_precentral	R	40.4	5.3	41.1	628.91	60217	-1.781	.01656
8	G_front_sup	R	16.3	27	48.1	232.89	123085	-1.765	.01718
9	G_precuneus	R	8.9	-52.3	24.9	74.42	106808	-1.665	.02163
10	S_circular_insula_ant	R	31.6	26.9	-6.5	100.99	43256	-1.631	.02339
11	S_pericallosal	R	7	-36.7	24.5	26.13	45858	1.581	.02624
12	G_and_S_cingul-Ant	R	15.9	42.8	5.5	42.73	67978	-1.577	.02649
13	G_Ins_lg_and_S_cent_ins	R	38.2	-0.6	-13.6	69.08	7013	-1.574	.02667
14	G_and_S_cingul-Mid-Post	R	4	-14.5	31	19.29	45843	-1.484	.03281
15	G_occipital_middle	R	39.2	-83.9	2	47.92	148866	1.474	.03357
16	G_and_S_subcentral	R	62.6	-9.4	12.9	18.05	153561	-1.391	.04064
17	G_oc-temp_med-Lingual	R	15.8	-78.5	-6.7	32.21	114309	-1.356	.04406
18	S_orbital-H_Shaped	R	20.1	32.8	-16.6	6.8	9116	-1.34	.04571
19	S_oc-temp_med_and_Lingual	R	23.6	-51.2	-2.9	6.59	148735	-1.321	.04775
20	S_calcarine	R	14.4	-65.8	14.3	7.59	125979	-1.308	.04920

| Anatomical Parcellation (aparc.a2009s): Annotation that VtxMax falls into
| VtxMax = Vertex of max sig. in cluster | Max = −log10 (p-value) of VtxMax | Sig. = *p*-value of VtxMax

BIBLIOGRAPHY

Allen, P., Stephan, K. E., Mechelli, A., Day, F., Ward, N., Dalton, J., Williams, S. C., McGuire, P. (2010). Cingulate activity and fronto-temporal connectivity in people with prodromal signs of psychosis. *NeuroImage*, *49*(1), 947-955.

Association, A. P. (2000). *DSM-IV-TR: Diagnostic and Statistical Manual of Mental Disorders, 4th Edition, Text Revision*.

Antonova, E., Sharma, T., Morris, R., Kumari, V. (2004). The relationship between brain structure and neurocognition in schizophrenia: a selective review. *Schizophr Res*, *70*(2-3), 117-145.

Atkinson, R. J., Michie, P. T., Schall, U. (2012). Duration Mismatch Negativity and P3a in First-Episode Psychosis and Individuals at Ultra-High Risk of Psychosis. *Biol Psychiatry*, *71*(2), 98-104.

Auther, A. M., Smith, C. W., Cornblatt, B. A. (2006). Global Functioning: Social Scale (GF: Social). *NY: Zucker-Hillside Hospital*.

Baron-Cohen, S., Wheelwright, S., Hill, J., Raste, Y., Plumb, I. (2001). The "Reading the Mind in the Eyes" Test revised version: a study with normal adults, and adults with Asperger syndrome or high-functioning autism. *J Child Psychol Psychiatry*, *42*(2), 241-251.

Beck, A. T., Epstein, N., Brown, G., Steer, R. A. (1988). An inventory for measuring clinical anxiety: psychometric properties. *J Consult Clin Psychol*, *56*(6), 893-897.

Beck, A. T., Steer, R. A., Ball, R., Ranieri, W. (1996). Comparison of Beck Depression Inventories -IA and -II in psychiatric outpatients. *J Pers Assess*, *67*(3), 588-597.

Becker, H. E., Nieman, D. H., Dingemans, P. M., Van de Fliert, J. R., de, H., L, Linszen, D. H. (2010). Verbal fluency as a possible predictor for psychosis. *Eur Psychiatry*, *25*(2), 105-110.

Beer, J. S., Ochsner, K. N. (2006). Social cognition: a multi level analysis. *Brain Res*, *1079*(1), 98-105.

Berge, D., Carmona, S., Rovira, M., Bulbena, A., Salgado, P., Vilarroya, O. (2011). Gray matter volume deficits and correlation with insight and negative symptoms in first-psychotic-episode subjects. *Acta Psychiatr Scand*, *123*(6), 431-439.

Bloemen, O. J., de Koning, M. B., Schmitz, N., Nieman, D. H., Becker, H. E., de Haan, L., Dingemans, P., Linszen, D. H., van Amelsvoort, T. A. (2010). White-matter markers for psychosis in a prospective ultra-high-risk cohort. *Psychol Med*, *40*(8), 1297-1304.

Bodatsch, M., Ruhrmann, S., Wagner, M., Muller, R., Schultze-Lutter, F., Frommann, I., Brinkmeyer, J., Gaebel, W., Maier, W., Klosterkotter, J., Brockhaus-Dumke, A. (2011). Prediction of psychosis by mismatch negativity. *Biol Psychiatry*, *69*(10), 959-966.

Bokat, C. E., Goldberg, T. E. (2003). Letter and category fluency in schizophrenic patients: a meta-analysis. *Schizophr Res*, *64*(1), 73-78.

Bonilha, L., Molnar, C., Horner, M. D., Anderson, B., Forster, L., George, M. S., Nahas, Z. (2008). Neurocognitive deficits and prefrontal cortical atrophy in patients with schizophrenia. *Schizophr Res*, *101*(1-3), 142-151.

Bora, E., Yucel, M., Pantelis, C. (2009). Theory of mind impairment in schizophrenia: meta-analysis. *Schizophr Res*, *109*(1-3), 1-9.

Borgwardt, S., McGuire, P., Fusar-Poli, P. (2011). Gray matters!--mapping the transition to psychosis. *Schizophr Res*, *133*(1-3), 63-67.

Bowie, C. R., Harvey, P. D. (2005). Cognition in schizophrenia: impairments, determinants, and functional importance. *Psychiatr Clin North Am*, *28*(3), 613-33, 626.

Bramon, E., Rabe-Hesketh, S., Sham, P., Murray, R. M., Frangou, S. (2004). Meta-analysis of the P300 and P50 waveforms in schizophrenia. *Schizophr Res*, *70*(2-3), 315-329.

Brewer, W. J., Wood, S. J., McGorry, P. D., Francey, S. M., Phillips, L. J., Yung, A. R., Anderson, V., Copolov, D. L., Singh, B., Velakoulis, D., Pantelis, C. (2003). Impairment of olfactory identification ability in individuals at ultra-high risk for psychosis who later develop schizophrenia. *Am J Psychiatry*, *160*(10), 1790-1794.

Brockhaus-Dumke, A., Schultze-Lutter, F., Mueller, R., Tendolkar, I., Bechdolf, A., Pukrop, R., Klosterkoetter, J., Ruhrmann, S. (2008). Sensory gating in schizophrenia: P50 and N100 gating in antipsychotic-free subjects at risk, first-episode, and chronic patients. *Biol Psychiatry*, *64*(5), 376-384.

Brodmann, K. (1909). Vergleichende Lokalisationslehre der Grosshirnrinde in ihren Prinzipien dargestellt auf Grund des Zellenbaues. *Johann Ambrosius Barth Verlag*.

Broome, M. R., Fusar-Poli, P., Matthiasson, P., Woolley, J. B., Valmaggia, L., Johns, L. C., Tabraham, P., Bramon, E., Williams, S. C., Brammer, M. J., Chitnis, X., Zelaya, F., McGuire, P. K. (2010). Neural correlates of visuospatial working memory in the 'at-risk mental state'. *Psychol Med*, *40*(12), 1987-1999.

Broome, M. R., Matthiasson, P., Fusar-Poli, P., Woolley, J. B., Johns, L. C., Tabraham, P., Bramon, E., Valmaggia, L., Williams, S. C., Brammer, M. J., Chitnis, X., McGuire, P. K. (2009). Neural correlates of executive function and working memory in the 'at-risk mental state'. *Br J Psychiatry*, *194*(1), 25-33.

Brune, M. (2005). "Theory of mind" in schizophrenia: a review of the literature. *Schizophr Bull*, *31*(1), 21-42.

Brune, M., Abdel-Hamid, M., Lehmkamper, C., Sonntag, C. (2007). Mental state attribution, neurocognitive functioning, and psychopathology: what predicts poor social competence in schizophrenia best? *Schizophr Res*, *92*(1-3), 151-159.

Buckner, R. L., Head, D., Parker, J., Fotenos, A. F., Marcus, D., Morris, J. C., Snyder, A. Z. (2004). A unified approach for morphometric and functional data analysis in young, old, and demented adults using automated atlas-based head size normalization: reliability and validation against manual measurement of total intracranial volume. *NeuroImage*, *23*(2), 724-738.

Cantor-Graae, E., Warkentin, S., Nilsson, A. (1995). Neuropsychological assessment of schizophrenic patients during a psychotic episode: persistent cognitive deficit? *Acta Psychiatr Scand*, *91*(4), 283-288.

Carrington, S. J., Bailey, A. J. (2009). Are there theory of mind regions in the brain? A review of the neuroimaging literature. *Hum Brain Mapp*, *30*(8), 2313-2335.

Chan, R. C., Di, X., McAlonan, G. M., Gong, Q. Y. (2011). Brain anatomical abnormalities in high-risk individuals, first-episode, and chronic schizophrenia: an activation likelihood estimation meta-analysis of illness progression. *Schizophr Bull*, *37*(1), 177-188.

Cheung, V., Chiu, C. P., Law, C. W., Cheung, C., Hui, C. L., Chan, K. K., Sham, P. C., Deng, M. Y., Tai, K. S., Khong, P. L., McAlonan, G. M., Chua, S. E., Chen, E. (2011). Positive symptoms and white matter microstructure in never-medicated first episode schizophrenia. *Psychol Med*, *41*(8), 1709-1719.

Chow, Y. W., Pietranico, R., Mukerji, A. (1975). Studies of oxygen binding energy to hemoglobin molecule. *Biochem Biophys Res Commun*, *66*(4), 1424-1431.

Chung, Y. S., Kang, D. H., Shin, N. Y., Yoo, S. Y., Kwon, J. S. (2008). Deficit of theory of mind in individuals at ultra-high-risk for schizophrenia. *Schizophr Res*, *99*(1-3), 111-118.

Cocchi, L., Walterfang, M., Testa, R., Wood, S. J., Seal, M. L., Suckling, J., Takahashi, T., Proffitt, T. M., Brewer, W. J., Adamson, C., Soulsby, B., Velakoulis, D., McGorry, P. D., Pantelis, C. (2009). Grey and white matter abnormalities are associated with impaired spatial working memory ability in first-episode schizophrenia. *Schizophr Res*, *115*(2-3), 163-172.

Cohen, M., Rasser, P. E., Peck, G., Carr, V. J., Ward, P. B., Thompson, P. M., Johnston, P., Baker, A., Schall, U. (2011). Cerebellar grey-matter deficits, cannabis use and first-episode schizophrenia in adolescents and young adults. *Int J Neuropsychopharmacol*, 1-11.

Corcoran, R., Mercer, G., Frith, C. D. (1995). Schizophrenia, symptomatology and social inference: investigating "theory of mind" in people with schizophrenia. *Schizophr Res*, *17*(1), 5-13.

Cornblatt, B. A., Auther, A. M., Niendam, T., Smith, C. W., Zinberg, J., Bearden, C. E., Cannon, T. D. (2007). Preliminary findings for two new measures of social and role functioning in the prodromal phase of schizophrenia. *Schizophr Bull*, *33*(3), 688-702.

Coyle, J. T. (2004). The GABA-glutamate connection in schizophrenia: which is the proximate cause? *Biochem Pharmacol*, *68*(8), 1507-1514.

Coyle, J. T. (2006). Glutamate and schizophrenia: beyond the dopamine hypothesis. *Cell Mol Neurobiol*, *26*(4-6), 365-384.

Crespo-Facorro, B., Roiz-Santianez, R., Perez-Iglesias, R., Rodriguez-Sanchez, J. M., Mata, I., Tordesillas-Gutierrez, D., Sanchez, E., Tabares-Seisdedos, R., Andreasen, N., Magnotta, V., Vazquez-Barquero, J. L. (2011). Global and regional cortical thinning in first-episode psychosis patients: relationships with clinical and cognitive features. *Psychol Med*, *41*(7), 1449-1460.

Crossley, N. A., Mechelli, A., Fusar-Poli, P., Broome, M. R., Matthiasson, P., Johns, L. C., Bramon, E., Valmaggia, L., Williams, S. C., McGuire, P. K. (2009). Superior temporal lobe dysfunction and frontotemporal dysconnectivity in subjects at risk of psychosis and in first-episode psychosis. *Hum Brain Mapp*, *30*(12), 4129-4137.

Darke, S., Ward, J., Hall, W., Heather, N., Wodak, A. (1991). The Opiate Treatment Index (OTI) Researcher's Manual. *National Drug and Alcohol Research Centre*.

Davis, K. L., Kahn, R. S., Ko, G., Davidson, M. (1991). Dopamine in schizophrenia: a review and reconceptualization. *Am J Psychiatry*, *148*(11), 1474-1486.

Delis, D. C., Kaplan, E., Kramer, J. H. (2001). Delis-Kaplan Executive Function System (D-KEFS). *The Psychological Corporation*.

Delis, D. C., Kramer, J. H., Kaplan, E., Ober, B. A. (1994). California Verbal Learning Test - Children's Version: Manual. *The Psychological Corporation*.

Delis, D. C., Kramer, J. H., Kaplan, E., Ober, B. A. (2000). California Verbal Learning Test: Second Edition. *The Psychological Corporation*.

Destrieux, C., Fischl, B., Dale, A., Halgren, E. (2010). Automatic parcellation of human cortical gyri and sulci using standard anatomical nomenclature. *NeuroImage*, *53*(1), 1-15.

Doty, R. L., Shaman, P., Kimmelman, C. P., Dann, M. S. (1984). University of Pennsylvania Smell Identification Test: a rapid quantitative olfactory function test for the clinic. *Laryngoscope*, *94*(2 Pt 1), 176-178.

Eastvold, A. D., Heaton, R. K., Cadenhead, K. S. (2007). Neurocognitive deficits in the (putative) prodrome and first episode of psychosis. *Schizophr Res*, *93*(1-3), 266-277.

Ellison-Wright, I., Glahn, D. C., Laird, A. R., Thelen, S. M., Bullmore, E. (2008). The anatomy of first-episode and chronic schizophrenia: an anatomical likelihood estimation meta-analysis. *Am J Psychiatry*, *165*(8), 1015-1023.

Elwood, R. W. (1995). The California Verbal Learning Test: psychometric characteristics and clinical application. *Neuropsychol Rev*, *5*(3), 173-201.

Eysenck, S. B. G., Eysenck, H. J., Barrett, P. (1985). A revised version of the psychoticism scale. *Personality and Individual Differences*, *6*(1), 21-29.

First, M. B., Spitzer, R. L., Gibbon, M. L., Janet, B. W. (1996). Structured Clinical Interview for DSM-IV Axis I Disorders, Clinician Version (SCID-CV). *American Psychiatric Press, Inc.*

Fischl, B., Dale, A. M. (2000). Measuring the thickness of the human cerebral cortex from magnetic resonance images. *Proc Natl Acad Sci U S A*, *97*(20), 11050-11055.

Fischl, B., Salat, D. H., Busa, E., Albert, M., Dieterich, M., Haselgrove, C., van der Kouwe, A., Killiany, R., Kennedy, D., Klaveness, S., Montillo, A., Makris, N., Rosen, B., Dale, A. M. (2002). Whole brain segmentation: automated labeling of neuroanatomical structures in the human brain. *Neuron*, *33*(3), 341-355.

Fischl, B., van der Kouwe, A., Destrieux, C., Halgren, E., Segonne, F., Salat, D. H., Busa, E., Seidman, L. J., Goldstein, J., Kennedy, D., Caviness, V., Makris, N., Rosen, B., Dale, A. M. (2004). Automatically parcellating the human cerebral cortex. *Cereb Cortex*, *14*(1), 11-22.

Flashman, L. A., Green, M. F. (2004). Review of cognition and brain structure in schizophrenia: profiles, longitudinal course, and effects of treatment. *Psychiatr Clin North Am*, *27*(1), 1-18, vii.

Friedman, D., Cycowicz, Y. M., Gaeta, H. (2001). The novelty P3: an event-related brain potential (ERP) sign of the brain's evaluation of novelty. *Neurosci Biobehav Rev*, *25*(4), 355-373.

Fusar-Poli, P., Borgwardt, S., Crescini, A., Deste, G., Kempton, M. J., Lawrie, S., Mc Guire, P., Sacchetti, E. (2011a). Neuroanatomy of vulnerability to psychosis: a voxel-based meta-analysis. *Neurosci Biobehav Rev*, *35*(5), 1175-1185.

Fusar-Poli, P., Broome, M. R., Matthiasson, P., Woolley, J. B., Johns, L. C., Tabraham, P., Bramon, E., Valmaggia, L., Williams, S. C., McGuire, P. (2010). Spatial working memory in individuals at high risk for psychosis: longitudinal fMRI study. *Schizophr Res*, *123*(1), 45-52.

Fusar-Poli, P., Broome, M. R., Matthiasson, P., Woolley, J. B., Mechelli, A., Johns, L. C., Tabraham, P., Bramon, E., Valmaggia, L., Williams, S. C., McGuire, P. (2011b). Prefrontal function at presentation directly related to clinical outcome in people at ultrahigh risk of psychosis. *Schizophr Bull*, *37*(1), 189-198.

Fusar-Poli, P., Broome, M. R., Woolley, J. B., Johns, L. C., Tabraham, P., Bramon, E., Valmaggia, L., Williams, S. C., McGuire, P. (2011c). Altered brain function directly related to structural abnormalities in people at ultra high risk of psychosis: longitudinal VBM-fMRI study. *J Psychiatr Res*, *45*(2), 190-198.

Fusar-Poli, P., Crossley, N., Woolley, J., Carletti, F., Perez-Iglesias, R., Broome, M., Johns, L., Tabraham, P., Bramon, E., McGuire, P. (2011d). Gray matter alterations related to P300 abnormalities in subjects at high risk for psychosis: longitudinal MRI-EEG study. *NeuroImage*, *55*(1), 320-328.

Fusar-Poli, P., Deste, G., Smieskova, R., Barlati, S., Yung, A. R., Howes, O., Stieglitz, R. D., Vita, A., McGuire, P., Borgwardt, S. (2012a). Cognitive functioning in prodromal psychosis: a meta-analysis. *Arch Gen Psychiatry*, *69*(6), 562-571.

Fusar-Poli, P., Radua, J., McGuire, P., Borgwardt, S. (2012b). Neuroanatomical Maps of Psychosis Onset: Voxel-wise Meta-Analysis of Antipsychotic-Naive VBM Studies. *Schizophr Bull*, *38*(6), 1297-1307.

Gaspar, P. A., Bustamante, M. L., Silva, H., Aboitiz, F. (2009). Molecular mechanisms underlying glutamatergic dysfunction in schizophrenia: therapeutic implications. *J Neurochem*, *111*(4), 891-900.

Glahn, D. C., Laird, A. R., Ellison-Wright, I., Thelen, S. M., Robinson, J. L., Lancaster, J. L., Bullmore, E., Fox, P. T. (2008). Meta-analysis of gray matter anomalies in schizophrenia: application of anatomic likelihood estimation and network analysis. *Biol Psychiatry*, *64*(9), 774-781.

Green, M. F., Kern, R. S., Braff, D. L., Mintz, J. (2000). Neurocognitive deficits and functional outcome in schizophrenia: are we measuring the "right stuff"? *Schizophr Bull*, *26*(1), 119-136.

Grillon, C., Courchesne, E., Ameli, R., Geyer, M. A., Braff, D. L. (1990). Increased distractibility in schizophrenic patients. Electrophysiologic and behavioral evidence. *Arch Gen Psychiatry*, *47*(2), 171-179.

Hagler, D. J. J., Saygin, A. P., Sereno, M. I. (2006). Smoothing and cluster thresholding for cortical surface-based group analysis of fMRI data. *NeuroImage*, *33*(4), 1093-1103.

Harris, M. G., Henry, L. P., Harrigan, S. M., Purcell, R., Schwartz, O. S., Farrelly, S. E., Prosser, A. L., Jackson, H. J., McGorry, P. D. (2005). The relationship between duration of untreated psychosis and outcome: an eight-year prospective study. *Schizophr Res*, *79*(1), 85-93.

Haut, M. W., Kuwabara, H., Leach, S., Arias, R. G. (2000). Neural activation during performance of number-letter sequencing. *Appl Neuropsychol*, *7*(4), 237-242.

Heinrichs, R. W., Zakzanis, K. K. (1998). Neurocognitive deficit in schizophrenia: A quantitative review of the evidence. *Neuropsychology*, *12*(3), 426-445.

Ho, B. C., Andreasen, N. C., Ziebell, S., Pierson, R., Magnotta, V. (2011). Long-term antipsychotic treatment and brain volumes: a longitudinal study of first-episode schizophrenia. *Arch Gen Psychiatry*, *68*(2), 128-137.

Honea, R., Crow, T. J., Passingham, D., Mackay, C. E. (2005). Regional deficits in brain volume in schizophrenia: a meta-analysis of voxel-based morphometry studies. *Am J Psychiatry*, *162*(12), 2233-2245.

Jacobson, S., Kelleher, I., Harley, M., Murtagh, A., Clarke, M., Blanchard, M., Connolly, C., O'Hanlon, E., Garavan, H., Cannon, M. (2010). Structural and functional brain correlates of subclinical psychotic symptoms in 11-13 year old schoolchildren. *NeuroImage*, *49*(2), 1875-1885.

Jahshan, C., Cadenhead, K. S., Rissling, A. J., Kirihara, K., Braff, D. L., Light, G. A. (2012). Automatic sensory information processing abnormalities across the illness course of schizophrenia. *Psychol Med*, *42*(1), 85-97.

Johnson-Selfridge, M., Zalewski, C. (2001). Moderator variables of executive functioning in schizophrenia: meta-analytic findings. *Schizophr Bull*, *27*(2), 305-316.

Jung, W. H., Jang, J. H., Byun, M. S., An, S. K., Kwon, J. S. (2010). Structural brain alterations in individuals at ultra-high risk for psychosis: a review of magnetic resonance imaging studies and future directions. *J Korean Med Sci*, *25*(12), 1700-1709.

Jung, W. H., Kim, J. S., Jang, J. H., Choi, J. S., Jung, M. H., Park, J. Y., Han, J. Y., Choi, C. H., Kang, D. H., Chung, C. K., Kwon, J. S. (2011). Cortical thickness reduction in individuals at ultra-high-risk for psychosis. *Schizophr Bull*, *37*(4), 839-849.

Kao, Y. C., Liu, Y. P. (2011). Suicidal behavior and insight into illness among patients with schizophrenia spectrum disorders. *Psychiatr Q*, *82*(3), 207-220.

Kaufman, J., Birmaher, B., Brent, D., Rao, U., Flynn, C., Moreci, P., Williamson, D., Ryan, N. (1997). Schedule for Affective Disorders and Schizophrenia for School-Age Children-Present and Lifetime Version (K-SADS-PL): initial reliability and validity data. *J Am Acad Child Adolesc Psychiatry*, *36*(7), 980-988.

Kaur, M., Battisti, R. A., Ward, P. B., Ahmed, A., Hickie, I. B., Hermens, D. F. (2011). MMN/P3a deficits in first episode psychosis: comparing schizophrenia-spectrum and affective-spectrum subgroups. *Schizophr Res*, *130*(1-3), 203-209.

Kim, K. R., Park, J. Y., Song, D. H., Koo, H. K., An, S. K. (2011). Neurocognitive performance in subjects at ultrahigh risk for schizophrenia: a comparison with first-episode schizophrenia. *Compr Psychiatry*, *52*(1), 33-40.

Klosterkotter, J., Hellmich, M., Steinmeyer, E. M., Schultze-Lutter, F. (2001). Diagnosing schizophrenia in the initial prodromal phase. *Arch Gen Psychiatry*, *58*(2), 158-164.

Klosterkotter, J., Schultze-Lutter, F., Bechdolf, A., Ruhrmann, S. (2011). Prediction and prevention of schizophrenia: what has been achieved and where to go next? *World Psychiatry*, *10*(3), 165-174.

Kuperberg, G. R., Broome, M. R., McGuire, P. K., David, A. S., Eddy, M., Ozawa, F., Goff, D., West, W. C., Williams, S. C., van der Kouwe, A. J., Salat, D. H., Dale, A. M., Fischl, B. (2003). Regionally localized thinning of the cerebral cortex in schizophrenia. *Arch Gen Psychiatry*, *60*(9), 878-888.

Laird, A. R., McMillan, K. M., Lancaster, J. L., Kochunov, P., Turkeltaub, P. E., Pardo, J. V., Fox, P. T. (2005). A comparison of label-based review and ALE meta-analysis in the Stroop task. *Hum Brain Mapp*, *25*(1), 6-21.

Langdon, R., Coltheart, M. (1999). Mentalising, schizotypy, and schizophrenia. *Cognition*, *71*(1), 43-71.

Lavoie, S., Murray, M. M., Deppen, P., Knyazeva, M. G., Berk, M., Boulat, O., Bovet, P., Bush, A. I., Conus, P., Copolov, D., Fornari, E., Meuli, R., Solida, A., Vianin, P., Cuenod, M., Buclin, T., Do, K. Q. (2008). Glutathione precursor, N-acetyl-cysteine, improves mismatch negativity in schizophrenia patients. *Neuropsychopharmacology*, *33*(9), 2187-2199.

Lencz, T., Smith, C. W., McLaughlin, D., Auther, A., Nakayama, E., Hovey, L., Cornblatt, B. A. (2006). Generalized and specific neurocognitive deficits in prodromal schizophrenia. *Biol Psychiatry*, *59*(9), 863-871.

Levine, S. Z., Rabinowitz, J. (2009). A population-based examination of the role of years of education, age of onset, and sex on the course of schizophrenia. *Psychiatry Res*, *168*(1), 11-17.

Lichtenberger, E. O., Kaufman, A. S., Lai, Z. C. (2002). Essentials of WMS-III assessment. *John Wiley & Sons, Inc.*, 271.

Light, G. A., Braff, D. L. (2005). Mismatch negativity deficits are associated with poor functioning in schizophrenia patients. *Arch Gen Psychiatry*, *62*(2), 127-136.

Light, G. A., Swerdlow, N. R., Braff, D. L. (2007). Preattentive sensory processing as indexed by the MMN and P3a brain responses is associated with cognitive and psychosocial functioning in healthy adults. *J Cogn Neurosci*, *19*(10), 1624-1632.

Linden, D. E. (2005). The P300: Where in the brain is it produced and what does it tell us? *Neuroscientist*, *11*(6), 563-576.

Lord, L. D., Allen, P., Expert, P., Howes, O., Lambiotte, R., McGuire, P., Bose, S. K., Hyde, S., Turkheimer, F. E. (2011). Characterization of the anterior cingulate's role in the at-risk mental state using graph theory. *NeuroImage*, *56*(3), 1531-1539.

Lui, S., Deng, W., Huang, X., Jiang, L., Ma, X., Chen, H., Zhang, T., Li, X., Li, D., Zou, L., Tang, H., Zhou, X. J., Mechelli, A., Collier, D. A., Sweeney, J. A., Li, T., Gong, Q. (2009). Association of cerebral deficits with clinical symptoms in antipsychotic-naive first-episode schizophrenia: an optimized voxel-based morphometry and resting state functional connectivity study. *Am J Psychiatry*, *166*(2), 196-205.

Magaud, E., Kebir, O., Gut, A., Willard, D., Chauchot, F., Olie, J.-P., Kazes, M., Krebs, M.-O. (2010). Altered semantic but not phonological verbal fluency in young help-seeking individuals with ultra high risk of psychosis. *Schizophr Res*, *123*(1), 53-58.

Malla, A. K., Bodnar, M., Joober, R., Lepage, M. (2011). Duration of untreated psychosis is associated with orbital-frontal grey matter volume reductions in first episode psychosis. *Schizophr Res*, *125*(1), 13-20.

Manoach, D. S. (2003). Prefrontal cortex dysfunction during working memory performance in schizophrenia: reconciling discrepant findings. *Schizophr Res*, *60*(2-3), 285-298.

Marek, G. J., Behl, B., Bespalov, A. Y., Gross, G., Lee, Y., Schoemaker, H. (2010). Glutamatergic (N-methyl-D-aspartate receptor) hypofrontality in schizophrenia: too little juice or a miswired brain? *Mol Pharmacol*, *77*(3), 317-326.

Marshall, M., Lewis, S., Lockwood, A., Drake, R., Jones, P., Croudace, T. (2005). Association between duration of untreated psychosis and outcome in cohorts of first-episode patients: a systematic review. *Arch Gen Psychiatry*, *62*(9), 975-983.

Mason, O., Startup, M., Halpin, S., Schall, U., Conrad, A., Carr, V. (2004). Risk factors for transition to first episode psychosis among individuals with 'at-risk mental states'. *Schizophr Res*, *71*(2-3), 227-237.

McGorry, P. D., Goodwin, R. J., Stuart, G. W. (1988). The development, use, and reliability of the brief psychiatric rating scale (nursing modification)--an assessment procedure for the nursing team in clinical and research settings. *Compr Psychiatry*, *29*(6), 575-587.

McGorry, P. D., Yung, A. R., Phillips, L. J. (2003). The "close-in" or ultra high-risk model: a safe and effective strategy for research and clinical intervention in prepsychotic mental disorder. *Schizophr Bull*, *29*(4), 771-790.

McGrath, J. J., Susser, E. S. (2009). New directions in the epidemiology of schizophrenia. *The Medical journal of Australia*, *190*(4 Suppl), S7-S9.

McGue, M., Gottesman, I. I. (1991). The genetic epidemiology of schizophrenia and the design of linkage studies. *Eur Arch Psychiatry Clin Neurosci*, *240*(3), 174-181.

Mechelli, A., Riecher-Rossler, A., Meisenzahl, E. M., Tognin, S., Wood, S. J., Borgwardt, S. J., Koutsouleris, N., Yung, A. R., Stone, J. M., Phillips, L. J., McGorry, P. D., Valli, I., Velakoulis, D., Woolley, J., Pantelis, C., McGuire, P. (2011). Neuroanatomical abnormalities that predate the onset of psychosis: a multicenter study. *Arch Gen Psychiatry*, *68*(5), 489-495.

Meijer, J. H., Schmitz, N., Nieman, D. H., Becker, H. E., van Amelsvoort, T. A., Dingemans, P. M., Linszen, D. H., de Haan, L. (2011). Semantic fluency deficits and reduced grey matter before transition to psychosis: A voxelwise correlational analysis. *Psychiatry Res*, *194*(1), 1-6.

Minassian, A., Feifel, D., Perry, W. (2007). The relationship between sensorimotor gating and clinical improvement in acutely ill schizophrenia patients. *Schizophr Res*, *89*(1-3), 225-231.

Minzenberg, M. J., Laird, A. R., Thelen, S., Carter, C. S., Glahn, D. C. (2009). Meta-analysis of 41 functional neuroimaging studies of executive function in schizophrenia. *Arch Gen Psychiatry*, *66*(8), 811-822.

Mitrushina, M. N., Boone, K. B. (2005). Handbook of normative data for neuropsychological assessment. *Oxford University Press, Inc.*, 1029.

Moghaddam, B., Javitt, D. (2012). From Revolution to Evolution: The Glutamate Hypothesis of Schizophrenia and its Implication for Treatment. *Neuropsychopharmacology*, *37*(1), 4-15.

Myles-Worsley, M., Ord, L., Blailes, F., Ngiralmau, H., Freedman, R. (2004). P50 sensory gating in adolescents from a pacific island isolate with elevated risk for schizophrenia. *Biol Psychiatry*, *55*(7), 663-667.

Näätänen, R. (1990). The role of attention in auditory information processing as revealed by event-related potentials and other brain measures of cognitive function. *Behavioral and Brain Sciences*, *13*(02), 201-233.

Näätänen, R., Kahkonen, S. (2009). Central auditory dysfunction in schizophrenia as revealed by the mismatch negativity (MMN) and its magnetic equivalent MMNm: a review. *Int J Neuropsychopharmacol*, *12*(1), 125-135.

Nakamura, K., Takahashi, T., Nemoto, K., Furuichi, A., Nishiyama, S., Nakamura, Y., Ikeda, E., Kido, M., Noguchi, K., Seto, H., Suzuki, M. (2013). Gray matter changes in subjects at high risk for developing psychosis and first-episode schizophrenia: a voxel-based structural MRI study. *Front Psychiatry*, *4*, 16.

Navari, S., Dazzan, P. (2009). Do antipsychotic drugs affect brain structure? A systematic and critical review of MRI findings. *Psychol Med*, *39*(11), 1763-1777.

Niendam, T. A., Bearden, C. E., Johnson, J. K., Cannon, T. D. (2006). Global Functioning: Role Scale (GF: Role). *CA: University of California*.

Nuechterlein, K. H., Barch, D. M., Gold, J. M., Goldberg, T. E., Green, M. F., Heaton, R. K. (2004). Identification of separable cognitive factors in schizophrenia. *Schizophr Res*, *72*(1), 29-39.

Olabi, B., Ellison-Wright, I., McIntosh, A. M., Wood, S. J., Bullmore, E., Lawrie, S. M. (2011). Are there progressive brain changes in schizophrenia? A meta-analysis of structural magnetic resonance imaging studies. *Biol Psychiatry*, *70*(1), 88-96.

Olney, J. W., Farber, N. B. (1995). Glutamate receptor dysfunction and schizophrenia. *Arch Gen Psychiatry*, *52*(12), 998-1007.

Ortiz-Gil, J., Pomarol-Clotet, E., Salvador, R., Canales-Rodriguez, E. J., Sarro, S., Gomar, J. J., Guerrero, A., Sans-Sansa, B., Capdevila, A., Junque, C., McKenna, P. J. (2011). Neural correlates of cognitive impairment in schizophrenia. *Br J Psychiatry*, *199*(3), 202-210.

Pantelis, C., Barnes, T. R., Nelson, H. E., Tanner, S., Weatherley, L., Owen, A. M., Robbins, T. W. (1997). Frontal-striatal cognitive deficits in patients with chronic schizophrenia. *Brain*, *120*(Pt 10), 1823-1843.

Pantelis, C., Velakoulis, D., McGorry, P. D., Wood, S. J., Suckling, J., Phillips, L. J., Yung, A. R., Bullmore, E. T., Brewer, W., Soulsby, B., Desmond, P., McGuire, P. K. (2003). Neuroanatomical abnormalities before and after onset of psychosis: a cross-sectional and longitudinal MRI comparison. *Lancet*, *361*(9354), 281-288.

Pantelis, C., Velakoulis, D., Wood, S. J., Yucel, M., Yung, A. R., Phillips, L. J., Sun, D. Q., McGorry, P. D. (2007). Neuroimaging and emerging psychotic disorders: the Melbourne ultra-high risk studies. *Int Rev Psychiatry*, *19*(4), 371-381.

Peters, B. D., de Haan, L., Dekker, N., Blaas, J., Becker, H. E., Dingemans, P. M., Akkerman, E. M., Majoie, C. B., van Amelsvoort, T., den Heeten, G. J., Linszen, D. H. (2008). White matter fibertracking in first-episode schizophrenia, schizoaffective patients and subjects at ultra-high risk of psychosis. *Neuropsychobiology*, *58*(1), 19-28.

Peters, B. D., Dingemans, P. M., Dekker, N., Blaas, J., Akkerman, E., van Amelsvoort, T. A., Majoie, C. B., den Heeten, G. J., Linszen, D. H., de Haan, L. (2010). White matter connectivity and psychosis in ultra-high-risk subjects: a diffusion tensor fiber tracking study. *Psychiatry Res*, *181*(1), 44-50.

Peters, B. D., Schmitz, N., Dingemans, P. M., van Amelsvoort, T. A., Linszen, D. H., de Haan, L., Majoie, C. B., den Heeten, G. J. (2009). Preliminary evidence for reduced frontal white matter integrity in subjects at ultra-high-risk for psychosis. *Schizophr Res*, *111*(1-3), 192-193.

Pflueger, M. O., Gschwandtner, U., Stieglitz, R. D., Riecher-Rossler, A. (2007). Neuropsychological deficits in individuals with an at risk mental state for psychosis - working memory as a potential trait marker. *Schizophr Res*, *97*(1-3), 14-24.

Preacher, K. J. (2001). Calculation for the chi-square test: An interactive calculation tool for chi-square tests of goodness of fit and independence [Computer software]. Available from http://quantpsy.org.

Raine, A. (1991). The SPQ: a scale for the assessment of schizotypal personality based on DSM-III-R criteria. *Schizophr Bull*, *17*(4), 555-564.

Rannikko, I., Paavola, L., Haapea, M., Huhtaniska, S., Miettunen, J., Veijola, J., Murray, G. K., Barnes, A., Wahlberg, K.-E., Isohanni, M., Jääskeläinen, E. (2012). Verbal learning and memory and their associations with brain morphology and illness course in schizophrenia spectrum psychoses. *J Clin Exp Neuropsychol*, *34*(7), 698-713.

Rasser, P. E., Johnston, P., Lagopoulos, J., Ward, P. B., Schall, U., Thienel, R., Bender, S., Toga, A. W., Thompson, P. M. (2005). Functional MRI BOLD response to Tower of London performance of first-episode schizophrenia patients using cortical pattern matching. *NeuroImage*, *26*(3), 941-951.

Rasser, P. E., Schall, U., Peck, G., Cohen, M., Johnston, P., Khoo, K., Carr, V. J., Ward, P. B., Thompson, P. M. (2010). Cerebellar grey matter deficits in first-episode schizophrenia mapped using cortical pattern matching. *NeuroImage*, *53*(4), 1175-1180.

Rasser, P. E., Schall, U., Todd, J., Michie, P. T., Ward, P. B., Johnston, P., Helmbold, K., Case, V., Soyland, A., Tooney, P. A., Thompson, P. M. (2011). Gray matter deficits, mismatch negativity, and outcomes in schizophrenia. *Schizophr Bull*, *37*(1), 131-140.

Rinne, T., Alho, K., Ilmoniemi, R. J., Virtanen, J., Naatanen, R. (2000). Separate time behaviors of the temporal and frontal mismatch negativity sources. *NeuroImage*, *12*(1), 14-19.

Rosen, K., Garety, P. (2005). Predicting recovery from schizophrenia: a retrospective comparison of characteristics at onset of people with single and multiple episodes. *Schizophr Bull*, *31*(3), 735-750.

Ruff, R. M., Light, R. H., Parker, S. B., Levin, H. S. (1997). The psychological construct of word fluency. *Brain Lang*, *57*(3), 394-405.

Salisbury, D. F., Kuroki, N., Kasai, K., Shenton, M. E., McCarley, R. W. (2007). Progressive and interrelated functional and structural evidence of post-onset brain reduction in schizophrenia. *Arch Gen Psychiatry*, *64*(5), 521-529.

Saunders, J. B., Aasland, O. G., Babor, T. F., de la Fuente, J. R., Grant, M. (1993). Development of the Alcohol Use Disorders Identification Test (AUDIT): WHO Collaborative Project on Early Detection of Persons with Harmful Alcohol Consumption--II. *Addiction*, *88*(6), 791-804.

Schall, U., Catts, S. V., Karayanidis, F., Ward, P. B. (1999). Auditory event-related potential indices of fronto-temporal information processing in schizophrenia syndromes: valid outcome prediction of clozapine therapy in a three-year follow-up. *Int J Neuropsychopharmacol*, *2*(2), 83-93.

Schall, U., Johnston, P., Lagopoulos, J., Juptner, M., Jentzen, W., Thienel, R., Dittmann-Balcar, A., Bender, S., Ward, P. B. (2003a). Functional brain maps of Tower of London performance: a positron emission tomography and functional magnetic resonance imaging study. *NeuroImage*, *20*(2), 1154-1161.

Schall, U., Johnston, P., Todd, J., Ward, P. B., Michie, P. T. (2003b). Functional neuroanatomy of auditory mismatch processing: an event-related fMRI study of duration-deviant oddballs. *NeuroImage*, *20*(2), 729-736.

Schultz, C. C., Koch, K., Wagner, G., Roebel, M., Schachtzabel, C., Gaser, C., Nenadic, I., Reichenbach, J. R., Sauer, H., Schlosser, R. G. (2010). Reduced cortical thickness in first episode schizophrenia. *Schizophr Res*, *116*(2-3), 204-209.

Schultze-Lutter, F., Ruhrmann, S., Berning, J., Maier, W., Klosterkotter, J. (2010). Basic symptoms and ultrahigh risk criteria: symptom development in the initial prodromal state. *Schizophr Bull*, *36*(1), 182-191.

Seeman, P. (2009). Glutamate and dopamine components in schizophrenia. *J Psychiatry Neurosci*, *34*(2), 143-149.

Segonne, F., Dale, A. M., Busa, E., Glessner, M., Salat, D., Hahn, H. K., Fischl, B. (2004). A hybrid approach to the skull stripping problem in MRI. *NeuroImage*, *22*(3), 1060-1075.

Semlitsch, H. V., Anderer, P., Schuster, P., Presslich, O. (1986). A solution for reliable and valid reduction of ocular artifacts, applied to the P300 ERP. *Psychophysiology*, *23*(6), 695-703.

Shaikh, M., Valmaggia, L., Broome, M. R., Dutt, A., Lappin, J., Day, F., Woolley, J., Tabraham, P., Walshe, M., Johns, L., Fusar-Poli, P., Howes, O., Murray, R. M., McGuire, P., Bramon, E. (2012). Reduced mismatch negativity predates the onset of psychosis. *Schizophr Res*, *134*(1), 42-48.

Shallice, T. (1982). Specific impairments of planning. *Philos Trans R Soc Lond B Biol Sci*, *298*(1089), 199-209.

Shelley, A. M., Ward, P. B., Catts, S. V., Michie, P. T., Andrews, S., McConaghy, N. (1991). Mismatch negativity: an index of a preattentive processing deficit in schizophrenia. *Biol Psychiatry*, *30*(10), 1059-1062.

Shenton, M. E., Dickey, C. C., Frumin, M., McCarley, R. W. (2001). A review of MRI findings in schizophrenia. *Schizophr Res*, *49*(1-2), 1-52.

Shin, K. S., Kim, J. S., Kang, D. H., Koh, Y., Choi, J. S., O'Donnell, B. F., Chung, C. K., Kwon, J. S. (2009). Pre-attentive auditory processing in ultra-high-risk for schizophrenia with magnetoencephalography. *Biol Psychiatry*, *65*(12), 1071-1078.

Simon, A. E., Gradel, M., Cattapan-Ludewig, K., Gruber, K., Ballinari, P., Roth, B., Umbricht, D. (2012). Cognitive functioning in at-risk mental states for psychosis and 2-year clinical outcome. *Schizophr Res*, *142*(1-3), 108-115.

Sled, J. G., Zijdenbos, A. P., Evans, A. C. (1998). A nonparametric method for automatic correction of intensity nonuniformity in MRI data. *IEEE Trans Med Imaging*, *17*(1), 87-97.

Smieskova, R., Allen, P., Simon, A., Aston, J., Bendfeldt, K., Drewe, J., Gruber, K., Gschwandtner, U., Klarhoefer, M., Lenz, C., Scheffler, K., Stieglitz, R. D., Radue, E. W., McGuire, P., Riecher-Rossler, A., Borgwardt, S. J. (2012). Different duration of at-risk mental state associated with neurofunctional abnormalities. A multimodal imaging study. *Hum Brain Mapp*, *33*(10), 2281-2294.

Smieskova, R., Fusar-Poli, P., Allen, P., Bendfeldt, K., Stieglitz, R. D., Drewe, J., Radue, E. W., McGuire, P. K., Riecher-Rossler, A., Borgwardt, S. J. (2009). The effects of antipsychotics on the brain: what have we learnt from structural imaging of schizophrenia?--a systematic review. *Curr Pharm Des*, *15*(22), 2535-2549.

Smieskova, R., Fusar-Poli, P., Allen, P., Bendfeldt, K., Stieglitz, R. D., Drewe, J., Radue, E. W., McGuire, P. K., Riecher-Rossler, A., Borgwardt, S. J. (2010). Neuroimaging predictors of transition to psychosis--a systematic review and meta-analysis. *Neurosci Biobehav Rev*, *34*(8), 1207-1222.

Smith, C. W., Park, S., Cornblatt, B. (2006). Spatial working memory deficits in adolescents at clinical high risk for schizophrenia. *Schizophr Res*, *81*(2-3), 211-215.

Smith, S. M. (2002). Fast robust automated brain extraction. *Hum Brain Mapp*, *17*(3), 143-155.

Sowell, E. R., Thompson, P. M., Tessner, K. D., Toga, A. W. (2001). Mapping continued brain growth and gray matter density reduction in dorsal frontal cortex: Inverse relationships during postadolescent brain maturation. *J Neurosci*, *21*(22), 8819-8829.

Stroop, J. R. (1935). Studies of interference in serial verbal reactions. *Journal of Experimental Psychology*, *18*(6), 643-662.

Sun, D., Phillips, L., Velakoulis, D., Yung, A., McGorry, P. D., Wood, S. J., van Erp, T. G., Thompson, P. M., Toga, A. W., Cannon, T. D., Pantelis, C. (2009). Progressive brain structural changes mapped as psychosis develops in 'at risk' individuals. *Schizophr Res*, *108*(1-3), 85-92.

Swerdlow, N. R., Geyer, M. A. (1998). Using an animal model of deficient sensorimotor gating to study the pathophysiology and new treatments of schizophrenia. *Schizophr Bull*, *24*(2), 285-301.

Swerdlow, N. R., Light, G. A., Cadenhead, K. S., Sprock, J., Hsieh, M. H., Braff, D. L. (2006). Startle gating deficits in a large cohort of patients with schizophrenia: relationship to medications, symptoms, neurocognition, and level of function. *Arch Gen Psychiatry*, *63*(12), 1325-1335.

Takeuchi, H., Taki, Y., Sassa, Y., Hashizume, H., Sekiguchi, A., Nagase, T., Nouchi, R., Fukushima, A., Kawashima, R. (2012). Regional gray and white matter volume associated with Stroop interference: evidence from voxel-based morphometry. *Neuroimage*, *59*(3), 2899-2907.

Tandon, R., Keshavan, M. S., Nasrallah, H. A. (2008). Schizophrenia, "just the facts" what we know in 2008. 2. Epidemiology and etiology. *Schizophr Res*, *102*(1-3), 1-18.

Thompson, P. M., Vidal, C., Giedd, J. N., Gochman, P., Blumenthal, J., Nicolson, R., Toga, A. W., Rapoport, J. L. (2001). Mapping adolescent brain change reveals dynamic wave of accelerated gray matter loss in very early-onset schizophrenia. *Proc Natl Acad Sci U S A*, *98*(20), 11650-11655.

Todd, J., Michie, P. T., Schall, U., Karayanidis, F., Yabe, H., Naatanen, R. (2008). Deviant matters: duration, frequency, and intensity deviants reveal different patterns of mismatch negativity reduction in early and late schizophrenia. *Biol Psychiatry*, *63*(1), 58-64.

Todd, J., Michie, P. T., Schall, U., Ward, P. B., Catts, S. V. (2012). Mismatch negativity (MMN) reduction in schizophrenia-impaired prediction--error generation, estimation or salience? *Int J Psychophysiol*, *83*(2), 222-231.

Turetsky, B. I., Raz, J., Alsop, D., Charbonnier, D., Schroeder, L., Gur, R. E. (2000). Integrated ERP/fMRI analysis of deviance processing in schizophrenia. *Biological Psychiatry*, *47*(8), S172.

Tuulio-Henriksson, A., Partonen, T., Suvisaari, J., Haukka, J., Lonnqvist, J. (2004). Age at onset and cognitive functioning in schizophrenia. *Br J Psychiatry*, *185*, 215-219.

Umbricht, D., Koller, R., Vollenweider, F. X., Schmid, L. (2002). Mismatch negativity predicts psychotic experiences induced by NMDA receptor antagonist in healthy volunteers. *Biol Psychiatry*, *51*(5), 400-406.

Umbricht, D., Krljes, S. (2005). Mismatch negativity in schizophrenia: a meta-analysis. *Schizophr Res*, *76*(1), 1-23.

Wechsler, D. (1997). Wechsler Memory Scale - Third Edition: Manual. *The Psychological Corporation*.

Wechsler, D. (1999). Wechsler Abbreviated Scale of Intelligence (WASI). *The Psychological Corporation*.

Weiss, E. M., Siedentopf, C., Golaszewski, S., Mottaghy, F. M., Hofer, A., Kremser, C., Felber, S., Fleischhacker, W. W. (2007). Brain activation patterns during a selective attention test--a functional MRI study in healthy volunteers and unmedicated patients during an acute episode of schizophrenia. *Psychiatry Res*, *154*(1), 31-40.

Wobrock, T., Ecker, U. K., Scherk, H., Schneider-Axmann, T., Falkai, P., Gruber, O. (2009). Cognitive impairment of executive function as a core symptom of schizophrenia. *World J Biol Psychiatry*, *10*(4 Pt 2), 442-451.

Wood, S. J., Pantelis, C., Proffitt, T., Phillips, L. J., Stuart, G. W., Buchanan, J. A., Mahony, K., Brewer, W., Smith, D. J., McGorry, P. D. (2003). Spatial working memory ability is a marker of risk-for-psychosis. *Psychol Med*, *33*(7), 1239-1247.

Yung, A. R., Phillips, L. J., Yuen, H. P., McGorry, P. D. (2004). Risk factors for psychosis in an ultra high-risk group: psychopathology and clinical features. *Schizophr Res*, *67*(2-3), 131-142.

Yung, A. R., Yuen, H. P., McGorry, P. D., Phillips, L. J., Kelly, D., Dell'Olio, M., Francey, S. M., Cosgrave, E. M., Killackey, E., Stanford, C., Godfrey, K., Buckby, J. (2005). Mapping the onset of psychosis: the Comprehensive Assessment of At-Risk Mental States. *Aust N Z J Psychiatry*, *39*(11-12), 964-971.

Zakzanis, K. K., Mraz, R., Graham, S. J. (2005). An fMRI study of the Trail Making Test. *Neuropsychologia*, *43*(13), 1878-1886.

Ziermans, T., Schothorst, P., Magnee, M., van Engeland, H., Kemner, C. (2011). Reduced prepulse inhibition in adolescents at risk for psychosis: a 2-year follow-up study. *J Psychiatry Neurosci*, *36*(2), 127-134.

Ziermans, T. B., Schothorst, P. F., Schnack, H. G., Koolschijn, P. C., Kahn, R. S., van Engeland, H., Durston, S. (2012). Progressive Structural Brain Changes During Development of Psychosis. *Schizophr Bull*, *38*(3), 519-530.

COLLABORATION WITH OTHER RESEARCHERS

This PhD project was carried out in conjunction with a prospective multi-centre study which provided a cross-sectional subset of its collected data (i.e. MRI brain scans, EEG recordings, and clinical/neuropsychological assessments) to be used for analysis and presentation in this thesis. As the PhD candidate, I conducted all MR image processing along with the statistical analyses of these data with clinical/neuropsychological and ERP data.